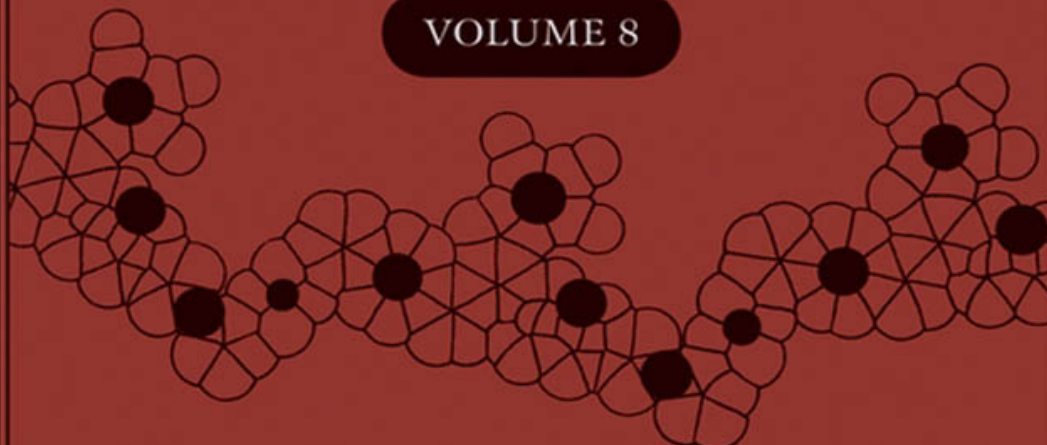


MACROMOLECULES  
CONTAINING METAL  
and METAL-LIKE  
ELEMENTS

VOLUME 8



BORON-CONTAINING POLYMERS

Edited by

ALAA S. ABD-EL-AZIZ  
CHARLES E. CARRAHER, JR.  
CHARLES U. PITTMAN, JR.  
MARTEL ZELDIN

---

# Macromolecules Containing Metal and Metal-Like Elements

## Volume 8

---

### Boron-Containing Polymers

Edited by

**Alaa S. Abd-El-Aziz**

*University of British Columbia Okanagan, Kelowna, British Columbia,  
Canada*

**Charles E. Carraher Jr.**

*Department of Chemistry and Biochemistry, Florida Atlantic University,  
Boca Raton, Florida, and Florida Center for Environmental Studies,  
Palm Beach Gardens, Florida*

**Charles U. Pittman Jr.**

*Department of Chemistry, Mississippi State University,  
Mississippi State, Mississippi*

**Martel Zeldin**

*Department of Chemistry, University of Richmond, Richmond, Virginia*

 **WILEY-INTERSCIENCE**

A John Wiley & Sons, Inc., Publication



---

**Macromolecules  
Containing Metal and  
Metal-Like Elements**

**Volume 8**

---



---

# Macromolecules Containing Metal and Metal-Like Elements

## Volume 8

---

### Boron-Containing Polymers

Edited by

**Alaa S. Abd-El-Aziz**

*University of British Columbia Okanagan, Kelowna, British Columbia,  
Canada*

**Charles E. Carraher Jr.**

*Department of Chemistry and Biochemistry, Florida Atlantic University,  
Boca Raton, Florida, and Florida Center for Environmental Studies,  
Palm Beach Gardens, Florida*

**Charles U. Pittman Jr.**

*Department of Chemistry, Mississippi State University,  
Mississippi State, Mississippi*

**Martel Zeldin**

*Department of Chemistry, University of Richmond, Richmond, Virginia*

 **WILEY-INTERSCIENCE**

A John Wiley & Sons, Inc., Publication

Copyright © 2007 by John Wiley & Sons, Inc. All rights reserved

Published by John Wiley & Sons, Inc., Hoboken, New Jersey  
Published simultaneously in Canada

No part of this publication may be reproduced, stored in a retrieval system, or transmitted in any form or by any means, electronic, mechanical, photocopying, recording, scanning, or otherwise, except as permitted under Section 107 or 108 of the 1976 United States Copyright Act, without either the prior written permission of the Publisher, or authorization through payment of the appropriate per-copy fee to the Copyright Clearance Center, Inc., 222 Rosewood Drive, Danvers, MA 01923, (978) 750-8400, fax (978) 750-4470, or on the web at [www.copyright.com](http://www.copyright.com). Requests to the Publisher for permission should be addressed to the Permissions Department, John Wiley & Sons, Inc., 111 River Street, Hoboken, NJ 07030, (201) 748-6011, fax (201) 748-6008, or online at <http://www.wiley.com/go/permission>.

**Limit of Liability/Disclaimer of Warranty:** While the publisher and author have used their best efforts in preparing this book, they make no representations or warranties with respect to the accuracy or completeness of the contents of this book and specifically disclaim any implied warranties of merchantability or fitness for a particular purpose. No warranty may be created or extended by sales representatives or written sales materials. The advice and strategies contained herein may not be suitable for your situation. You should consult with a professional where appropriate. Neither the publisher nor author shall be liable for any loss of profit or any other commercial damages, including but not limited to special, incidental, consequential, or other damages.

For general information on our other products and services or for technical support, please contact our Customer Care Department within the United States at (800) 762-2974, outside the United States at (317) 572-3993 or fax (317) 572-4002.

Wiley also publishes its books in a variety of electronic formats. Some content that appears in print may not be available in electronic formats. For more information about Wiley products, visit our web site at [www.wiley.com](http://www.wiley.com).

Wiley Bicentennial Logo: Richard J. Pacifico

***Library of Congress Cataloging-in-Publication Data:***

ISBN 978-0-471-73012-5  
ISSN 1545-438X

Printed in the United States of America

10 9 8 7 6 5 4 3 2 1

---

# Contributors

---

**Samuel Bernard**, Laboratoire des Multimatériaux et Interfaces, Université Lyon 1, Villeurbanne, France

**Yoshiki Chujo**, Department of Polymer Chemistry, Graduate School of Engineering, Kyoto University, Katsura Nishikyo-ku, Kyoto 615-8510, Japan

**David Cornu**, Laboratoire des Multimatériaux et Interfaces, Université Lyon 1, Villeurbanne, France

**Teddy M. Keller**, Advanced Materials Section, Materials Chemistry Branch, Chemistry Division, Naval Research Laboratory, Washington, DC 20375

**Manoj K. Kolel-Veetil**, Advanced Materials Section, Materials Chemistry Branch, Chemistry Division, Naval Research Laboratory, Washington, DC 20375

**Noriyoshi Matsumi**, Department of Biotechnology, Tokyo University of Agriculture and Technology, Koganei, Tokyo 184-8588, Japan

**Philippe Miele**, Laboratoire des Multimatériaux et Interfaces, Université Lyon 1, Villeurbanne, France

**Yuuya Nagata**, Department of Polymer Chemistry, Graduate School of Engineering, Kyoto University, Katsura Nishikyo-ku, Kyoto 615-8510, Japan

**Hiroyuki Ohno**, Department of Biotechnology, Tokyo University of Agriculture and Technology, Koganei, Tokyo 184-8588, Japan

**Mogon Patel**, Atomic Weapons Establishment (AWE), Aldermaston, Reading, RG7 4PR, UK

**Anthony C. Swain**, Atomic Weapons Establishment (AWE), Aldermaston, Reading, RG7 4PR, UK

**Bérangère Toury**, Laboratoire des Multimatériaux et Interfaces, Université Lyon 1, Villeurbanne, France



---

# Contents

---

<b>Preface</b>	<b>xi</b>
<b>Series Preface</b>	<b>xiii</b>
<b>1. The State of the Art in Boron Polymer Chemistry</b>	<b>1</b>
<i>Manoj K. Kolel-Veetil and Teddy M. Keller</i>	
I. Introduction	2
A. A Brief Historical Perspective on Boron and Its Polymers	2
II. Recent Advances in Boron-Containing Polymers	8
A. Polymers Containing Boron Atoms in the Backbone or in Pendent Groups	8
i. $\pi$ -Conjugated Organoboron Polymers Used in Optical and Sensing Applications	8
a. Formed by the Hydroboration Route	9
b. Formed by Other Synthetic Routes	11
ii. Boron Polymers Containing P, Si, or Organometallic Units	15
a. Boron Polymers Containing P Atoms	15
b. Silicon-Containing Boron Polymers	17
c. Boron Polymers Containing Organometallic Moieties	17
iii. Organoboron Polymers Used as Catalysts in Organic Transformations	22
a. Boron Ligands/Polymers Used in Olefin Polymerization Reactions	22
b. Organoboron Polymers Used in Other Organic Transformations	29
iv. Organoboron Polymers that Function as Flame-Retardant Materials	31
B. Polymers Containing Boron Ring Systems in the Backbone or in Pendent Groups	33
i. Organoboron Polymers that Contain Borazine or 9-BBN with Utility in the Production of High-Performance Fibers	34
a. SiC-Producing Borazine Polymer Systems	34
b. Si/B/C/N-Producing Systems	36

---

ii. Organoboron Polymers that Contain Boroxine or Triphosphatriborin Ring Systems	37
iii. Organoboron Polymers that Contain Polypyrazolyborate or Pyrazabole Ring Systems	37
iv. Organoboron Polymers that Contain Other Boron Ring Systems	38
C. Polymers Containing Boron Clusters in the Backbone or in Pendent Groups	38
i. Monomeric and Polymeric Organic Analogs of Boron Cluster Systems	38
ii. Poly(carboranylenesiloxanes) and Related Polymers	42
iii. Conducting Polymers Containing Carborane Clusters	52
iv. Carborane Polymers in Medicine	54
v. Carborane Polymers Used in the Production of High-Performance Fibers	57
vi. Miscellaneous Carborane Polymers	60
a. Carborane Polymers of Polyetherketones	60
b. Carborane Polymers for Use in Catalytic Reactions	61
vii. Carborane Supramolecular Chemistry	63
III. Summary	71
IV. References	71
<b>2. Polymers Incorporating Icosahedral Closo-Dicarbaborane Units</b>	<b>77</b>
<i>Mogon Patel and Anthony C. Swain</i>	
I. Introduction	78
A. Polymers Incorporating Decaborane	79
B. Polymers with Pendant Carborane Groups	80
II. Poly( <i>M</i> -Carborane-Siloxane) Rubbers	81
III. Synthesis	82
A. Bis(ureido)silanes: Condensation Polymerization	86
B. Dilithiocarborane: Salt Elimination Route	88
IV. Characterization	88
A. Nuclear Magnetic Resonance Spectroscopy	88
B. Gel-Permeation Chromatography	89
C. Thermal and Chemical Properties	89
V. Thermal and Radiation Stability	93
A. Stability to Neutrons	96
VI. Other Carborane-Containing Polymers	97
A. Poly(ether-ketone-carbaborane)	97
B. Polyphosphazene Incorporating Carboranyl Units	98
VII. Energetic Carborane Polymer Systems	99
VIII. Summary	100
IX. References	101

---

<b>3. Boron- and Nitrogen-Containing Polymers for Advanced Materials</b>	<b>103</b>
<i>Philippe Miele and Samuel Bernard</i>	
I. Introduction	104
II. Polymeric Precursors of BN Fibers	105
A. tris(Alkylamino)boranes–Derived Poly[ <i>B</i> -(alkylamino)borazines]	105
B. tris( <i>B</i> -Alkylamino)borazine–Derived Poly[ <i>B</i> -(alkylamino)borazines]	107
C. Polymeric Precursors Derived from tris(Borylamino)borazines	112
i. Two-Step Polycondensation (Thermal Route)	112
ii. One-Step Polycondensation	116
III. Outlook	118
IV. Summary	118
V. References	119
<b>4. Organoboron Polymers</b>	<b>121</b>
<i>Yuuya Nagata and Yoshiki Chujo</i>	
I. Introduction	122
II. Hydroboration Polymerization	123
A. Hydroboration Polymerization of Diene Monomers	123
B. Reactions of Organoboron Polymers Prepared by Hydroboration Polymerization	124
C. Hydroboration Polymerization of Diyne Monomers	129
D. Conjugated Organoboron Polymers	130
E. Poly(cyclodiborazane)s Prepared by Hydroboration Polymerization of Dicyano Monomers	132
F. Conjugated Poly(cyclodiborazane)s	134
G. Organoboron Polymers as an Anion Sensor	137
III. Other Boration Polymerizations	138
A. Haloboration Polymerization	138
B. Phenylboration Polymerization	139
C. Alkoxyboration Polymerization	140
IV. Organometallic Routes	141
A. Grignard and Organolithium Reagents	141
B. Poly(cyclodiborazane)s via Cross-Coupling Reactions	142
C. Poly(pyrazabole)s via Cross-Coupling Reactions	143
V. Summary	145
VI. References	145
<b>5. Boron- and Nitrogen-Containing Polymers</b>	<b>149</b>
<i>Philippe Miele, David Cornu and Bérangeère Toury</i>	
I. Introduction	150
II. Background	151

III. Polymers Derived from Borazine	151
IV. Polymers Derived from <i>B</i> -Chloroborazine	156
A. Poly( <i>B</i> -amino)borazines Prepared in a One-Step Process	156
B. Poly( <i>B</i> -borylamino)borazines Prepared in a One-Step Process	159
C. Poly( <i>B</i> -amino)borazines Prepared in a Two-Step Process	161
D. Poly( <i>B</i> -borylamino)borazines Prepared in a Two-Step Process	166
V. Polymers Derived from tris(Alkylamino)boranes	169
VI. Summary	171
VII. References	172
<b>6. Organoboron Polymer Electrolytes for Selective Lithium Cation Transport</b>	<b>175</b>
<i>Noriyoshi Matsumi and Hiroyuki Ohno</i>	
I. Introduction	176
II. Anion-Trapping-Type Organoboron Polymer Electrolytes via Hydroborane Monomer	177
III. Comblike Organoboron Polymer Electrolytes	180
IV. Facile Preparation of Organoboron Polymer Electrolytes via Dehydrocoupling Reaction of 9-Borabicyclo[3.3.1]nonane and Poly(propylene oxide)	182
V. Poly(organoboron halide)-imidazole Complexes	183
VI. Lithium Borate-Type Polymers via Polymer Reactions	186
VII. Direct Synthesis of Poly(lithium organoborate)s	188
VIII. Polymer/Salt Hybrid Including Boron-Stabilized Imidoanion	190
IX. Summary	193
X. References	194
<b>Index</b>	<b>197</b>

---

# Preface

---

Boron has been known as an element since its discovery in 1808 by Davy, Gay-Lussac, and Thenard, but it was not purified until 1909. The first polymers containing boron were synthesized by Stock about 80 years ago. Since then there has been a growing number and variety of boron-containing polymers produced. The emphasis for much of the development of boron polymers involves boron's ability for delocalizing electrons because of the presence of an empty p orbital. Furthermore, boron's ability to capture neutrons and its ability to form protective coatings have been driving forces to produce polymers. Finally, boron polymers with high percentages of nitrogen and boron have been sought as precursors to the ceramic boron nitride and boron nitride fibers. This volume presents the state-of-the-art developments with respect to boron-containing polymers. It captures the explosive development of these important materials in the areas of ceramics, coatings, nanomaterials, catalysts, therapeutic agents, and especially electronic applications such as nonlinear optical and fluorescent light-emitting materials. The chapters give supportive and historical developments that allow a person unfamiliar with boron polymers to appreciate and understand the topics presented. Practical application of boron-containing materials is also emphasized. Thanks to the efforts of the leading scientists in the fields represented, the full range of activity is included in this volume.



---

# Series Preface

---

Most traditional macromolecules are composed of less than 10 elements (mainly C, H, N, O, S, P, Cl, F), whereas metal and semi-metal-containing polymers allow properties that can be gained through the inclusion of nearly 100 additional elements. Macromolecules containing metal and metal-like elements are widespread in nature with metalloenzymes supplying a number of essential physiological functions including respiration, photosynthesis, energy transfer, and metal ion storage.

Polysiloxanes (silicones) are one of the most studied classes of polymers. They exhibit a variety of useful properties not common to non-metal-containing macromolecules. They are characterized by combinations of chemical, mechanical, electrical, and other properties that, when taken together, are not found in any other commercially available class of materials. The initial footprints on the moon were made by polysiloxanes. Polysiloxanes are currently sold as high-performance caulks, lubricants, antifoaming agents, window gaskets, O-rings, contact lenses, and numerous and variable human biological implants and prosthetics, to mention just a few of their applications.

The variety of macromolecules containing metal and metal-like elements is extremely large, not only because of the large number of metallic and metalloid elements, but also because of the diversity of available oxidation states, the use of combinations of different metals, the ability to include a plethora of organic moieties, and so on. The appearance of new macromolecules containing metal and metal-like elements has been enormous since the early 1950s, with the number increasing explosively since the early 1990s. These new macromolecules represent marriages among many disciplines, including chemistry, biochemistry, materials science, engineering, biomedical science, and physics. These materials also form bridges between ceramics, organic, inorganic, natural and synthetic, alloys, and metallic materials. As a result, new materials with specially designated properties have been made as composites, single- and multiple-site catalysts, biologically active/inert materials, smart materials, nanomaterials, and materials with superior conducting, nonlinear optical, tensile strength, flame retardant, chemical inertness, superior solvent resistance, thermal stability, solvent resistant, and other properties.

There also exist a variety of syntheses, stabilities, and characteristics, which are unique to each particular material. Further, macromolecules containing metal and metal-like elements can be produced in a variety of geometries, including linear, two-dimensional, three-dimensional, dendritic, and star arrays.

In this book series, macromolecules containing metal and metal-like elements are defined as large structures where the metal and metalloid atoms are (largely) covalently bonded into the macromolecular network within or pendant to the polymer backbone.

This includes various coordination polymers where combinations of ionic, sigma-, and pi-bonding interactions are present. Organometallic macromolecules are materials that contain both organic and metal components. For the purposes of this series, we define metal-like elements to include both the metalloids as well as materials that are metal-like in at least one important physical characteristic such as electrical conductance. Thus the term includes macromolecules containing boron, silicon, germanium, arsenic, and antimony as well as materials such as poly(sulfur nitride), conducting carbon nanotubes, polyphosphazenes, and polyacetylenes.

The metal and metalloid-containing macromolecules that are covered in this series will be essential materials for the twenty-first century. The first volume is an overview of the discovery and development of these substances. Succeeding volumes will focus on thematic reviews of areas included within the scope of metallic and metalloid-containing macromolecules.

Alaa S. Abd-El-Aziz  
Charles E. Carraher Jr.  
Charles U. Pittman Jr.  
Martel Zeldin

---

## CHAPTER 1

# The State of the Art in Boron Polymer Chemistry

**Manoj K. Kolel-Veetil and Teddy M. Keller**

*Advanced Materials Section, Materials Chemistry Branch, Chemistry Division, Naval Research Laboratory, Washington, DC 20375*

### CONTENTS

I. INTRODUCTION	2
A. A Brief Historical Perspective on Boron and Its Polymers	2
II. RECENT ADVANCES IN BORON-CONTAINING POLYMERS	8
A. Polymers Containing Boron Atoms in the Backbone or in Pendent Groups	8
i. $\pi$ -Conjugated Organoboron Polymers Used in Optical and Sensing Applications	8
a. Formed by the Hydroboration Route	9
b. Formed by Other Synthetic Routes	11
ii. Boron Polymers Containing P, Si, or Organometallic Units	15
a. Boron Polymers Containing P Atoms	15
b. Silicon-Containing Boron Polymers	17
c. Boron Polymers Containing Organometallic Moieties	17
iii. Organoboron Polymers Used as Catalysts in Organic Transformations	22
a. Boron Ligands/Polymers Used in Olefin Polymerization Reactions	22
b. Organoboron Polymers Used in Other Organic Transformations	29

*Macromolecules Containing Metal and Metal-Like Elements,  
Volume 8: Boron-Containing Polymers*, edited by Alaa S. Abd-El-Aziz,  
Charles E. Carraher Jr., Charles U. Pittman Jr., and Martel Zeldin.  
Copyright © 2007 John Wiley & Sons, Inc.

iv. Organoboron Polymers that Function as Flame-Retardant Materials	31
B. Polymers Containing Boron Ring Systems in the Backbone or in Pendent Groups	33
i. Organoboron Polymers that Contain Borazine or 9-BBN with Utility in the Production of High-Performance Fibers	34
a. SiC-Producing Borazine Polymer Systems	34
b. Si/B/C/N-Producing Systems	36
ii. Organoboron Polymers that Contain Boroxine or Triphosphatriborin Ring Systems	37
iii. Organoboron Polymers that Contain Polypyrazolylborate or Pyrazabole Ring Systems	37
iv. Organoboron Polymers that Contain Other Boron Ring Systems	38
C. Polymers Containing Boron Clusters in the Backbone or in Pendent Groups	38
i. Monomeric and Polymeric Organic Analogs of Boron Cluster Systems	38
ii. Poly(carboranylenesiloxanes) and Related Polymers	42
iii. Conducting Polymers Containing Carborane Clusters	52
iv. Carborane Polymers in Medicine	54
v. Carborane Polymers Used in the Production of High-Performance Fibers	57
vi. Miscellaneous Carborane Polymers	60
a. Carborane Polymers of Polyetherketones	60
b. Carborane Polymers for Use in Catalytic Reactions	61
vii. Carborane Supramolecular Chemistry	63
III. SUMMARY	71
IV. REFERENCES	71

## I. INTRODUCTION

### A. A Brief Historical Perspective on Boron and Its Polymers

Boron (*Buraq* in Arabic/*Burah* in Persian, which is the word for “white,” the color being attributed to borax (sodium tetraborate,  $\text{Na}_2\text{B}_4\text{O}_7 \cdot 10\text{H}_2\text{O}$ )) was discovered in 1808 independently by the British Chemist, Sir Humphry Davy, and two French chemists, Joseph Louis Gay-Lussac and Loius Jacques Thenard.<sup>1</sup> They isolated boron in 50% purity by the reduction of boric acid with sodium or magnesium. The Swedish chemist Jons Jakob Berzilius identified boron as an *element* in 1824. The first pure sample of boron was produced by the American chemist William Weintraub in 1909. Boron does not appear in nature in elemental form, but is found in its compounded

forms of borax, boric acid, colemanite, kernite, ulexite, and borates. In ancient times, compounds of borax ores known as tincal were exported from Tibet. Historically, boron is known to have been used for refining gold and silver in Arabia, for ceramic glazes in China, and for embalming in Egypt. Egyptians are known to have used the salt natron, which contains borates along with other common salts such as sodium bicarbonate, and sodium chloride in the mummification process. Marco Polo is believed to have brought natron to Italy where it was used by the artisans of the time.<sup>2</sup>

The United States and Turkey are the world's largest producers of boron.<sup>1</sup> Economically important sources are from the ores rasorite (kernite) and tincal, which are both found in the Mojave Desert of California, with borax being the most important source there. The famous "20-Mule-Team Borax," now a part of chemistry folklore, originates from the time when teams of 20 mules used to haul colemanite from Furnace Creek in Death Valley 166 miles south to Mojave. Elemental boron in its impure form can be obtained by the reduction of the oxide  $B_2O_3$  by magnesium, and in the pure form by the reduction of  $BCl_3$  by hydrogen on hot filaments.<sup>1</sup>

Boron with an atomic number of 5 is electron deficient, possessing a vacant p orbital (one of the 2p orbitals) making it a good electrophile. In terms of hybridization of atomic orbitals, boron has three  $sp^2$  hybridized orbitals pointing to the vertices of an equilateral triangle with its vacant p orbital positioned perpendicular to the plane of the equilateral triangle containing the  $sp^2$  orbitals. Thus, compounds of boron often behave as Lewis acids, readily bonding with electron-rich substances to compensate for its electron deficiency. Boron, on reaction with hydrogen, is known to form clusters of borohydrides called boranes.<sup>3</sup> Borane clusters, wherein a few of the boron atoms have been substituted by carbon atoms, yield a class of compounds known as carboranes. Boron also exists in "inorganic benzene-like" ring systems such as borazine, boroxine, and triphosphatriborin with nitrogen, oxygen, and phosphorus, respectively. The element boron exists in nature in high abundance both as boron 10 and boron 11 isotopes, with the nucleus of the latter possessing one additional neutron.<sup>2</sup> Boron 10 nucleus is the only *light* element that is capable of binding a slow neutron (or thermal neutron) to yield an excited boron-11 nucleus.<sup>2</sup>

The first reports on the formation of boron polymers were from Alfred Stock in the 1920s on the generation of a boron hydride polymer during his pioneering studies on boron hydride (borane) chemistry.<sup>4</sup> He discovered that fairly complicated compounds analogous to hydrocarbons could be built up from boron and its hydrides. Following Stock's work, Herbert Schlesinger and Anton Burg raised the chemistry of boron hydrides to new heights.<sup>5</sup> Based on the aminoborane adducts ( $R_3N \cdot B_2H_5$ ), with electron deficient bonds (or B—H—B three-centered bonds), obtained from amines such as  $NH_3$  or  $NHMe_2$  and diborane, Burg and co-workers explored the chemistry of similar diborane adducts with phosphine. Phosphine and diborane were found to yield the trimer  $[(CH_3)_2PBH_2]_3$  (**1**) (Fig. 1), which was discovered to be stable when heated to 400°C, with little decomposition, and to reduction by sodium in liquid ammonia.<sup>6</sup> This result, originating from a project sponsored by the Office of Naval Research (ONR), was a serendipitous one, as the initial intent was to make highly water-reactive boron hydride derivatives that might be used to propel underwater torpedos much faster. From then on, ONR extensively supported the development

of stable rubbers containing B—H bonds. Out of such efforts, the carboranosiloxane rubbers, renowned under the tradename DEXSIL, was engineered into existence by Heying and Schroeder at the Olin Laboratories in New Haven, Connecticut.<sup>7</sup> Burg and co-workers discovered that when the  $(\text{CH}_3)_2\text{PBH}_2$  unit was made in the presence of a slight excess of base, a long open-chain compound with as many as 300 repeating units was formed. In anticipation of their high-temperature stability and flame retardancy, the exploration of polyphosphinoboranes, materials based on skeletons of alternating phosphorus and boron atoms, was undertaken in the 1950s and 1960s.<sup>8</sup> However, these pioneering forays could only produce products with low yields and low molecular weights.<sup>9</sup>

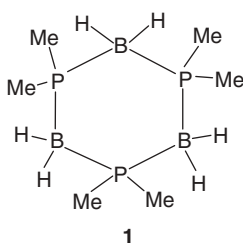


**Figure 1** The triphosphatriborin cyclic product  $[(\text{CH}_3)_2\text{PBH}_2]_3$  (**1**) obtained from  $\text{PMe}_3$  and  $\text{B}_2\text{H}_6$ . (Adapted from ref. 6.)

In their search for thermally stable polymers, the team of Schroeder and Heying at Olin Laboratories synthesized the first polymer (**2**) (Fig. 2) with P—O—P linkages containing the open boron cluster decaborane within the chain architecture (with a molecular weight of ca. 27,000) by the triethylamine-catalyzed condensation reaction between bis(chlorodiphenylphosphine)decaborane and bis(hydroxydiphenylphosphine)decaborane.<sup>10</sup> The selection of boron as the primary element was based both on bond-strength considerations (after Burg's results) and its ability to form appropriate cluster compounds. Simultaneously, they synthesized a P—N=P (phosponitrile) bonded decaborane polymer by the reaction of two difunctional monomers, a diphosphine and a diazide compound derived from diborane. Both of these thermally stable polymers were observed to flow during cross-linking through their dicarborane units. However, these materials were found to be unsuitable for use as molding compounds. Subsequently, in the interest of making elastomeric high-temperature rubbers, the Olin team focused its efforts on the synthesis of silylcarborane systems involving the icosahedral carboranes, *o*-, *m*-, and *p*-carborane.

In Olin's attempts to derivatize dilithiated products of *o*-carborane with chlorosilanes for further reaction with ammonia, it was observed that cyclic compounds, instead of polymers, were produced by the interaction of the substituents on the adjacent carbon atoms in the *o*-carborane units.<sup>11</sup> However, when a linear dimethoxy intermediate of *m*-carborane was reacted as an equimolar mixture with dichlorosilane in the presence of the catalyst  $\text{FeCl}_3$ , the quantitative evolution of  $\text{CH}_3\text{Cl}$  was observed

producing a crystalline polymer, which Olin named as DEXSIL 200 (SiB-2) (**3**) (Fig. 2); (M.P. = 151°C).<sup>12</sup> Since the number of repeating units in these polymers was low (5–10 units), some siloxyl moieties with pendant 1-vinyl-*o*-carboranyl groups were introduced in these polymers to improve their curing characteristics, resulting in DEXSIL 201 (**4**) (Fig. 2).<sup>13</sup> DEXSIL 201, upon curing, was found to have a tensile strength of 100 to 150 psi and an elongation of 120 to 250%, both of which were improvable upon addition of selected fillers.<sup>14</sup> Subsequently, it was discovered that carborane polymers (**5**) (Fig. 2) containing tin bridges were amenable to synthesis with higher molecular weights than **3** or **4**. These polymers (with a M.P. of 250–255°C) were produced by the reaction of (C<sub>6</sub>H<sub>5</sub>)<sub>2</sub>SnCl<sub>2</sub> with *m*-B<sub>10</sub>H<sub>10</sub>C<sub>2</sub>Li<sub>2</sub> and contained up to 30 repeating units when formed in Decalin.<sup>15</sup> Continuing its quest for high-temperature polymers, the Olin team attempted the inclusion of *p*-carborane units in these polymers. When the dilithio salt of *p*-carborane was treated with diphenyltin chloride, the polymers were observed to form with an average chain length of only 11 repeating units melting in the 300–400°C range.<sup>16</sup>

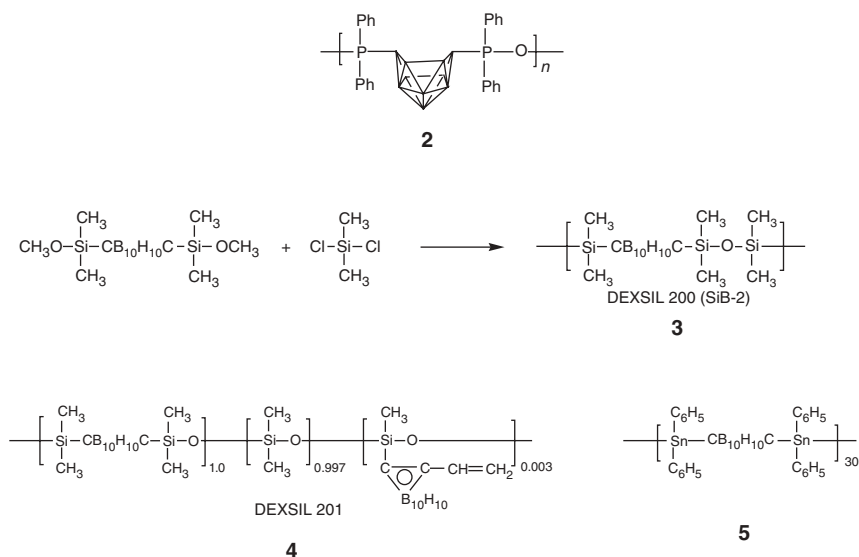


**Figure 2** Schematic representations of the Olin polymers: **2** (with —P—O—P— linkages), **3** and **4** (DEXSIL carborane polymers), and **5** (carborane polymers with tin bridges). (Adapted from ref. 7.)

While the Olin efforts on the production of high-temperature polymers were centered mainly on FeCl<sub>3</sub>-catalyzed condensation reactions, subsequent efforts from Union Carbide, Inc. utilized an aminosilane route and a ureidosilane route (Fig. 3) to synthesize carboranylenesiloxane polymers of high molecular weights. Using the former route, the polymer was produced by a condensation reaction between a carborane-disilanol and bis(dimethylamino)dimethylsilane, during which an expulsion of a

dimethylamine by-product occurred.<sup>17</sup> In the latter route, the bis(dimethylamino) dimethylsilane reagent was replaced with a bisureidosilane monomer to yield phenyl urea as the by-product during the polymerization.<sup>18</sup> The aminosilane reaction had the advantage that it did not require a catalyst and was performable between  $-10$  and  $25^{\circ}\text{C}$ . However, the molecular weights of the polymers synthesized by this route seldom exceeded 20,000. The low molecular weights were attributed to the scission of the backbone of the polymer by the dimethylamine by-product. The aminosilane route was abandoned and the ureidosilane route was seriously pursued. In the initial trials of the reaction, where the bisureidosilane monomers were prepared and utilized *in situ*, the molecular weights of the resulting polymers were found to be quite low. At the high polymerization temperature of  $160$ – $170^{\circ}\text{C}$ , the carboranedisilanol underwent self-condensation, thereby causing the molecular weights of the polymers to drop. This self-condensation problem was circumvented by the development of a low-temperature, solution polycondensation reaction, that included the slow addition of the solid carboranedisilanol monomer into a solution of the bisureidosilane.<sup>19</sup> The molecular weights of the polymers obtained by this modified route were as high as 200,000. Subsequently, the synthesis of ultra-high molecular weight (molecular weight of several millions) carboranylenesiloxane polymers was achieved by the Union Carbide team by a modification of the low temperature ureidosilane procedure.<sup>20</sup>

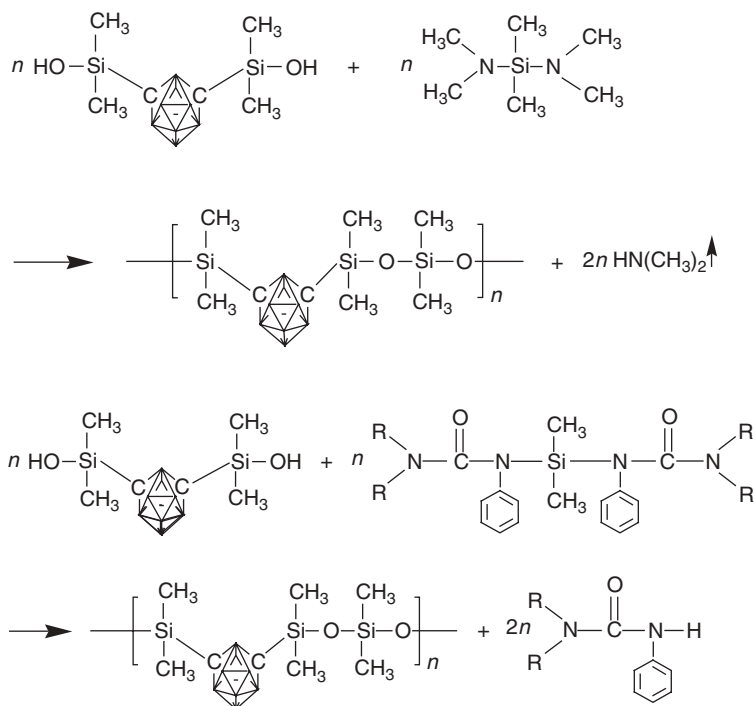


**Figure 3** Reaction schemes for the aminosilane (top) and the ureidosilane (bottom) routes for the synthesis of carboranylenesiloxane polymers. (Adapted from ref. 23.)

The Union Carbide team also utilized the dilithiocarborane chemistry to produce carboranylenesiloxane polymers by the metal–halogen interchange reaction (Fig. 4) between dilithiocarboranes and dichlorosiloxanes.<sup>21</sup> Polymers with molecular weights up to 52,000 were synthesized by this procedure.

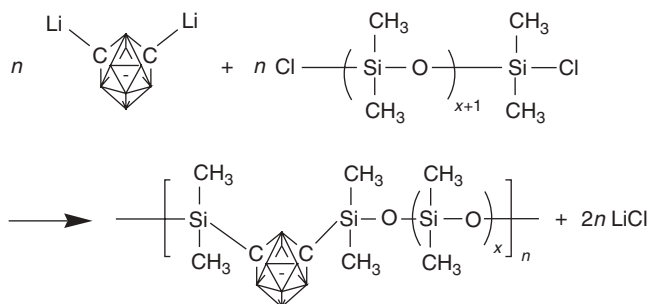


**Figure 4** Reaction scheme for the metal–halogen interchange reaction between dilithiocarboranes and dichlorosiloxanes for the synthesis of carboranylenesiloxane polymers. (Adapted from ref. 23.)

In addition to the icosahedral carboranes, the incorporation of smaller carboranes such as  $\text{C}_2\text{B}_5\text{H}_7$  and/or  $\text{C}_2\text{B}_8\text{H}_{10}$  in carboranylenesiloxane polymers was also achieved by the utilization of their dilithio, diethoxysilyl and dichlorosilyl derivatives in  $\text{FeCl}_3$ -catalyzed polycondensation reactions. A series of homo- and co-polymers were synthesized by this procedure. However, the molecular weights of these polymers were observed to be low, with the highest being 12,500.<sup>22</sup> A more descriptive history of the Olin and the Union Carbide works on carboranylenesiloxane polymers is available in the excellent book on high-temperature siloxane elastomers by Dvornic and Lenz.<sup>23</sup>

During the time of the Olin reports, the first examples of oligomeric boron-bridged (1-pyrazolyl)borate systems appeared from the laboratory of Trofimenko at DuPont Chemicals.<sup>24</sup> He reported the synthesis of poly(1-pyrazolyl)borates (**6**) (Fig. 5) from the reactions of alkali metal borohydrides with the pyrazole ligand. The (1-pyrazolyl)borate ligand was obtained from two pyrazole units when bridged by a  $\text{BR}_2$  unit on one side and by a metal or onium ion on the other. Even though reports

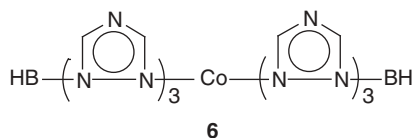


**Figure 5** The first reported poly(1-pyrazolyl)borate (**6**) containing a cobalt bridge. (Adapted from ref. 24.)

of the syntheses of a number of pyrazolyl borate and pyrazabole (a ligand obtained by the bridging of two pyrazole units by two  $BR_2$  units) complexes have appeared in the literature since Trofimenko's account, there are relatively few examples of polymers containing these ligands.

Since these early studies on poly(phosphinoboranes), poly(carboranylensiloxanes) and poly(1-pyrazolyl)borates, the polymer chemistry of boron has burgeoned into an eclectic field that now encompasses areas such as polymeric precursors for high-performance composites and fibers, supramolecular nanomaterials, polymer-supported catalysts for polymeric and organic transformations, therapeutic agents in medicine, optical polymers, and so forth. In a rudimentary sense, these developments in the polymer chemistry of boron may be considered to have been driven by two fundamental characteristics of boron: first, its electronic characteristics; that of its  $\pi$ -delocalizing ability due to the presence of an empty p orbital, and second, its nuclear characteristics; that of its neutron capturing ability due to its natural existence in the form of two isotopes. In addition, a third characteristic of boron, that of its ability to react at high temperatures with oxygen to form a protective intumescent  $B_2O_3$  char, has also contributed to its utilization in high-performance polymers, composites, and fibers, besides other applications.<sup>25</sup>

This review summarizes the significant developments in the area of boron-containing polymers during the past 10 years. The review is divided into three sections, each of which covers a unique group of boron-containing polymers. The first section covers polymers in which boron exists as a backbone element (rather than as part of a ring or a cluster system) or in a pendent group in the polymer. The second section covers polymers wherein boron is present as a part of a ring system. The third section includes polymers where boron exists as a part of a cluster. Within each section, polymers have been grouped in terms of their applications or some other common characteristics such as the presence of a common element (e.g., P, Si, etc.), etc. When a boron polymer deserves inclusion in more than one section, it has been placed in the most appropriate section as deemed by the authors.

## II. RECENT ADVANCES IN BORON-CONTAINING POLYMERS

### A. Polymers Containing Boron Atoms in the Backbone or in Pendent Groups

#### *i. $\pi$ -Conjugated Organoboron Polymers Used in Optical and Sensing Applications*

The electron delocalizing capability of a boron atom arising from its empty p-orbital positions it as an ideal candidate for incorporation in conjugated polymers for use in optical and sensing applications. The majority of the examples of boron-atom-containing conjugated polymers have been synthesized via the hydroboration reaction. However, other synthetic procedures have also been utilized.

*a. Formed by the Hydroboration Route*

The ubiquitous hydroboration reaction (Fig. 6),<sup>26</sup> which involves the addition of a B—H bond across an organic unsaturation, has been used extensively by researchers for the production of various organoboron polymers, especially for optical [light-emitting diodes (LED), energy storage systems (batteries), nonlinear optical (NLO), etc.] and sensing applications. Chujo and co-workers have utilized this reaction strategy for constructing an impressive library of fluorescent polymers (7) (Fig. 7).<sup>27</sup> A detailed account of their research is present in Chapter 3 of this book. On boron incorporation, the optical and sensing properties of these polymers benefit from the extension of their  $\pi$ -conjugation through the utilization of the reactivity of the vacant p-orbital of the boron atom.<sup>27</sup>

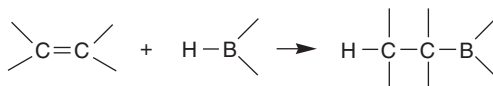


**Figure 6** The hydroboration reaction.

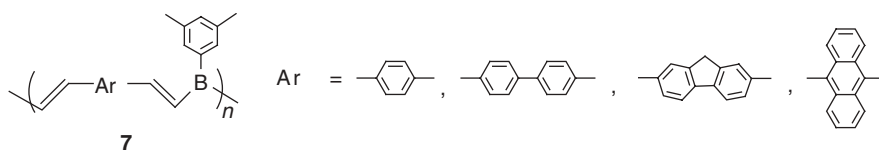


**Figure 7** Some  $\pi$ -conjugated fluorescent organoboron polymers (7) synthesized by the hydroboration polymerization reaction. (Adapted from ref. 27.)

In one of their notable examples, the hydroboration polymerization of low molecular weight allyl-telechelic polyisobutylene with tripropylborane (trip = 2,4,6-triisopropylphenyl) was found to yield air-stable organoboron segmented block copolymers. These boron main-chain polymers (8) (Fig. 8), unlike the general ones, were stable to air. The stability was due to the steric hindrance of the bulky tripropyl groups preventing oxygen attack of the borons.<sup>28</sup>

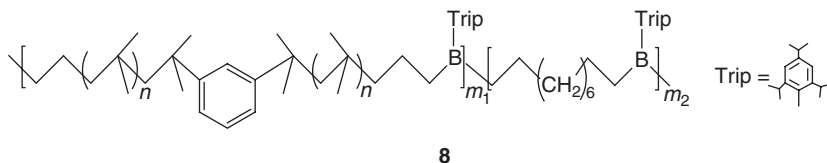


**Figure 8** The air-stable  $\pi$ -conjugated organoboron segmented block copolymer (8) obtained by the hydroboration polymerization of allyl-telechelic polyisobutylene, 1,9-decadiene, and tripropylborane. (Adapted from ref. 28.)

In addition to hydroboration, haloboration and phenylboration have also been used in the synthesis of  $\pi$ -conjugated organoboron polymers (**9**)<sup>29</sup> (Fig. 9) and polymers containing B—N bonds.<sup>30</sup>

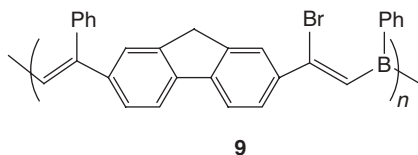


**Figure 9** The  $\pi$ -conjugated organoboron polymer (**9**) produced by haloboration-phenylboration polymerization between 2,7-diethynylfluorene and  $\text{Ph}_2\text{BBr}$ . (Adapted from ref. 29.)

The synthesis of unsaturated polymers (**10**) (Fig. 10) containing boron atoms and thiophene units in the backbone was reported by Corriu and Douglas.<sup>31</sup> Polythiophenes, an important class of conjugated electroactive polymers, are known to have the potential for such applications as energy storage, electrochromic devices and electrochemical sensors.<sup>32</sup> The efficacy of polythiophenes in these applications depends on the nature and extent of their doping, usually with electron acceptors. The Corriu/Douglas polymers, possessing both electron-donor (sulfur) and electron-acceptor (boron) sites, were expected to show interesting properties, since the boron sites with vacant 2p orbitals were available to act as *in situ* electron-acceptor dopants.

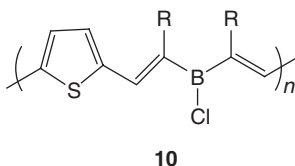


**Figure 10** The  $\pi$ -conjugated polythiophene (**10**) containing thiophene units and boron atoms in its backbone. (Adapted from ref. 31.)

In the area of ion sensing, cation recognition by electrodes containing functionalized redox-active polymers has been an area of considerable interest. Fabre and co-workers have reported the development of a boronate-functionalized polypyrrole as a fluoride anion-responsive electroactive polymer film. The electropolymerizable polypyrrole precursor (**11**) (Fig. 11) was synthesized by the hydroboration reaction of 1-(phenylsulfonyl)-3-vinylpyrrole with diisopinocampheylborane followed by treatment with pinacol and the deprotection of the pyrrole ring.<sup>33</sup> The same methodology was utilized for the production of several electropolymerizable aromatic compounds (of pyrrole (**12**) (Fig. 11), thiophene (**13** and **14**) (Fig. 11), and aniline) bearing boronic acid and boronate substituents as precursors of fluoride- and/or chloride-responsive conjugated polymer.<sup>34</sup>

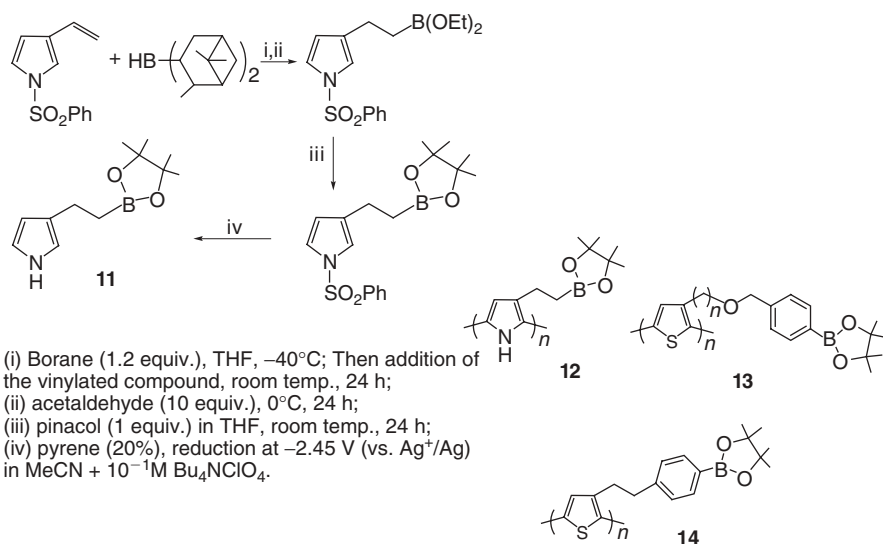


**Figure 11** The reaction scheme for the polypyrrole precursor (**11**) synthesis (left; top) with reagents and conditions (left; bottom). Representative pyrrole (**12**) and thiophene (**13** and **14**)-based redox-active polypyrroles. (Adapted from refs. 32 and 33.)

### b. Formed by Other Synthetic Routes

Grignard chemistry was used as an alternative to hydroboration reaction by the Chujo team in its search for new n-type conjugated polymers for utilization in polymer energy storage systems. By this route, the syntheses of  $\pi$ -conjugated poly(*p*-phenyleneboranes) (**15**)<sup>35</sup> (Fig. 12) and poly(ethynylene-phenylene-ethynylene-borane)s were reported.<sup>36</sup>

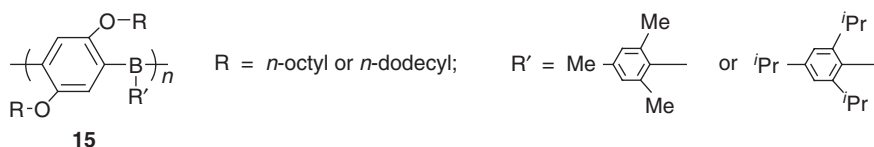


**Figure 12** Some  $\pi$ -conjugated poly(*p*-phenylene-boranes) (**15**). (Adapted from ref. 35.)

NLO materials (**16** and **17**) (Fig. 13) have been obtained from polyurethanes by the incorporation of sidechains with boron chromophores.<sup>37</sup> The dihydroxy ligand of an azobenzene ligand containing a dimesityl boron acceptor was reacted in a polycondensation fashion with the diisocyanate groups of the polyurethanes to yield the desired polymers. Halogen displacement and transmetallation reactions have been utilized in the development of extended  $\pi$ -conjugated systems of tri-9-anthrylborane with dendritic structures.<sup>38</sup> In one (**18**) (Fig. 14) of the novel compounds, three identical

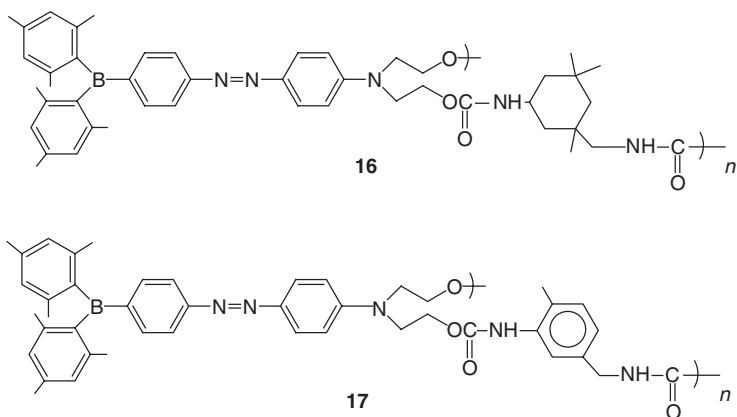


**Figure 13** Boron chromophore-containing polyurethanes (**16** and **17**) for NLO applications. (Adapted from ref. 37.)

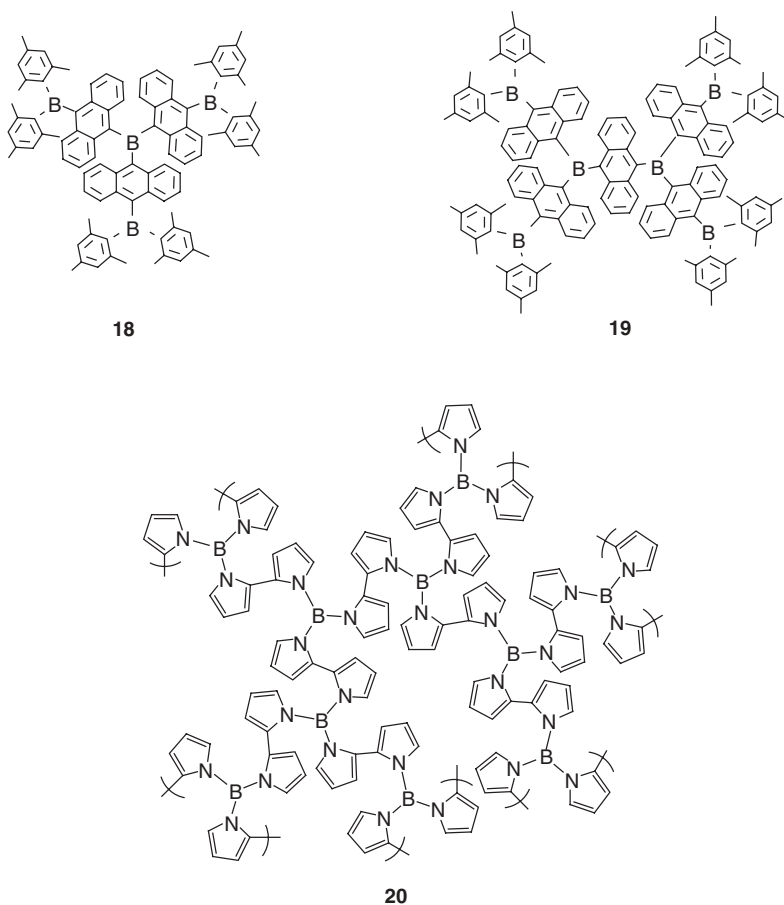


**Figure 14**  $\pi$ -Conjugated dendritic polymers (**18** and **19**) obtained from tri-9-anthrylborane. The branched conducting polymer **20** was obtained from tris(*N*-pyrrolyl)borane. (Adapted from refs. 38 and 39.)

$\pi$ -electron systems were introduced onto a planar boron atom, which made it possible to extend the lowest unoccupied molecular orbital (LUMO) over the three  $\pi$ -systems across the vacant p-orbital of boron. The generation of a similar  $\pi$ -extended conducting polymeric system (**20**) (Fig. 14) has been realized by the electrochemical oxidation in THF of tris(*N*-pyrrolyl)borane. The data from pendant group analysis and the number of electrons consumed during electropolymerization suggested the formation of a branched conducting polymer with boron as the diverging center. The conductivity of the polymer film was evaluated to be ca.  $7 \times 10^{-4} \text{ S cm}^{-1}$ .<sup>39</sup>

The synthesis of luminescent organoboron quinolate polymers (**21**) (Fig. 15) via a three-step procedure starting from a silylated polystyrene has been communicated. The synthesis was initiated by the highly selective borylation of poly(4-trimethylsilylstyrene) (PS-Si), followed by the replacement of the bromine substituents in poly(4-dibromoborylstyrene) (PS-BBr) with substituted thienyl groups (R = H, 3-hexyl, 5-hexyl). In the final step, the 8-hydroxyquinolato moiety was introduced. The hexyl-substituted polymers efficiently emitted light at 513–514 nm upon excitation at 395 nm.<sup>40</sup>

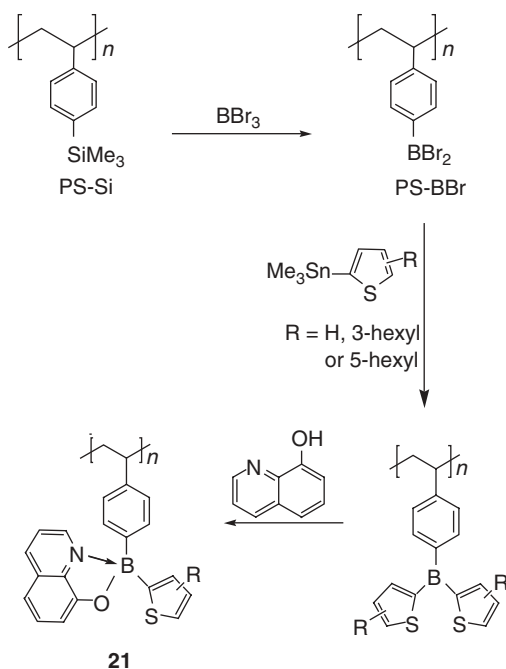


**Figure 15** Luminescent organoboron quinolate polymers (**21**) produced from silylated polystyrene. (Adapted from ref. 40.)

Several other organoboron polymers have been developed by various synthetic strategies and utilized to construct polymeric sensing systems for cations, dopamine, saccharides, and so on. Fabre and co-workers have reported the preparation of a conjugated trifluoroborate-substituted polythiophene system for sensing cations such as

$\text{Li}^+$ ,  $\text{Na}^+$ ,  $\text{K}^+$ , and  $\text{Bu}_4\text{N}^+$ . The monomer **22** (Fig. 16) used for the synthesis of the polymer was produced in one step from 3-thiopheneboronic acid by reacting it with potassium hydrogen difluoride. The electrochemical and UV-visible spectroscopic responses of the polymer were found to be dependent on the nature of the cation.<sup>41</sup>

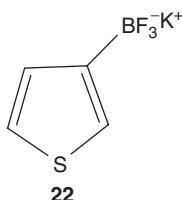


**Figure 16** Trifluoroborate-substituted thiophene monomer (**22**) used in the synthesis of a conjugated polythiophene system. (Adapted from ref. 41.)

A poly(aniline boronic acid)-based conductimetric sensor for dopamine consisting of an interdigitated microarray electrode coated with poly(aniline boronic acid) has also been developed by the Fabre team. The sensor was found to show a reversible chemoresistive response to dopamine without interference by ascorbic acid from their mixtures.<sup>42</sup>

Boronic acid-containing polyaniline has also been utilized in diabetes-related research. One such polymer (**23**) (Fig. 17) has been observed to exhibit a linear near-infrared optical response to saccharides.<sup>43</sup> The polymer was prepared by the copolymerization of aniline with 3-aminophenylboronic acid using 10 mM  $(\text{NH}_4)_2\text{S}_2\text{O}_8$  in 1 M HCl. The films were observed to undergo changes in the absorption spectra on addition of saccharides at pH 7.2.

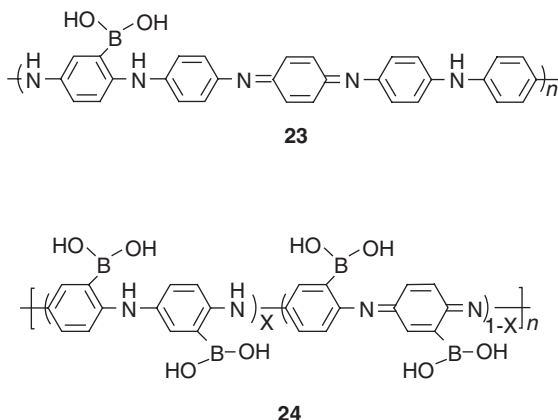


**Figure 17** Boronic acid-containing polyanilines (**23** and **24**) used in the detection of saccharides. (Adapted from refs. 43 and 44.)

Similar boronic acid-containing polyaniline-based potentiometric sensors (**24**) (Fig. 17) have been demonstrated to be effective for the nonenzymatic detection of glucose.<sup>44</sup> The studies on the selectivity of the polymer-bound boronic acid in its complexation reaction toward different sugars ( $\alpha$ -methyl-D-glucoside, D-glucose, and fructose) revealed that for D-glucose, in a pH 7.4 phosphate buffer saline, reversible responses were obtainable within the physiological relevant range of 4–6 mM.

## ii. Boron Polymers Containing P, Si, or Organometallic Units

### a. Boron Polymers Containing P Atoms

After Burg's and the Olin team's studies on phosphorus-containing boron polymers, new discoveries of boron polymers with phosphorus–boron bonds and an appreciable molecular weight (up to a  $M_w$  of 31,000) had to wait until 1999. Research by Manners and co-workers revealed that the phosphane–borane adduct  $\text{PhPH}_2\cdot\text{BH}_3$  undergoes dehydrocoupling in refluxing toluene to produce an off-white polymeric product poly(phenylphosphinoborane)  $[\text{PhPH-BH}_2]_n$  (**25**) (Fig. 18), when it was carried out (110°C, 14 h) in the presence of a 0.3 mol%  $[\text{Rh}(1,5\text{-cod})_2][\text{Otf}]$  catalyst.<sup>45</sup> This polymer, which could be considered an analog of polystyrene with phosphorus–boron backbone, was obtained as an air- and moisture-stable solid with an absolute weight average molecular weight ( $M_w$ ) of 5600. However, when the polymerization was achieved in the absence of a solvent by heating  $\text{PhPH}_2\cdot\text{BH}_3$  and one of the catalysts from Rh(I) [ $\{\text{Rh}(\mu\text{-Cl})(1,5\text{-cod})\}_2$ , anhydrous  $\text{RhCl}_3$  or  $\text{RhCl}_3$  hydrate (ca. 1 mol % Rh)] at slightly elevated temperatures (3 h at 90°C and 3 h at 130°C), a polymeric product with a higher molecular weight ( $M_w = 31,000$ ) was observed to have formed.

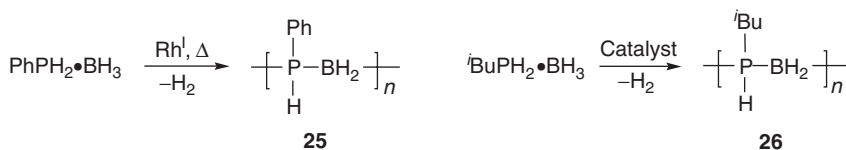


**Figure 18** Syntheses of poly(phenylphosphinoborane)  $[\text{PhPH-BH}_2]_n$  (**25**) and poly(isobutylphosphinoborane)  $[\text{}^i\text{-BuPH-BH}_2]_n$  (**26**) from their respective phosphane–borane adducts. (Adapted from ref. 45.)

In subsequent studies by the Manners team on the catalytic dehydrocoupling of alkyl-substituted phosphine–borane adduct  $\text{}^i\text{-BuPH}_2\cdot\text{BH}_3$ , that were performed under neat conditions at 120°C in the presence of  $[\text{Rh}(\mu\text{-Cl})(1,5\text{-cod})_2]$ , the phosphinoborane polymer poly(isobutylphosphinoborane)  $[\text{}^i\text{-BuPH-BH}_2]_n$  (**26**) (Fig. 18) was observed to form in 80% yield. When the polymers **25** and **26** were subjected to prolonged heating at elevated temperatures in the presence of a catalyst, insoluble but solvent-swallowable gels were obtained, presumably due to light interchain crosslinking through the P–B bonds.<sup>46</sup>

The transition metal-catalyzed synthetic methodology was further expanded by the Manners group to synthesize  $[(p\text{-}n\text{-BuC}_6\text{H}_4)\text{PH-BH}_2]_n$  (**27**) and  $[(p\text{-dodecylC}_6\text{H}_4)\text{PH-BH}_2]_n$  (**28**) (Fig. 19) via the rhodium-catalyzed dehydrocoupling procedure at elevated temperatures (ca. 90–130°C) of the corresponding phosphine–borane adducts.<sup>47</sup> Molecular-weight determinations by gel permeation chromatography (GPC) or light scattering methods revealed that the molecular-weight distributions of the two polymers were significantly broad. The irreproducibility of the molecular weights, owing to high viscosity and facile solidification of the reaction mixture, suggested the need for the development of improved catalysts that were sufficiently active to allow the formation of high molecular-weight polymers in solution.

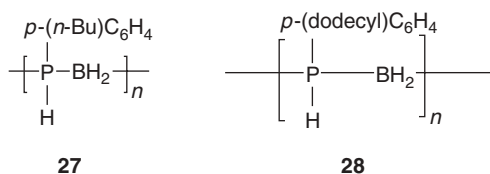


**Figure 19** Poly(phosphinoborane)s,  $[(p\text{-}n\text{-BuC}_6\text{H}_4)\text{PH-BH}_2]_n$  (**27**) and  $[(p\text{-dodecylC}_6\text{H}_4)\text{PH-BH}_2]_n$  (**28**). (Adapted from ref. 47.)

In an effort to understand the mechanism of these dehydrocoupling reactions, the Manners group undertook further studies of several phosphine–borane adducts. The studies revealed that the dehydrocoupling of phosphine–borane adducts,  $\text{Ph}_2\text{PH}\cdot\text{BH}_3$ , proceeded by a homogeneous mechanism even when the catalysts in question were in the  $\text{Rh}(0)$  state. However, analogous  $\text{Rh}$ -catalyzed dehydrocoupling of amine–borane adducts were discovered to proceed via a heterogeneous mechanism involving  $\text{Rh}(0)$  colloids.<sup>48</sup>

In a recent report, the same group has discussed the influence that the electronic nature of the substituents located on phosphorus in the phosphine–borane adducts might have on both the rate of dehydrocoupling and the polymer properties.<sup>49</sup>  $[\text{Rh}(\mu\text{-Cl})(1,5\text{-cod})_2]_2$ -catalyzed dehydrocoupling of the primary phosphine–borane adduct,  $\text{RPH}_2\cdot\text{BH}_3$  ( $\text{R} = p\text{-CF}_3\text{C}_6\text{H}_4$ ) (**29**) (Fig. 20) was observed to proceed at 60°C to yield high molecular-weight polyphosphinoborane polymer  $[\text{RPH-BH}_2]_n$

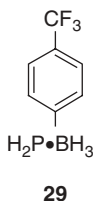


**Figure 20** The primary phosphine–borane adduct  $\text{RPH}_2\cdot\text{BH}_3$  (**29**) with the highly electron-withdrawing aromatic group  $\text{R} = p\text{-CF}_3\text{C}_6\text{H}_4$ . (Adapted from ref. 49.)

( $M_w = 56,170$ , PDI = 1.67). The electron-withdrawing nature of the fluorinated aryl substituents appeared to have had an important influence on the reactivity, as the dehydrocoupling process was observed to occur efficiently at the mildest temperatures observed with such polymerizations to date.<sup>49</sup>

### b. Silicon-Containing Boron Polymers

The most studied class of boron polymers containing boron–silicon bonds are the carboranylenesiloxane polymers. The history of these polymers was discussed at the beginning of this chapter. The more recent advances in this group of polymers and in silicon-containing borazine and boroxine polymers are discussed in later sections of this chapter. In this section, some remaining groups of silicon-containing boron polymers are discussed.

Sundar and Keller have reported the synthesis of linear boron–silicon–diacetylene polymers (**31**) (Fig. 21) using phenylboron dichloride (PBD) as the source for boron.<sup>50</sup> The compositions of the thermally stable boron–silicon–diacetylene copolymers **31a–d** are summarized in Figure 21. These polymers were observed to possess exceptional thermooxidative stabilities.

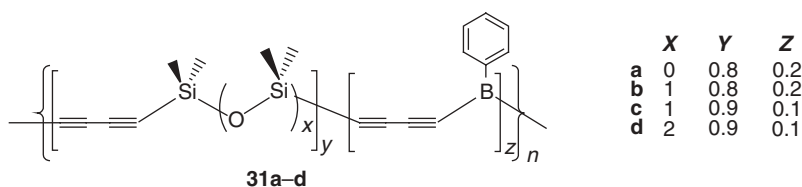


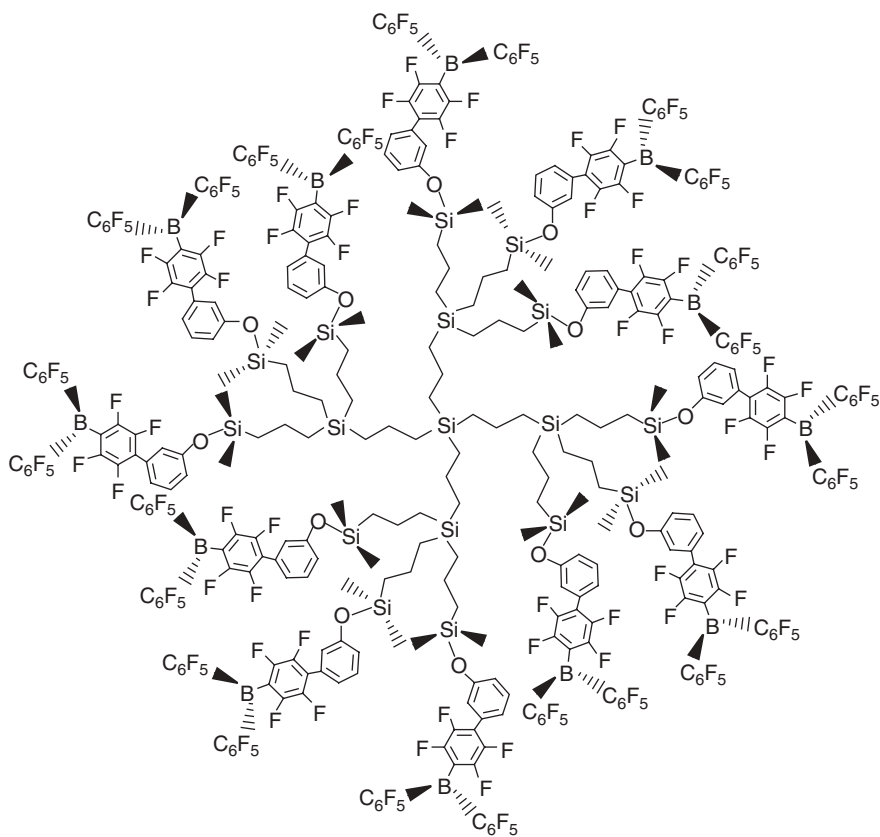
**Figure 21** The linear (boron–silicon–diacetylene) copolymers (**31a–d**) with their respective compositions. (Adapted from ref. 50.)

The synthesis of a variety of lithium ion conducting borosiloxane polymers have been reported.<sup>51</sup> The incorporation of the Lewis acidic boron and silicon into the polymer backbone was expected to facilitate their interaction with anions and thereby increase the  $T_+$  (transference numbers) of the resulting polymers.<sup>52</sup>

Carbosilane dendrimers capped with 4, 8, and 12 (**32**) (Fig. 22) perfluoroarylborane Lewis acids have been synthesized for use as Lewis-acid catalysts for the hydrosilation of acetophenone.<sup>53</sup> The dendrimers were found to be rather effective, exhibiting only slightly inferior activities in comparison to  $B(C_6F_5)_3$ .

### c. Boron Polymers Containing Organometallic Moieties

The presence of metals in coordination polymers has been hypothesized to produce interesting electrical, magnetic and optical characteristics as a result of electron delocalization.<sup>54</sup> When an atom such as boron is incorporated in metal-containing coordination polymers, it can conceivably expand the polymer's  $\pi$ -conjugation further by virtue of its empty p-orbital. This property of boron makes it an exciting atom for synthetic manipulations of coordination/organometallic polymers.



32

**Figure 22** Carbosilane dendrimeric Lewis-acid catalyst (**32**) capped with perfluoroarylborane Lewis acids. (Adapted from ref. 53.)

The chemistry of ferrocene compounds appears to have benefited most from the inclusion of boron atoms. Wagner and coworkers have developed coordination polymers with charge-transfer properties from reactions of diborylated ferrocenes (**33**) (Fig. 23) with 4,4'-bipyridine (bipy) or 1,2-bis(4-pyridyl)ethane (pyetpy).<sup>55</sup> The polymer  $[\mathbf{33}\cdot\text{bipy}]_n$  or  $[\mathbf{33}\cdot\text{pyetpy}]_n$  was prepared by layering a one equivalent solution of the corresponding pyridine in  $\text{CH}_2\text{Cl}_2$  over a diborylated ferrocene solution in  $\text{CHCl}_3$ . In the solid state, the polymer  $[\mathbf{33}\cdot\text{bipy}]_n$  exhibited an intense blue to purple color indicative of the charge-transfer reaction between the electron-rich ferrocene moieties and the viologen-like  $\text{R}_3\text{B}\text{-bipy}\text{-R}_3\text{B}$  units. In the  $[\mathbf{33}\cdot\text{pyetpy}]_n$  polymer, the disruption of the extended  $\pi$ -system due to the insertion of an ethylene spacer into the central C—C bond of the bipy ligand was observed to destroy its viologen-like electron accepting ability. As a consequence, it was found to lose its intense color, thereby rendering it yellow in appearance. The solid  $[\mathbf{33}\cdot\text{bipy}]_n$  polymer

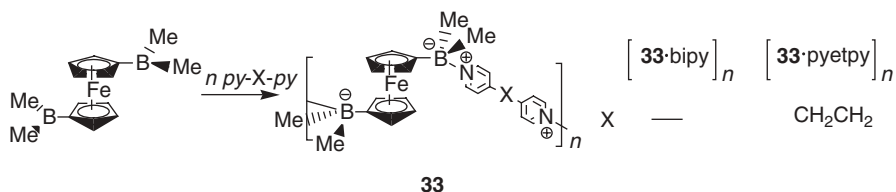


**Figure 23** Charge transfer coordination polymers (**33**) obtained from diborylated ferrocenes with 4,4'-bipyridine (bipy) or 1,2-bis(4-pyridyl)ethane (pyetpy) bridges. (Adapted from ref. 55.)

was thermally stable to 240°C under He. However, in toluene, the polymerization was observed to be reversible at 85°C.

Similar polymers (**34**) (Fig. 24) of diborylated ferrocenes linked by pyrazine units were developed that had an unusual dark-green appearance indicative of charge-transfer interactions between the iron centers and the electron-poor pyrazine adduct bridges.<sup>56</sup>

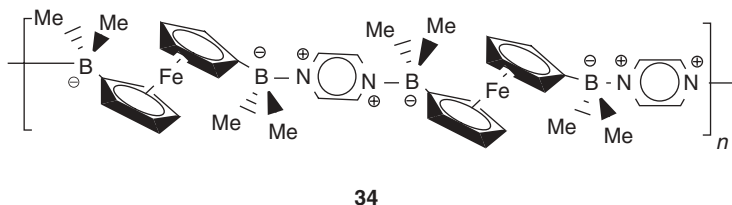


**Figure 24** Charge-transfer coordination polymer (**34**) of diborylated ferrocenes with pyrazine bridges. (Adapted from ref. 56.)

The ring-opening polymerization (ROP) strategy was utilized by Manners and co-workers for the polymerization of boron-bridged [1]ferrocenophanes.<sup>57</sup> The monomers, **35a** ( $R = R' = \text{SiMe}_3$ ), **35b** ( $R = \text{SiMe}_3$ ,  $R' = t\text{-Bu}$ ) and **35c** ( $R = R' = i\text{-Pr}$ ) (Fig. 25), were thermally polymerized in sealed and evacuated Pyrex tubes in the 180–200°C range. While the poly(ferrocenylborane)s **36a** and **36b** were found to be virtually insoluble in common organic solvents, the **35c**-derived low molecular-weight polymer (**36c**) had solubilities in polar organic solvents such as toluene, THF,  $\text{CH}_2\text{Cl}_2$ , and  $\text{CHCl}_3$ . The ROP enthalpy for **35a** (ca. 95  $\text{kJ mol}^{-1}$ ) was found to be lower than expected and was attributed to the presence of bulky substituents at boron.<sup>58</sup> The Manners team further reported the selective ring-opening reactions of [1]ferrocenophanes with boron halides resulting in the production of functionalized ferrocenylboranes and boron-containing oligo- and poly(ferrocene)s.<sup>59</sup> The transition metal-catalyzed ROP of sila[1]ferrocene in the presence of Si—H functionalized diferrocenylborane was also reported to yield the ferrocene polymer **37** (Fig. 26).

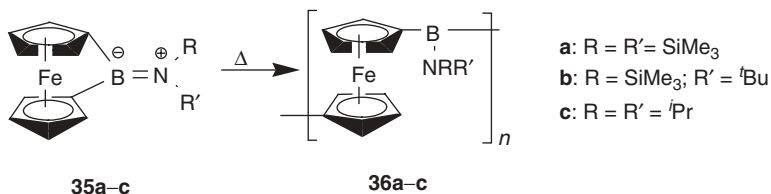


**Figure 25** The ring-opening polymerization of strained boron-bridged [1]ferrocenophanes (**35a–c**) to produce poly(ferrocenylboranes) (**36a–c**). (Adapted from ref. 57.)

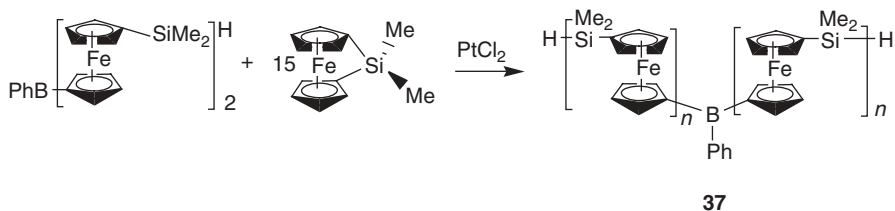


**Figure 26** The transition metal-catalyzed ROP of sila[1]ferrocene in the presence of Si—H functionalized diferrocenylborane to the ferrocene polymer **37**. (Adapted from ref. 59.)

While the boron-bridged [1]ferrocenophanes was observed to undergo polymerization via a transition metal-catalyzed ROP, the phosphorus(III)-bridged [1]ferrocenophanes were discovered to be resistant to a similar polymerization route, presumably due to the ligation of the catalyst by the phosphorus lone pair. However, when the phosphorus lone pair was protected through the formation of a borane adduct  $[(\eta\text{-C}_5\text{H}_4)\text{FeP}(\text{Ph})\text{BX}_3]$  (**38H** ( $X = \text{H}$ ) or **38Cl** ( $X = \text{Cl}$ )) (Fig. 27), the ROP was observed to proceed either thermally or in the presence of a transition metal catalyst to yield insoluble polymeric products,  $[(\eta\text{-C}_5\text{H}_4)\text{FeP}(\text{Ph})\text{BX}_3]_n$  (**39H** ( $X = \text{H}$ ) or **39Cl** ( $X = \text{Cl}$ )) (Fig. 27).<sup>60</sup> This approach has the advantage that subsequent deborylation of the poly(ferrocenylphosphine)borane adduct can afford a route to the production of poly(ferrocenylphosphines) with controlled molecular weights. Such materials have potential applications as catalytic materials based on the reactivity of the phosphorus lone pair.<sup>61</sup>

Jakle and Wagner have communicated the synthesis of bromo-substituted, boranediyl-bridged poly(ferrocenylene)s (**40**) (Fig. 28) by the reaction of  $\text{Fc}(\text{BBr}_2)_2$  with three equivalents of  $\text{HSiEt}_3$ . The polymer **40** was transformed into the corresponding mesityl-substituted polymer (**40Mes**) by treating its slurry in toluene with  $[\text{CuMes}]_n$  ( $n = 4, 5$ ).<sup>62</sup>

Ferrocene-bridged tris(1-pyrazolylborate) oligomeric systems have been synthesized by Wagner and co-workers.<sup>62</sup> The examples are described in more detail in the section on pyrazolylborate and pyrazabole polymers in this chapter.

In addition to the ferrocene-derived polymers, there have been reports of a few other metal-containing polymers with incorporated boron atoms. One such polymer

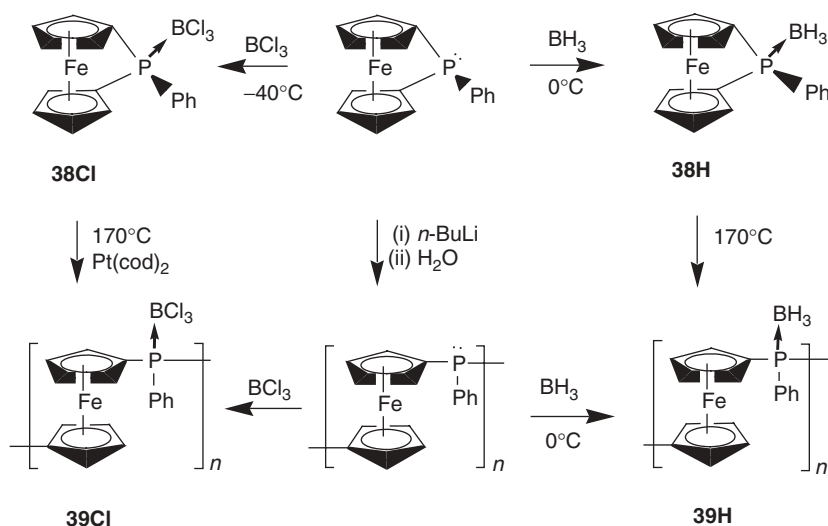


**Figure 27** The protection of the phosphorus lone pair during ROP of a phosphorus(III)-bridged [1]ferrocenophanes by  $\text{BCl}_3$  (**38Cl**) or  $\text{BH}_3$  (**38H**), leading to the production of the poly(ferrocenylphosphines) **39Cl** and **39H**, respectively. (Adapted from ref. 60.)

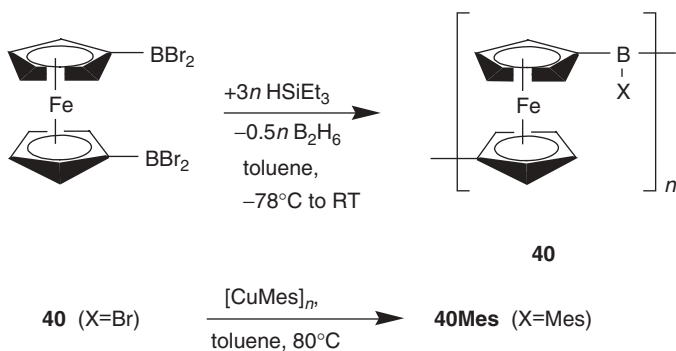


**Figure 28** Synthesis of bromo-substituted, boranediyl-bridged poly(ferrocenylene)s (**40**) from  $\text{Fc}(\text{BBr}_2)_2$ . (Adapted from ref. 62.)

is the  $\pi$ -conjugated organoboron polymer (**41**) (Fig. 29) containing ruthenium–phosphine moieties that was developed by Chujo and Lavastre by a hydroboration polymerization route.<sup>63</sup> Similar  $\pi$ -conjugated boron polymers (**42a** or **42b**) (Fig. 29) containing Pt or Pd in place of Ru in the polymer backbone have also been developed. The number-average molecular weight of the polymers was determined to be 9000 from gel permeation chromatographic analysis.<sup>63</sup>

Recently, Rauchfuss and co-workers have reported the synthesis of a one-dimensional  $[\text{PhB}(\text{CN})_3\text{Cu}(\text{PCy}_3)_2]$  polymer formed from the reaction between the anionic  $[\text{PhB}(\text{CN})_3]^-$  and  $[\text{Cu}(\text{PCy}_3)_2(\text{NCMe})_x]\text{PF}_6$ .<sup>64</sup>

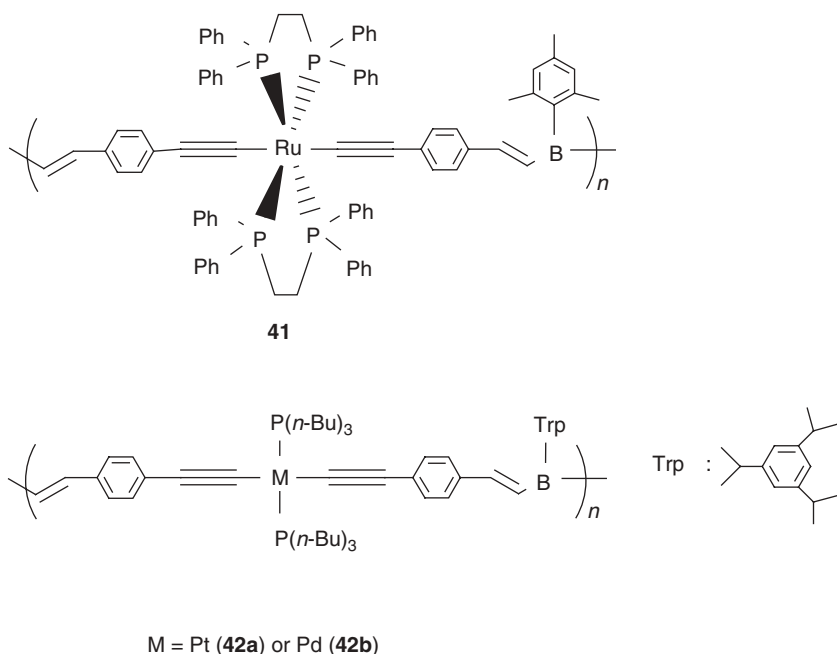


**Figure 29**  $\pi$ -Conjugated organoboron polymer containing phosphine ligands with Ru (**41**), Pt (**42a**), or Pd (**42b**) in the polymer backbone. (Adapted from refs. 62 and 63.)

### iii. Organoboron Polymers Used as Catalysts in Organic Transformations

#### a. Boron Ligands/Polymers Used in Olefin Polymerization Reactions

In recent times, boron-containing organic groups have found extensive use as protecting groups for functionalizing olefinic monomers for copolymerization with olefins in the Ziegler–Natta (Z-N) and other metal-catalyzed polymerization reactions. This methodology has been popularized especially by Chung and co-workers.<sup>65</sup> Among the boron ligands, boranes have been particularly effective due to their stability to transition metal catalysts, easy solubility in typical solvents used in Z-N polymerization such as hexane and toluene, and their versatility. In general, a borane-containing olefinic monomer is found to effectively copolymerize with most  $\alpha$ -olefins in the presence of an appropriate catalyst system. The incorporated borane groups in the polyolefins, in turn, function as manipulatable sites for selective functionalization under mild reaction conditions.

One such reported example is the synthesis of polypropylene-*b*-polymethylmethacrylate (PP-*b*-PMMA) copolymers utilizing metallocene catalysis and the borane chemistry. In the initial step, PP with chain-end olefinic unsaturations was prepared using metallocene catalysts such as Et(Ind)<sub>2</sub>ZrCl<sub>2</sub>/MAO. The unsaturation sites were then hydroborated by 9-borabicyclo[3.3.1]nonane (9-BBN) to produce borane-terminated PP (**43**) (Fig. 30), which was selectively oxidized and interconverted to a

polymeric radical. This radical then proceeded to initiate the polymerization to produce diblock copolymers (**44**) (Fig. 30).<sup>66</sup> A similar strategy was used for the synthesis of PP/maleic anhydride (MA) copolymers **45** (single MA unit-terminated PP) and **46** (styrene(S)/MA diblock copolymers of PP) (Fig. 30).<sup>67</sup> MA-modified PP has recently found applications especially in glass fiber-reinforced PP and anticorrosive coatings for metal pipes and containers.<sup>68</sup>

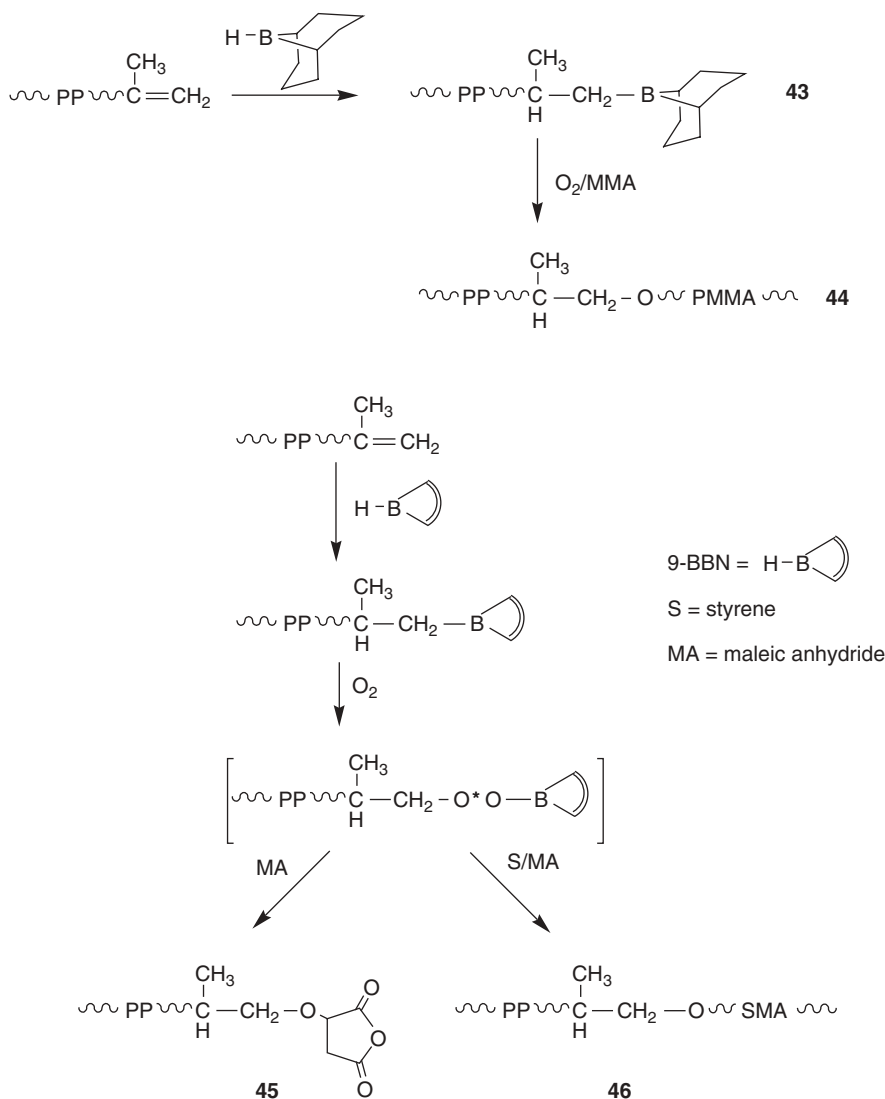


**Figure 30** The hydroboration strategy of chain end olefinic unsaturation in polypropylene with 9-BBN for further conversion into block copolymers via polymer radicals. (Adapted from refs. 66 and 67.)

A radical initiator based on the oxidation adduct of an alkyl-9-BBN (**47**) has been utilized to produce poly(methylmethacrylate) (**48**) (Fig. 31) from methylmethacrylate monomer by a living anionic polymerization route that does not require the mediation of a metal catalyst. The relatively broad molecular weight distribution ( $PDI = (M_w/M_n) \sim 2.5$ ) compared with those in living anionic polymerization cases was attributed to the slow initiation of the polymerization.<sup>69</sup> A similar radical polymerization route aided by **47** was utilized in the synthesis of functionalized syndiotactic polystyrene (PS) polymers by the copolymerization of styrene.<sup>70</sup> The borane groups in the functionalized syndiotactic polystyrenes were transformed into free-radical initiators for the *in situ* free-radical graft polymerization to prepare *s*-PS-*g*-PMMA graft copolymers.

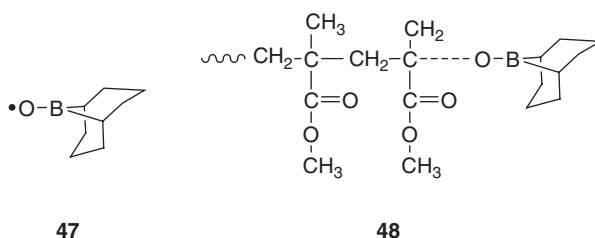


**Figure 31** The radical initiator (**47**) based on the oxidation adduct of an alkyl-9-BBN used for the production of poly(methylmethacrylate) (**48**) from methylmethacrylate monomer by the radical polymerization route. (Adapted from ref. 69.)

A dimeric organoborane chain-transfer agent, the 9-BBN dimer (**49**) (Fig. 32) afforded a very convenient method for the preparation of polyolefins containing a terminal polar group. This first appeared in the literature in 1999.<sup>71</sup> This reagent, which is stable to hydroboration of olefins, incorporates the B-containing group in polyolefins *in situ* during the termination of a metallocene-catalyzed polymerization. The termination of the polymer chains is achieved by quenching the polymer solution with anhydrous/anaerobic MeOH. This borane dimer was utilized in the synthesis of diblock copolymers containing syndiotactic PS and polar polymers.<sup>72</sup>

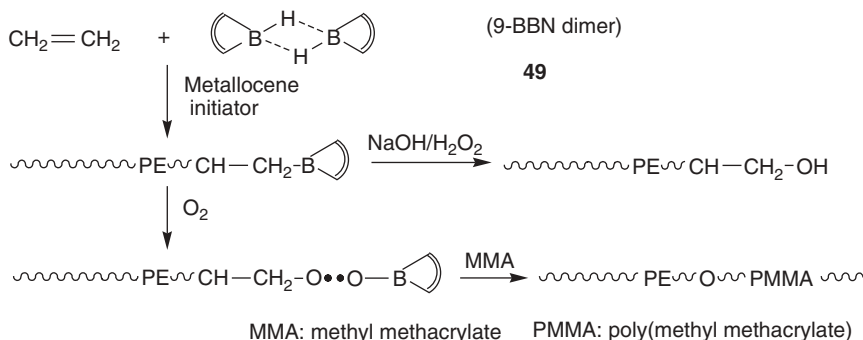


**Figure 32** The dimeric organoborane chain-transfer agent, 9-BBN dimer (**49**), used for the *in situ* incorporation of B-containing group in polyolefins during the termination of a metallocene-catalyzed polymerization. (Adapted from ref. 71.)

The extension of the olefin protection and chain-transfer strategies to the synthesis of a broad range of polyolefin homo- and copolymers has been achieved by the judicious manipulations of borane chain-transfer agents, metallocene catalyst systems, and reaction conditions. The polymers utilized include polyethylene, polypropylene, syndiotactic polystyrene, poly(ethylene-*co*-propylene), poly(ethylene-*co*-1-octene), and poly(ethylene-*co*-styrene). The molecular weight of the borane-terminated polyolefin was found to be proportional to the molar ratio of [olefin]/[borane]. The reactive terminal borane was then converted to various functional groups or selectively oxidized to yield a stable polymeric radical for living free-radical polymerization of desired functional monomers. The preceding steps in effect produced an elegant transformation from a metallocene polymerization to a living free-radical transformation via the borane terminal group. This afforded functional polyolefin diblock copolymers, which ordinarily are difficult to be prepared using conventional initiators.<sup>73</sup>

In a recent development, a new process of preparing borane-terminated isotactic polypropylene (*i*-PPs) via an *in situ* chain-transfer reaction was achieved by a styrene/hydrogen consecutive chain-transfer reagent, which avoids the use of a B—H containing chain-transfer agent.<sup>74</sup> This has resulted in the utilization of milder polymerization conditions due to the use of the alkylaluminumoxane cocatalyst (MAO) (**50**) (Fig. 33), which cannot normally be used in the presence of a B—H chain-transferring

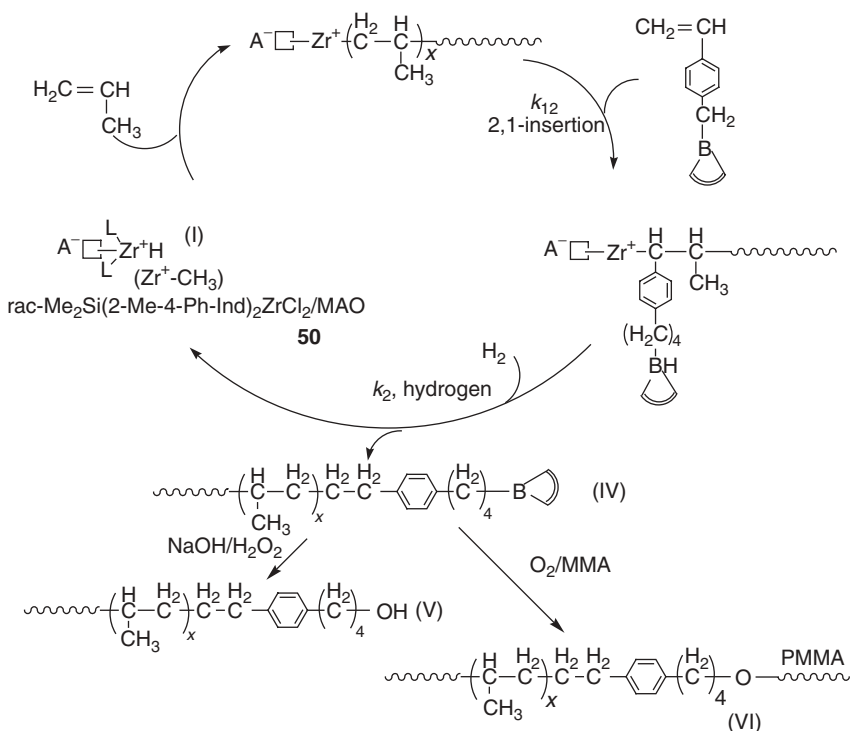


**Figure 33** The catalytic mechanism for the production of borane-terminated isotactic polypropylene (*i*-PPs) via *in situ* chain-transfer reaction by a styrene/hydrogen consecutive chain-transfer reagent allowing the utilization of MAO cocatalyst (**50**). (Adapted from ref. 74.)

agent due to ligand exchange reaction between the B—H and the alkyl groups on the aluminum. The undesirable hydroboration of the olefins by the B—H chain-transferring agent during the polymerization can also be avoided by this method.<sup>74</sup>

In addition to their use as olefin protecting groups, boron ligands have also been utilized in the modification of polymer-supported metallocene catalysts for olefin polymerization. Roscoe et al. have reported the preparation of metallocene catalysts supported on noninteracting polystyrene to avoid the destructive interaction of highly reactive metallocene catalysts with classic silica-based supports.<sup>75</sup> Supported catalysts (**51**) (Fig. 34) for the polymerization of  $\alpha$ -olefins were prepared by treating lightly cross-linked, chloromethylated polystyrene beads consecutively with a secondary amine, an ammonium salt of a weakly coordinating anion,  $[\text{B}(\text{C}_6\text{F}_5)_4]^-$ , and a neutral dialkyl metallocene. The copolymerization of ethylene and 1-hexene at 40°C, facilitated by the homogeneously distributed catalytic sites on the support particle, afforded discrete spherical polyolefin beads with a size (0.3 to 1.4 mm) that varied according to the polymerization time.

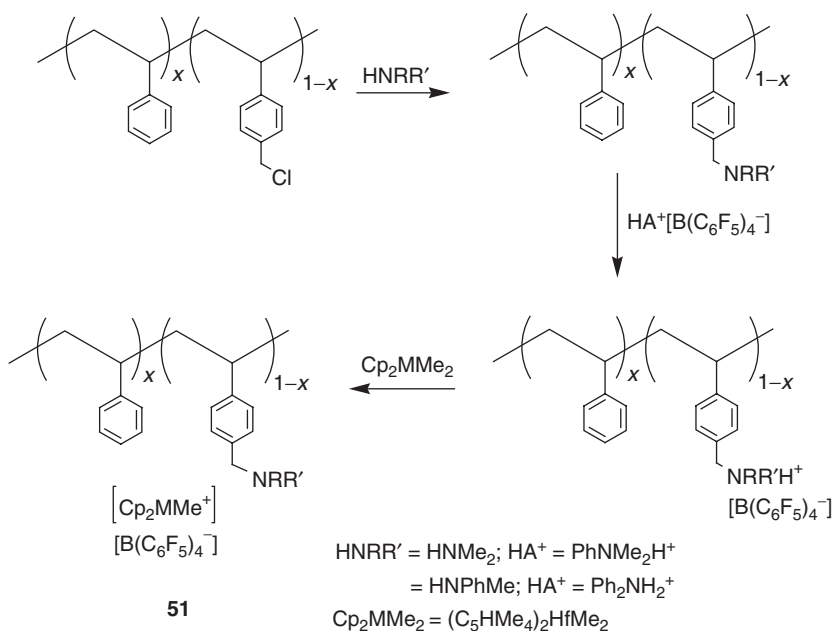


**Figure 34** A polymer-supported metallocene catalyst (**51**) with a weakly coordinating anion,  $[\text{B}(\text{C}_6\text{F}_5)_4]^-$ , produced from lightly cross-linked, chloromethylated polystyrene beads for olefin polymerization. (Adapted from ref. 75.)

There also have been other reports of polymer-supported catalysts with incorporated boron moieties resulting from multistep polymer modification reactions to incorporate the boron moiety.<sup>76</sup>

It is well known that the nature of the cocatalyst used in the metallocene-catalyzed olefin polymerization has a significant effect on the kinetics of the polymerization. The most important industrial cocatalysts are (MAO),<sup>77</sup> a condensation product prepared from  $\text{AlMe}_3$  and water, and the perfluorophenylborane  $\text{B}(\text{C}_6\text{F}_5)_3$ .<sup>78</sup> Research has recently focused on the design of borane anions, which are even more noncoordinating than  $\text{B}(\text{C}_6\text{F}_5)_3$ . Such cocatalysts are expected to improve the activity and the lifetime of the catalytically active species and to better the chain-termination and chain-transfer reactions as well as regio- and stereoregularity.<sup>79</sup> Nager et al. have recently reported the synthesis of a highly noncoordinating carborasilane dendrimeric polyanion terminated with  $\text{BR}_3$  groups (**52**) (Fig. 35).<sup>80</sup>

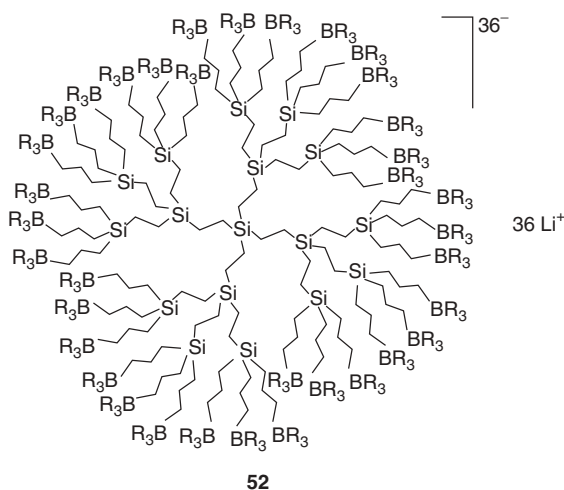


**Figure 35** A noncoordinating carborasilane dendrimeric polyanion terminated with  $\text{BR}_3$  groups (**52**) used as a cocatalyst in the metallocene-catalyzed olefin polymerization. (Adapted from ref. 80.)

In a series of reports, Jakle and co-workers have reported a new route to organoboron polymers of PS that contained well-defined boron-containing Lewis acids.<sup>81</sup> These acidic polymers have the potential for use as cocatalysts in olefin polymerization and as catalysts in organic syntheses. The initial step in the synthesis involved the production of a dibromoborylated PS (PS-BBr) from the reaction of 4-trimethylsilylstyrene in anisole (50%) by a typical atom-transfer radical polymerization (ATRP)<sup>82</sup> initiated with 2 mol % 1-phenylethyl bromide. PS-BBr was found to readily react with nucleophiles, thereby serving as a precursor to a number of other polymers with boron centers of variable Lewis acidity. When PS-BBr was treated with  $\text{Me}_3\text{SiOEt}$  or tetrahydrofuran (THF), PS-BOEt (**53**) and PS-BOBuBr (**54**) (Fig. 36), were obtained in 90 and 83% yield, respectively. PS-BOEt, on reaction with pinacol, yielded the polymer PS-BPin (**55**) (Fig. 36). The molecular weight and dispersity of PS-BOBuBr were determined by GPC analysis (relative to polystyrene standards) to be 7180 and 1.13, respectively.<sup>81a</sup>

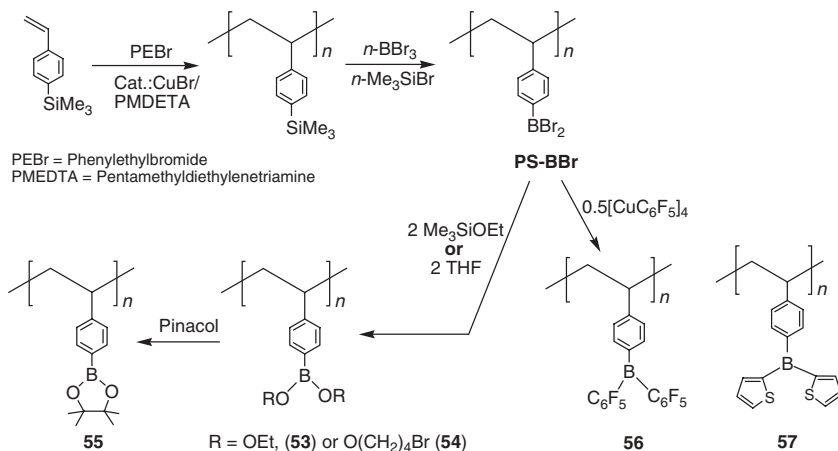


**Figure 36** Organoboron polymers of PS with well-defined boron-containing Lewis acids for use as a cocatalyst in metallocene-catalyzed olefin polymerizations. (Adapted from ref. 81.)

Using the same synthetic strategy, the synthesis of polymeric Lewis acids PS-BAr (**56**) and PS-BTh (**57**) (Fig. 36) were produced by the respective reactions of PS-BBr with pentafluorophenylcopper and trimethylstannylthiophene.<sup>81b,c</sup> The molecular weight and dispersity of the pinacol derivative were determined by GPC methods to be 13,830 and 1.09, respectively.

Hartwig and Hillmyer have recently reported the Rh-catalyzed borylation of polyolefins to yield boronate-functionalized polymers (**58**) (Fig. 37) in a single step.<sup>83</sup> The number-average molecular weight of the borylated polymer that was obtained at a B<sub>2</sub>pin<sub>2</sub>:polyethylene ratio of 0.3 was found to be the highest ( $M_n = 52,000$  and PDI = 1.09) among the developed boronate-functionalized polyolefins.

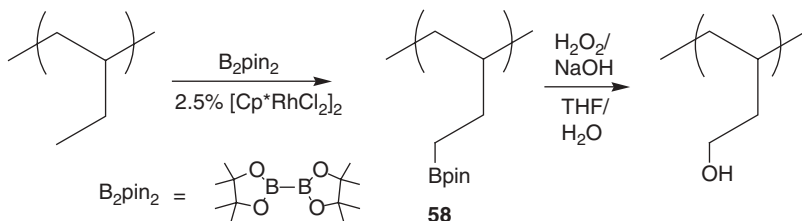


**Figure 37** The boronate-functionalized polymer (**58**) obtained by the Rh-catalyzed borylation of polyolefins. (Adapted from ref. 83.)

Wolfe and Wagener have developed *main-chain* boronate polymers (**59**) (Fig. 38) by the acyclic diene metathesis (ADMET) polymerization of symmetrical  $\alpha,\omega$ -dienes, containing both methyl- and phenyl-substituted boronate functionalities using Mo and Ru catalysts.<sup>84</sup> The ring-opening metathesis polymerization (ROMP) of several norbornene monomers containing methyl- and phenyl-substituted boronates into

unsaturated polymers (**60**) (Fig. 38) has also been achieved. The Ru and the Mo metathesis catalysts were observed to be sensitive to the isomeric form of the norbornene monomer. While the Ru alkylidene generated only the *cis* polymer using the *exo* monomer, the Mo alkylidene was found to produce a completely *trans* polymer from the *endo* monomer. It was discovered that the long-term stability and solution characteristics of both sets of polymers were dramatically influenced by ligand-exchange reactions within the boronate moiety. When the boronates were placed pendent to the main chain, this phenomenon was found to be obviated.

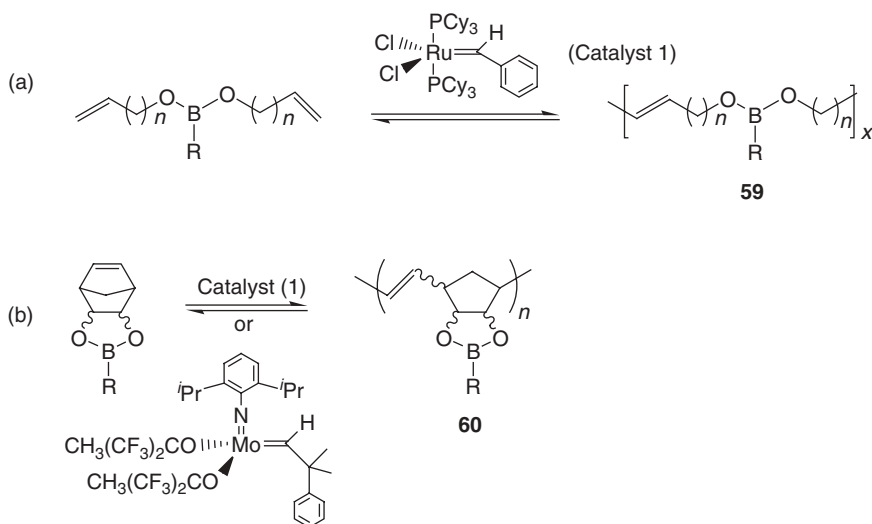
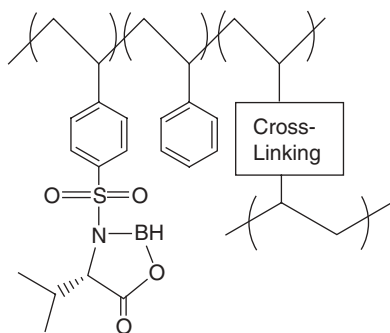


**Figure 38** (a) The ADMET polymerization (using Mo and Ru catalysts) of symmetrical  $\alpha,\omega$ -dienes that yield main-chain boronate polymers (**59**). (b) The ROMP of several norbornene monomers containing methyl- and phenyl-substituted boronates into unsaturated polymers (**60**). (Adapted from ref. 84.)

### b. Organoboron Polymers Used in Other Organic Transformations

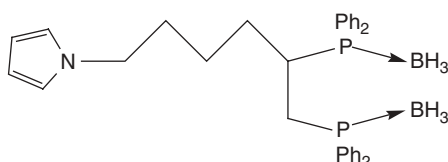
Polymer-supported organoboron catalysts have been finding increasing use in catalytic asymmetric syntheses. The anchoring of catalysts on polymer supports aids in the recycling of the catalysts, which is of great importance in homogeneous catalysis for the development of new industrial processes. Itsuno and co-workers have reported the design of highly enantioselective polymer-supported catalysts (**61**) (Fig. 39) of chiral oxazaborolidinone having different cross-linking structures for use in the Diels–Alder reaction of methacrolein with cyclopentadiene. The polymer-supported catalysts **61** having oxyethylene cross-linkages were found to exhibit better performance in promoting the enantioselective Diels–Alder reaction than their nonpolymeric counterparts.<sup>85</sup>

The development of polypyrroles bearing supported diphosphine ligands protected from oxidation by borane groups has been reported.<sup>86</sup> The polymer was produced by the electropolymerization of 1-(*N*-but-4-yl-pyrrol)-1,2-bis(diphenylphosphinoborane) (**62**) (Fig. 40). These preformed polymeric films lend themselves to the incorporation



61

**Figure 39** The enantioselective polymer-supported catalysts (**61**) of chiral oxazaborolidinone with cross-linking structures for use in the Diels–Alder reaction of methacrolein with cyclopentadiene. (Adapted from ref. 85.)

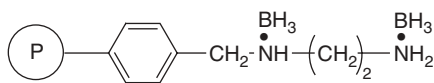


62

**Figure 40** The pyrrole monomer, 1-(*N*-but-4-yl-pyrrol)-1,2-bis(diphenylphosphinoborane) (**62**), used for electropolymerization to yield polypyrroles with diphosphine ligands protected from oxidation by borane groups. (Adapted from ref. 86.)

of palladium, thus generating palladium(0) catalysts that have applications in allylic-catalyzed alkylation reactions.<sup>86</sup>

Devaky and Rajasree have reported the production of a polymer-bound ethylenediamine-borane reagent (**63**) (Fig. 41) for use as a reducing agent for the reduction of aldehydes.<sup>87</sup> The polymeric reagent was derived from a Merrifield resin and a 1,6-hexanediol diacrylate-cross-linked polystyrene resin (HDODA-PS). The borane reagent was incorporated in the polymer support by complexation with sodium borohydride. When this reducing agent was used in the competitive reduction of a 1:1 molar mixture of benzaldehyde and acetophenone, benzaldehyde was found to be selectively reduced to benzyl alcohol.



63

**Figure 41** The polymer-bound ethylenediamine-borane reagent (**63**) for use as a reducing agent for the reduction of aldehydes. (Adapted from ref. 87.)

#### iv. Organoboron Polymers that Function as Flame-Retardant Materials

Borates and boric acid have been well known to function as flame retardants, particularly in a synergistic fashion with halogenated polymers and halogen additive polymeric systems.<sup>88</sup> The flame retardancy of boron compounds is known to have its origin in the ability of the compounds to form a surface layer of an intumescent protective char, which acts as a barrier to oxygen, and consequently to the oxidation of carbon.

Recently, several reports of the flame-retardant properties of boron-containing bisphenol-A resins have appeared from Gao and Liu.<sup>89</sup> The synthesis of a boron-containing bisphenol-A formaldehyde resin (**64** and **65**) (Fig. 42) from a mixture of bisphenol-A, formaldehyde, and boric acid, in the mole ratio 1:2.4:0.5, has been reported.<sup>89a</sup> The kinetics of the thermal degradation and thermal stability of the resins were determined by thermal analysis. The analysis revealed that the resin had higher heat resistance and oxidative resistance than most common phenol-formaldehyde resins.

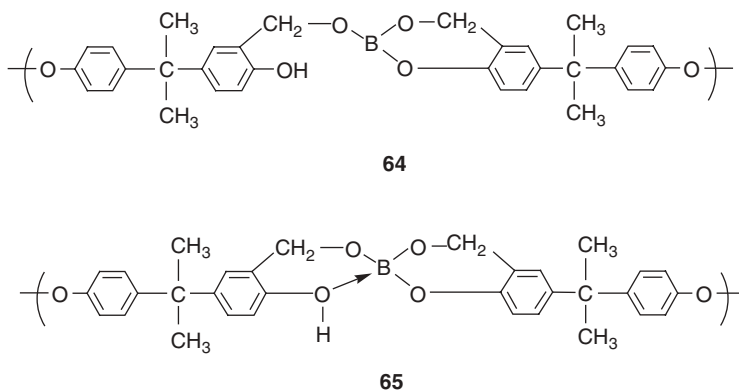


**Figure 42** The boron-containing bisphenol-A formaldehyde resin [**64** and **65** (obtained from **64** on further heat treatment)] produced from a mixture of bisphenol-A, formaldehyde and boric acid, in the mole ratio 1:2.4:0.5. (Adapted from ref. 89.)

The development of a solvent reaction between triphenyl borate and paraformaldehyde to produce a boron-modified phenolic resin that flowed at usual processing temperatures has been reported.<sup>90</sup>

Cadiz and co-workers have reported the synthesis of a boron-containing Novolac resin (**66**) (Fig. 43) by the modification of the commercially available Novolac (phenolic) resin with different amounts of bis(benzo-1,3,2-dioxaborolanyl)oxide.<sup>91</sup> These modified Novolac resins were further cross-linked (**67**) (Fig. 43) with diglycidyl ether of bisphenol-A. The thermal degradation study of the boron-containing Novolac resin monitored by Fourier transform infrared (FTIR) spectroscopy revealed that they generated boric acid at high temperatures to give an intumescent char that slowed down the thermal degradation of the resin.

The syntheses of a homopolymer and a copolymer (**68**) (Fig. 44) of the boron-containing styrenic monomer, 5-benzyl-2-phenyl-5-(4-vinylbenzyl)-[1,3,3]-dioxaborinane with styrene have been achieved.<sup>92</sup> A similar monomer without boron

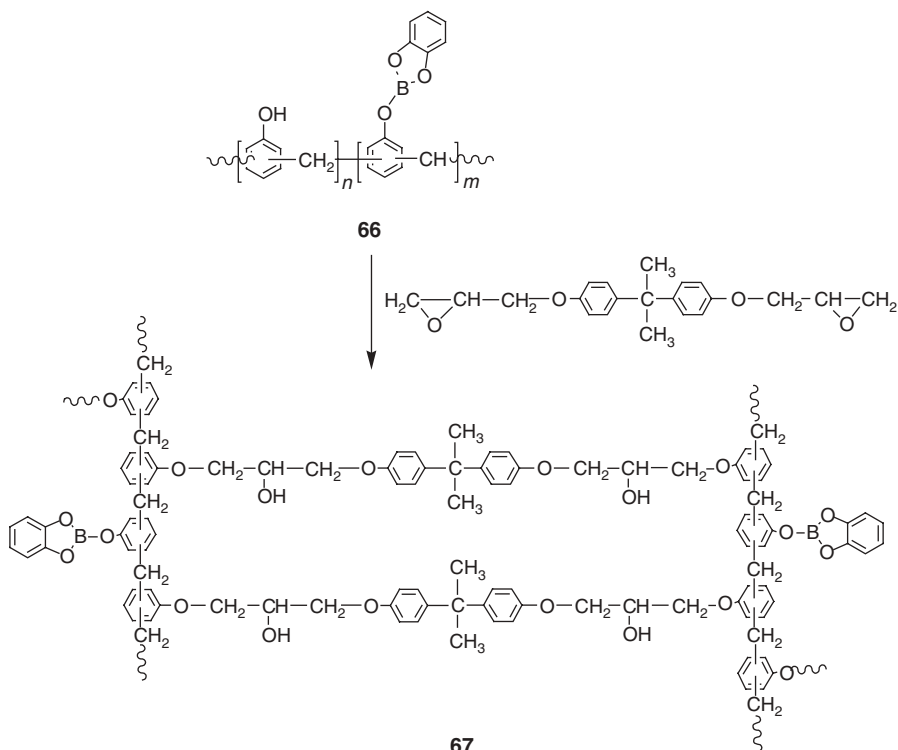
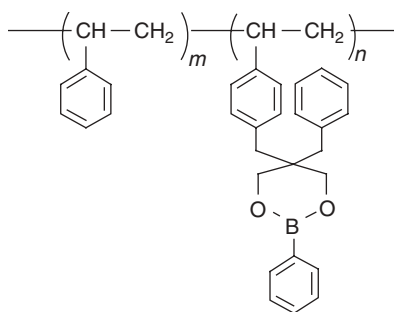


**Figure 43** The cross-linking reaction of the boron-containing Novolac resin (**66**) (obtained by the modification of the commercially available Novolac resin) with bis(benzo-1,3,2-dioxaborolanyl)oxide. (Adapted from ref. 91.)



**68**

**Figure 44** The boron-containing styrenic monomer, 5-benzyl-2-phenyl-5-(4-vinylbenzyl)-[1,3,3]-dioxaborinane (**68**) used in the syntheses of a homopolymer and a copolymer with styrene. (Adapted from ref. 92.)

was also prepared and polymerized so that its properties could be compared with the boron-containing polymers. The boron-containing polymers were found to have higher limiting oxygen indices and to give greater char yields than those without boron.

Boronic acids (**69** and **70**) (Fig. 45) with more than one boronic acid functionality are known to form a polymer system on thermolysis through the elimination of water.<sup>93</sup> Specifically, they form a boroxine (a boron ring system) glass that could lead to high char formation on burning. Tour and co-workers have reported the synthesis of several aromatic boronic acids and the preparation of their blends with acrylonitrile-butadiene-styrene (ABS) and polycarbonate (PC) resins. When the materials were tested for burn resistance using the UL-94 flame test, the burn times for the ABS samples were found to exceed 5 minutes, thereby showing unusual resistance to consumption by fire.<sup>94</sup>

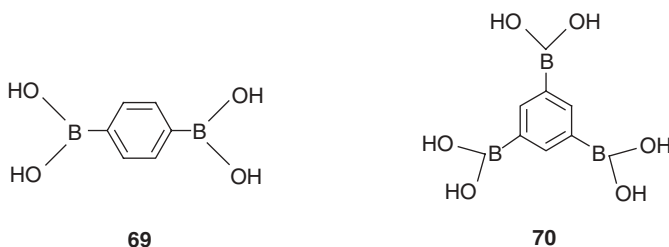


**Figure 45** Boronic acids (**69** and **70**) with multiple boronic acid functionalities that form boroxine ring systems on thermolysis through the elimination of water. (Adapted from ref. 93.)

## B. Polymers Containing Boron Ring Systems in the Backbone or in Pendent Groups

The best known boron-containing ring systems are the so-called “inorganic benzenes,” namely, borazine (**71**), boroxine (**72**), and triphosphatiborin (**73**) (Fig. 46), which are isoelectronic and isostructural with benzene. These ring systems are obtained by the interaction of boron with nitrogen, oxygen, and phosphorus, respectively.<sup>4</sup>

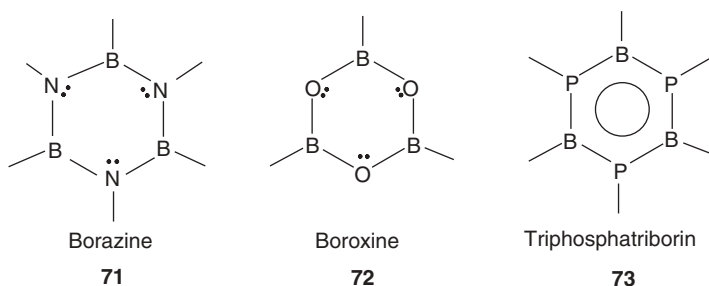


**Figure 46** The planar structures of the boron ring systems, borazine (**71**) and boroxine (**72**), with nonexistent aromaticities and of triphosphatiborin (**73**) with an appreciable degree of aromaticity. (Adapted from ref. 95.)

Previous studies on electronic delocalization in borazine, boroxine, and triphosphatriborin in comparison to benzene have indicated that there is no significant aromatic character in borazine, boroxine, or triphosphatriborin.<sup>95</sup> In addition, the borazine and boroxine ring systems were found to possess very similar localized electronic densities.<sup>95</sup> Recent valence bond (VB) theory and ring-current map studies have indicated that in borazine and boroxine there is a localization of lone pairs on the electronegative atoms, nitrogens, and oxygens, respectively, and as a consequence, there is no resonance energy stabilization arising from any Kekule-like structures.<sup>96</sup> However, in the case of triphosphatriborin some benzene-like features were observed in its planar form with a significant contribution to its VB wave function from two Kekule-like structures, resulting in an appreciable resonance energy and a discernible diatropic ring current. The observed resonance stabilization in the planar confirmation of triphosphatriborin was found to be lost when it was allowed to relax to its optimal nonplanar chair conformation.<sup>96</sup> However, in a contrasting report on the calculations of the protonation and methylation energies of  $C_6H_6$  and  $B_3N_3H_6$ , it was claimed that the aromaticity of borazine is about half that of benzene.<sup>97</sup> Even though the debate on the electronic nature of these ring systems is ongoing, their unique and beneficial chemistries have propelled their incorporation, especially that of the borazine ring system, in various polymeric materials.

The area of organoboron polymers containing borazine and its derivatives is covered in Chapter 5 of this book by Miele and co-workers. Miele and Bernard also describe the utilization of these polymers in ceramics, fibers, and so on, in Chapter 3 of this book. In this section, the utilization of polymers containing borazine or in some cases the bicyclic boron ligand, 9-BBN, for the production of SiC or Si/C/B fibers is briefly described. Recent advances in polypyrazolylborate or pyrazabole-containing polymers and other boron ring system-derived polymers also have been briefly described.

### ***i. Organoboron Polymers that Contain Borazine or 9-BBN with Utility in the Production of High-Performance Fibers***

#### ***a. SiC-Producing Borazine Polymer Systems***

The major impetus for the incorporation of boron in silicon-containing polymers has been the utilization of such polymers in the high-performance fiber industry. The high-performance nonoxide ceramics such as silicon carbide (SiC)<sup>98</sup> and silicon nitride ( $Si_3N_4$ )<sup>99</sup> are conventionally made from polycarbosilanes, polysilazanes, or polycarbosilazanes, respectively. The production of industrial SiC fibers such as NICALON and TYRANNO resulted from the seminal work of Verbeek<sup>100</sup> and Yajima.<sup>101</sup> According to Yajima's strategy, precursor dichlorosilane materials are converted to polysilanes which are in turn converted to polycarbosilanes (PCS) by thermolysis. However, PCS can also be synthesized directly without the mediation of polysilane.<sup>102</sup> The addition of organoborate additive during the thermolysis of polysilane to PCS or during the final pyrolytic conversion to the fiber can improve the mechanical properties of the fiber by decreasing the oxygen and free carbon content and by improving its sintering properties. Additives such as  $B_2H_6$ ,<sup>103</sup>  $BCl_3$ ,<sup>104</sup> or boron vapor<sup>105</sup> have been used in the past toward this goal.

In recent times, polyborazine has been used as an additive to both polysilanes (specifically, polymethylsilane)<sup>106</sup> and PCS<sup>107</sup> separately to improve the yield of oxygen-free SiC fibers. Sneddon and co-workers have reported the use of a borazine, namely, diethylborazine (**74**), for the modification of poly(vinylsiloxane)s (PVS) (Fig. 47) for the production of boron-modified SiC by the  $\text{RhH}(\text{CO})(\text{PPh}_3)_3$ -catalyzed reaction of PVS with diethylborazine.<sup>108</sup> The same report also discusses the synthesis of pinacolborane-modified PVS polymers (**77**) (Fig. 47), which happen to be the first examples of a melt-processable poly(borosiloxane) single-source precursor for the formation of small-diameter SiOCB fibers. This synthetic strategy is an alternative way of introducing boron into SiC-producing resins. This is conventionally achieved by the blending of boron-containing materials into the resin before processing or by the treatment of the processed green fibers with a gaseous boron reagent.<sup>108</sup> The pinacolborane product was synthesized by the reaction of PVS with pinacolborane (**76**) (Fig. 47) in the presence of the catalyst  $\text{RhH}(\text{CO})(\text{PPh}_3)_3$ . The ceramic chars obtained at 1800°C were found to contain reduced grain growth and more uniform grain distribution compared to the ceramics obtained from unmodified PVS, demonstrating the pronounced effect that the addition of even a small amount of boron (<1%) has had on the ceramic properties of the chars.

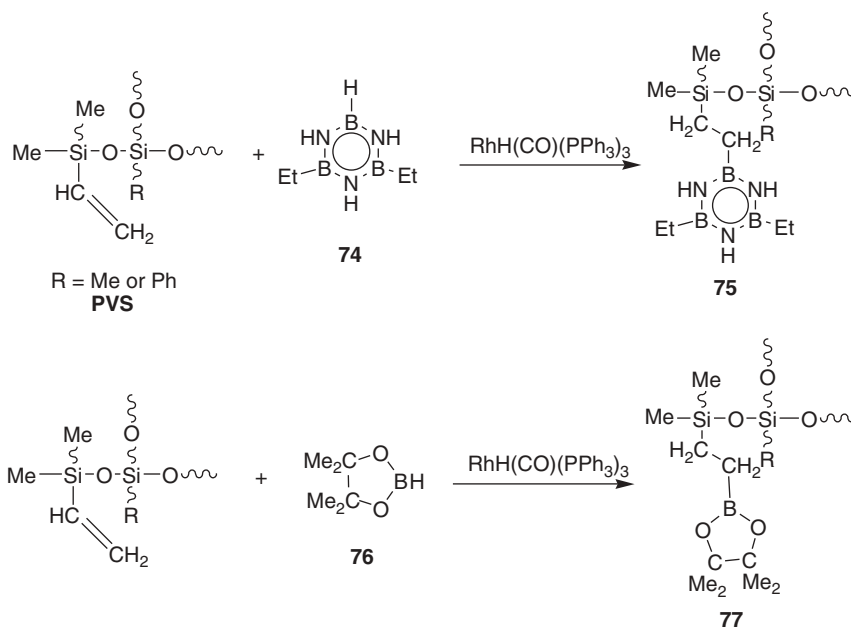


**Figure 47** Synthesis of diethylborazine-modified (**75**) (top) and pinacolborane-modified (**77**) (bottom) polyvinylstyrene polymers. (Adapted from ref. 108.)

Recently, the modification of polycarbosilane polymers with 9-BBN (**78**) (Fig. 48) was reported by the Sneddon group.<sup>109</sup> To improve sintering in SiC ceramics, allylhydridopolycarbosilane (AHPCS) polymers were reacted with 9-BBN at room temperature in toluene. Typical reactions required  $\sim 20$  h for the complete consumption of the 9-BBN ligand. The ceramic yields of the AHPCS-9-BBN polymers (**79**) (Fig. 48) were found to be significantly higher than that of the parent AHPCS polymer due to an additional cross-linking reaction involving the 9-BBN ligand. In addition, the presence of boron was found to increase the density of the ceramic fibers obtained at 1800°C and 2000°C from the BBN-modified polymers compared to those produced from the unmodified polymers.

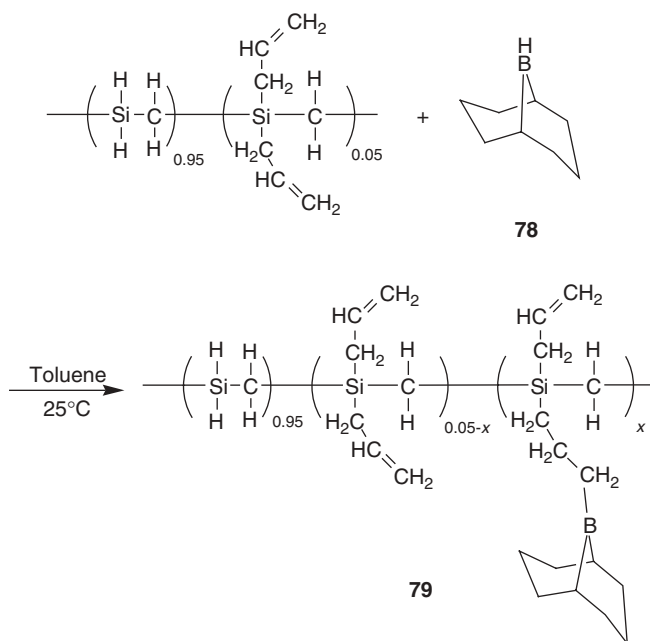


**Figure 48** Synthesis of 9-BBN-modified allylhydridopolycarbosilane polymers (**79**). (Adapted from ref. 109.)

#### *b. Si/B/C/N-Producing Systems*

The introduction of small amounts of boron into precursors that produce silicon nitride have been known to improve the ceramic yields of silicon nitride and Si—B—C—N ceramics as first reported in 1986.<sup>110</sup> Several reports have appeared in the past couple of years alone that utilize borazine precursors such as 2,4-diethylborazine and other cyclic boron precursors, such as pinacolborane, 1,3-dimethyl-1,3-diaza-2-boracyclopentane, for their reactions with silanes, polysilazanes, and polysilylcarbodiimides for the high-yield production of Si—B—N—C ceramics.<sup>111</sup>

These developments are discussed in depth by Miele and Bernard in Chapter 3 of this book.

### ii. Organoboron Polymers that Contain Boroxine or Triphosphatriborin Ring Systems

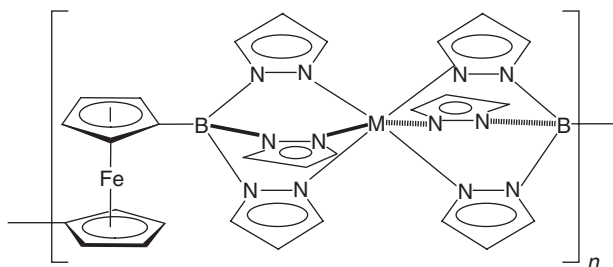
Boroxine ring-containing polymers have found extensive use in the development of polymeric electrolyte materials used in ion-selective transport membranes. Matsumi and Ohno cover this area in Chapter 6 of this book.

There have been no recent examples of polymers that contain the triphosphatriborin ring system.

### iii. Organoboron Polymers that Contain Polypyrazolylborate or Pyrazabole Ring Systems

Over 2000 papers have appeared on the chemistry of polypyrazolylborate/pyrazabole ring systems, but there have only been a few examples of polymers containing these ligands.<sup>112</sup>

Wagner and co-workers have reported the synthesis of ferrocene-bridged tris(1-pyrazolylborate) oligomeric systems (**80**) (Fig. 49).<sup>62</sup> Such polymers are of interest, as they offer a multiplicity of options for tailoring the access space to a metal held by the tris(1-pyrazolylborate) ligand, as well as a means to electronically influence the environment of a transition metal.<sup>113,114</sup>

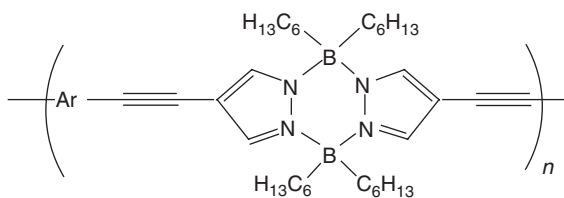


**80**

**Figure 49** Ferrocene-bridged tris(1-pyrazolylborate) oligomeric systems (**80**). (Adapted from ref. 62.)

Pyrazabole ligands have been introduced into fluorescent organoboron polymers (**81**) (Fig. 50) by the Heck-Sonogashira coupling between diyne monomers and pyrazabole derivatives by Chujo and Matsumoto.<sup>115</sup> The number-average molecular weights (9000–34,000) of the polymers obtained by this method were comparatively higher than that of similar polymers obtained from hydroboration reactions.

Using the same strategy, new pyrazabole polymers containing electron-withdrawing aromatic units, such as tetrafluorophenylene, pyridinediyl, and nitrophenylene, have also been synthesized in good yields. The number-average molecular weights of the polymers ranged between 2800 and 11,400.<sup>116</sup>



81

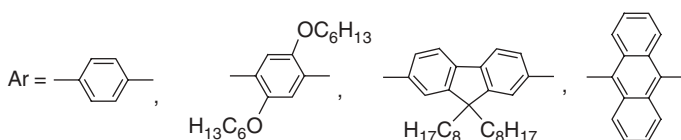
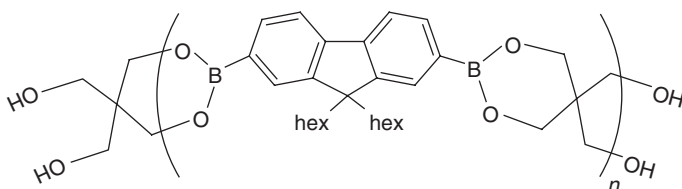


**Figure 50** Fluorescent organoboron polymers (**81**) obtained by Heck–Sonagashira coupling between diyne monomers and pyrazabole derivatives. (Adapted from ref. 115.)

#### *iv. Organoboron Polymers that Contain Other Boron Ring Systems*

Poly(dioxaboralane)s (**82**) (Fig. 51) with controllable molecular weights were reported to be readily obtained through the condensation reaction between 9,9-dihexylfluorene-2,7-diboric acid and pentaerythritol in toluene with an associated azeotropic removal of water. The molecular weights of the resulting polymers, which ranged between 10,000 and 76,900, were found to depend on the processing conditions of the polymers.<sup>117</sup>



82

**Figure 51** Poly(dioxaboralane)s (**82**) obtained through the condensation reaction between 9,9-dihexylfluorene-2,7-diboric acid and pentaerythritol in toluene. (Adapted from ref. 117.)

## **C. Polymers Containing Boron Clusters in the Backbone or in Pendent Groups**

### *i. Monomeric and Polymeric Organic Analogs of Boron Cluster Systems*

The polyhedral clusters of boranes and carboranes are groups of cluster systems that are present ubiquitously in organoboron polymers. As in the case with the

boron ring systems, there have been numerous comparisons of these systems to organic analogs. Recently, Balakrishnarajan and Hoffmann have evaluated the similarities in electronic structures of quinones such as the dioxobenzene dianion (**83**) and polyhedral boranes such as the polyhedral dioxoborane tetraanion (**84**) (Fig. 52)

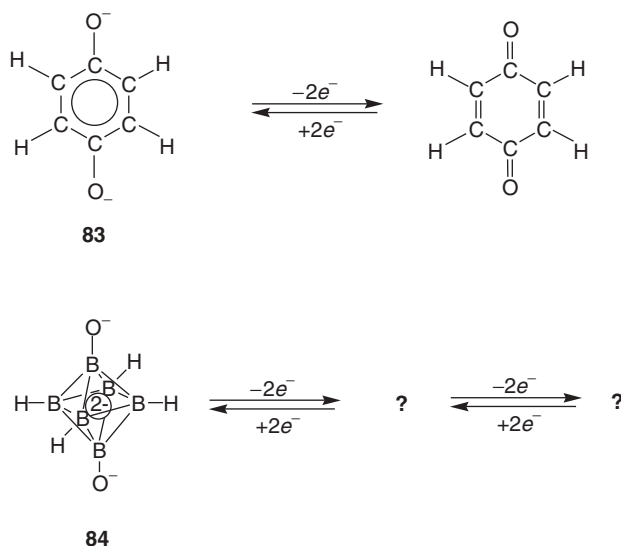


**Figure 52** The redox equilibria in the compared dioxobenzene dianion (**83**) and dioxoborane dianion (**84**) systems. (Adapted from ref. 118.)

that contain exo multiple bonds.<sup>118</sup> Hybrid Density Functional Theory (DFT) and extended Huckel calculations revealed that the exopolyhedral B—O bond lengths decreased steadily and dramatically when **84** was oxidized in a sequence to its dianion and its neutral form, as has been observed during the oxidation of **83** to the neutral quinone. The carborane cluster systems, which can be represented by the general formula  $C_pB_qH_{p+q}$ , can be thought of as being derived from borane clusters by the substitution of some of their boron atoms by carbon atoms.<sup>119</sup> All of the known carborane clusters fall into three categories, namely, the closo-, nido- and arachno-carboranes, where the first are built of closed polyhedral cages, while the latter two include those carboranes in which the boron-carbon polyhedra resemble the shapes of nest skeletons. The closed-shell structures of the closo-dicarbaboranes are known to contribute to their astonishing chemical inertness, especially to acids, with the 1,2-, 1,7-, and 1,12-dicarba-closo-dodecaboranes, better known by the more popular names *o*- (**85**), *m*- (**86**) and *p*-carborane (**87**) (Fig. 53), respectively, being the most stable. Carboranes, in general, and icosahedral carboranes, in particular, in their neutral and anionic forms are also known for their exceptional characteristics, such as low nucleophilicity

and high hydrophobicity, in addition to their electron-withdrawing properties having highly polarizable-aromatic character.<sup>25,119</sup> A weak point of carboranes is their susceptibility to alkaline degradation. This weakness, however, applies practically only to the species with adjacent carbon atoms such as *o*-carborane.<sup>25</sup>

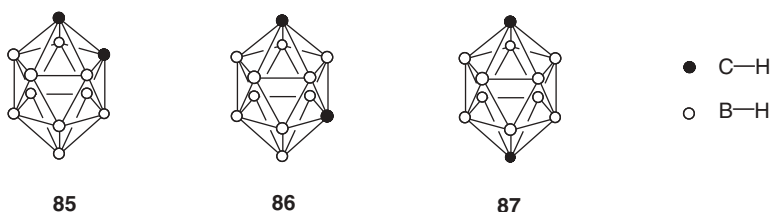


**Figure 53** The 1,2-, 1,7-, and 1,12-dicarba-closo-dodecaboranes, better known by the more popular names *o*- (**85**), *m*- (**86**), and *p*-carborane (**87**), respectively. (Adapted from ref. 119.)

Icosahedral carboranes have been described as “superaromatic” due to the optimal occupancy of their 13 bonding molecular orbitals by the 26 framework electrons. They have been known to undergo electrophilic substitution, which is a hallmark of aromatic compounds.<sup>120</sup> Recent reports of the syntheses of carborane analogs of organic aromatic systems have further established this inorganic–organic relationship. Jones and co-workers have reported the reaction of 1,2-dehydro-*o*-carborane with acetylenes that produced the carborane analog of benzocyclobutadiene.<sup>121</sup> 1,2-Dehydro-*o*-carborane (**88**) (Fig. 54), which is obtained from *o*-carborane by treatment with *n*-BuLi and Br<sub>2</sub>, was found to add 3-hexyne to give the product of an ene reaction and with 1-phenyl-1-propyne (**87**) to give the products of both an ene reaction (**89**) and a 2+2 reaction (**90**) similar to the reactivity of benzene (Fig. 54).

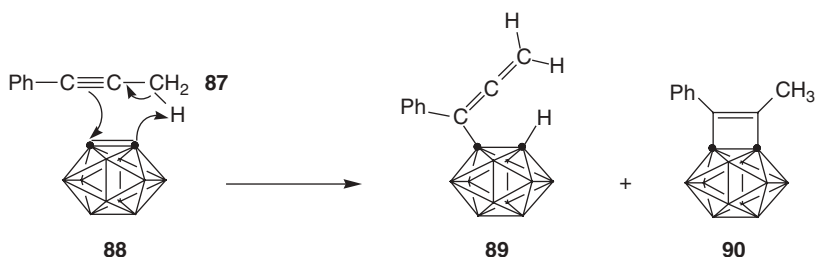
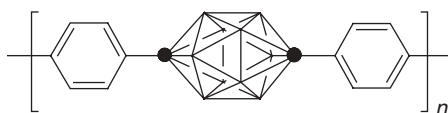


**Figure 54** The ene reaction (**89**) and 2+2 reaction (**90**) products obtained from reaction between 1-phenyl-1-propyne (**87**) and 1,2-dehydro-*o*-carborane (**88**). (Adapted from ref. 121.)

Wade and Williams have reported the synthesis of a carborane-based analog of poly(*p*-phenylene).<sup>122</sup> The rodlike polymer (**91**) (Fig. 55) was prepared by the catalytic

[using Zn and Ni(PPh<sub>3</sub>)<sub>4</sub>] polycondensation of 1,12-bis-(4-chlorophenyl)-1,12-dicarbadoecaborane. The aromatic rings in the polymer were found to be effectively coplanar and the torsion angle ( $\Delta$ ) between a carborane cage and its associated aromatic rings was found to be 18°. The polymer was found to yield a very high ceramic yield (ca. 92%) at 1000°C in argon.



91

**Figure 55** The rodlike polymer (**91**) that is the carborane-based analog of poly(*p*-phenylene). (Adapted from ref. 123.)

Several reported examples of carboranophane analogs of cyclophanes, compounds obtained by the bridging of 1,4- or 1,3-positions of benzene rings, further emphasize this inorganic–organic analogy. Jones and co-workers have reported the synthesis of carboranophanes starting from *m*-carborane, in which the carbons are in a 1,3-relationship with each other.<sup>123</sup> This compound was converted to the known dithiol, which was further reacted in the presence of KOH in ethanol with 1,*n*-dibromoalkane ( $n = 6, 7, \text{ or } 8$ ) to produce three [*n*]carboranophanes (**92** and **93**) (Fig. 56).

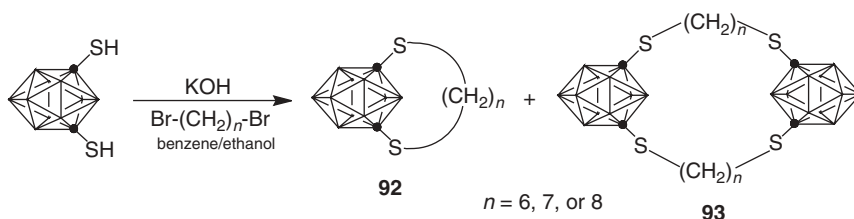


**Figure 56** Two sets of [*n*]carboranophanes (**92** and **93**) derived from the dithiol derivative of *m*-carborane. (Adapted from ref. 123.)

A novel cyclooctaphane (**94**) (Fig. 57) was assembled by the condensation reaction between the C,C'-dicopper(I) derivative of *m*-carborane and 1,2-bis(4-iodophenyl)-*o*-carborane.<sup>124</sup> The macrocycle was found to adopt a butterfly (dihedral angle 143°) confirmation with the *o*-carborane units at the wingtips and the phenylene ring planes roughly perpendicular to the wing planes of the confirmation.

Many other carboracycles and carborands, another group of organic ring systems, have been reported and are discussed in the section on carborane supramolecular chemistry later in this chapter.

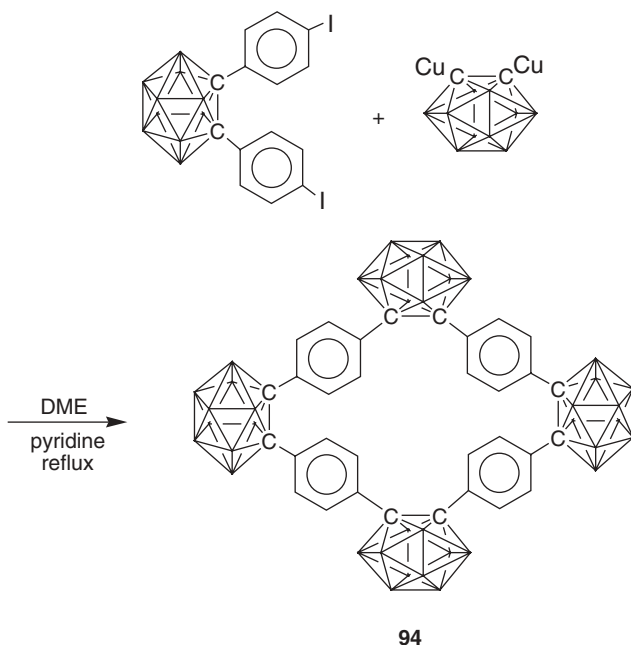


**Figure 57** The cyclooctaphane (**94**) assembled by the condensation reaction between C,C'-dicopper(I) derivative of *m*-carborane and 1,2-bis(4-iodophenyl)-*o*-carborane. (Adapted from ref. 124.)

### *ii. Poly(carboranylenesiloxanes) and Related Polymers*

Developments in the chemistry of poly(carboranylenesiloxanes) were sparse in the 1980s following the initial bursts of work from the Olin and the Union Carbide teams. However, there has been renewed interest in this chemistry since the mid-1990s owing especially to the work originating from Keller and co-workers.

A significant development in this area resulted from the inclusion of a thermally cross-linkable diacetylene unit in the backbone of poly(carboranylenesiloxanes).<sup>125</sup> This facilitated the conversion of the starting oligomeric materials into extended networked polymers. Until then, the traditional sites of cross-linking in poly(carboranylenesiloxanes) had consisted of either pendent methyl and vinyl groups on Si atoms of the oligomers, or some reactive sites on the carborane moieties; the chemistry of which was not easily controllable.<sup>25</sup> The inclusion of a diacetylene group in a poly(carboranylenesiloxane) yielded a useful handle to control the extent of curing in the produced networked systems by the selection of appropriate curing temperatures.<sup>125</sup> The first oligomer generated of this kind, **95** (Fig. 58), on complete conversion to a networked system, was found to yield a plastic product. These extremely thermooxidatively stable networked systems exhibited high char yields of ca. 92 and 85% in air and N<sub>2</sub>, respectively.

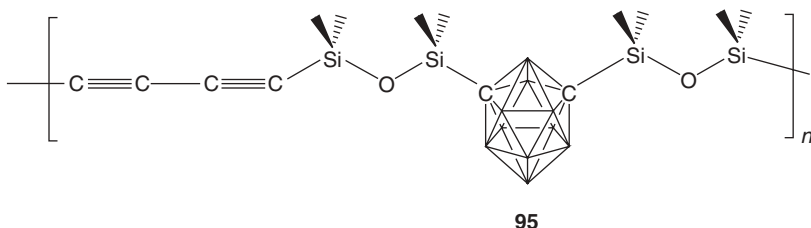


**Figure 58** The carboranylenesiloxane (**95**) containing the cross-linking diacetylene group. (Adapted from ref. 125.)

The inclusion of an organometallic system in these polymers, reported by Houser and Keller, resulted in the synthesis of linear ferrocenyl-carboranylenesiloxyl-diacetylene polymers (**96**) (Fig. 59), which could be deemed as a diacetylene-containing carboranylenesiloxane polymer with some of its carborane groups having been replaced by the bridging ferrocenyl groups.<sup>126</sup> The polymers were produced by the reaction of dilithiobutadiyne with two equivalents of 1,7-bis(chlorotetramethyl-disiloxyl)-*m*-carborane (Dexsil 200 monomer) followed by the treatment with dilithioferrocene-*t*-meda (1 equiv.). The molecular weight of this material was determined to be ca. 10,000 (relative to polystyrene) by GPC, thus accounting for ~10 repeat units of the monomer. On thermal treatment, this oligomer was found to yield an elastomeric material.

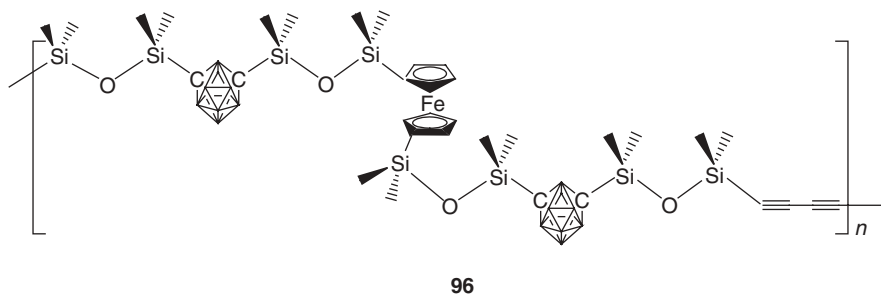


**Figure 59** The carboranylenesiloxane (**96**) containing both the organometallic ferrocene moiety and the cross-linking diacetylene group. (Adapted from ref. 126.)

To produce elastomeric materials from **95**, Kolel-Veetil and Keller studied the effects of reducing the concentration of the diacetylene units in **95** on the plasticities of the resulting networks.<sup>127</sup> The ratio (1:2:1) of the carborane, disiloxane, and diacetylene moieties in **95** was altered to 2:3:1, 4:5:1, and 9:10:1, respectively, to produce polymers containing progressively lower amounts of diacetylene units. Two sets of the polymers, one an alternating type (**97**) and the other a blocky type (**98**) (Fig. 60), were synthesized. The networked polymers produced from both the blocky and the alternating sets were found to be slightly elastomeric with  $T_g$  values around

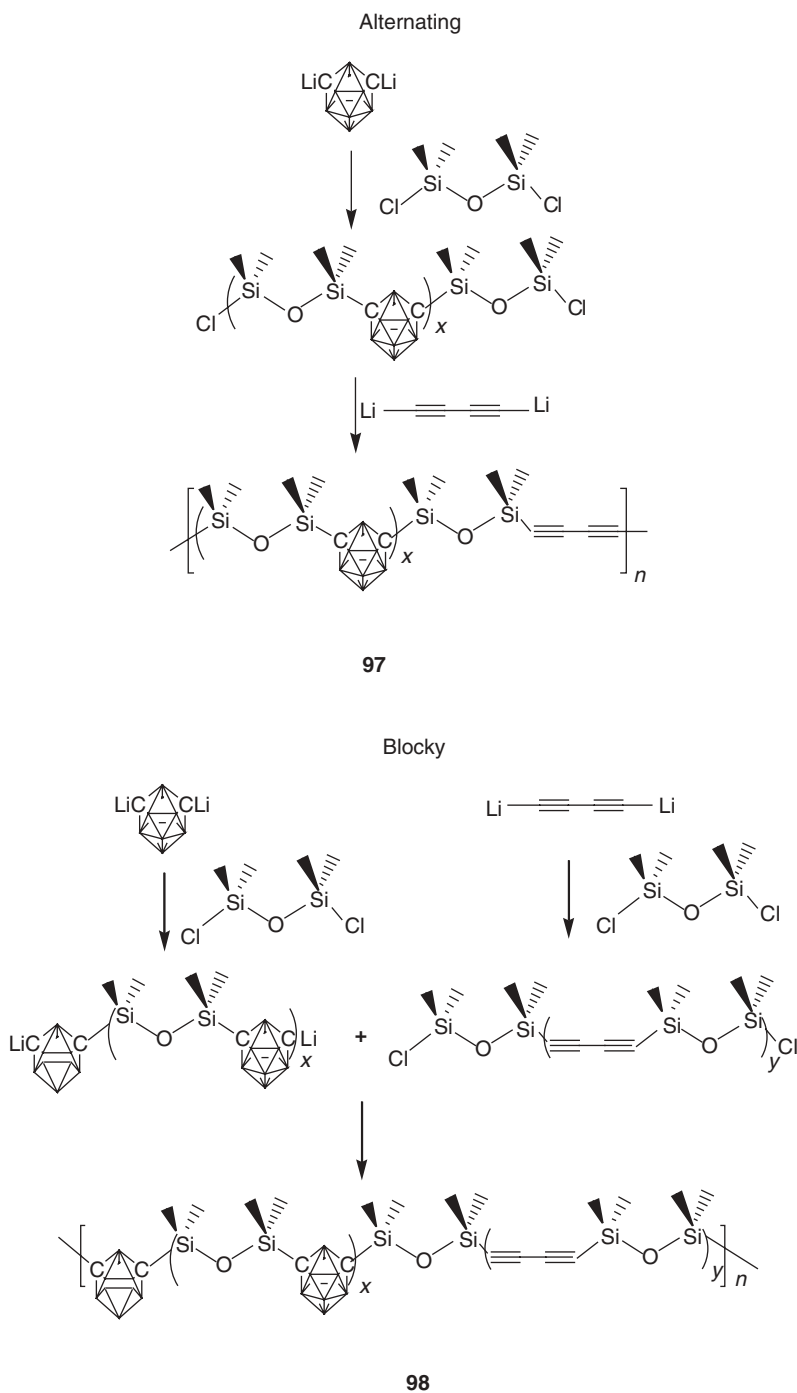
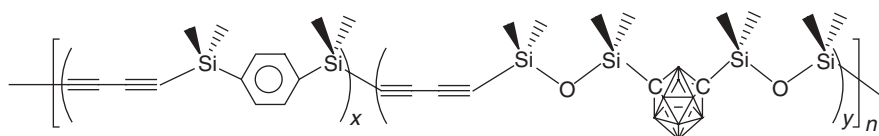


**Figure 60** The synthetic schemes for the diacetylene-diluted (a) alternating (**97**) (left) and (b) blocky poly(*m*-carborane-disiloxane-diacetylene)s (**98**). (Adapted from ref. 127.)

56, 45, and 35°C for the 2:3:1, 4:5:1, and 9:10:1 ratios, respectively, demonstrating the utility of this method for the introduction of elastomeric properties in these materials.

A further improvement in the elasticity of these polymers was realized when the disiloxyl groups in the alternating and blocky type polymers were substituted with the more flexible trisiloxyl groups.<sup>128</sup> The  $T_g$  values of the cured networks produced from the blocky and alternating set of polymers with ratios of 10:9:1, 5:4:1, and 3:2:1 were -49, -34, and -27°C, and -46, -39, and -30°C, respectively. The thermal stabilities of the cross-linked networks were analyzed thermogravimetrically by heating to 1000°C in N<sub>2</sub>. For a given siloxane:carborane:diacetylene ratio, the char yields were discovered to be about 4–6% higher for the blocky type of copolymers when compared to the alternating type of copolymers.

The synthesis of block polymers of diacetylene–silarylene and diacetylene–carboranylenesiloxane polymers (**99a–e**) (Fig. 61) by the polycondensation reaction of 1,4-dilithiobutadiyne with 1,4-bis(dimethylchlorosilyl) benzene and/or 1,7-bis(tetramethylchlorodisiloxane)-*m*-carborane have been reported by Sundar and Keller.<sup>129</sup> These polymers are a hybrid between the carboranylenesiloxane and silarylene-siloxane polymers and have high char yields (up to 85%) at 1000°C in N<sub>2</sub> and in air, reflecting the thermal stabilizing effects of the carborane and aromatic units in the polymeric backbone.



**99a–e**

a:  $x = 1, y = 0$ ; b:  $x = 3, y = 1$ ; c:  $x = 1, y = 1$ ; d:  $x = 1, y = 3$ ; e:  $x = 0, y = 1$ .

**Figure 61** The hybrid silarylene-siloxane/carboranylenesiloxane polymers, **99a–e**. (Adapted from ref. 129.)

In addition to their utility as cross-linking sites, the diacetylene units in **95** have been used for functionalization with organometallic moieties yielding pyrolyzable precursors of nanomaterials with diverse conducting characteristics. In a recent report, Kolel-Veetil and Keller have utilized the substitution reaction of **95** with cyclopentadienylmolybdenum tricarbonyl dimer, Cp<sub>2</sub>Mo<sub>2</sub>(CO)<sub>6</sub>, containing labile carbonyl ligands for the production of superconducting nanoparticles of β-Mo<sub>2</sub>C.<sup>130</sup> When **95** and Cp<sub>2</sub>Mo<sub>2</sub>(CO)<sub>6</sub> were reacted at unimolar concentrations in tetrahydrofuran at 80°C, an oligomeric product mixture containing partially reacted, completely reacted, and unreacted diacetylene groups was observed to form (Fig. 62). The unreacted and partially reacted diacetylene units in the metal-derivatized oligomeric mixture were utilized further for the cross-linking reaction leading to tight cross-linked matrixes in which Mo moieties were spatially confined following the liberation of labile carbonyl and cyclopentadienyl ligands. This Mo-containing

cross-linked network, on pyrolysis to 1000°C, was observed to yield nanoparticles of superconducting  $\beta$ -Mo<sub>2</sub>C nanoparticles ( $T_c = 8$  K) and multiwalled carbon nanotubes in an amorphous matrix of unidentified molybdenum compounds of boron and silicon (Fig. 62). In light of this result, the production of various nanomaterials of metallic carbides, borides, and silicides by the pyrolysis of the appropriate metal derivatives of **95** seems possible.

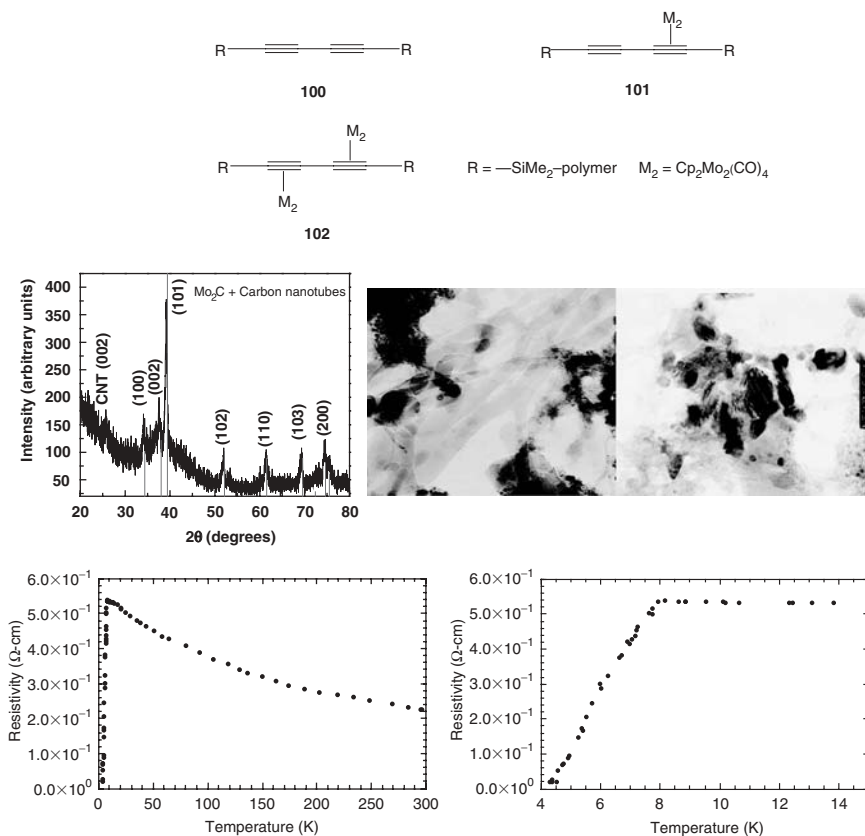


**Figure 62** The unreacted (**100**), partially reacted (**101**), and completely reacted (**102**) diacetylene group-containing oligomers in the product from the reaction between **95** and  $\text{Cp}_2\text{Mo}_2(\text{CO})_6$  (top). The X-ray diffraction spectrum (middle, left), TEM micrographs (middle, right), and conductivity plots (bottom) of the product from the reaction between **95** and  $\text{Cp}_2\text{Mo}_2(\text{CO})_6$  after pyrolysis to 1000°C. (Adapted from ref. 130.)

The original  $\text{FeCl}_3$ -catalyzed condensation reaction strategy has been exploited recently by Patel and co-workers for the synthesis of poly(*m*-carborane-siloxane) rubbers (**103**) (Fig. 63) in the reactions between dimethoxy-*m*-carborane terminated monomers and dichlorodimethylsilane.<sup>131</sup> They have also synthesized similar polymers

where Si–Me groups have been substituted either with phenyl or vinyl groups. While the unmodified polymer had some crystallinity, the modified polymers were observed to be amorphous with good elastomeric properties. A detailed account of their research is present in Chapter 2 of this book.

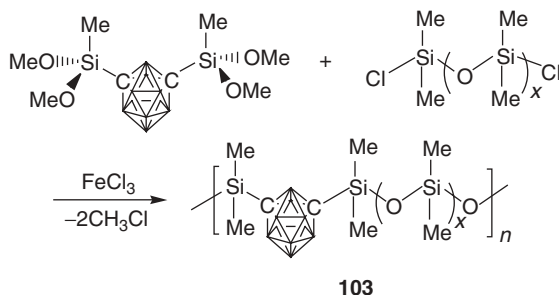


**Figure 63** The poly(*m*-carborane-siloxane) rubbers (**103**) synthesized by the  $\text{FeCl}_3$ -catalyzed condensation reaction between dimethoxy-*m*-carborane terminated monomers and dichlorodimethylsilane. (Adapted from ref. 131.)

The ubiquitous hydrosilation reaction, popular especially in silicone manufacturing,<sup>132</sup> has been utilized by Houser and Keller for the synthesis of the networked polymers (**104**) (Fig. 64) from the reaction of the 1,7-bis(vinyltetramethyldisiloxy)-*m*-carborane monomer with the polymeric crosslinker, poly(methylhydrosiloxane).<sup>133</sup> The reactions were catalyzed by the Speier's catalyst,  $\text{H}_2\text{PtCl}_6$ . Three samples were

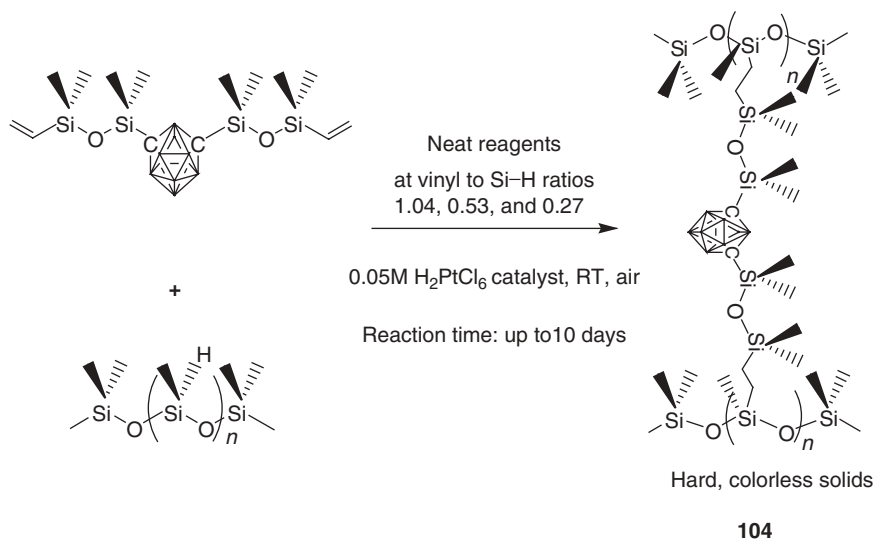


**Figure 64** Hydrosilation reactions between 1,7-bis(vinyltetramethyldisiloxy)-*m*-carborane monomer and the polymeric cross-linker, poly(methylhydrosiloxane), producing hard, colorless networked plastics. (Adapted from ref. 133.)



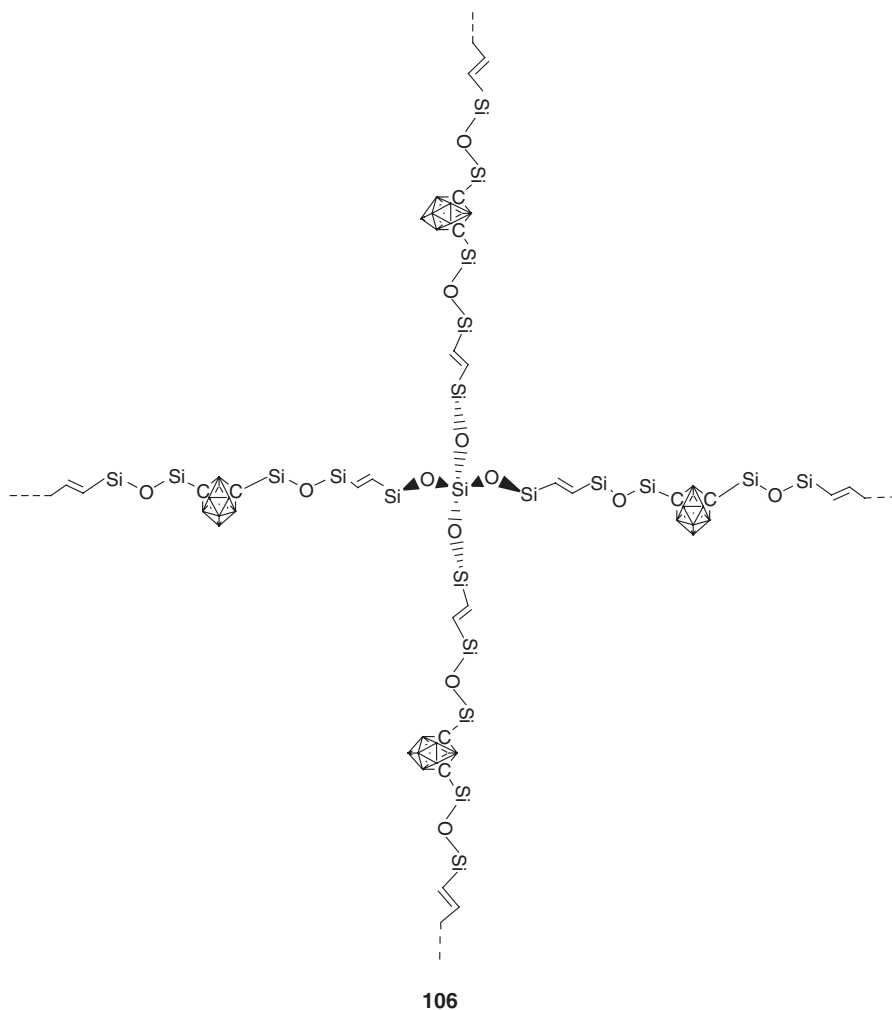


**Figure 65** (Continued)

pletely saturated (**107**) (Fig. 65) set of networked polymers. The Karstedt catalyst was preferred over the Speier's catalyst for its greater activity due to its ability to form finer colloidal Pt particles during the catalyst initiation step.<sup>135</sup> The reactions proceeded rapidly to generate elastomeric networked polymers in contrast to the slow formation of the hard, colorless solid **104**. The flexible and transparent films of the saturated elastomeric networked polymers (**105**) from the vinyl monomer had  $T_g$  values below  $-35^\circ\text{C}$ , while the  $T_g$  values of the films (**106** and **107**) formed from the ethynyl monomers were below  $0^\circ\text{C}$ . Preliminary studies of the three elastomeric products have indicated that the materials retain their elastomeric nature on extended use (3–4 days) in air at a temperature of  $200^\circ\text{C}$ . The clarity of the products was also

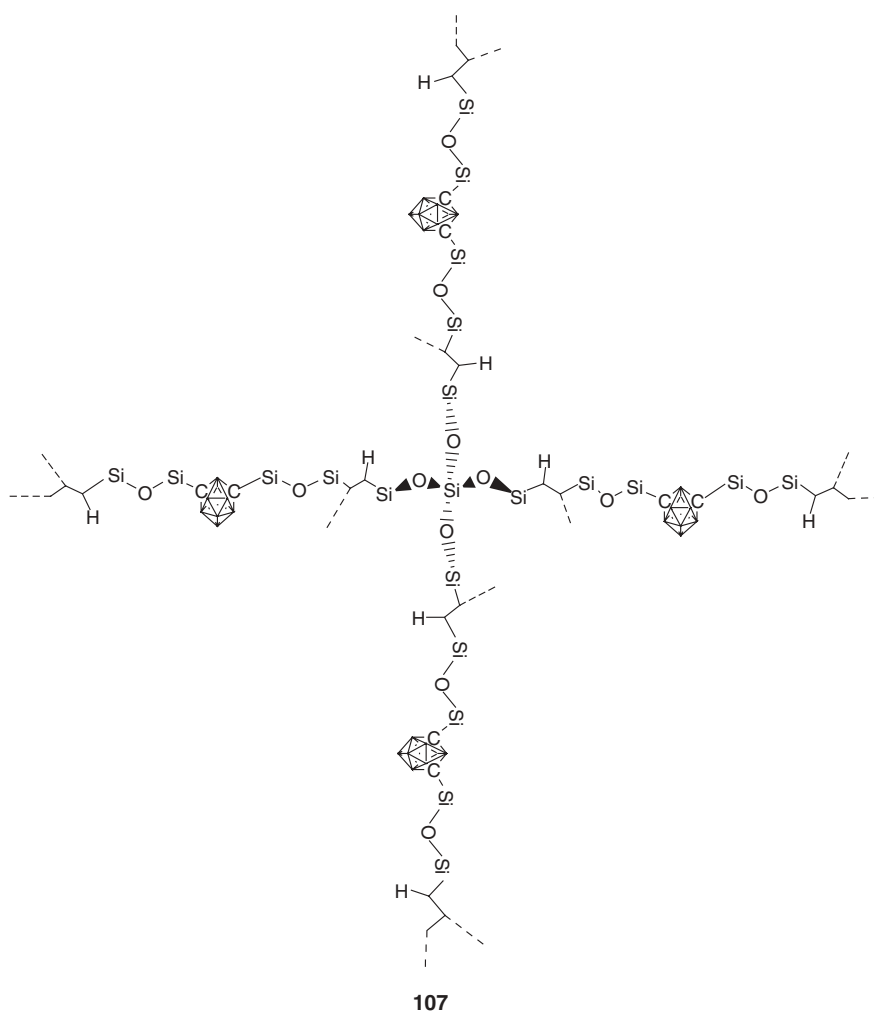
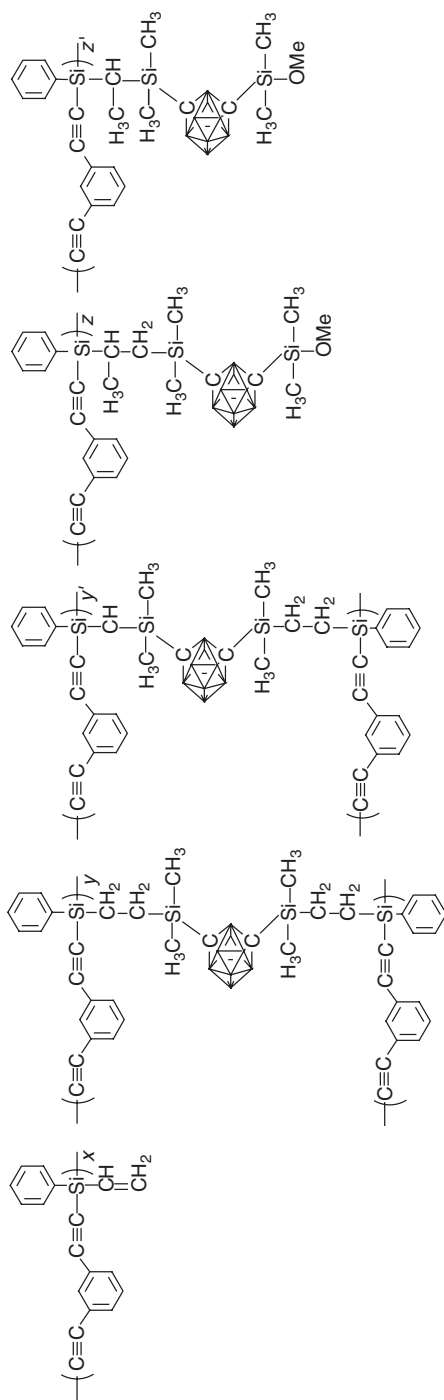


**Figure 65** (Continued)

observed to have been maintained during such exposures. At temperatures above 350°C, these materials were observed to lose their clarity, presumably due to further cross-linking reactions of Si-bound methyl groups. The degradation temperature defined as the temperature at 5% weight loss of the material for the three networks was determined to be in the range of 500–550°C.

Ando and co-workers have reported the synthesis of a silyl-carborane hybrid diethynylbenzene-silylene polymer (**108**) (Fig. 66) possessing high thermal stability.<sup>136</sup> The polymer contained Si and  $\text{—C}\equiv\text{C—}$  group in the main chain and *m*-carborane and vinyl groups in the side chain. The 5% weight-loss temperature of the cured polymer in air was over 1000°C as determined by thermogravimetric analysis.



108

**Figure 66** The thermooxidatively stable silyl-carborane hybrid diethynylbenzene-silylene polymer **108** containing various carbon-carbon unsaturations. (Adapted from ref. 136.)

During heat treatment between 250 and 500°C, the formation of three-dimensional networks by diene and addition reactions of Ph—C≡C, C≡C, and *m*-carborane groups in this system has been characterized by  $^{11}\text{B}$  MQ-MAS NMR and  $^{13}\text{C}$  and  $^{29}\text{Si}$  CP-MAS NMR methods.

### iii. Conducting Polymers Containing Carborane Clusters

Carboranes due to their exceptional characteristics in both their neutral and anionic forms have evoked extreme interest in their use as doping agents and covalently bound functionalities in conducting polymers.<sup>137</sup> Teixidor and co-workers have reported the use of an organometallic complex of a carborane  $\text{Cs}[\text{Co}(\text{C}_2\text{B}_9\text{H}_{11})_2]^-$  (**109**) (Fig. 67) as doping agents in organic conducting polymers.<sup>138</sup> The synthesis of the polypyrrole, (PPy)[Co(C<sub>2</sub>B<sub>9</sub>H<sub>11</sub>)<sub>2</sub>] polymer, by the electropolymerization of the pyrrole monomer in the presence of **109** has been achieved. On electropolymerization, the carborane clusters were found to be incorporated and uniformly distributed in the PPy polymer. The incorporation of the carborane clusters resulted in a dramatic improvement in the overoxidation threshold (1.25 V) of the polymer when compared to other doping anions (commonly near 0.6 V) such as Cl<sup>-</sup>, (NO<sub>3</sub>)<sup>-</sup>, and so on.

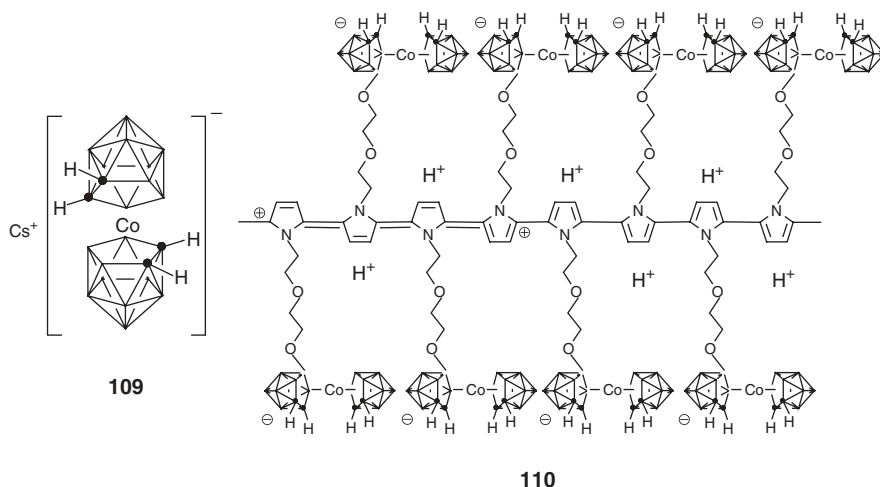


**Figure 67** The cobaltabisdicarbollide  $\{\text{Cs}[\text{Co}(\text{C}_2\text{B}_9\text{H}_{11})_2]^-$  (**109**) that was doped in or covalently bound to a pyrrole monomer to produce conducting polymers (**110** being one of them). (Adapted from refs. 138 and 139.)

The Teixidor team further improved upon this chemistry by covalently linking units of **109** to the polypyrrole monomer prior to electropolymerization.<sup>139</sup> A  $[3,3'-\text{Co}(\text{C}_2\text{B}_9\text{H}_{11})_2]^-$  anion was covalently bound to a pyrrole via a spacer through one of its boron atoms by the reaction of the species  $[3,3'-\text{Co}(8-\text{C}_4\text{H}_8\text{O}_2-1,2-\text{C}_2\text{B}_9\text{H}_{10})(1',2'-(\text{C}_2\text{B}_9\text{H}_{11})_2)]^-$  with potassium pyrrole, as functionalization through

its carbon atoms proved impractical due to poor yield of the product. This covalently carborane-bound polymer (**110**) (Fig. 67) did not exhibit overoxidation in the 0–1.8 V range and was found to be better than the noncovalently linked system.<sup>139</sup>

Further studies by this group centered on comparisons of the overoxidation resistance limit (ORL) of polypyrrole materials doped with monoanionic borane clusters  $[B_{12}H_{11}NH_3]^-$  or dianionic borane  $[B_{12}H_{12}]^{2-}$  or carborane  $[Co(C_2B_9H_{11})_2]^{2-}$  clusters. The monoanionic boron clusters were found to offer the highest stability to the PPy doped materials against overoxidation than any other charged dopant. They were also found to be far superior to the dianionic clusters in their ability to impart an ORL rise.<sup>140</sup>

The synthesis of the first covalently attached carborane-containing polypyrrole was reported by Fabre and co-workers.<sup>141</sup> The initial step involved the production of 2-*t*-butoxycarboranylpyrrole from 1-allyl-2-methyl-*o*-carborane by the addition of phenylsulfonyl chloride, followed by oxidation, dehydrochlorination and condensation under Barton–Zard conditions. This product was cleaved and decarboxylated using 2% TFA/THF to produce **111** (Fig. 68) in 70% overall yield. The monomer 3-carboranymethyl-pyrrole (**111**) (**112** being its *nido* version) (Fig. 68) was subsequently electropolymerized to produce the polymer (**115**) (Fig. 68), which exhibited an overoxidation threshold of 1.5 V and a high hyperpolarizability ( $\beta$ ) value.

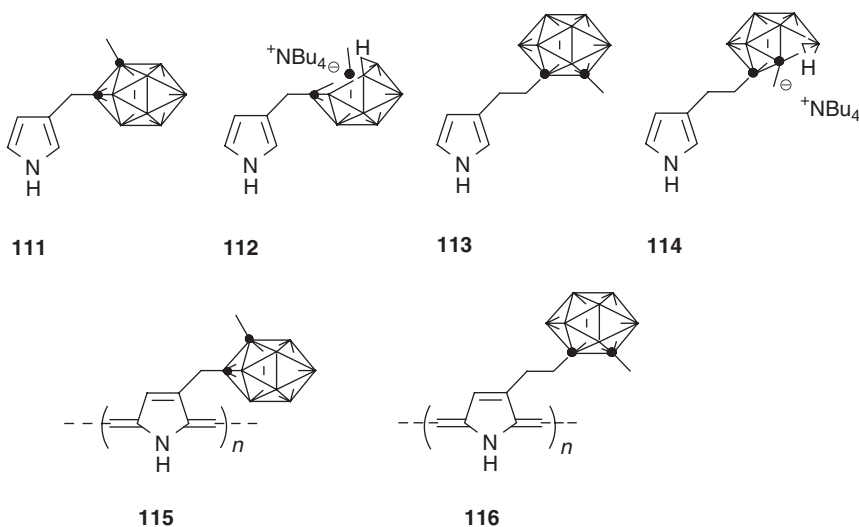


**Figure 68** The neutral *ortho*- or anionic *nido*-carborane attached pyrrole molecule (**111**, **112**, **113**, and **114**) used in the synthesis of conducting organic polymers **115**, **116**, etc. (Adapted from refs. 141 and 142.)

The Fabre group has further developed the chemistry of covalently attached carborane-containing polypyrrole by synthesizing pyrrole derivatives that are covalently

linked to neutral *ortho*- or anionic *nido*-carborane cage via an ethylene spacer arm attached to the pyrrole molecule [3-(2-methyl-*o*-carboranyl)ethyl-1H-pyrrole (**113**) and **114** (being the *nido* version of **113**)] (Fig. 68) at one of its ring 3-(2-methyl-*o*-carboranyl)ethyl-1H-pyrrole (**113**) carbons.<sup>142</sup> The electrochemical studies under anodic oxidation of both of the polymers (**115** and **116**) (Fig. 68) revealed that while the neutral carborane-containing PPy exhibited conductivity, the anionic derivative caused the passivation of the electrode.

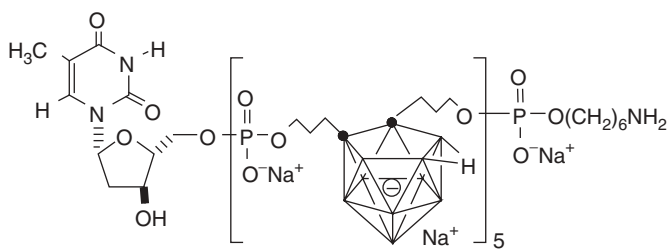
The assembly of a soluble, air-stable, supramolecular structure from the metal-containing porphyrin-carborane moiety  $\{\text{Cp}^*\text{Ir}[\text{S}_2\text{C}_2(\text{B}_{10}\text{H}_{10})]\}$ , through bridging via nitrogen-based organic spacers has been reported.<sup>143</sup> In the resulting polymeric material,  $\{\{\text{Zn-TPyP}\}[\text{Cp}^*\text{Ir}\{\text{S}_2\text{C}_2(\text{B}_{10}\text{H}_{10})\}]_2 \cdot 6(\text{CHCl}_3)\}_n$ , the strong luminescence of the zinc porphyrin was observed to be completely quenched due to an intramolecular electron transfer between the porphyrin site and the binding cluster in the phthalocyanine site to the photoexcited singlet state.

#### *iv. Carborane Polymers in Medicine*

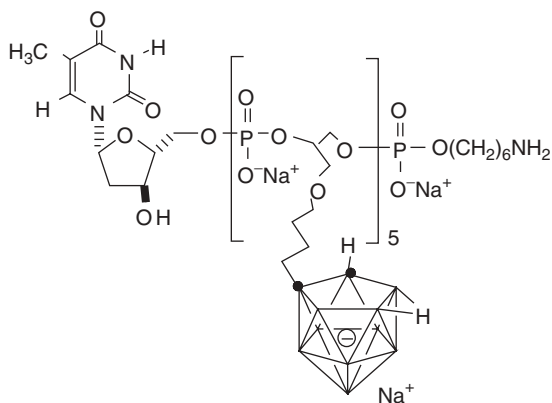
Boron exists in nature in the form of two stable isotopes;  $^{10}\text{B}$  (abundance 19.9%) and  $^{11}\text{B}$  (80.1%), with the latter's nucleus possessing an extra neutron.<sup>2</sup> Boron-10 nucleus is the only *light* element that is capable of binding a slow neutron (or thermal neutron) to yield an excited boron-11 nucleus. This unstable nucleus undergoes fission to form a lithium-7 nucleus and a helium-4 nucleus along with a gamma photon. The neutron-capturing ability of boron has facilitated the use of its boron-10 nucleus for localized treatment of cancers. The use of boron compounds for the treatment of cancer was first proposed by Locher in 1936.<sup>144</sup> In the therapy, known as boron neutron-capture therapy (BNCT), a tumor target is selectively loaded with high concentrations of stable boron-10 ( $^{10}\text{B}$ ) isotope, followed by irradiation with thermal neutrons. The heavy ions ( $^7\text{Li}$ ,  $^4\text{He}$ ) emitted on irradiation have a limited translational path (approximately one cell diameter), and hence, the BNCT-produced cytotoxicity is limited only to the tumor target that contains elevated levels of the  $^{10}\text{B}$  nuclei.

Since the initial discovery by Locher, Hawthorne and co-workers, among others, have pioneered the use of  $^{10}\text{B}$  nucleus in cancer therapy research. Lately, the research in BNCT has centered on the utilization of immunoproteins as vehicles to transport carborane nuclei to targeted cancerous cells. In a recent report, the tethering of oligomeric *nido*-carboranyl phosphodiester to an engineered immunoprotein (a chimeric IgG3 protein) at its exposed cysteine residues was achieved by the coupling of two boron-rich phosphodiester to sulfhydryls (of cysteine) that had been introduced to the  $\text{C}_H2$  domain of the IgG3 protein.<sup>145</sup> The resulting boron-rich immunconjugates (**117** and **118**) (Fig. 69) were found to have promising *in vitro* and *in vivo* characteristics for boron delivery.

Hawthorne and co-workers have reported the selective uptake of homogeneous fluorescein-labeled *nido*-carboranyl oligomeric phosphate diesters (*nido*-OPDs) by cell nuclei within 2 h after microinjection. The location in the cell of *nido*-OPDs uptake was found to depend on the location of the carboranyl moiety in the *nido*-OPDs. When the carborane cage was located on a side chain attached to the oligomeric



117



118

**Figure 69** The boron-rich immunoconjugates (**117** and **118**) obtained by the tethering of oligomeric *nido*-carboranyl phosphodiester to an engineered immunoprotein (a chimeric IgG3 protein). (Adapted from ref. 145.)

backbone (**120**) (Fig. 70), the *nido*-OPDs were found to distribute between both the cytoplasm and the nucleus. However, when the carborane cage was located along the oligomeric backbone (**119**) (Fig. 70), the *nido*-OPDs were found to remain primarily in the nucleus. In comparative studies, the *ortho*-OPDs (**121**) (Fig. 70) were found to be not as effective as the *nido*-OPDs for boron delivery.<sup>146</sup>

Several dendrimeric borane and carborane systems have been developed for use as boron-delivery agents.<sup>147</sup> *In vitro* tests with a boronated dendrimer-epidermal growth factor bioconjugates indicated that they are endocytosed, resulting in the accumulation of boron in lysosomes.

Thomas and Hawthorne have synthesized unimolecular, nanospherical boron-rich dodeca(carboranyl)-substituted closomers (**122**) (Fig. 71) for their potential application as drug-delivery platforms for BNCT.<sup>148</sup> The substituted closomers were synthesized by reacting carborane acid chloride with the dodecahydroxy dodecaborate closomer in methylene chloride by utilizing a threefold excess of the former in triethylamine. The twelve pendant *closo*-1,2-carborane units in the closomer could

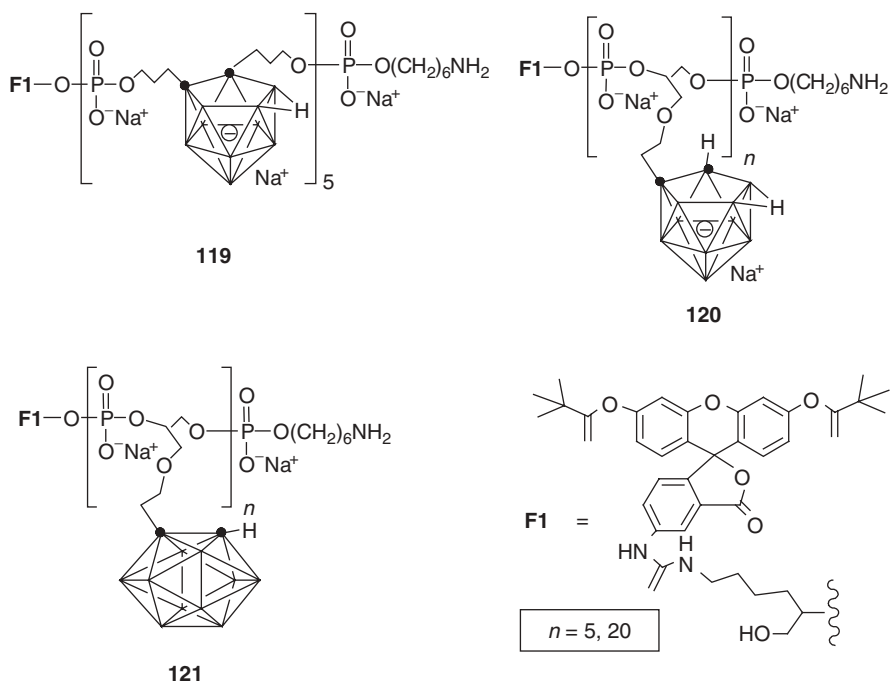


**Figure 70** The fluoresein (F1)-labeled *nido*-OPDs (**119** and **120**) and *ortho*-OPDs (**121**) boron delivery systems. (Adapted from ref. 146.)

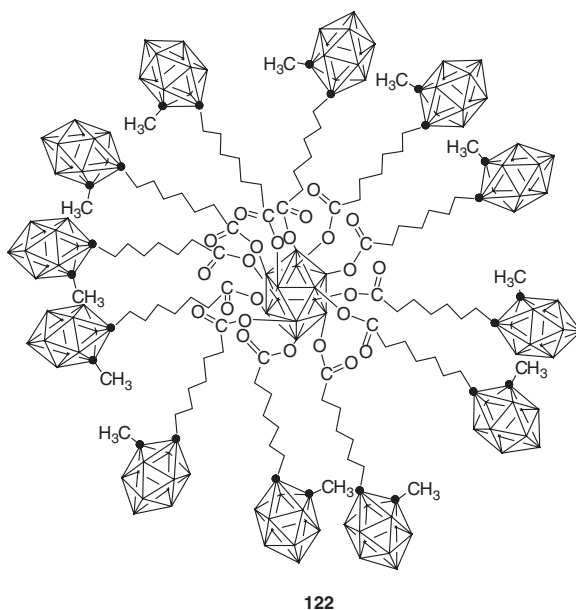


**Figure 71** Nanospherical boron-rich dodeca(carboranyl)-substituted closomers (**122**) with potential for boron delivery in BNCT. (Adapted from ref. 148.)

also be degraded to anionic *nido*-7,8-carborane cages by refluxing with a large excess of CsF in absolute ethanol for 4 days.

Qualmann and Kessels have reported the synthesis of carborane-containing lysine dendrimers (**123**) (Fig. 72), with a better defined number of boron atoms, for use as protein labels in immunocytochemistry using electron microscopic techniques such as electron energy loss spectroscopy (EELS) and electron spectroscopic imaging (ESI).<sup>149</sup>

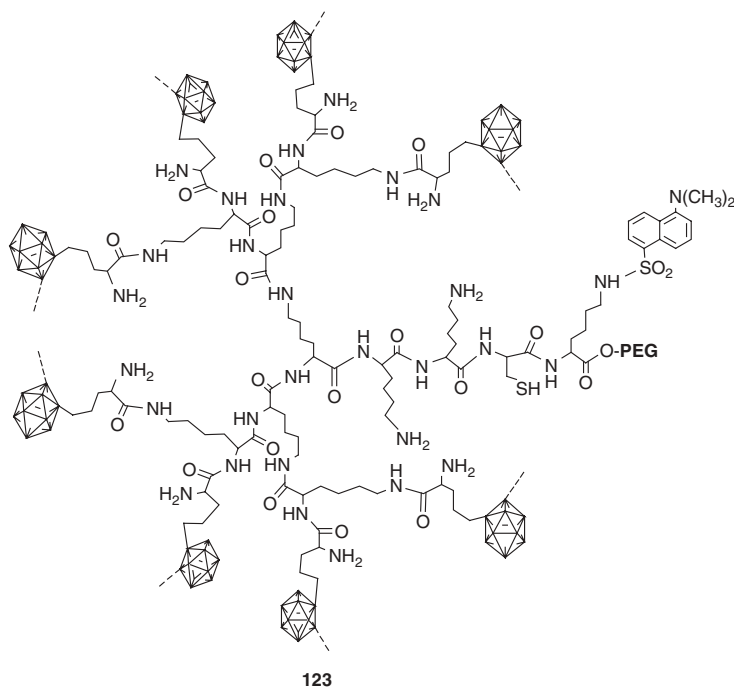


**Figure 72** Carborane-containing lysine dendrimers (**123**), with a defined number of boron atoms, for use as protein labels. (Adapted from ref. 149.)

Several reports of carboranylated porphyrins have appeared for utilization in the BNCT of cancer.<sup>150</sup> The examples include both *nido*- (**126**) (Fig. 73) and *closo*-carborane cluster-containing (**124** and **125**) (Fig. 73) materials. Metal-free *nido*-carboranylporphyrins were able to deliver a higher amount of boron to cells than the corresponding zinc complexes.

#### *v. Carborane Polymers Used in the Production of High-Performance Fibers*

Carborane-derived polymers have been used in the production of boron carbide ceramic fibers and matrices. Polyhexenyldodecaborane (**128**) (Fig. 74), a dodecaborane-based polymeric material, has been reported to be an ideal source for the production of nanostructured boron carbide materials by new nanoscale templating methods utilizing porous alumina templates having a thickness of 60  $\mu\text{m}$  and a nominal pore

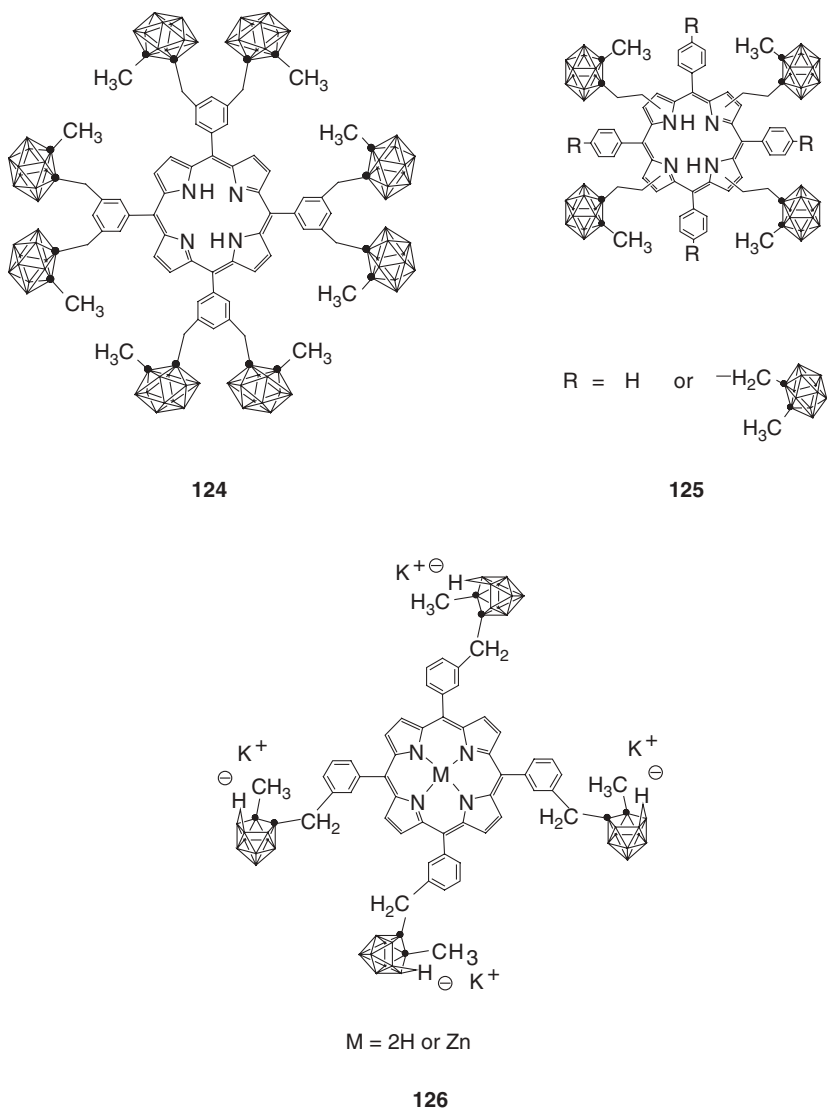


**Figure 73** The *closo*- (**124** and **125**) and *nido*- (**126**) carborane cluster-containing porphyrins for BNCT. (Adapted from ref. 150.)

size of  $\sim 250$  nm.<sup>151</sup> The monomeric building block, 6-hexynyl-decaborane (**127**) (Fig. 74), was constructed from a  $\text{Cp}_2\text{Ti}(\text{CO})_2$ -catalyzed reaction of hexadiene and decaborane. The polymerization was then achieved by employing the  $\text{Cp}_2\text{ZrMe}_2/\text{B}(\text{C}_6\text{F}_5)_3$  catalyst.



**Figure 74** The polyhexenyldecaborane (**128**) used in the production of nanostructured boron carbide materials by nanoscale templating methods utilizing porous alumina templates. (Adapted from ref. 151.)

Other monomeric precursors similar to 6-hexynyl-decaborane such as 6-norbornenyl-decaborane (**129**) and 6-cyclooctenyl-decaborane (**131**) (Fig. 75) underwent ROMP in the presence of either first- or second-generation Grubbs catalysts to produce the corresponding poly(norbornenyl-decaborane) (**130**) (Fig. 75) and poly(cyclooctenyl-decaborane) (**132**) (Fig. 75) with  $M_n > 30$  kDa and polydispersities between 1.1 and 1.8.<sup>152</sup> Electrostatic spinning and pyrolysis of poly(norbornenyl-decaborane) was discovered to produce nanoscale, free-standing porous boron-carbide/carbon, ceramic fiber matrices.<sup>153</sup>

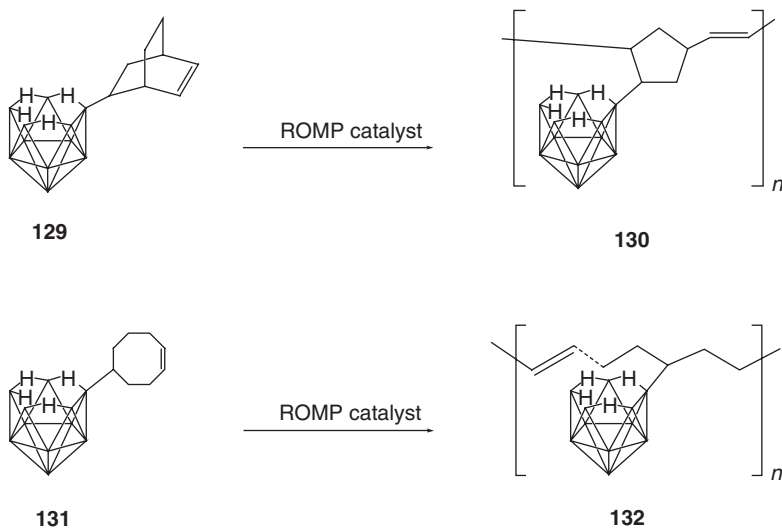


**Figure 75** The conversion of the monomeric precursors, 6-norbornenyl-decaborane (**129**) and 6-cyclooctenyl-decaborane (**131**), by ROMP into poly(norbornenyl-decaborane) (**130**) and poly(cyclooctenyl-decaborane) (**132**). (Adapted from ref. 152.)

The incorporation of decaborane into polycarbosilane-based polymers has been used in the densification of the polymer-derived SiC fibers. Improved densification resulted in the formation of fibers with density as high as 2840 kg/m<sup>3</sup> corresponding to an increase of 89%.<sup>154</sup>

## vi. Miscellaneous Carborane Polymers

### a. Carborane Polymers of Polyetherketones

Colquhoun and Wade have reported the synthesis of fire-resistant carborane-containing polyetherketones [133, 134, and 135 (*meta*-derivatives) and 136, 137, and 138 (*ortho*-derivatives)] (Fig. 76) from the trifluoromethanesulfonic acid-promoted polycondensation reaction of various bis(4-phenoxyphenyl) derivatives of *meta*- or *ortho*-carborane with aromatic or aliphatic dicarboxylic acids.<sup>155</sup> The weight-average molecular weights of the polymers ranged between 50,000 and 170,000. On thermolysis to 850°C under nitrogen or air, these polymers were observed to lose only 7 or 3% of the weight, respectively, demonstrating their exceptional thermal stability and extreme resistance to combustion.

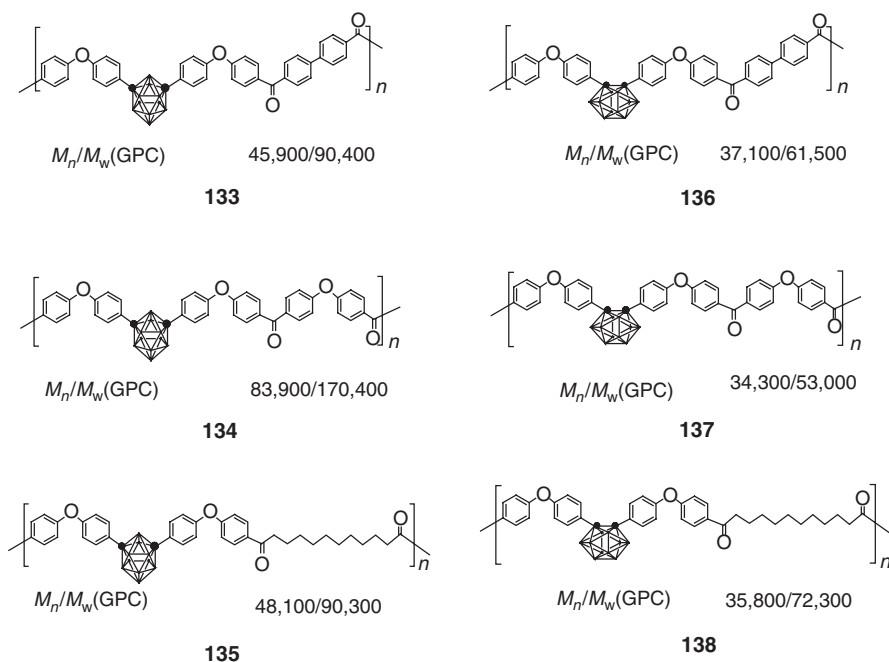


**Figure 76** Fire-resistant carborane-containing polyetherketones [133, 134 and 135 (*meta*-derivatives) and 136, 137 and 138 (*ortho*-derivatives)]. (Adapted from ref. 155.)

The trifluoromethanesulfonic acid (TFSA)-promoted polycondensation reaction between diarylcarborane dicarboxylic acid (139) and diaryl carborane diether

monomer acid (**140**) (Fig. 77) was utilized in the construction of a similar carborane-containing polyetherketone acid (**141**) (Fig. 77) with two ortho-carborane units in a repeating unit.<sup>156</sup> The polymer was found to lose a much smaller proportion of its weight on pyrolysis up to 1000°C compared to conventional aromatic ether-ketones (e.g., ICI's VICTREX).

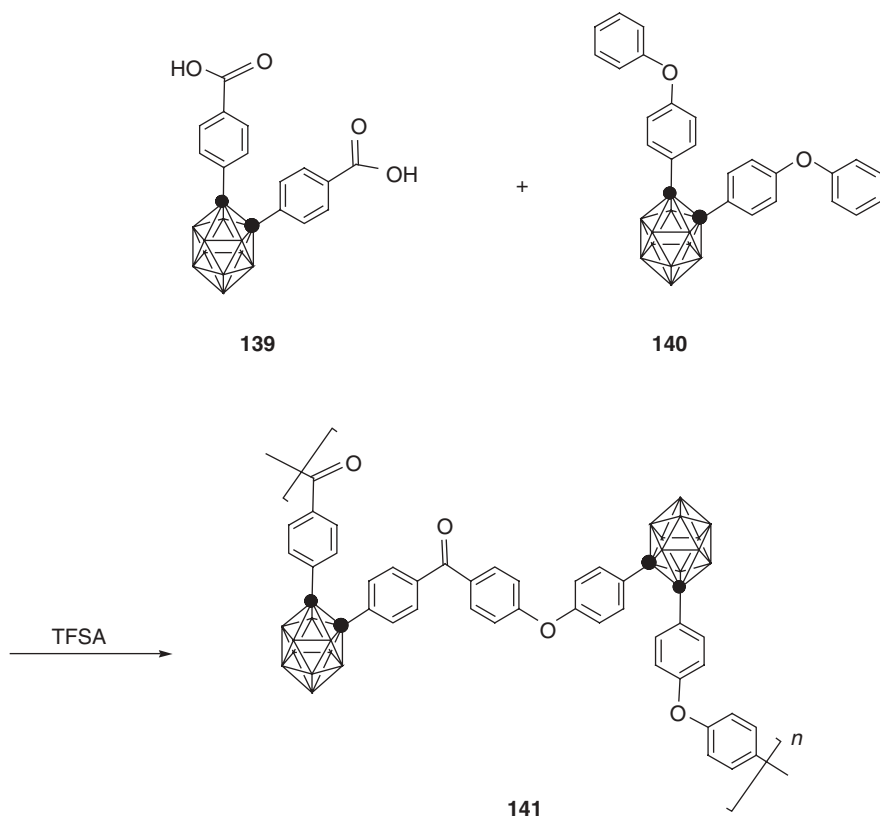
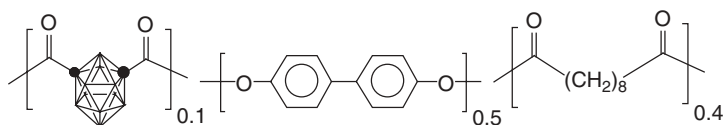


**Figure 77** The trifluoromethanesulfonic acid-promoted polycondensation reaction between diarylcaborane dicarboxylic acid (**139**) and diaryl carborane diether monomer acid (**140**) to yield the polyetherketone acid, **141**. (Adapted from ref. 156.)

A polycondensation reaction of 4,4'-dihydroxybiphenyl, sebacic, and *m*-carboranedicarboxylic acids was reported to produce a carborane-containing polymer (**142**) (Fig. 78) that led to the production of a new columnar phase at elevated temperatures.<sup>157</sup> This new phase was formed in addition to the crystalline and liquid crystalline smectic phases typically formed from only 4,4'-dihydroxybiphenyl and sebacic acids.

#### *b. Carborane Polymers for Use in Catalytic Reactions*

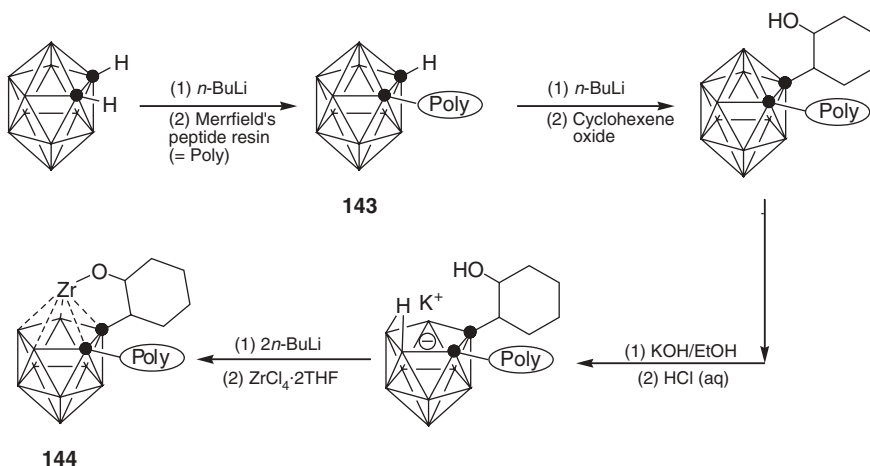
The polymer-supported *o*-carborane, **143**, was utilized further for cage decapitation, deprotonation, and reaction with  $\text{ZrCl}_4 \cdot 2\text{THF}$  to generate a polymer-supported



142

**Figure 78** The carborane-containing polymer (**142**) obtained from the polycondensation reaction of 4,4'-dihydroxybiphenyl, sebacic, and *m*-carboranedicarboxylic acids. (Adapted from ref. 157.)

single-site polymerization catalyst (**144**) (Fig. 79). This catalyst was used for the polymerization of ethylene and vinyl chloride in toluene to give high molecular weight polyethylene [ $9.4 \times 10^3$  ( $M_w/M_n = 1.8$ )] and polyvinyl chloride [ $9.4 \times 10^3$  ( $M_w/M_n = 1.8$ )], respectively.<sup>158</sup>



144

**Figure 79** The polymer-supported *o*-carborane (**143**) utilized further for its decapitation, deprotonation and reaction with  $ZrCl_4 \cdot 2THF$  to generate a polymer-supported single-site polymerization catalyst (**144**) for the polymerization of ethylene and vinyl chloride. (Adapted from ref. 158.)

Carborane clusters, consisting of their  $B_{10}H_{10}$  portions, that have been grafted onto the surface of organometallic dendrimers have been reported.<sup>159</sup>  $B_{10}H_{10}$  has been linked to a terpyridine group in a ruthenium complex. The reaction of this complex with a tetra(terpyridine) core afforded a first-generation organometallic dendrimer (**145**) (Fig. 80).

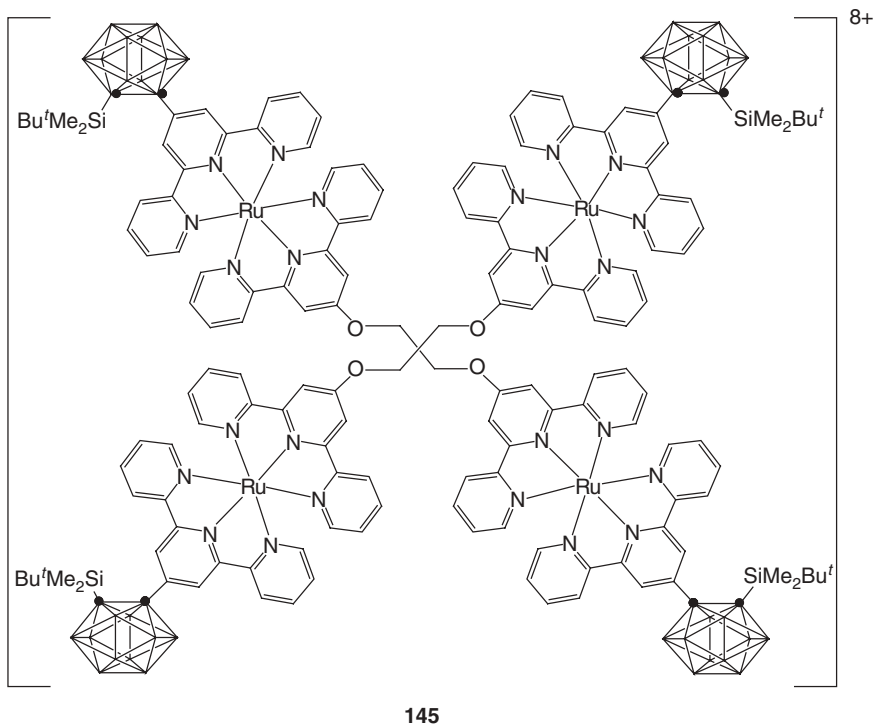


**Figure 80** A first-generation organometallic dendrimer (**145**) containing grafted carborane clusters on tetra(terpyridine) cores. (Adapted from ref. 159.)

### vii. Carborane Supramolecular Chemistry

The supramolecular chemistry of boron, as with other elements, has witnessed a spectacular explosion in its growth in recent times. Supramolecular chemistry, which deals with the chemistry and collective behavior of organized ensembles of molecules, has obtained one of its perfect assembling tools in the structurally symmetric carborane molecule. The supramolecular architectures produced from carboranes have included such varied examples as carboracycles, mercuracarborands, grid-shaped polymers, and coordination-driven polymers. Hawthorne and co-workers have developed a family of carboracycles (**146**, **147**, **148**, and **149**) (Fig. 81), from carborane icosahedra and bridging organic groups, as alluded to in a previous section, highlighting the suggested carborane–benzene analogy.<sup>160</sup> The organic bridging groups have included 1,3-trimethylene,  $\alpha,\alpha'$ -1,3-xylylene or  $\alpha,\alpha'$ -2,6-lutidylene, among others. These types of nanometer-scaled, structurally well-defined rigid molecules are expected to bridge the gap between discrete molecules and bulk materials.

Carboracycle systems (**150** and **151**) (Fig. 82) with aromatic urea as bridging groups have been constructed by Endo and co-workers.<sup>161</sup> The presence of ureas along with carboranes was expected to be useful for the construction of

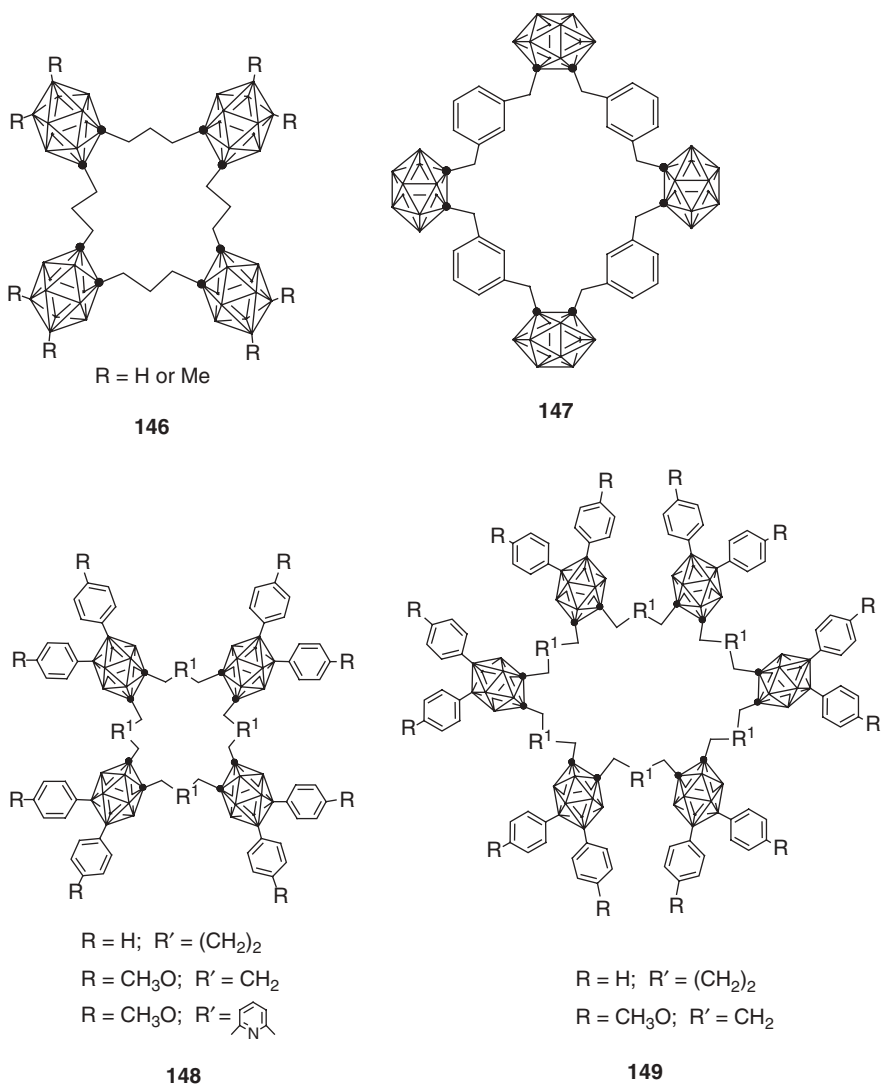
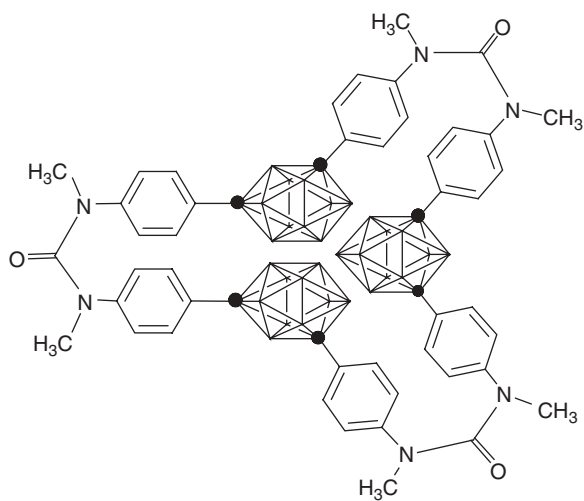


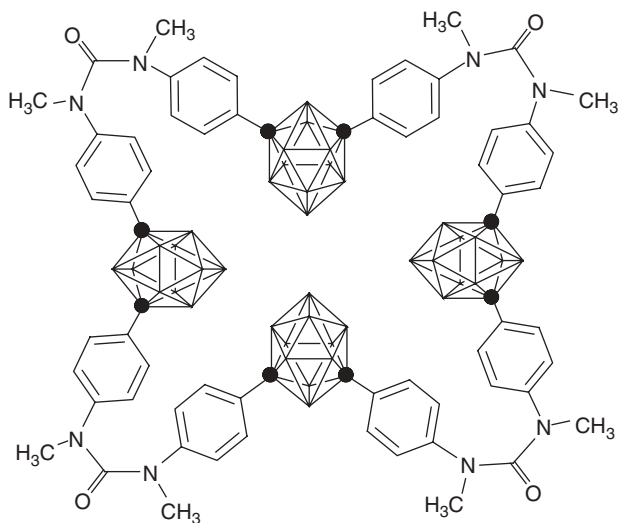
**Figure 81** A few examples (**146**, **147**, **148**, and **149**) from the extensive family of carboracycles. (Adapted from ref. 160.)

cyclic, layered, or helical molecules with both hydrophobic and hydrogen-bonding characters.

Grimes and co-workers have constructed similar cyclic metallocarborane oligomers with highly symmetric geometries such as squares, triangles, or rectangles for assembling them into extended systems.<sup>162</sup> These symmetric oligomers (**152**, **153**, **154**, and **155**) (Fig. 83) are expected to have useful electronic, optical, magnetic, and catalytic properties along with other properties.



150



151

**Figure 82** Carboracycle systems (**150** and **151**) with aromatic urea as bridging groups. (Adapted from ref. 161.)

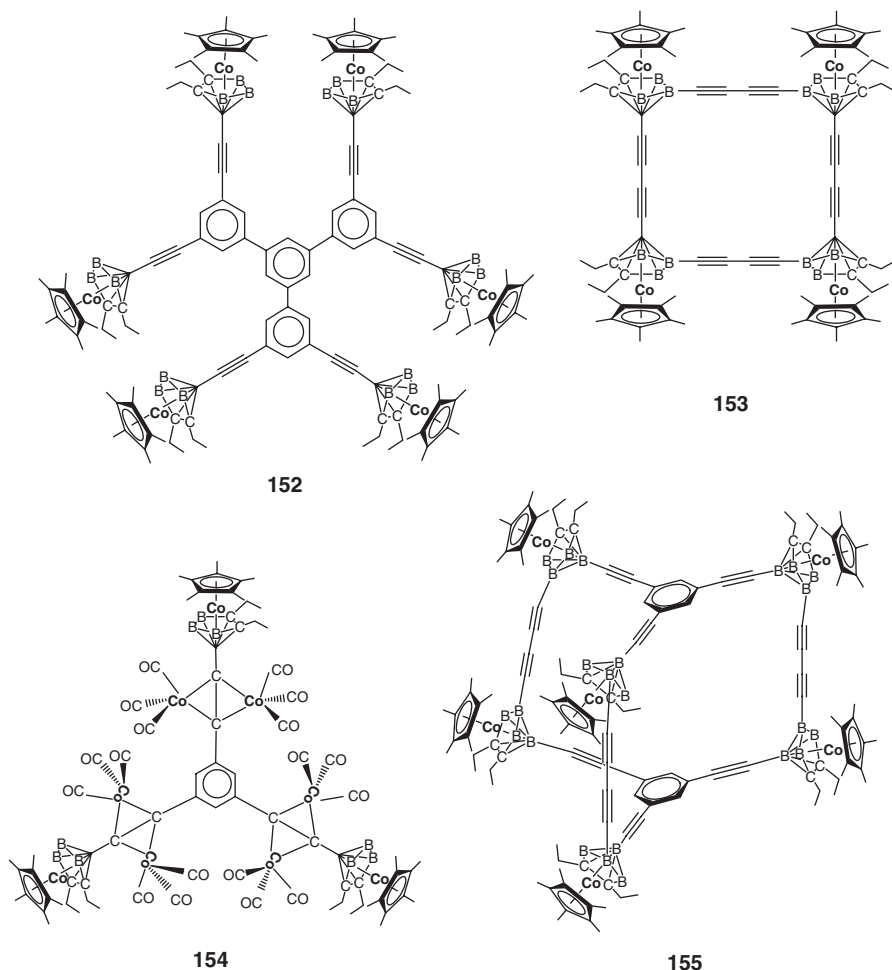


**Figure 83** Symmetric cyclic metallacarborane oligomers (**152**, **153**, **154**, and **155**) for assemblage into extended systems. (Adapted from ref. 162.)

Hawthorne and co-workers have also produced a series of macrocyclic Lewis acid hosts called mercuracarborands (**156**, **157**, and **158**) (Fig. 84) with structures incorporating electron-withdrawing icosahedral carboranes and electrophilic mercury centers. They were synthesized by a kinetic halide ion template effect that afforded tetrameric cycles or cyclic trimers in the presence or absence of halide ion templates, respectively.<sup>163</sup> These complexes, which can bind a variety of electron-rich guests, are ideal for catalytic and ion-sensing applications, as well as for the assembly of supramolecular architectures.

A molecular-size construction kit (**159**, **160**, and **161**) (Fig. 85) for the assembly of carborane-containing grid-shaped polymers has been developed by Michl and co-workers.<sup>164</sup> By synthesizing firmly connected, regular two-dimensional grid-shaped

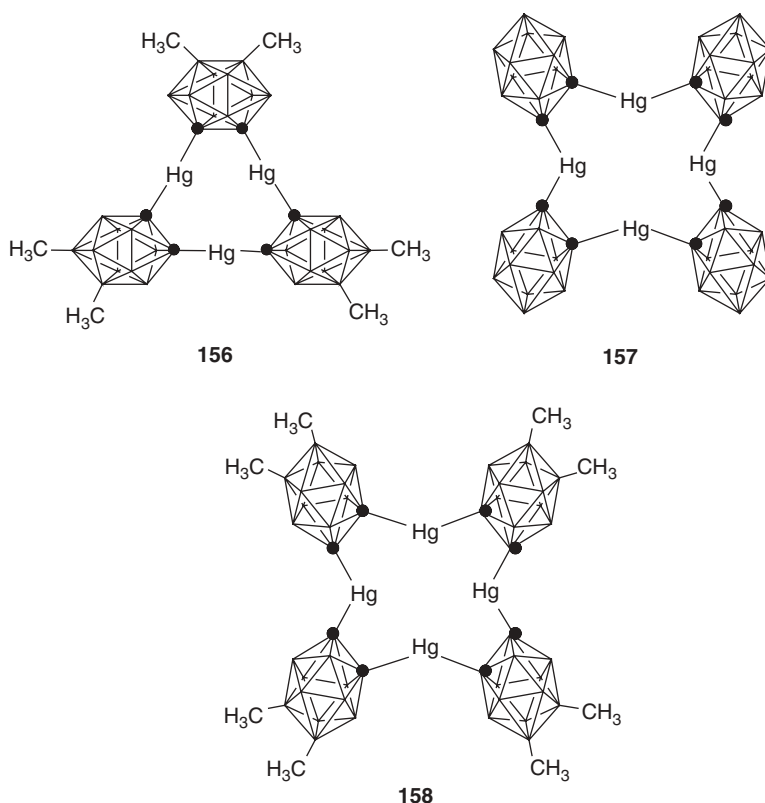


**Figure 84** Macrocyclic mercuracarborands (**156**, **157**, and **158**) with structures incorporating electron-withdrawing icosahedral carboranes and electrophilic mercury centers. (Adapted from ref. 163.)

polymers with a trigonal, square, or hexagonal lattice, it was anticipated that the chance existed for the covalent attachment of additional regular grid layers one at a time on top of the first layer. Thus, as an ultimate goal, the construction of thin layers of materials whose structure is periodic in two wide dimensions and aperiodic in one thin dimension was envisaged for applications in nanotechnology.

Coordination-driven carborane-containing self-assembled polymers (**162**, **163**, and **164**) (Fig. 86) have been reported by Stang et al.<sup>165</sup> Two linear carborane building blocks, 1,12-(4-C≡C(C<sub>5</sub>H<sub>4</sub>N)<sub>2</sub>-*p*-C<sub>2</sub>B<sub>10</sub>H<sub>10</sub>) and 1,12-(*trans*-(Pt(PEt<sub>3</sub>)<sub>2</sub>I)C≡C)-*p*-C<sub>2</sub>B<sub>10</sub>H<sub>10</sub>), were utilized to design and self-assemble five supramolecular complexes (a rectangle, a triangle, a hexagon, and two squares). The coordination originated from interactions of the pyridine ligand's nitrogen atoms and the Pt centers. These systems were expected to have potential applications as host–guest materials, sensors, and catalysts.

Hardie et al. have utilized the coordination strategy for constructing coordination polymers by mixing silver carborane salts Ag(CB<sub>11</sub>H<sub>12</sub>) (**165**) or Ag[Co(C<sub>2</sub>B<sub>9</sub>H<sub>11</sub>)<sub>2</sub>]

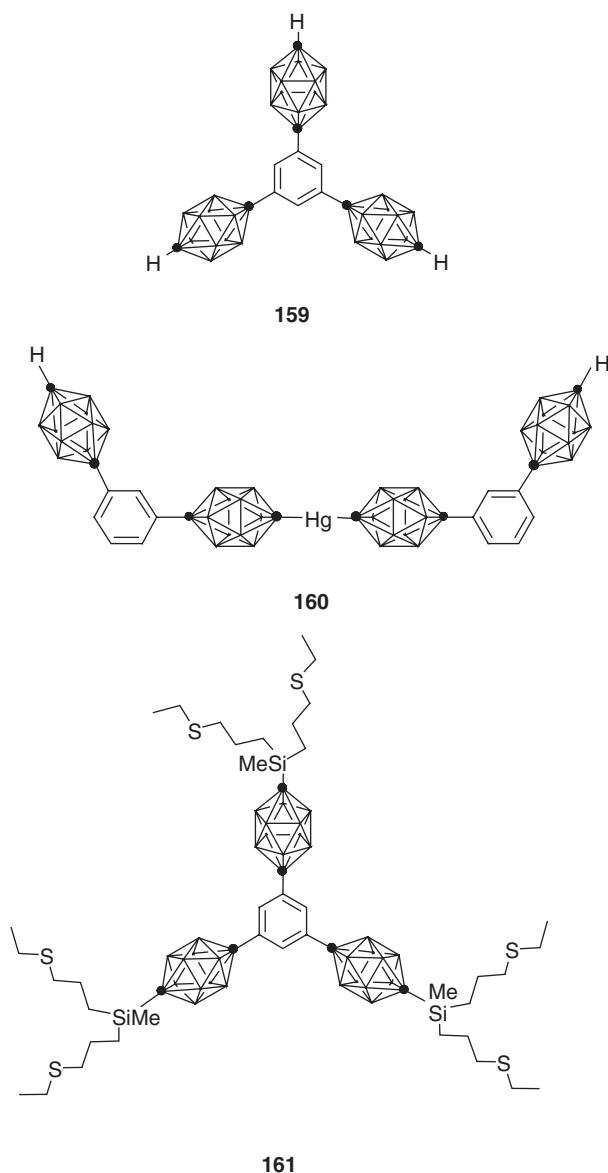


**Figure 85** Some carborane-containing molecular tools (**159**, **160**, and **161**) in the molecular construction kit for the construction of carborane-containing grid-shaped polymers. (Adapted from ref. 164.)

(**166**) with nitrile ligands (**167**, **168**, **169**, and **170**) (Fig. 87).<sup>166</sup> The coordination originated from B—H···Ag interactions between the silver center and carborane anion.

In another example of hydrogen-bond interaction-driven coordination, Teixidor and Lledos have exploited C—H···S—H···H—B hydrogen/dihydrogen-bond

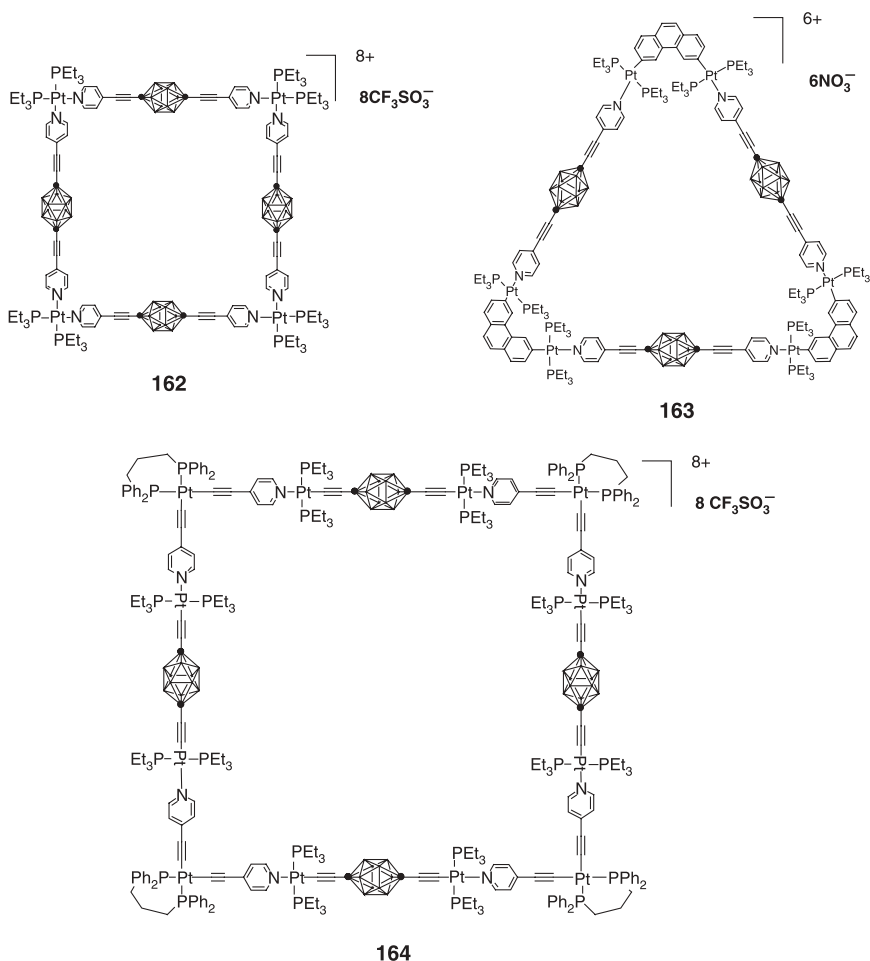


**Figure 86** The coordination-driven carborane-containing self-assembled polymers, **162**, **163**, and **164**. (Adapted from ref. 165.)

interactions between mercaptane and metallacarborane complexes to assemble supramolecular architectures (**171**) (Fig. 88).<sup>167</sup> This is the first instance of the structural elucidation of a S—H···(H—B)<sub>2</sub> dihydrogen bond.

Finally, in a brilliant piece of nanoscale assembly, Tour and co-workers have constructed a “motorized nanocar” structure (**172**) (Fig. 89) that contains a light-activated unidirectional molecular motor and an oligo(phenylene ethynylene) chassis and axle system with four carboranes to serve as the wheels.<sup>168</sup> These authors have demonstrated the rotation of the motor in solution upon irradiation with 365-nm light. This in turn resulted in the turning of the wheels and the movement of the “motorized nanocar” forward. Against its backdrop, it does not seem as a huge leap of faith for one to fathom the construction of a motorized nanotrain and other complex nanostructures in the very near future.

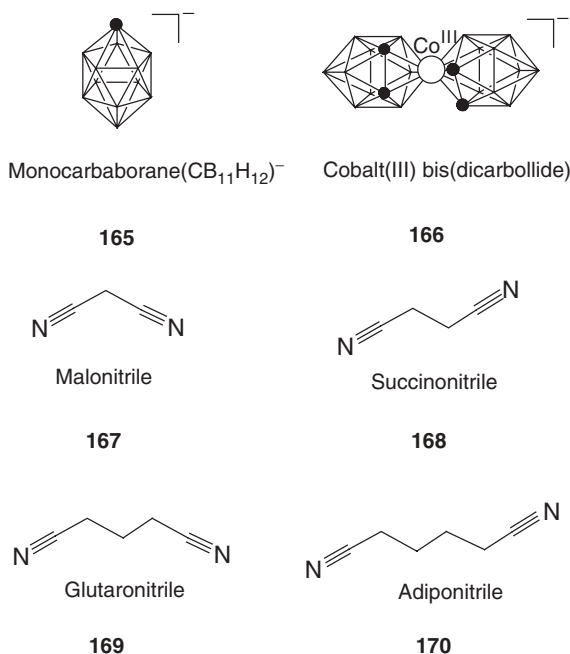


**Figure 87** The silver carborane salts  $\text{Ag}(\text{CB}_{11}\text{H}_{12})$  (**165**) and  $\text{Ag}[\text{Co}(\text{C}_2\text{B}_9\text{H}_{11})_2]$  (**166**), and the nitrile ligands (**167**, **168**, **169**, and **170**) utilized in the construction of coordination polymers. (Adapted from ref. 166.)

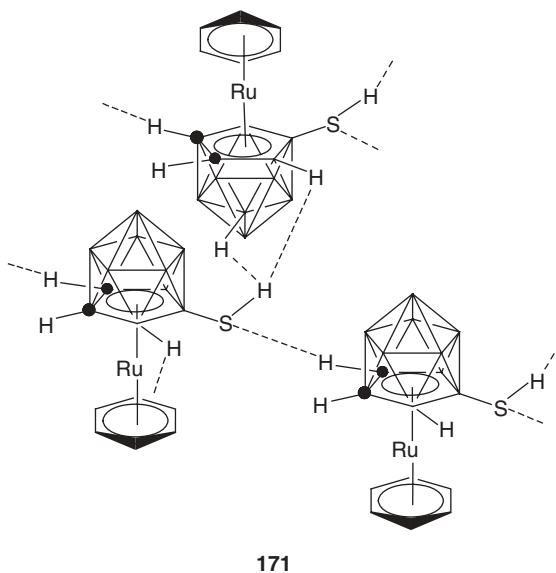
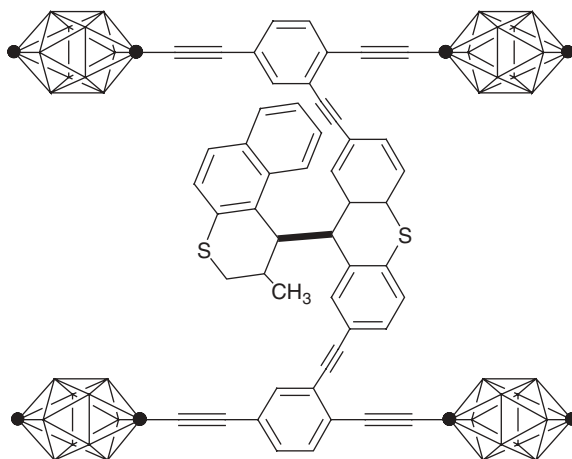


**Figure 88** The supramolecular architectures (**171**) assembled by the  $\text{C}-\text{H}\cdots\text{S}-\text{H}\cdots\text{H}-\text{B}$  hydrogen/dihydrogen-bond interactions between mercaptane and metallacarborane complexes. (Adapted from ref. 167.)



172

**Figure 89** The “motorized nanocar” structure (172) that contains a light-activated unidirectional molecular motor and an oligo(phenylene ethynylene) chassis and axle system with four carboranes to serve as the wheels. (Adapted from ref. 168.)

### III. SUMMARY

Since the pioneering studies of Stocks, Schlesinger, and Burg on the chemistry of borane compounds, the science of boron polymers has blossomed to claim its position among the major polymeric fields, including those of carbon, silicon, and phosphorous. Polymers of boron have now found their niches in virtually every field of chemistry. The only limiting factor for the further unimpeded growth of this polymer field may be the facile and low-cost availability of such boron precursors as carboranes. A concerted effort toward alleviating this deficiency is bound to catalyze even more unique and fascinating polymeric architectural outcomes from this neighbor of carbon.

### IV. REFERENCES

1. I. Asimov, *The Search for the Elements*, Fawcett World Library, New York, 1962.
2. M. F. Hawthorne, 79th Faculty Research Lecture, University of California at Los Angeles, November 29, 1995.
3. A. Stock, C. Massenez, *Ber. Dtsch. Chem. Ges.*, **45**, 3539 (1912).
4. A. Stock, R. Wierl, *Z. Anorg. Allgem. Chem.*, **203**, 228 (1931).
5. H. I. Schlesinger, A. B. Burg, *Chem. Rev.*, **31**, 1 (1942).
6. A. B. Burg, R. I. Wagner, *J. Am. Chem. Soc.*, **75**, 1515 (1953).
7. H. A. Schroeder, *Inorg. Macromol. Rev.*, **1**, 45 (1970).
8. G. W. Parshall, in *The Chemistry of Boron and Its Compounds*, E. L. Muetterties, Ed., p. 617, Wiley, New York, 1967; I. Haiduc, *The Chemistry of Inorganic Ring Systems*, Wiley, New York, 1970.
9. A. B. Burg, R. I. Wagner, *J. Am. Chem. Soc.*, **75**, 3872 (1953); R. I. Wagner, F. F. Caserio, *J. Inorg. Nucl. Chem.*, **11**, 258 (1959); A. B. Burg, R. I. Wagner, U.S. Patent No. 3,071,553 (1963).

10. H. A. Schroeder, J. R. Reiner, T. A. Knowles, *Inorg. Chem.*, **2**, 393 (1963).
11. S. Papetti, T. L. Heying, *Inorg. Chem.*, **2**, 1105 (1963).
12. S. Papetti, B. B. Schaffer, A. P. Gray, T. L. Heying, *J. Polym. Sci., A-1*, **4**, 1623 (1966).
13. H. A. Schroeder, *Inorg. Macromol. Rev.*, **1**, 45 (1970).
14. H. A. Schroeder, *Rubber Age*, **101**, 58 (1969).
15. H. A. Schroeder, S. Papetti, R. P. Alexander, J. F. Sieckhaus, T. L. Heying, *Inorg. Chem.*, **8**, 2441 (1969).
16. H. A. Schroeder, *Inorg. Macromol. Rev.*, **1**, 45 (1970).
17. E. Hedaya, J. H. Kawakami, P. W. Kopf, G. T. Kwiatkowski, D. W. McNeil, D. A. Owen, E. N. Peters, R. W. Tulis, *J. Polym. Sci., Polym. Chem. Ed.*, **15**, 2229 (1977).
18. E. N. Peters, D. D. Stewart, J. J. Bohan, R. Moffitt, C. D. Beard, G. T. Kwiatkowski, E. Hedaya, *J. Polym. Sci., Polym. Chem. Ed.*, **15**, 973 (1977); K. O. Knollmueller, R. N. Scott, H. Kwansnik, J. F. Sieckhaus, *J. Polym. Sci., A-1*, **9**, 1071 (1971).
19. K. A. Barker, C. D. Beard, J. J. Bohan, G. B. Dunks, E. Hedaya, B. L. Joesten, J. H. Kawakami, P. W. Kopf, G. T. Kwiatkowski, D. W. McNeil, R. B. Moffitt, D. A. Owen, E. N. Peters, M. L. Poutsma, D. D. Stewart, R. W. Tulis, *Report MPD-T-871*, Union Carbide Tarrytown Technical Center, Tarrytown, NY, and Chemical and Plastics Laboratory, Bound Brook, NJ (1977).
20. D. D. Stewart, E. N. Peters, C. D. Beard, G. B. Dunks, E. Hedaya, G. T. Kwiatkowski, R. B. Moffitt, J. J. Bohan, *Macromolecules*, **12**, 373 (1979).
21. E. N. Peters, D. D. Stewart, *J. Polym. Sci., Polym. Chem. Ed.*, **17**, 405 (1979).
22. R. E. Williams, *Boron Compounds*, Butterworths, London, 569 (1977); R. E. Kesting, K. F. Jackson, J. M. Newman, *J. Appl. Polym. Sci.*, **15**, 2645 (1971); R. E. Kesting, K. F. Jackson, J. M. Newman, *J. Appl. Polym. Sci.*, **15**, 1527 (1971).
23. P. R. Dvornic, R. W. Lenz, *High Temperature Siloxane Elastomers*, Huthig & Wepf, Heidelberg (1990).
24. S. Trofimenko, *J. Am. Chem. Soc.*, **89**, 3170 (1967).
25. L. G. Sneddon, *Advances in Boron Chemistry*, **201**, 491 (1997).
26. H. C. Brown, B. C. Subba Rao, *J. Am. Chem. Soc.*, **78**, 5694 (1956).
27. N. Matsumi, Y. Chujo, *Polym. Bull.*, **38**, 531 (1997); N. Matsumi, K. Naka, Y. Chujo, *J. Am. Chem. Soc.*, **120**, 5112 (1998); N. Sato, H. Ogawa, F. Matsumoto, Y. Chujo, T. Matsuyama, *Synth. Met.*, **154**, 113 (2005); M. Miyata, Y. Chujo, *Poly. Bull.*, **51**, 9 (2003).
28. M. Miyata, F. Meyer, Y. Chujo, *Polym. Bull.*, **46**, 23 (2001); M. Miyata, F. Meyer, Y. Chujo, *Polym. Bull.*, **52**, 25 (2004).
29. M. Miyata, N. Matsumi, Y. Chujo, *Polym. Bull.*, **42**, 505 (1999).
30. N. Matsumi, K. Kotera, K. Naka, Y. Chujo, *Macromolecules*, **31**, 3155 (1999); N. Matsumi, K. Kotera, Y. Chujo, *Macromolecules*, **33**, 2801 (2000).
31. R. J. P. Corriu, T. Deforth, W. E. Douglas, G. Guerrero, W. E. Siebert, *Chem. Commun.*, 963 (1998).
32. J. Roncali, *Chem. Rev.*, **92**, 711 (1992).
33. M. Nicolas, B. Fabre, J. Simonet, *Chem. Commun.*, **52**, 1881 (1999).
34. M. Nicolas, B. Fabre, G. Marchand, J. Simonet, *Eur. J. Org. Chem.*, **9**, 1703 (2000); M. Nicolas, B. Fabre, J. Simonet, *J. Electroanal. Chem.*, **509**, 73 (2001).
35. N. Matsumi, K. Naka, Y. Chujo, *J. Am. Chem. Soc.*, **120**, 10776 (1998).
36. M. Miyata, Y. Chujo, *Polym. Bull.*, **51**, 9 (2003).
37. C. Branger, M. Lequan, M. Large, F. Kajzar, *Chem. Phys. Lett.*, **272**, 265 (1997).
38. S. Yamaguchi, S. Akiyama, K. Tamao, *J. Am. Chem. Soc.*, **122**, 6335 (2000); S. Yamaguchi, S. Akiyama, K. Tamao, *J. Am. Chem. Soc.*, **123**, 11372 (2001).
39. G. Douglade, B. Fabre, *Polym. Bull.*, **129**, 309 (2002).
40. Y. Qin, C. Pagba, P. Piotrowiak, F. Jakle, *J. Am. Chem. Soc.*, **126**, 7015 (2004).
41. B. Fabre, *Electrochem. Commun.*, **3**, 6549 (2001).
42. B. Fabre, L. Taillebois, *Chem. Commun.*, 2982 (2003).

43. E. Pringsheim, E. Terpetsching, S. A. Pilletsky, O. S. Wolfbeis, *Adv. Mater.*, **11**, 865 (1999).
44. E. Shoji, M. S. Freund, *J. Am. Chem. Soc.*, **123**, 3383 (2001).
45. H. Dorn, R. A. Singh, J. A. Massey, A. J. Lough, I. Manners, *Angew. Chem. Int. Ed.*, **38**, 3321 (1999).
46. H. Dorn, R. A. Singh, J. A. Massey, J. M. Nelson, C. A. Jaska, A. J. Lough, I. Manners, *J. Am. Chem. Soc.*, **122**, 6669 (2000).
47. H. Dorn, J. M. Rodenzo, B. Brunnhofer, E. Rivard, J. A. Massey, I. Manners, *Macromolecules*, **36**, 291 (2003).
48. C. A. Jaska, I. Manners, *J. Am. Chem. Soc.*, **126**, 9776 (2004).
49. T. J. Clark, J. M. Rodenzo, S. B. Clendenning, S. Aoubam, P. M. Brodersen, A. J. Lough, H. E. Ruda, I. Manners, *Chem. Eur. J.*, **11**, 4526 (2005).
50. R. A. Sundar, T. M. Keller, *Macromolecules*, **29**, 3647 (1996).
51. R. Kurono, M. A. Mehta, T. Inoue, T. Fujinami, *Electrochim. Acta.*, **47**, 483 (2001).
52. M. Inoue, S. Sekiyama, K. Nakamura, S. Shishiguchi, A. Matsuura, T. Fukuda, H. Yanazawa, Y. Uchimaru, *Rev. Adv. Mater. Sci.*, **5**, 392 (2003).
53. R. Roesler, B. J. N. Har, W. E. Piers, *Organometallics*, **21**, 4300 (2002).
54. I. Manners, *Angew. Chem.*, **108**, 1712 (1996); I. Manners, *Angew. Chem. Int. Ed.*, **35**, 1602 (1996).
55. M. Fontani, F. Peters, W. Scherer, W. Wachter, M. Wagner, P. Zanello, *Eur. J. Inorg. Chem.*, **10**, 1453 (1998).
56. M. Grosche, E. Herdtweck, F. Peters, M. Wagner, *Organometallics*, **18**, 4669 (1999).
57. A. Berenbaum, H. Braunschweig, R. Dirk, U. Englert, J. C. Green, F. Jakle, A. J. Lough, I. Manners, *J. Am. Chem. Soc.*, **122**, 5765 (2000).
58. F. Jakle, A. Berenbaum, A. J. Lough, I. Manners, *Chem. Eur. J.*, **6**, 2762 (2000).
59. C. E. B. Evans, A. J. Lough, H. Grondy, I. Manners, *New J. Chem.*, **24**, 447 (2000).
60. C. H. Honeyman, T. J. Peckham, J. A. Massey, I. Manners, *Chem. Commun.*, **22**, 2589 (1996); T. J. Peckham, C. H. Honeyman, J. A. Massey, I. Manners, *Macromolecules*, **32**, 2830 (1999).
61. J. B. Heilmann, M. Scheibitz, Y. Qin, A. Sundararaman, F. Jakle, T. Kretz, M. Bolte, H.-W. Lerner, M. C. Holthausen, M. Wagner, *Angew. Chem. Int. Ed.*, **45**, 920 (2006).
62. K. Ma, M. Scheibitz, S. Scholz, M. Wagner, *J. Organomet. Chem.*, **11–19**, 652 (2002).
63. N. Matsumi, Y. Chujo, O. Lavastre, P. H. Dixneuf, *Organometallics*, **20**, 2425 (2001); F. Matsumoto, N. Matsumi, Y. Chujo, *Polym. Bull.*, **46**, 257 (2001).
64. H. Yao, M. L. Kuhlman, T. B. Rauchfuss, S. R. Wilson, *Inorg. Chem.*, **44**, 6256 (2005).
65. T. C. Chung, *Macromolecules*, **21**, 865 (1988); S. Ramakrishnan, E. Berluche, T. C. Chung, *Macromolecules*, **23**, 378 (1990).
66. T. C. Chung, H. L. Lu, W. Janvikul, *Polymer*, **38**, 1495 (1997).
67. B. Lu, T. C. Chung, *Macromolecules*, **31**, 5943 (1998); B. Lu, T. C. Chung, *Macromolecules*, **32**, 2525 (1999).
68. B. C. Trivedi, B. M. Culbertson, *Maleic Anhydride*, Plenum Press, New York, 1982.
69. T. C. Chung, W. Janvikul, H. L. Lu, *J. Am. Chem. Soc.*, **118**, 705 (1996).
70. J. Y. Dong, E. Manias, T. C. Chung, *Macromolecules*, **35**, 3439 (2002).
71. G. Xu, T. C. Chung, *J. Am. Chem. Soc.*, **121**, 6763 (1999).
72. G. Xu, T. C. Chung, *Macromolecules*, **32**, 8689 (1999).
73. T. C. Chung, G. Xu, Y. Lu, Y. Hu, *Macromolecules*, **34**, 8040 (2001).
74. F. Fan, J. Y. Dong, Z. Wang, T. C. Chung, *J. Polym. Sci.: Part A: Polym. Chem.*, **44**, 539 (2006).
75. S. B. Roscoe, J. M. J. Frechet, J. F. Walzer, A. J. Dias, *Science*, **280**, 270 (1998).
76. K. Kamahori, K. Ito, S. Itsuno, *J. Org. Chem.*, **61**, 8321 (1996); K. Smith, G. A. El-Hiti, D. J. Hou, G. A. DeBoos, *J. Chem. Soc., Perkin Trans.*, **1**, 2807 (1999); B. R. Stranix, J. P. Gao, R. Barghi, J. Salha, G. D. Darling, *J. Org. Chem.*, **62**, 8987 (1997); G. Belogi, T. Zhu, G.-J. Boons, *Tetrahedron Lett.*, 6965 (2000).

77. H. Sinn, W. Kaminsky, *Adv. Organomet. Chem.*, **18**, 99 (1980).
78. T. X. Yang, C. L. Stern, T. J. Marks, *J. Am. Chem. Soc.*, **113**, 3623 (1991).
79. P. A. Deck, T. J. Marks, *J. Am. Chem. Soc.*, **117**, 6128 (1995).
80. M. Nager, S. Becke, H. Windisch, U. Denninger, *Angew. Chem. Int. Ed.*, **40**, 1898 (2001).
81. (a) Y. Qin, G. Cheng, A. Sundararaman, F. Jakle, *J. Am. Chem. Soc.*, **124**, 12672 (2002).  
(b) Y. Qin, G. Cheng, K. Parab, A. Sundararaman, F. Jakle, *Macromol. Symp.*, **196**, 337 (2003).  
(c) Y. Qin, G. Cheng, O. Achara, K. Parab, F. Jakle, *Macromolecules*, **37**, 7123 (2004).
82. K. Matyjaszewski, J. H. Xia, *Chem. Rev.*, **101**, 2921 (2001).
83. Y. Kondo, D. Garcia-Cuarrado, J. F. Hartwig, N. K. Boen, N. L. Wagner, M. A. Hillmyer, *J. Am. Chem. Soc.*, **124**, 1164 (2002).
84. P. S. Wolfe, K. B. Wagener, *Macromolecules*, **32**, 7961 (1999).
85. K. Kamahori, K. Ito, S. Itsuno, *J. Org. Chem.*, **61**, 8321 (1996).
86. O. Stephan, N. Riegel, S. Juge, *J. Electroanal. Chem.*, **421**, 5 (1997).
87. K. Rajasree, K. S. Devaky, *J. Appl. Polym. Sci.*, **82**, 593 (2001).
88. S. M. Lomakin, G. E. Zaikov, *Ecological Aspects of Flame Retardancy*, VSP, Utrecht, 1999.
89. (a) J. Gao, Y. Liu, L. Yang, *Polym. Degrad. Stab.*, **63**, 19 (1999). (b) J. Gao, Y. Liu, *J. Appl. Polym. Sci.*, **76**, 1054 (2000). (c) J. Gao, Y. Liu, F. Wang, *Eur. Polym. J.*, **37**, 207 (2001).  
(d) J. Gao, Y. Liu, L. Xia, *Polym. Degrad. Stab.*, **83**, 71 (2004).
90. M. O. Abdalla, A. L. Ludwick, T. Mitchell, *Polymer*, **44**, 7353 (2003).
91. C. Martin, J. C. Ronda, V. Cadiz, *Polym. Degrad. Stab.*, **91**, 747 (2006); C. Martin, J. C. Ronda, V. Cadiz, *J. Polym. Sci. Part A: Polym. Chem.*, **44**, 1701 (2006).
92. C. Martin, B. J. Hunt, J. R. Ebdon, J. C. Ronda, V. Cadiz, *J. Polym. Sci. Part A: Polym. Chem.*, **43**, 6419 (2005).
93. D. R. Nielsen, W. E. McEwen, *J. Am. Chem. Soc.*, **44**, 3081 (1957).
94. A. B. Morgan, J. L. Jurs, J. M. Tour, *J. Appl. Polym. Sci.*, **76**, 1257 (2000).
95. D. L. Coopera, S. C. Wright, J. Gerratt, P. A. Hyams, M. Raimondi, *J. Chem. Soc., Perkin Trans. II*, **6**, 719 (1989).
96. J. J. Engelberts, R. W. A. Havenith, J. H. V. Lenthe, L. W. Jenneskens, P. W. Fowler, *Inorg. Chem.*, **44**, 5266 (2005).
97. B. Kiran, A. K. Phukan, E. D. Jemmis, *Inorg. Chem.*, **40**, 3615 (2001).
98. Y. Hasegawa, K. Okamura, *J. Mater. Sci.*, **18**, 3633 (1983).
99. R. M. Laine, Y. D. Blum, D. Tse, R. Glaser, *Inorganic and Organometallic Polymers*, M. Zeldin, K. J. Wynne, H. R. Allcock, eds., ACS Symposium Series **360**, American Chemical Society, Washington, DC, p. 124, 1988.
100. W. Verbeek, G. Winter, *German Patent 2,236,078* (1974); *Chem. Abstr.*, **81**, 50,911 (1974).
101. S. Yajima, J. Hayashi, M. Otori, *Jpn. Appl.*, **75**, 50,223 (1975); *Chem. Abstr.*, **86**, 30,940 (1977).
102. M. Birot, J.-P. Pillot, J. Dunogues, *Chem. Rev.*, **95**, 1443 (1995).
103. J. Lipowitz, *U.S. Patent 4,743,662* (1988); *Chem. Abstr.*, **109**, 42,570 (1988).
104. D. C. Deleeuw, J. Lipowitz, P. P. Y. Lu, *European Patent Appl.* 438,117 (1991); *Chem. Abstr.*, **115**, 138,149 (1991).
105. C. P. Jacobson, L. C. De Jonghe, *International Patent Appl.* 94, 02,430 (1994); *Chem. Abstr.*, **120**, 171,546 (1994).
106. J. G. Kho, D. S. Min, D. P. Kim, *J. Mater. Sci. Lett.*, **19**, 303 (2000); F. Cao, X. D. Li, D. P. Kim, *J. Mater. Chem.*, **12**, 1213 (2002).
107. F. Cao, X.-D. Li, J.-H. Ryu, D.-P. Kim, *J. Mater. Chem.*, **13**, 1941 (2003).
108. A. R. Brunner, D. R. Bujalski, E. S. Moyer, K. Su, L. G. Sneddon, *Chem. Mater.*, **12**, 2770 (2000).
109. A. R. Puerta, E. E. Remsen, M. G. Bradley, W. Sherwood, L. G. Sneddon, *Chem. Mater.*, **15**, 478 (2003).
110. M. Takamizawa, T. Kobayashi, A. Hayashida, Y. Takeda, U.S. Patent 4,604,367 (1986).

111. A. Kienzle, W. Dressler, L. Ruwisch, J. Bill, F. Aldinger, *Nature*, **382**, 796 (1996); Q. D. Nghiem, J. K. Jeon, L. Y. Hong, D. P. Kim, *J. Organomet. Chem.*, **688**, 27 (2003); J. K. Jeon, Q. D. Nghiem, D. R. Kim, J. Lee, *J. Organomet. Chem.*, **689**, 2311 (2004); K. Moraes, J. Vosburg, D. Wark, L. V. Interrante, A. R. Puerta, L. G. Sneddon, M. Narisawa, *Chem. Mater.*, **16**, 125 (2004); J. Haberecht, F. Krumeich, H. Grutzmacher, R. Nesper, *Chem. Mater.*, **16**, 418 (2004).
112. S. Trofimenko, *Polyhedron*, **23**, 197 (2004).
113. P. J. Steel, *Coord. Chem. Rev.*, **106**, 227 (1990); A. P. Sadimenko, S. S. Basson, *Coord. Chem. Rev.*, **147**, 247 (1996).
114. S. Trofimenko, *Chem. Rev.*, **93**, 943 (1993).
115. F. Matsumoto, Y. Chujo, *Macromolecules*, **36**, 5516 (2003).
116. F. Matsumoto, Y. Nagata, Y. Chujo, *Polym. Bull.*, **53**, 155 (2005).
117. W. Niu, C. O'Sullivan, B. M. Rambo, M. D. Smith, J. J. Lavigne, *Chem. Commun.*, **53**, 4342 (2005).
118. M. Balakrishnarajan, R. Hoffmann, *Angew. Chem. Int. Ed.*, **42**, 3777 (2003).
119. R. E. Williams, "Carboranes," in *Progress in Boron Chemistry*, Vol. 2, Pergamon Press, New York, 1970, Chapter 2; G. B. Dunks, M. F. Hawthorne, *Acc. Chem. Res.*, **6**, 124 (1973).
120. G. A. Olah, G. K. Surya Prakash, R. E. Williams, L. D. Field, K. Wade, *Hypercarbon Chemistry*, Wiley, New York, 1987; E. Muettterties, *Boron Hydride Chemistry*, Academic Press, New York, 1975; R. N. Grimes, *Carboranes*, Academic Press, New York, 1970; T. Onak, *Organoborane Chemistry*, Academic Press, New York, 1975; V. I. Bregadze, *Chem. Rev.*, **92**, 209 (1992).
121. D. M. Ho, R. J. Cunningham, J. A. Brewer, N. Bian, M. Jones, Jr., *Inorg. Chem.*, **34**, 5274 (1995).
122. H. M. Colquhoun, P. L. Herbertson, K. Wade, I. Baxter, D. J. Williams, *Angew. Chem. Int. Ed.*, **42**, 3777 (2003).
123. L. Barnett-Thamattoor, J. J. Wu, D. M. Ho, M. Jones, Jr., *Tetrahedron Lett.*, **37**, 7221 (1996).
124. M. A. Fox, J. A. K. Howard, J. A. H. MacBride, A. Mackinnon, K. Wade, *J. Organomet. Chem.*, **680**, 155 (2003).
125. L. J. Henderson, T. M. Keller, *Macromolecules*, **27**(6) 1660 (1994).
126. E. J. Houser, T. M. Keller, *Macromolecules*, **31**, 4038 (1998).
127. M. K. Kolel-Veetil, T. M. Keller, *J. Mater. Chem.*, **13**(7) 1652 (2003).
128. M. K. Kolel-Veetil, H. W. Beckham, T. M. Keller, *Chem. Mater.*, **16**, 3162 (2004).
129. R. A. Sundar, T. M. Keller, *J. Polym. Sci. Part A: Polym. Chem.*, **35**, 2387 (1997).
130. M. K. Kolel-Veetil, S. B. Qadri, M. Osofsky, T. M. Keller, *Chem. Mater.*, **17**(24), 6101 (2005).
131. M. Patel, A. C. Swain, A. R. Skinner, L. G. Mallinson, G. F. Hayes, *Macromol. Symp.*, **202**, 47 (2003); A. C. Swain, M. Patel, J. J. Murphy, *Mater. Res. Soc. Symp. Proc.*, **851**, 363 (2005).
132. W. Noll, *Chemistry and Technology of Silicones*, Academic Press, New York, 1968.
133. E. J. Houser, T. M. Keller, *J. Polym. Sci. Part A: Polym. Chem.*, **36**, 1969 (1998).
134. M. K. Kolel-Veetil, T. M. Keller, *J. Polym. Sci. Part A: Polym. Chem.*, **44**, 147 (2006).
135. L. N. Lewis, N. J. Lewis, *J. Am. Chem. Soc.*, **108**, 7228 (1986).
136. M. Ichitani, K. Yonezawa, K. Okada, T. Sugimoto, *Polym. J.*, **31**, 908 (1999); H. Kimura, K. Okita, M. Ichitani, T. Sugimoto, S. Kuroki, I. Ando, *Chem. Mater.*, **15**, 355 (2003).
137. K. Shelly, C. A. Reed, Y. J. Lee, W. R. Scheidt, *J. Am. Chem. Soc.*, **108**, 3117 (1986).
138. C. Masalles, S. Borros, C. Vinas, F. Teixidor, *Adv. Mater.*, **12**, 1199 (2000).
139. C. Masalles, J. Llop, C. Vinas, F. Teixidor, *Adv. Mater.*, **14**, 826 (2002).
140. S. Gentil, E. Crespo, I. Rojo, A. Friang, C. Vinas, F. Teixidor, B. Gruner, D. Gabel, *Polymer*, **46**, 12,218 (2005).
141. B. Fabre, S. Chayer, M. G. H. Vicente, *Electrochem. Commun.*, **5**, 431 (2003).
142. B. Fabre, J. C. Clark, M. G. H. Vicente, *Macromolecules*, **39**, 112 (2006).
143. J. Q. Wang, C. X. Ren, L. H. Weng, G. X. Jin, *Chem. Commun.*, 162 (2006).
144. G. L. Locher, *Am. J. Roentgenol. Radium Ther.*, **36**, 1 (1936).

145. L. Guan, L. A. Wims, R. R. Kane, M. B. Smuckler, S. L. Morrison, M. F. Hawthorne, *Proc. Natl. Acad. Sci. USA*, **95**, 13206 (1998).
146. A. Nakanishi, L. Guan, R. R. Kane, H. Kasamatsu, M. F. Hawthorne, *Proc. Natl. Acad. Sci. USA*, **96**, 238 (1999).
147. J. Capala, R. F. Barth, M. Bendayan, M. Lauzon, D. M. Adams, A. H. Soloway, R. A. Fernstermaker, J. Carlsson, *J. Bioconjugate Chem.*, **7**, 7 (1996).
148. J. Thomas, M. F. Hawthorne, *Chem. Commun.*, **18**, 1884 (2001).
149. B. Qualmann, M. M. Kessels, H. J. Musiol, W. D. Sierralta, P. W. Jungblut, L. Moroder, *Angew. Chem. Int. Ed.*, **35**, 909 (1996).
150. M. G. H. Vicente, S. J. Shetty, A. Wickramasinghe, K. M. Smith, *Tetrahedron Lett.*, **41**, 7623 (2000); M. G. H. Vicente, B. F. Edwards, S. J. Shetty, Y. Hou, J. E. Boggan, *Bioorg. Med. Chem.*, **10**, 481 (2002); M. G. H. Vicente, A. Wickramasinghe, D. J. Nurco, H. J. H. Wang, M. M. Nawrocky, M. S. Makar, M. Miura, *Bioorg. Med. Chemun.*, **11**, 3101 (2003); J. C. Clark, F. R. Fronczek, M. G. H. Vicente, *Tetrahedron Lett.*, **46**, 2365 (2005).
151. M. J. Pender, L. G. Sneddon, *ACS Polym. Prep.*, **41**, 551 (2000); M. J. Pender, K. M. Forsthoefel, L. G. Sneddon, *Pure Appl. Chem.*, **75**, 1287 (2003).
152. X. Wei, P. J. Carroll, L. G. Sneddon, *Organometallics*, **23**, 163 (2004); X. Wei, P. J. Carroll, L. G. Sneddon, *Chem. Mater.*, **18**, 1113 (2006).
153. D. T. Welna, J. D. Bender, X. Wei, L. G. Sneddon, H. R. Allcock, *Adv. Mater.*, **17**, 859 (2005).
154. G. J. Choi, W. Toreki, C. D. Batich, *J. Mater. Sci.*, **35**, 2421 (2000).
155. H. M. Colquhoun, P. L. Herbertson, K. Wade, *J. Polym. Sci., Part A: Polym. Chem.*, **34**, 2521 (1996); H. M. Colquhoun, D. F. Lewis, J. A. Daniels, P. L. Herbertson, J. A. H. MacBride, I. R. Stephenson, K. Wade, *Polymer*, **38**, 2447 (1997); H. M. Colquhoun, D. F. Lewis, P. L. Herbertson, K. Wade, *Polymer*, **38**, 4539 (1997).
156. M. A. Fox, K. Wade, *J. Mater. Chem.*, **12**, 1301 (2002).
157. E. M. Antipov, V. A. Vasnev, M. Stamm, E. W. Fischer, N. A. Plate, *Macromol. Rapid Commun.*, **20**, 185 (1999).
158. Z. Yinghuai, Z. Yulin, K. Carpenter, J. A. Maguire, N. S. Hosmane, *J. Organomet. Chem.*, **690**, 2802 (2005).
159. D. Armspach, M. Cattalini, E. C. Constable, C. E. Housecroft, D. Phillips, *Chem. Commun.*, **15**, 1823 (1996).
160. W. Jiang, I. T. Chizhevsky, W. Chen, C. B. Knobler, S. E. Johnson, F. A. Gomez, M. F. Hawthorne, *Inorg. Chem.*, **35**, 5417 (1996); M. J. Bayer, A. Herzog, M. Diaz, G. A. Harakas, H. Lee, C. B. Knobler, S. E. Johnson, F. A. Gomez, M. F. Hawthorne, *Chem. Eur. J.*, **9**, 2732 (2003).
161. C. Songkram, R. Yamasaki, A. Tanatani, K. Tkaishi, K. Yamaguchi, H. Kagechika, Y. Endo, *Tetrahedron Lett.*, **42**, 5913 (2001).
162. H. Yao, M. Sabat, R. N. Grimes, F. Fabrizi di Biani, P. Zanello, *Angew. Chem. Int. Ed.*, **42**, 1002 (2003); H. Yao, R. N. Grimes, *J. Organomet. Chem.*, **680**, 51 (2003); R. N. Grimes, *Pure Appl. Chem.*, **75**, 1211 (2003).
163. Z. Zheng, C. B. Knobler, M. D. Mortimer, G. Kong, M. F. Hawthorne, *Inorg. Chem.*, **35**, 1235 (1996); H. Lee, C. B. Knobler, M. F. Hawthorne, *Angew. Chem. Int. Ed. Engl.*, **40**, 3058 (2001); H. Lee, C. B. Knobler, M. F. Hawthorne, *J. Am. Chem. Soc.*, **123**, 8543 (2001); T. J. Wedge, M. F. Hawthorne, *Coord. Chem. Rev.*, **240**, 111 (2003).
164. U. Schoberl, T. F. Magnera, R. M. Harrison, F. Fleischer, J. L. Pflug, P. F. H. Schwab, X. Meng, D. Lipiak, B. C. Noll, V. S. Allured, T. Rudalevige, S. Lee, J. Michl, *J. Am. Chem. Soc.*, **119**, 3907 (1997).
165. H. Jude, H. Disteldorf, S. Fischer, T. Wedge, A. J. Hawkrigde, A. M. Arif, M. F. Hawthorne, D. C. Muddiman, P. J. Stang, *J. Am. Chem. Soc.*, **127**, 12,131 (2005).
166. A. Westcott, N. Whitford, M. J. Hardie, *Inorg. Chem.*, **43**, 3663 (2004).
167. J. G. Planas, C. Vinas, F. Teixidor, A. Comas-Vives, G. Ujaque, A. Lledos, M. E. Light, M. B. Hursthouse, *J. Am. Chem. Soc.*, **127**, 15,976 (1997).
168. J. F. Morin, Y. Shirai, J. M. Tour, *Org. Lett.*, **8**, 1713 (2006).

---

## CHAPTER 2

# Polymers Incorporating Icosahedral Closo-Dicarbaborane Units

**Mogon Patel and Anthony C. Swain**

*Atomic Weapons Establishment (AWE), Aldermaston, Reading, RG7 4PR, UK*

### CONTENTS

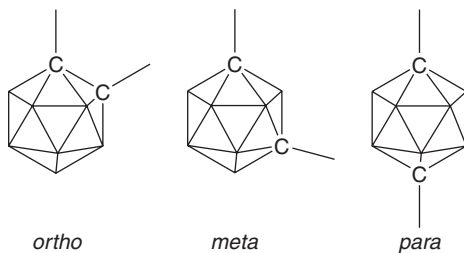
I. INTRODUCTION	78
A. Polymers Incorporating Decaborane	79
B. Polymers with Pendant Carborane Groups	80
II. POLY( <i>m</i> -CARBORANE-SILOXANE) RUBBERS	81
III. SYNTHESIS	82
A. Bis(ureido)silanes: Condensation Polymerization	86
B. Dilithiocarborane: Salt Elimination Route	88
IV. CHARACTERIZATION	88
A. Nuclear Magnetic Resonance Spectroscopy	88
B. Gel-Permeation Chromatography	89
C. Thermal and Chemical Properties	89
V. THERMAL AND RADIATION STABILITY	93
A. Stability to Neutrons	96
VI. OTHER CARBORANE-CONTAINING POLYMERS	97
A. Poly(ether-ketone-carbaborane)	97
B. Polyphosphazene Incorporating Carboranyl Units	98

*Macromolecules Containing Metal and Metal-Like Elements,*  
*Volume 8: Boron-Containing Polymers*, edited by Alaa S. Abd-El-Aziz,  
Charles E. Carraher Jr., Charles U. Pittman Jr., and Martel Zeldin.  
Copyright © 2007 John Wiley & Sons, Inc.

VII. ENERGETIC CARBORANE POLYMER SYSTEMS	99
VIII. SUMMARY	100
IX. REFERENCES	101

## I. INTRODUCTION

Boron is a nonmetallic refractory element that exists in the form of two stable isotopes,  $^{10}\text{B}$  (19.8%) and  $^{11}\text{B}$  (80.2%). It has a relatively high melting point of  $2300^\circ\text{C}$  and is able to combine with other elements to form a variety of boron cluster compounds having unique molecular architectures and unusual properties.<sup>1</sup> These compounds include pentaborane, decaborane, and the closo-dicarbaboranes. The latter compounds are generally expressed by the molecular formula  $\text{C}_2\text{B}_n\text{H}_{n+2}$  ( $n = 3-10$ ) and include the carba-closo-dodecaboranes, better known as the icosahedral *o*-, *m*-, and *p*-carboranes, see **1**. These compounds exhibit rather specific properties, in particular, high thermal and chemical stability, and show unusual chemistry not encountered in other materials. These properties have not been fully exploited or investigated, possibly because of the general limited availability (and therefore high cost) of the closo-dicarbaboranes.



Icosahedral *o*-, *m*-, and *p*-carboranes.

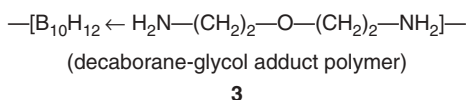
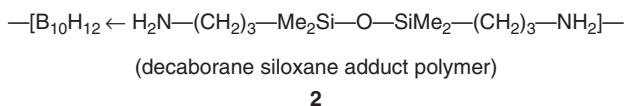
**1**

Carborane polyhedra, particularly those containing the icosahedral  $\text{C}_2\text{B}_{10}$  unit, and the octahedral units  $\text{C}_2\text{B}_4$ , display remarkable stability despite their inherent electron deficiency, thus making them well suited to high-temperature applications. The carborane cage is generally chemically robust and displays useful derivative chemistry. Thermal stability generally increases with cage size and with increased separation of the two carbon atoms (see **1**). Furthermore, the closed structure of the icosahedral carboranes result in enhanced chemical stability, with good stability in highly acidic media. However, under the driving conditions of reflux in concentrated sulfuric acid, followed by an aqueous work-up, the carborane cage is hydroxylated. Here the  $\text{B}-\text{H}$  vertices are converted to  $\text{B}-\text{OH}$  functionality.<sup>2</sup> Carboranes are also susceptible to attack from alkaline reagents; thus, *o*-carborane is slowly converted to the nido-[7,8- $\text{C}_2\text{B}_9\text{H}_{12}$ ]<sup>-</sup> anion by sodium hydroxide in ethanolic mixture.



treatment of decaborane with acetonitrile results in the formation of 6,9-bis(acetonitrile)-decaborane and hydrogen.<sup>4</sup>

Polymers derived from the preceding type of reaction with nitriles,<sup>5</sup> amines,<sup>6</sup> and phosphines,<sup>7</sup> have been reported. Green<sup>8</sup> has reported the preparation of a resin-type material composed of at least 10 repeat units from the reaction between decaborane and adiponitrile (NC(CH<sub>2</sub>)<sub>4</sub>CN). Also reported,<sup>9</sup> is the inclusion of flexible siloxanes and ether linkages into a diamine, and of their subsequent reaction with decaborane to give adduct polymers (see **2**, **3**).

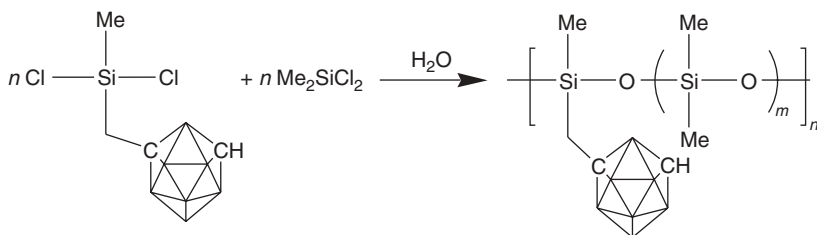


In general, the polymers incorporating decaborane that have been reported in the literature tend to be soluble in polar solvents, and generally have poor stability in solution with degradation of the decaborane cage.<sup>4</sup>

## B. Polymers with Pendant Carborane Groups

Carborane-containing polymers may be conveniently divided into two broad classes: (1) polymers incorporating carboranyl fragments within the pendent group attached to the main chain, and (2) polymers containing carboranyl fragments within their main chain.

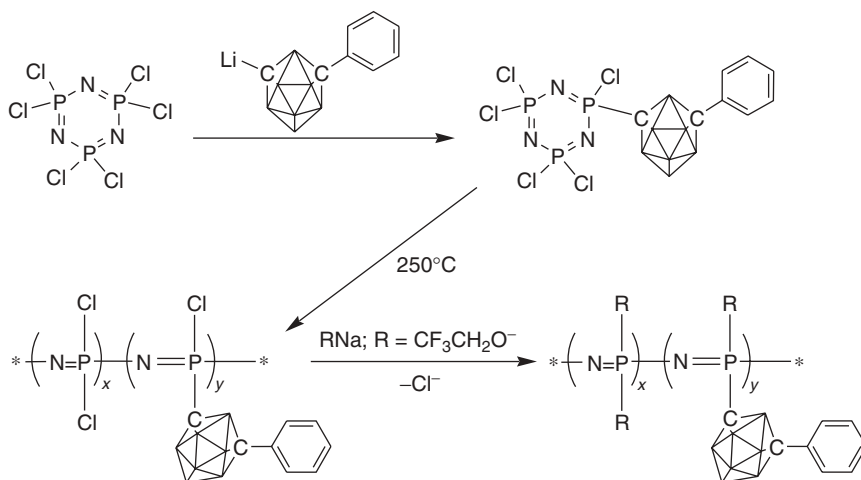
A typical synthetic route to the incorporation of pendent carboranyl units into a polymer chain is shown in scheme 3. Poly(*o*-carboranyl-organo-siloxane)s have been successfully prepared through hydrolysis of dimethyldichlorosilane in the presence of carboranedichloromethylsilane. The polymer has some of the elastomeric characteristics of the parent poly(siloxane); however, the thermal-oxidative cleavage of the *o*-carboranyl pendent group is reported to occur at lower temperatures than that for the thermo-oxidative cleavage of Si—O and Si—C bonds.<sup>10</sup> Thermal studies have



**Scheme 3** Synthesis of poly(*o*-carboranyl-organo-siloxane)s.

shown that the carborane functionality, in this mode of incorporation does not appear to impart any significant thermal stability improvements on the base siloxane, unlike that for main-chain incorporation. The presence of pendent carborane units does, however, affect the thermal decomposition pathway of the polysiloxane.<sup>11</sup> The incorporation of such bulky fragments into the polymer architecture reduces the torsional mobility, thereby increasing the glass transition temperature ( $T_g$ ) of the parent material.

This effect has also been observed in polyphosphazenes containing alkyl- or phenyl-carborane as pendent groups.<sup>12</sup> A typical synthetic route to poly(phenyl-carboranyl-di-trifluoroethoxy-phosphazene) having pendent phenyl-carborane groups is shown in scheme 4. A substantial improvement in the thermal stability of the polymer was observed. This is attributed to a retardation of the ring-chain de-polymerization mechanism due to steric hindrance effects of the carborane units, inhibiting helical coil formation.



**Scheme 4** Polyphosphazenes containing alkyl- or phenyl-carborane as pendent groups.

## II. POLY(*m*-CARBORANE-SILOXANE) RUBBERS

The preparation of high carbonyl content (and high boron content) polymers typically involves the coupling of carborane units with very short linking units. Thus, a polymer comprising meta-carborane repeat units will attain the maximum boron content of 76%; however, such systems are not elastomeric. Replacement of alternate carborane with, for example, a 1,4-phenylene unit gives a boron content of approximately 50%; similar replacement with bi-phenylene lowers the theoretical content to approximately 37%. The literature contains several papers on this theme, but all polymers of this type suffer from the same problems: low molecular weights, insolubility, high glass transition temperature ( $T_g$ ), and so on. These properties are very similar to those displayed by the poly (*para*-phenylene) class of polymers ("rigid-rod"-type polymers) that are generally insoluble and/or low molecular-weight crystalline materials.

However, elastomeric behavior can be introduced into carboranyl polymer systems by carefully selecting copolymer systems where one component imparts the rubbery character by increasing segmental motion (thereby reducing  $T_g$ ). The most popular choice for imparting rubbery characteristics into carborane polymer systems is through the incorporation of siloxane units. These units can be connected to the skeletal carbon atom, that is, *ortho*-, *meta*-, or *para*-arrangements, thereby allowing either bent or linear structures to be prepared.<sup>13</sup>

Decarborane and icosahedral carboranes are generally viewed as polymer building blocks, as well as three-dimensional "energy sinks." These properties were first successfully exploited by the Olin Corporation with the development of highly heat-resistant poly(*m*-carborane-siloxane)s type polymers.<sup>14</sup> These families of polymers were known under the trade name of DEXSIL. Typically, they comprise dialkyl or diarylsiloxane repeat units linked by *m*-carboranyl fragments, together with a small fraction of a vinyl functionality to promote cross-linking. The elastomeric properties of the polymer may be altered by increasing the proportion of Si—O repeat units and adjusting the cross-link density. The resulting materials contain known proportions of "soft block" siloxane and "hard block" carborane units held together within a cross-linked matrix.

The ratio of siloxane to carborane is important in not only determining the polymer melting temperature ( $T_m$ ) and  $T_g$ , but also its overall susceptibility to thermal and oxidative degradation. In general, the inclusion of carboranyl units into the backbone of a polymer reduces chain flexibility, resulting in  $T_g$  values being raised well above room temperature.<sup>15</sup> Additional elastomeric properties can, however, be imparted and controlled by introducing a number of tri- or tetra-functional silicon groups into the chain, usually as comonomers in the original reaction mixture. Table 1 shows that increasing the number of siloxane units in the polymer tend to decrease the  $T_g$  values. Since the hydrocarbon groups attached to silicon are the most vulnerable points for chemical attack, increasing the siloxane content typically reduces the chemical resistance of the polymer.

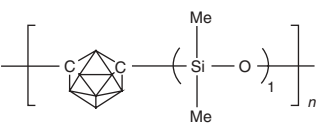
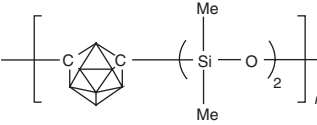
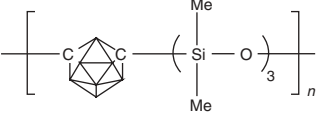
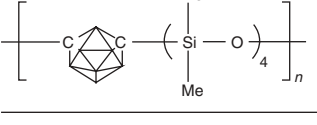
### III. SYNTHESIS

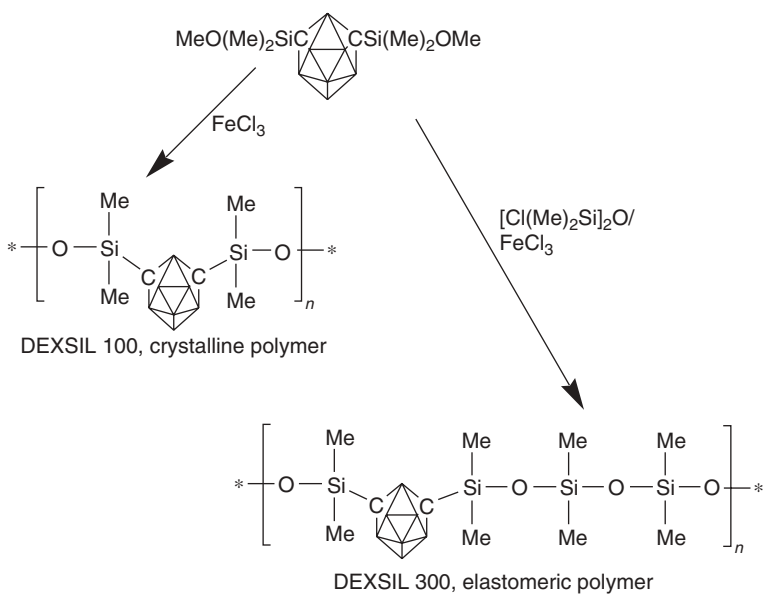
One of the earliest and most popular systems investigated are the highly heat-resistant poly(*m*-carborane-siloxane)s. A review of the general literature on the methods used in the synthesis of these materials is reported in the following sections.

Poly(*m*-carborane-siloxane) rubbers are most commonly prepared by a ferric chloride-catalyzed bulk condensation copolymerization of dichloro- and dimethoxy-terminated monomers with alkylchloro- or arylchloro-siloxanes.<sup>16</sup>

However, the synthesis process, depicted in scheme 5, is rather idealized. In reality, the chemistry appears to be quite complex, resulting in a partially cross-linked rubber and the evolution of gaseous species other than chloromethane. Dietrich et al.<sup>17</sup> reported that the progress of the polymerization at 116°C, as measured by gas evolution and polymer molecular weight, significantly slowed at around 50% conversion. The reaction could, however, be driven further forward by increasing the temperature to >150°C.

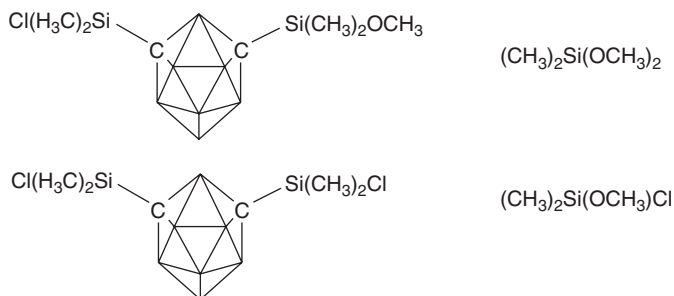
**Table 1** Glass Transition as a Function of Siloxane Content

Poly( <i>m</i> -carborane-siloxane)	$T_g/^\circ\text{C}$
	25
	-42
	-68
	-75


**Scheme 5** Poly(*m*-carborane-siloxane) using ferric chloride.

Our studies at Atomic Weapons Establishment (AWE) have confirmed that at elevated temperatures, especially when using dry inert gas conditions, there is considerable difficulty in pushing the reaction (see scheme 5) to completion.<sup>18</sup> Moisture was found to affect the rate of the reaction and the nature of the synthesized polymer. The introduction of additional catalyst to the reaction mixture was found to aid the forward reaction. Overall, our observations suggest the existence of a complex series of reactions, possibly having distinctly different activation energies.

The process is now recognized to take place through a series of stepwise reactions.<sup>17</sup> Initially a series of end group exchange reactions generates poly(ox-dimethylsilanediy)s as well as carbaborane containing monomers (see 4). At higher temperatures, the end-group reactions are replaced by a polymerization process between the carbaborane monomers and silanes to produce the polymer. Due to the chemical stabilizing influence of the carbaborane cage, the monomers require higher temperatures and more rigorous conditions to react.

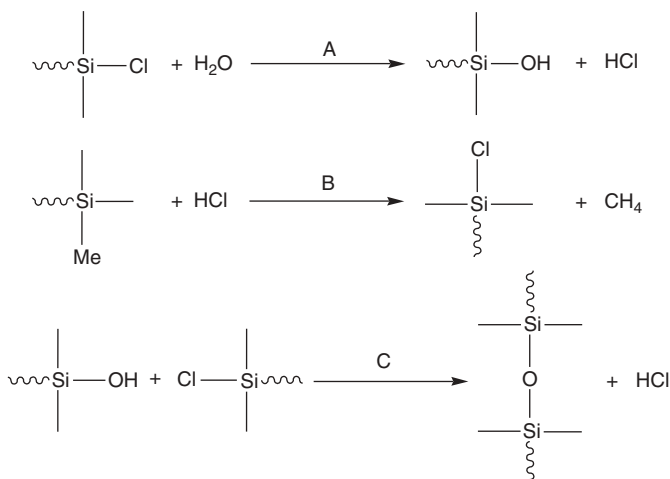


Species produced from end group reactions.

4

The resulting material is typically a soft spongy polymer that is insoluble in aromatic solvents. This is indicative of a cross-linked material. It is now recognized that moisture and/or hydrogen chloride play an important role in determining the extent of cross-linking of the polymer. The water most probably results in the production of silanol groups, either at chain ends or as pendent hydroxyl species. These can readily react with chloro-silane species generating a cross-linked network (see scheme 6). An additional source of cross-linking most probably arises from the reaction of chlorine radicals generated from the reduction of ferric chloride to  $\text{FeCl}_2$ . Such radicals would readily undergo abstraction and recombination reactions, thus contributing to the cross-link density of the rubber.

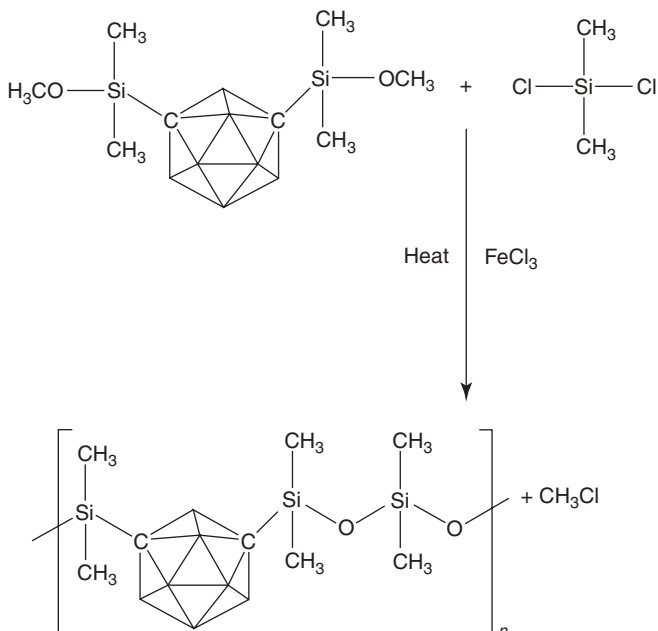
In order to avoid some of the side reactions that are inherent in the use of  $\text{FeCl}_3$ , alternative catalyst systems have been investigated.<sup>17</sup> Of these, antimony pentachloride ( $\text{SbCl}_5$ ) has shown good promise. This cationic catalyst readily initiates condensation reactions at room temperature and the reaction progresses without causing significant cross-linking of the polymer. The resulting polymer was reported to be readily soluble in aromatic or chlorinated solvents. However, if higher temperatures are used in the condensation reaction, the catalyst seems to behave very similar to  $\text{FeCl}_3$ , producing side reactions that generate a cross-linked elastomer.



**Scheme 6** Typical condensation reactions leading to a cross-linked polymer.

A typical polymerization method used at AWE to make poly(*m*-carborane-siloxane) rubbers is detailed briefly in the following paragraphs.

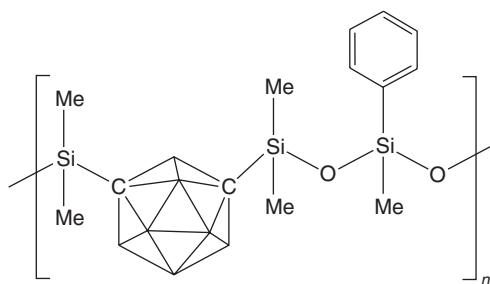
1,7-Bis-(di-methylmethoxysilyl)-*m*-carborane was used as the carborane-containing precursor. Briefly, a typical reaction mix included 1,7-bis-(di-methylmethoxysilyl)-*m*-carborane (40 g), di-chloro-di-methylsilane (16 g), and anhydrous ferric chloride (1 mol % of the carborane) as a catalyst. The reactions are shown in scheme 7. The



**Scheme 7** Reaction scheme used at AWE.

equimolar condensation reaction between chloro- and methoxy- (on the *m*-carborane precursor) generates chloromethane gas, producing a polymer. In order to drive the reaction forward, it was necessary to add two portions of catalyst at different times during the polymerization. In addition, it was also necessary to raise the temperature from 110°C to 180°C. The resulting product was a brownish-black material that was washed with acetone to reduce residual catalyst levels.

Phenyl and vinyl modified versions of poly(*m*-carborane-siloxane) were readily prepared using the procedure just described, by introducing the appropriate silane feed into the reaction mix.<sup>19</sup> Typically, 1 to 3 mol % di-chloro-methylvinylsilane was added to the di-chlorosilane feed in the syntheses described earlier. The repeat unit of the phenyl modified poly(*m*-carborane-siloxane) is shown in 5.



Typical repeat unit of the phenyl modified polymer.

5

After synthesis, the modified carborane-siloxane gums were fabricated into shaped components using standard siloxane vulcanization and fabrication technology. Di-chlorobenzyl peroxide (1% by wt) was used as the cross-linking agent and mixed into the polymer formed in scheme 7. Shaped rubber components were readily prepared by compression molding operations at 70°C. Postcure operations were typically at 120°C for 24 hours.

### A. Bis(ureido)silanes: Condensation Polymerization

An alternative route to poly(*m*-carborane-siloxane) rubbers is via the condensation reaction between *m*-carborane di-hydrocarbyl-disilanol and a bis-ureidosilane.<sup>20</sup> This mild reaction allows the incorporation of desired groups into the polymer via both the dihydrocarbyl-disilanol and the bis-ureidosilane (see scheme 8). The first step involves the formation of the carborane silanol from the butyl lithium carborane derivative. The bis-ureidosilane is prepared from the phenyl isocyanate (see step 2), and the final step involves reacting the dihydrocarbyl-disilanol with bis-ureidosilane.

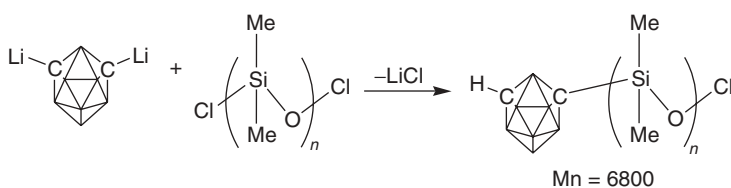
Polymers that have been successfully produced using this route are typically linear, high molecular weight ( $>10^6$  daltons), and show excellent thermal stability in both air and in nitrogen up to 800°C.

This approach allows the  $T_g$  of prepared polymers to be readily changed by altering the steric hindrance properties of the alkyl groups within the bis(*N*-pyrrolidino-*N*-phenylureido) dialkyl reagent. Thus, 33% diphenylsiloxane incorporation into the



## B. Dilithiocarbaborane: Salt Elimination Route

The preparation of poly(*m*-carborane-siloxane) polymers has also been successfully achieved directly from the carborane monomer.<sup>22</sup> The reaction used is shown in scheme 9. Here, the direct salt elimination reaction between dilithiocarbaborane and a dichlorosiloxane (e.g., 1,5-dichlorohexamethyltrisiloxane) results in the formation of linear polymers with a molecular-weight ( $M_n$ ) typically of 6800 dalton. However, the reported literature detailing this approach is very limited indeed, and the reaction has not found significant use. This is most probably because only relatively low molecular-weight polymers can be produced, ultimately restricting the flexibility to produce materials of controlled mechanical properties.



Scheme 9 Dilithiocarbaborane route.

## IV. CHARACTERIZATION

At AWE, the Lewis acid-catalyzed bulk polymerization route has been the main synthesis route to poly(*m*-carborane-siloxane) elastomers. Our selection has been based on considerations of safety, availability of key reagents, and ease of scale-up operations. An understanding of the physical and chemical properties of these materials, and how these properties can be modified through the synthesis process, is essential in order to develop materials of controlled characteristics.

In the following sections, details are provided on a selection of analytical techniques that have been typically used to characterize poly(*m*-carborane-siloxane) elastomers.

### A. Nuclear Magnetic Resonance Spectroscopy

The presence of four kinds of nuclear magnetic resonance (NMR) observable nuclei ( $^1\text{H}$ ,  $^{11}\text{B}$ ,  $^{13}\text{C}$ , and  $^{29}\text{Si}$ ) allows poly(*m*-carborane-siloxane) to be readily investigated using NMR spectroscopy. In addition,  $^1\text{H}$  spin-echo NMR relaxation techniques can provide an insight into polymer segmental chain dynamics and therefore useful information on material viscoelastic characteristics.

$^{11}\text{B}$  and  $^{11}\text{B}\{^1\text{H}\}$  solution-state NMR spectra (see Fig. 1a) clearly show the different boron environments within the *m*-carborane unit. The eight peaks in the  $-10$  to  $0$  ppm range are indicative of the different boron environments in the *m*-carborane cage, including B—B, B—C, and B—H bonds. The spectrum also contains

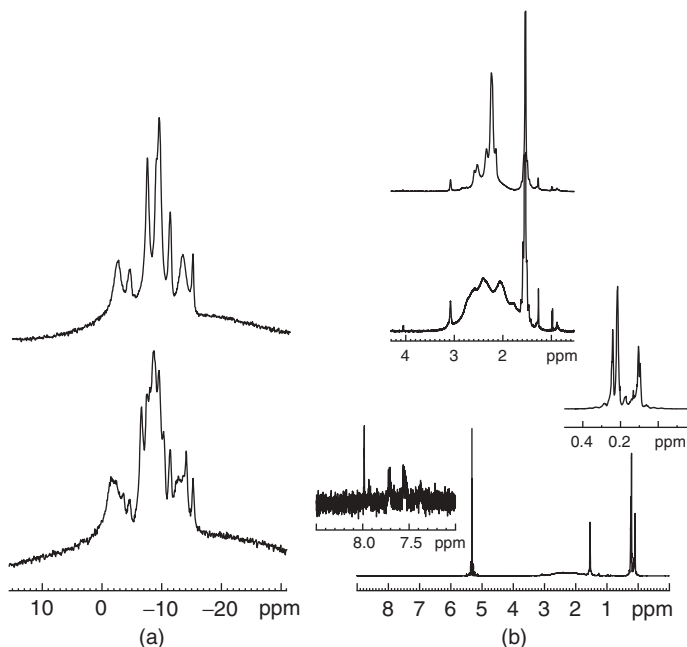


**Figure 1** Solution-state NMR spectra of the  $\text{CD}_2\text{Cl}_2$  soluble fraction of phenyl modified poly (*m*-carboranyl-siloxane) rubber. (a)  $^{11}\text{B}$  and  $^{11}\text{B}[^1\text{H}]$  NMR; (b)  $^1\text{H}$  and  $^1\text{H}[^{11}\text{B}]$  NMR.

characteristic broad lines due to unresolved  $^{11}\text{B}$ — $^{11}\text{B}$  and  $^{11}\text{B}$ — $^{10}\text{B}$  couplings. These results are in general agreement with that obtained by Kimura.<sup>23</sup> The  $^1\text{H}$  and  $^1\text{H}\{^{11}\text{B}\}$  solution-state NMR spectra of the soluble fraction are shown in Figure 1b. Three proton environments representative of the carborane, methyl, and phenyl groups were observed.<sup>24</sup> The application of  $^{11}\text{B}$  decoupling (depicted in the inset) shows the increased resolution afforded by heteronuclear decoupling.

## B. Gel-Permeation Chromatography

Polymer molecular-mass characteristics can be readily assessed using gel-permeation chromatography (GPC). GPC on the tetrahydrofuran (THF) soluble fraction shows a single broad molecular-mass distribution with a polydispersity of approximately 3.9. In addition, the weight-average molecular weight ( $M_w$ ) was typically 154,000 daltons, demonstrating that the synthetic route generates relatively linear high molar-mass polymer. Further details on the GPC analysis of these materials have been reported in an earlier publication.<sup>25</sup>

## C. Thermal and Chemical Properties

Both the glass-transition temperature ( $T_g$ ) and the melting temperature ( $T_m$ ) of a polymer dictate whether the material is likely to be elastomeric at service

temperature and indicate temperatures at which behavior is likely to change. It is therefore important that these transition temperatures are controlled and, preferably, outside the temperature range envisaged for possible future applications.

The  $T_g$  of elastomers synthesized at AWE was generally found to be within the range  $-30^\circ$  to  $-40^\circ\text{C}$  (see Table 2), which is significantly higher than that for standard poly(dimethylsiloxane). The introduction of the bulky *m*-carborane unit into the siloxane backbone has clearly elevated the  $T_g$ . However, although the carborane unit introduces conformational rigidity, the polymer chains retain sufficient flexibility and mobility to have a  $T_g < -30^\circ\text{C}$ .

**Table 2** Thermal Transition Temperatures

Thermal Transition Property	Standard Polysiloxane	Unmodified	Phenyl Modified	Phenyl-vinyl Modified
Glass transition ( $^\circ\text{C}$ )	-115	-39	-35	-35
Melting point ( $^\circ\text{C}$ )	-45	60	No melting	No melting
Enthalpy of melting ( $\text{Jg}^{-1}$ )	22.7	10		

The unmodified poly(*m*-carborane-siloxane) elastomer exhibits crystallinity, with a melting midpoint of  $60^\circ\text{C}$  and a  $10 \text{ J/g}$  endotherm. In view of the relatively bulky carborane unit in the polymer backbone, the presence of crystallinity in these materials is quite surprising. However, it may be explained through electron-deficient sites (carborane) along their main chains having increased affinity for electronegative sites (oxygen), resulting in greater cohesive energies between chains. This electrostatic attraction will aid the formation of crystalline regions.

A melting midpoint of  $60^\circ\text{C}$  is very undesirable, as it is very close to room temperature and/or in-service temperature range. Fortunately, the properties of these polymers, such as transition temperatures and thermal stability, can be readily altered by changes to pendant groups or by altering the number of siloxane groups per repeat unit. Thus, the phenyl-modified poly(*m*-carborane-siloxane) shows a slightly higher glass transition at  $-35^\circ\text{C}$ , and fortunately, no evidence of crystallinity. The introduction of pendent phenyl groups along the polymer chain readily suppresses the formation of crystalline domains. As a result the phenyl-modified poly(*m*-carborane-siloxane) rubbers show amorphous behaviour.<sup>26</sup>

Other material properties that are of general interest to the polymer chemist are shown in Table 3. Linear toluene swell is indicative of cross-link density in the material. The vinyl-phenyl modified rubber showed the lowest degree of swell. This is due to additional cross-links introduced by the vinyl groups during synthesis. The unmodified rubber was found to swell considerably in toluene and was found to dissolve partially in the solvent.

Atomic emission spectroscopy (AES) studies on these materials show a boron content of approximately 28.8%. Because of the dilution effects of the vinyl/phenyl

**Table 3** Summary of Physical and Chemical Properties

Property	Standard Polysiloxane	Unmodified	Phenyl Modified	Phenyl-vinyl Modified
Linear toluene swell (% of thickness) per unit density	70	Dissolves	40	19
% B from atomic emission spectroscopy (calculated from repeat unit)	0	28.8 ± 0.4 (31)	29.5 ± 0.2 (30)	26.4 ± 0.2 (30)

units, the vinyl-phenyl-modified polymer shows the lowest boron content. Surprisingly, the phenyl-modified polymer showed a higher boron content than the unmodified rubber (29.5% compared with 28.8%). This difference could be because the synthesis of the unmodified material resulted in some moisture deactivation of the carborane precursor (thus reducing the amount of carborane incorporated in the polymer). Moisture (hydrolysis) of the chlorosilane in the preparation of the phenyl-modified rubber is also possible and would lead to higher than expected boron in the polymer network. Overall, the measured boron content was in agreement with those values predicted from the polymer repeat unit. In comparison, a polymer comprising purely meta-carborane repeat units show a maximum boron content of 76%; however, such systems are not elastomeric in nature.

An understanding of the residual catalyst content of prepared materials is important as it could potentially influence materials ageing and reliability. For  $\text{FeCl}_3$ , the co-ordination by water to the  $\text{Fe}^{3+}$  will result in the formation of acidic species that could induce hydrolysis and scission of the Si—O—Si linkage. We have utilised Mössbauer spectroscopy to assess the nature of the  $\text{FeCl}_3$  catalyst in the final polymer. Our work in this area is quite original, as there are no reports of any such studies being performed previously on these materials.

Our  $^{57}\text{Fe}$  Mössbauer studies show that the catalyst reverts typically to  $\text{Fe}^{3+}$  and  $\text{Fe}^{4+}$  oxides (Fig. 2). The quadruple splitting pattern and the isomer shift values are typical of iron oxides. Our studies show no evidence of residual  $\text{FeCl}_3$ , suggesting that the high-temperature postcure operations in particular have resulted in the conversion of  $\text{FeCl}_3$  to the metal oxide. This is quite beneficial, as it is likely that these oxides will act as conventional reinforcing particulate fillers, increasing the rigidity of the elastomer without causing significant degradation of the polymer.

Some original work currently being investigated at AWE is the synthesis of foamed polysiloxanes incorporating carborane cages. Briefly, a series of tin-catalyzed condensation reactions results in the evolution of hydrogen gas (blowing reaction) and a cross-linked polysiloxane network. The introduction of functionalized carborane cages into the reaction mix results in a filled polymer or a copolymer where the carborane is bound directly to the polymer chains.

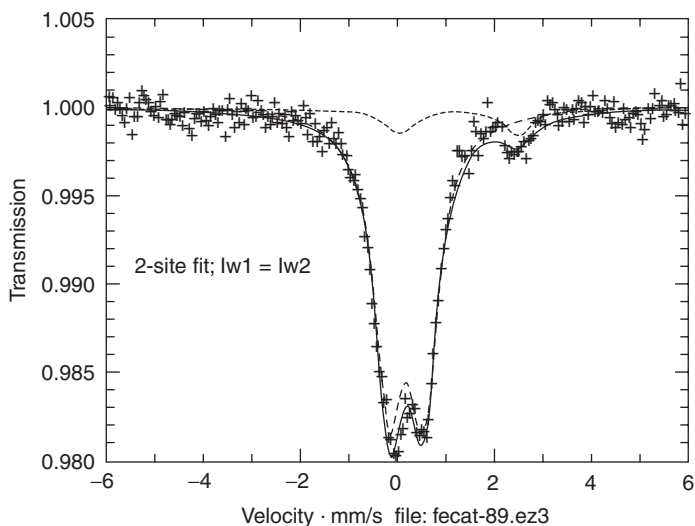


**Figure 2**  $^{57}\text{Fe}$  Mössbauer spectrum for a poly(*m*-carborane-siloxane).



**Figure 3** 3D computerized tomography (CT) image of a foamed polysiloxane incorporating a small admixture of carborane cages.

Successful development of such systems will lead to foamed materials having useful stress-absorbing characteristics in addition to controlled “physics” properties. Although our work in this area is currently in a very early stage, prototype materials have been successfully synthesized and assessed structurally using three-dimensional (3D) X-ray microtomography. The technique offers a unique insight into the internal microstructure of cellular materials (see Fig. 3). The diameter of the mainly open cell pores varies from approximately 100 to 250  $\mu\text{m}$  (the resolution of the instrument is 5  $\mu\text{m}$ ), with cell walls of variable thickness.

## V. THERMAL AND RADIATION STABILITY

Since icosahedral carboranes are generally viewed as 3D “energy sinks” as well as polymer building blocks, the thermal and radiation stability that these units impart on the base rubbery material needs to be explored. While the thermal stability of these materials has been studied and reported by a number of workers, there is little reported work on the stability of these materials to ionizing radiation. A brief account of our work within this area is detailed below.

Our investigations have shown that the incorporation of electron-deficient carborane cages into the polysiloxane main chain tends to strengthen the siloxane bond to thermal degradation. The typical high-temperature degradation process in siloxanes, depolymerization, or unzipping of the base siloxane rubber, is modified/hindered.<sup>27</sup> Presumably, the addition of a carborane cage into the main chain of the siloxane reduces the ability of chains to attain the necessary conformation for cyclic decomposition to occur. This stabilizing effect has been attributed to increased inductive  $d\pi-p\pi$  bond contributions and has been discussed in more detail by Kesting et al.<sup>28</sup>

On heating in air at 10°C per min, poly(*m*-carborane-siloxane) shows typically only 4% mass loss at 450°C and 7% mass loss at 600°C (see Fig. 4). In comparison, siloxanes without carborane units, show an approximate 50% mass loss at 450°C. As a consequence of the relatively high boron and carbon content of these materials, pyrolysis is expected to generate ceramic residues of boron carbide/silicon carbide.

These elastomers show good resistance to oxidative thermal degradation; however, a carborane moiety containing 10 boron atoms will take up to 15 oxygen atoms on oxidation. Hence, carborane-siloxane polymers can typically undergo considerable weight increases (up to 50%) largely due to the incorporation of up to 15 oxygen per cage of the repeat unit. Figure 4 shows an increase in mass of approximately 10%.

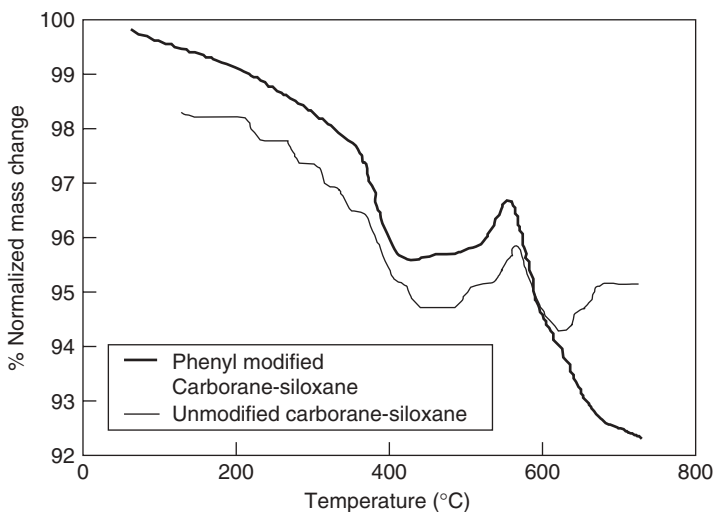


**Figure 4** Weight loss vs. temperature for poly(*m*-carborane-siloxane)s in air.

In thick samples, a boron oxide/boron carbide crust has been detected on the surface of the polymer. This inorganic surface layer has a shielding effect on the inner polymer layers, further enhancing the thermal stability of the material. Poly(*m*-carborane-siloxane)s have therefore been considered as surface coatings for organic materials, providing protection from erosion effects.

In general, as the length of the dimethylsiloxane chain sequence increases, reducing the concentration of the carborane within the polymer, the weight loss as a function of temperature increases. Their studies showed that the weight loss is linearly related to the number of dimethylsiloxane groups within the repeat unit. Thus, the incorporation of the carborane cage into the polymer backbone increases its resistance toward reversion. Figure 4 also shows a concomitant mass loss with temperature. This is in agreement with observations reported on similar poly(siloxane)-based materials by Knollmueller et al.<sup>18</sup> This mass loss most probably arises from the production and evolution of volatile products such as hydrogen and methane through chain scission followed by radical combination reactions. There is evidence of damage to the *m*-carborane moiety, as indicated by significant mass loss at temperatures approaching 580°C.

The impact of heat and of ionizing radiation on the carborane cage is evident in the <sup>11</sup>B Magic Angle Spinning Nuclear Magnetic Resonance (<sup>11</sup>B MAS) NMR spectrum shown in Figure 5. At 580°C, the broad resonance that appeared as a shoulder at 480°C dominates the spectrum. The broad lineshape and the range of chemical shifts of this peak are consistent with both amorphous boron oxides and boron carbide. The final residues of some of these experiments are of a ceramic nature. The broad and

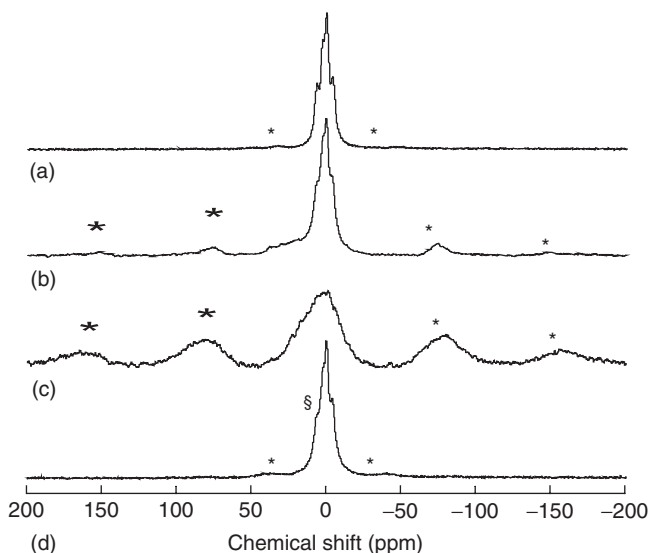


**Figure 5** <sup>11</sup>B MAS NMR spectra: (a) pristine phenyl modified elastomer; (b) heated at 480°C for 2 h; (c) heated at 580°C for 2 h; (d) after 1 MGy gamma exposure. (\* represents spinning sidebands.)

extensive manifold of spinning sidebands (\*) indicates that the boron species are, for the most part, immobile, reflecting the damage of the carborane cage at high temperatures. Figure 5 also shows that gamma radiation to an absorbed dose of 1 MGy appears to cause little damage to the carborane cage.

To further assess the thermal stability of these materials, we have carried out NMR relaxation measurements. NMR relaxation data of stereochemically different nuclei will give useful information on the local environments of these nuclei. The more restricted the environment around a given group type, the more rapidly it will relax. The spin-spin or transverse relaxation time ( $T_2$ ) is diagnostic of the rigidity of the material. A rubber with high cross-link density results in spins being held in close proximity to other spin active species, resulting in rapid  $T_2$  relaxation times. Materials that are more mobile will exhibit longer  $T_2$  regimes.

$^1\text{H}$  spin-echo decay measurements have been made on poly(*m*-carborane-siloxane)s (see Fig. 6). The rapidly decaying component is generally assigned to the network species, while the slower decaying component is assigned to the nonnetwork solvent soluble fractions or dangling chain ends. The results confirm a decrease in segmental mobility caused by oxidative cross-linking effects. In addition, our studies show that exposure to gamma radiation (dose of 1 MGy) leads only to a small

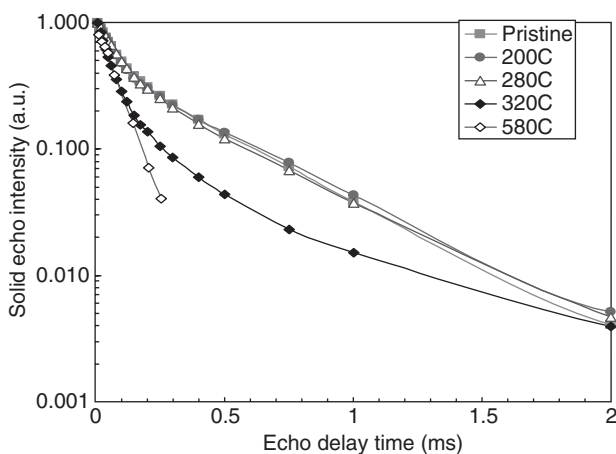


Figure 6 NMR proton spin-echo intensity vs. time.

change in the  $^1\text{H}$  spin-echo relaxation profile (see Fig. 7). The indicated trend suggests slight stiffening (through cross-linking effects) and slowing of chain dynamics. Taking into account the large gamma dose, this change is not however too pronounced, suggesting that the material shows in general good stability in radiation environments. The stabilizing effect of the carborane cage most probably arises through different resonance states of the boron cage, a mechanism through which the cage may act as an energy sink or sponge for both gamma radiation and heat.

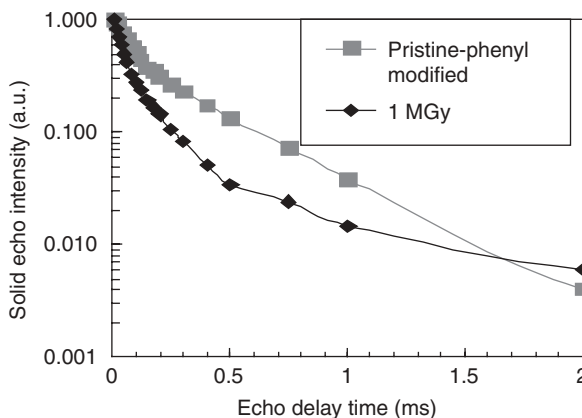
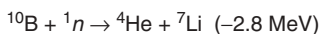


Figure 7  $^1\text{H}$  spin-echo profiles for a poly(*m*-carborane-siloxane).

### A. Stability to Neutrons

There are a number of papers in the open literature explicitly reporting on the properties of boron cluster compounds for potential neutron capture applications.<sup>1</sup> Such applications make full use of the  $^{10}\text{B}$  isotope and its relatively high thermal neutron capture cross section of  $3.840 \times 10^{-28} \text{ m}^2$  (barns). Composites of natural rubber incorporating  $^{10}\text{B}$ -enriched boron carbide filler have been investigated by Gwaily et al. as thermal neutron radiation shields.<sup>29</sup> Their studies show that thermal neutron attenuation properties increased with boron carbide content to a critical concentration, after which there was no further change.

An interesting application utilizing the neutron capture approach is the treatment of tumors and some forms of melanoma. Thus,  $^{10}\text{B}$  enriched compounds are functionalized and delivered so that they target tumor cells. The targeted cells are then irradiated with thermal neutrons. The resulting nuclear reaction (see scheme 10) generates energetic alpha particles with a penetration range of approximately  $10 \mu\text{m}$ . Targeted cells are destroyed, leaving the healthy tissue undamaged.



Scheme 10 The neutron capture reaction of  $^{10}\text{B}$ .

It is generally recognized that all polymers incorporating icosahedral carboranes should be efficient neutron shields. This is because neutron irradiation deposits energy in a system by two principal mechanisms: elastic scattering of fast neutrons by light atoms (e.g., hydrogen), and absorption (predominantly thermal) by atoms with large effective cross sections. Icosahedral carborane cages ( $\text{C}_2\text{B}_n\text{H}_{n+2}$ ) contain high concentrations of both boron and hydrogen, and thus should show good potential in neutron capture properties. There is, however, no reported information on the stability or

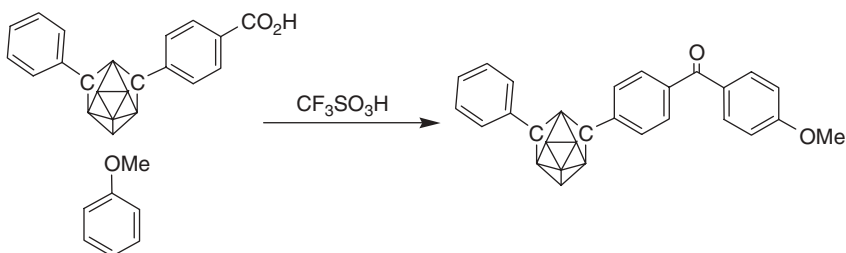
extent of damage of the carborane unit after neutron capture by boron atoms within the structure. The release of energetic alpha particles may initiate significant bond scission effects within the cage, causing significant disruption to the carborane structure.

## VI. OTHER CARBORANE-CONTAINING POLYMERS

Carborane-containing polymers other than polysiloxanes are reported in the open literature and will be briefly mentioned here to give a “flavor” for the area.

### A. Poly(ether-ketone-carborane)

In the development of materials with enhanced thermal stability, the effects of incorporating icosahedral carborane units into the chains of an already thermally stable polymer, the aromatic poly(ether-ketone)s, have been reported.<sup>30</sup> Materials were prepared using trifluoromethanesulphonic acid ( $\text{CF}_3\text{SO}_3\text{H}$ ) as both catalyst and solvent for the electrophilic polycondensation of certain aromatic ethers with carboxylic acids at room temperature (see scheme 11). This afforded relatively high molecular-weight linear materials and confirmed the high stability of the carborane unit in strongly acidic media. Prepared polymers were all amorphous and showed glass-transition temperatures in the range 174–214°C. Strong transparent polymer films could be readily prepared by dissolving in chloroform and casting.



**Scheme 11** Condensation of aromatic ethers and acids.

In comparison to conventional poly(ether-ketone)s, their thermal stability is generally reduced; however, the materials exhibited enhanced mass retention properties on pyrolysis (see Fig. 8). Thermogravimetric analysis studies in nitrogen at 10°C/min show that poly(ether-ketone-carborane) show a lower onset temperature for volatile evolution, but the weight loss to elevated temperatures is less than 11%. In comparison, poly(ether-ketone)s show a higher onset temperature for volatile loss (approximately 540°C) and a total weight loss of 50% by mass. Because of the high carbon-to-boron ratio in the poly(ether-ketone-carborane), pyrolysis is expected to lead to ceramic residues comprising a mix of boron carbide dispersed in a graphitic matrix.

An area of work closely related to poly(ether-ketone-carborane) that attracted significant interest in the late 1990s, is the synthesis of poly(aryletherketone-carborane)s. Studies were conducted investigating the incorporation of carborane units into the

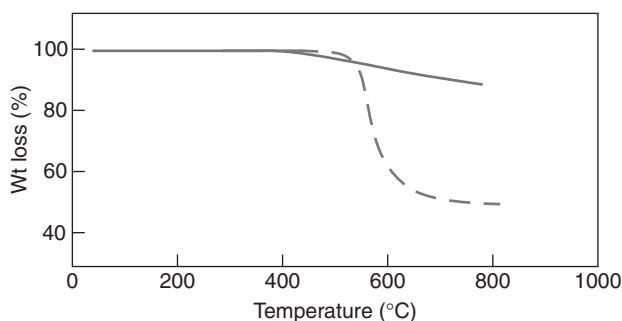
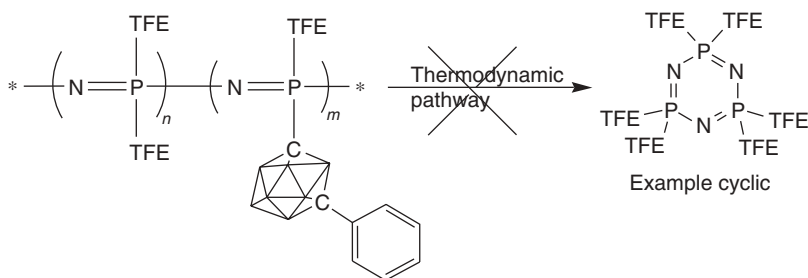


**Figure 8** Mass loss of poly(ether-ketone-carbaborane) relative to that of PEEK (dashed).

backbone of aromatic polyetherketone chains.<sup>31</sup> This modification causes the aromatic polyetherketone chains to lose the ability to crystallize, suggesting the carbaborane unit is essentially incompatible with the crystal lattice. Poly(aryletherketone-carborane)s are therefore generally amorphous materials with relatively high glass-transition temperatures ( $>200^{\circ}\text{C}$ ). Prepared polymers also showed good mechanical strength and chemical stability, including solubility in dipolar aprotic solvents. These materials showed good potential as thin-film separation membranes.

## B. Polyphosphazene Incorporating Carboranyl Units

The final class of polymers containing carboranyl units to be mentioned here is the polyphosphazenes. These polymers comprise a backbone of alternating phosphorous and nitrogen atoms with a high degree of torsional mobility that accounts for their low glass-transition temperatures ( $-60^{\circ}\text{C}$  to  $-80^{\circ}\text{C}$ ). The introduction of phenyl-carboranyl units into a polyphosphazene polymer results in a substantial improvement in their overall thermal stability. This is believed to be due to the steric hindrance offered by the phenyl-carborane functionality that inhibits coil formation, thereby retarding the preferred thermodynamic pathway of cyclic compound formation (see scheme 12).



**Scheme 12** The influence of steric congestion on thermal degradation pathway.

## VII. ENERGETIC CARBORANE POLYMER SYSTEMS

When one considers the potential high-energy release on rupture of a carborane unit, together with the thermodynamic stability of combustion products, it is hardly surprising that there is a body of literature that reports on the use of carboranes within propellant compositions. Their use in energetic applications is to be expected when the enthalpy of formation ( $\Delta H_f^\theta$ ) data for the products of combustion for boron are compared to those of carbon. Thermodynamic data for the enthalpy of formation of *o*-carborane and of typical boron and carbon combustion products is shown in Table 4. Measurements of the standard enthalpy of combustion<sup>32</sup> for crystalline samples of *ortho*-carborane show that complete combustion is a highly exothermic reaction,  $\Delta H_c^\theta = -8994 \text{ KJmol}^{-1}$ .

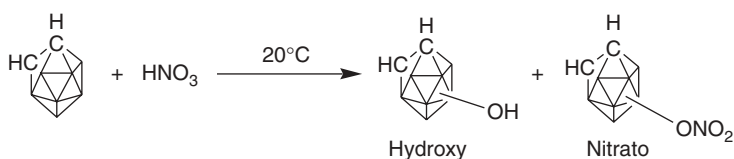
**Table 4** Enthalpy of Formation for *o*-Carborane and Combustion Products

Compound	$\Delta H_f^\theta$ (KJmol <sup>-1</sup> )
BO (g)	+25.0
BO <sub>2</sub> (g)	-300.4
B <sub>2</sub> O <sub>3</sub> (g)	-843.8
H <sub>2</sub> O (g)	-241.8
CO (g)	-110.5
CO <sub>2</sub> (g)	-393.5
<i>o</i> -C <sub>2</sub> B <sub>10</sub> H <sub>12</sub> (s)	-170

Vinyl- and allylcarborane containing polymers<sup>33</sup> and copolymers<sup>34</sup> have been used as solid propellant binders. The incorporation of oxidizers, for example, NH<sub>4</sub>ClO<sub>4</sub>, KClO<sub>4</sub>, or NH<sub>4</sub>NO<sub>3</sub>, makes high-impulse-type propellants having high flame speeds and high heats of combustion. The mechanical strength and burning characteristics of the propellant can be greatly altered by the addition of a resin based on either urea- or phenol-formaldehydes. Composite propellants with burning rates in the range 4 to 20 in. s<sup>-1</sup> are formed when carboranyl ballistic modifiers (burn rate modifiers), for example, alkylcarboranes, geminal NF carboranes, and siloxy- or silylcarboranes, are incorporated into the formulation. Burn rates up to 400% (when compared to a control propellant) are obtained for 10–14% weight percent of ballistic modifier.<sup>35</sup>

In the literature, there are reports of carborane units bearing energetic groups, including nitro- and nitro-phenyl. The treatment of *o*-carborane with 100% nitric acid at room temperature is reported<sup>36</sup> to yield a B-hydroxyl and a B-nitrato-*o*-carborane (see scheme 13).

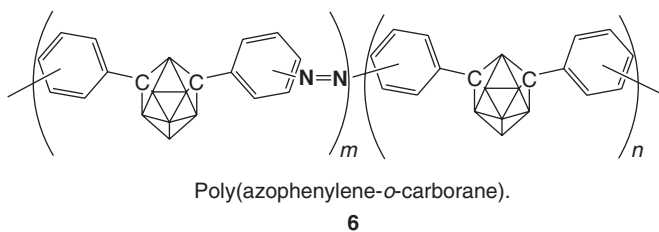
The nitrate was reported as being extremely unstable and detonated on heating, presumably due in part to the electron-withdrawing nature of the carborane. However, the reaction between nitric acid and either phenyl- or hydroxymethyl-*o*-carborane derivatives yields products where the position of nitration is directed



**Scheme 13** Formation of nitro-*o*-carborane via dissolution in nitric acid.

toward the substituent and not the carborane cage. Thus, 1-hydroxymethyl- and 1,2-bis(hydroxymethyl)-*o*-carborane is converted to the highly explosive 1-nitro- and 1,2-dinitro-*o*-carboranes, respectively, by cold nitric acid.<sup>37</sup> Rather encouragingly 1-phenyl-*o*-carborane reacts with 100% nitric acid or with a mixture of nitric and sulfuric acids in an inert solvent, forming predominantly 1-(*p*-nitrophenyl)-*o*-carborane.<sup>38</sup> Interestingly, nitroso derivatives of *o*-carborane have been synthesized from lithio-carboranes and nitrosyl chloride at very low temperatures.<sup>39</sup>

Poly(azophenylene-*o*-carborane) (see **6**) has been prepared from diphenyl-*o*-carborane by means of nitration, reduction, and acylation to initially give 1,2-bis(*N*-nitroso-acetylaminophenyl)-*o*-carborane (NAFC). Rapid decomposition in solution affords phenylene amino phenyl carborane (PAFC) by recombination of phenylene and azophenylene radicals.<sup>40</sup> These radicals have also been utilized to form copolymers of carborane-containing copolymers from monomers polymerizable via radical mechanisms. Thus, copolymers of polystyrene and poly(azophenylene) can be readily formed by means of emulsion copolymerization of styrene with NAFC decomposition products.



## VIII. SUMMARY

In this chapter we have attempted to capture the general synthesis chemistry and material properties of some important polymer systems incorporating icosahedral closo-dicarbaborane cages. In particular, we have focused on the development of poly(*m*-carborane-siloxane)s, as they show good potential for properties that are of special interest to AWE. Potential envisaged applications include corrosion-resistant protective layers, high-temperature-resistant polymers, and radiation absorbing/shielding systems.

The present limited availability of raw carborane materials, combined with the relatively high cost, has resulted in relatively few specialists active within this area

of science. However, we expect the interest within this field to increase as the potential of closo-dicarbaborane cages in the development of materials with specially tailored properties becomes recognized. Clearly, more needs to be done to fully exploit these materials. Hopefully, this chapter will provide a useful reference for chemists and material scientists who wish to explore this relatively challenging and novel area of chemistry.

## IX. REFERENCES

1. J. Plesek, *Chem. Rev.*, **92**(2), 269 (1992).
2. M. J. Bayer, M. F. Hawthorne, *Inorg. Chem.*, **43**(6), 2018 (2004).
3. H. Beall, *Inorg. Chem.*, **11**(3), 637 (1972).
4. J. Green, *Polym. Lett.*, **2**, 987 (1964).
5. R. H. Cragg, M. S. Fortuin, N. N. Greenwood, *J. Chem. Soc. A*, 1817 (1970).
6. H. C. Beachell, B. F. Dietrich, *J. Am. Chem. Soc.*, **83**, 1347 (1961).
7. W. Jeffers, *J. Chem. Soc.*, 1919 (1963).
8. J. Green, M. M. Fein, N. Mayes, G. Donovan, M. Israel, M. S. Cohen, *J. Polym. Sci., Polym. Lett.*, **2**, 987 (1964).
9. S. Packirisamy, *Prog. Polym. Sci.*, **21**, 707 (1996).
10. L. Noristi, E. Marchetti, G. Barruzi, P. Sgarzi, *J. Polym. Sci. Part A: Polym. Chem.*, **32**, 3047 (1994).
11. A. D. Delman, J. J. Kelly, A. A. Stein, B. B. Simms, *J. Polym. Sci. Part A-1*, **5**, 2119 (1967).
12. L. L. Fewell, *J. Appl. Polym. Sci.*, **28**, 2659 (1983).
13. H. Colquhoun, D. Lewis, *Polymer*, **38**(17), 4539 (1997).
14. W. A. Fort, "Carborane Polymers" Weapons Chemistry Branch, Memo. No. 645, AWE, Aldermaston, UK (1979).
15. V. V. Korshak, M. M. Teplyakov, Ts. L. Gelashvili, S. M. Komarov, V. N. Kalinin, L. I. Zhakarkin, *J. Polym. Sci., Polym. Lett. Ed.*, **17**(3), 115 (1979).
16. K. O. Knollmueller, Robert. N. Scott, *J. Polym. Sci. Part A-1*, 1071 (1971).
17. H. J. Dietrich, R. P. Alexander, T. L. Haying, *Die Makromolekulare*, **175**, 425 (1974).
18. K. O. Knollmueller, R. N. Scott, H. Kwasnik, J. F. Sieckhaus, *J. Polym. Sci., A-1*, **9**, 1071 (1971).
19. M. Patel, A. C. Swain, *Polym. Deg. Stab.*, **91**, 548 (2006).
20. D. D. Stewart, E. N. Peters, C. D. Beard, G. B. Dunks, E. Hedaya, G. T. Kwiatkowski, R. B. Moffitt, J. J. Bohan, *Macromolecules*, **12**(3), 373 (1979).
21. E. N. Peters, E. Hedaya, J. H. Kawakami, G. T. Kwiatkowski, D. W. McNeil, R. W. Tulis, *Rubber Chem. Technol.*, **48**, 14 (1975).
22. E. N. Peters, U.S. Patent 4,235,987 (Nov 25, 1980).
23. H. Kimura, K. Okita, M. Ichitani, T. Sugimoto, S. Kuroki, I. Ando, *Chem. Mater.* **15**, 355 (2003).
24. M. Patel, A. C. Swain, J. L. Cunningham, R. S. Maxwell, S. C. Chinn, *Polym. Deg. Stab.*, **91**, 548 (2006).
25. M. Patel, A. C. Swain, A. R. Skinner, L. G. Mallinson, G. F. Hayes, *Macromol. Symp.*, **47**, 202 (2003).
26. R. E. Kesting, K. F. Jackson, E. B. Klusman, F. J. Gerhart, *J. Appl. Polym. Sci.*, **14**, 2525 (1970).
27. M. Patel, A. R. Skinner, ACS Symp. Ser. 838, p. 138 (2003).

28. R. E. Kesting, K. F. Jackson, E. B. Klusmann, F. J. Gerhart, *J. Appl. Polym. Sci.*, **14**, 2525 (1970).
29. S. E. Gwaily, M. M. Badawy, H. H. Hassan, M. Madani, *Polym. Testing*, **21**, 129 (2002).
30. H. M. Colquhoun, J. A. Daniels, I. R. Stephenson, K. Wade, *Polym. Commun.*, **32**(9), 272 (1991).
31. H. M. Colquhoun, D. F. Lewis, P. L. Herbertson, K. Wade, *Polymer*, **38**(17), 539 (1997).
32. Gal'chenko, G. L. Martynouskaya, I. V. Stanko, *Zh. Obshch. Khim.*, **40**, 2410 (1970).
33. S. L. Clark, H. L. Goldstein, T. Heying, U.S. Patent, 3,121,117.
34. H. L. Goldstein, T. L. Heying, U.S. Patent, 3,109,031 (Oct 29, 1963).
35. W. E. Hill, L. R. Beason, U.S. Patent, 3,764,417.
36. L. I. Zakharkin, V. N. Kalinin, L. S. Podvisotskaya, *Zh. Obshch. Khim.*, **36**, 1786 (1966).
37. L. I. Zakharkin, V. A. Brattsev, V. I. Stanko, *Zh. Obshch. Khim.*, **36**, 886 (1966).
38. V. I. Stanko, A. V. Bodrov, *Zh. Obshch. Khim.*, **35**, 2003 (1965).
39. J. M. Kauffman, J. Green, M. S. Cohen, M. M. Fein, E. L. Cottrill, *J. Am. Chem. Soc.*, **86**, 4210 (1964).
40. A. A. Berlin, B. G. Gerasimov, A. A. Ivanov, A. P. Masliukov, V. N. Kalinin, *J. Macromol. Sci. Chem.*, **A14**, 999 (1980).

---

## CHAPTER 3

# Boron- and Nitrogen-Containing Polymers for Advanced Materials

**Philippe Miele and Samuel Bernard**

*Laboratoire des Multimatériaux et Interfaces, Université Lyon 1, Villeurbanne, France*

### CONTENTS

I. INTRODUCTION	104
II. POLYMERIC PRECURSORS OF BN FIBERS	105
A. tris(Alkylamino)boranes–Derived Poly[ <i>B</i> -(alkylamino)borazines]	105
B. tris( <i>B</i> -Alkylamino)borazine–Derived Poly[ <i>B</i> -(alkylamino)borazines]	107
C. Polymeric Precursors Derived from tris(Borylamino)borazines	112
i. Two-Step Polycondensation (Thermal Route)	112
ii. One-Step Polycondensation	116
III. OUTLOOK	118
IV. SUMMARY	118
V. REFERENCES	119

*Macromolecules Containing Metal and Metal-like Elements,*  
*Volume 8: Boron-Containing Polymers,* edited by Alaa S. Abd-El-Aziz,  
Charles E. Carraher Jr., Charles U. Pittman Jr., and Martel Zeldin.  
Copyright © 2007 John Wiley & Sons, Inc.

## I. INTRODUCTION

Boron-containing nonoxide amorphous or crystalline advanced ceramics, including boron nitride (BN), boron carbide ( $B_4C$ ), boron carbonitride (B/C/N), and boron silicon carbonitride Si/B/C/N, can be prepared via the preceramic polymers route called the polymer-derived ceramics (PDCs) route, using convenient thermal and chemical processes. Because the preparation of BN has been the most in demand and widespread boron-based material during the past two decades, this chapter provides an overview of the conversion of boron- and nitrogen-containing polymers into advanced BN materials.

Boron nitride is an artificial ceramic material of great importance for advanced technological applications, particularly for high-temperature structural purposes. Since the B—N bond is isoelectronic with the C—C bond, BN and carbon share common polymorphisms, the two main ones being the cubic form, for example, diamond and *c*-BN, and the hexagonal form, for example, graphite and *h*-BN. The hexagonal form appears to be the most thermodynamically stable phase under standard conditions and thus the easiest to obtain. This structure is composed of layers of hexagons, that is,  $B_3N_3$ , in which the hexagonal rings contain alternating boron and nitrogen atoms. The atoms are linked by covalent bonds within the sheets (*a* axis). The  $B_3N_3$  hexagons are packed in such a way that the atoms of two consecutive layers are below each other, with alternating boron and nitrogen atoms along the *c* axis. This array implies that the layers are linked by van der Waals-type bonds (*c* axis). According to this anisotropic structure, hexagonal BN displays a unique set of mechanical, optical, and thermal properties.<sup>1-3</sup> In particular, the mechanical properties along the *a* axis, the chemical and thermal stability, the oxidation resistance, and the low coefficient of thermal expansion along the *a* axis have led to an interest in, and a demand for, BN coatings, matrices, and fibers. Such specific morphologies, which cannot be prepared by classic high-temperature methods, have proffered new interest in boron- and nitrogen-containing molecular precursors and related preceramic polymers.

The nonoxide precursors route represents a chemical approach based on the use of air- and/or moisture-sensitive (molecular or polymeric) precursors by means of standard Schlenk techniques and vacuum/argon lines. This route allows the chemistry (elemental composition, compositional homogeneity, and atomic architecture) of molecular precursors to be controlled and tailored to provide the ensuing preceramic polymers with desirable composition, structure, and thermal properties. The preceramic polymers have received increased attention in order to prepare advanced nonoxide ceramics. This attention has enabled the tailoring of chemical composition to obtain a closely defined nanostructural organization by convenient thermal/chemical treatments (curing and thermolysis processes) under a selected oxygen-free atmosphere.<sup>4-9</sup> Compared to other methods of preparing ceramics, the main advantage of the PDCs route lies in the control of the rheological properties of preceramic polymers. This, in turn, allows the preparation of near-net shapes in a way not known from other techniques.

This chapter focuses on the description of boron-containing preceramic polymers, which are currently used for the preparation of complex shapes and have been

developed in our group. Our overall goal is to provide a detailed picture of the physicochemical criteria that define preceramic polymers in terms of processing shapes. Because processing ceramic fibers is the most challenging application, this chapter is exclusively dedicated to the description of requirements that define a proper melt-spinnable BN polymer candidate for fiber formation through the PDCs route. In the final section, some projections for future development of this area are drawn, and we shed some light on further scientific challenges.

## II. POLYMERIC PRECURSORS OF BN FIBERS

The conceptual preparation of BN materials from preceramic polymers chemistry was historically reported through works dedicated to the preparation of ceramic fibers. These fibers are of great interest as reinforcing agents for the fabrication of continuous fiber-reinforced ceramic matrix composites. These materials are known to have better potential against oxidation (thermal stability up to 900°C) than their structural analogs, that is, the carbon fibers, which undergo oxidation starting from 450°C. Numerous papers have been devoted to this subject in the relatively recent past.<sup>10–12</sup>

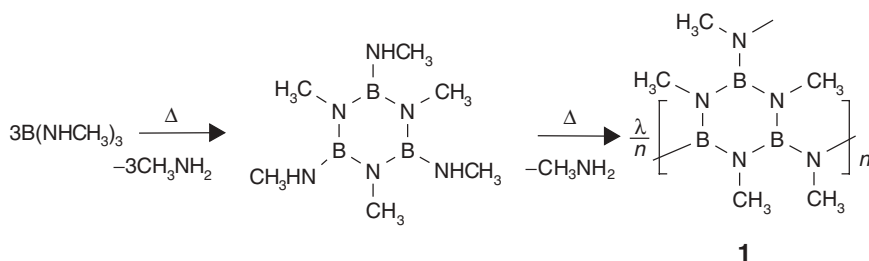
According to the correct 1:1 boron-to-nitrogen ratio and the symmetry of borazine, all these studies showed clearly that borazine-based polymers are suitable compounds for the preparation of BN fibers by the preceramic polymers route. However, to be spinnable, a polymer should offer a set of properties, including solubility (spinning in solution), adjusted melt-viscosity (melt-spinning), controllable thermal decomposition, and high ceramic yield. Such studies provided some prerequisite characteristics to improve the melt-stability of borazine-based polymers. They pointed out that good processing properties are always related to both the presence of alkyl chains linked to the polymer backbone and the type of connections between the monomeric units. In much of the same way, our investigations of polymer-derived BN fibers highlighted the need for tailoring borazine-based polymers for the preparation of boron nitride fibers via the melt-spinning and thermal-decomposition processes. In particular, they revealed that poly[*B*-(alkylamino)borazines] are well suited to filling the requirements as fiber precursors and that their architecture strongly influences their processing properties. Therefore, to explore properly the subject area of this chapter, we first define the potential of poly[*B*-(alkylamino)borazines] as precursors of BN fibers. Then we focus on the description of polyborylborazines, which are a new class of BN polymers that exhibit increased ring spacing and are potential melt-spinnable candidates.

### A. tris(Alkylamino)boranes–Derived Poly[*B*-(alkylamino)borazines]

Poly[*B*-(alkylamino)borazines] can be prepared through a multistep thermolysis process involving tris(monoalkylamino)boranes of the type B(NHR)<sub>3</sub> (R = Me, Pr<sup>*i*</sup>). Heating these molecular precursors under reduced pressure or in an inert atmosphere

results in their conversion to an intermediate *B*-(alkylamino)-*N*-(alkyl)borazine of the type  $[R(H)N]_3B_3N_3R_3$ , and then to the related poly[*B*-(alkylamino)borazine].

We focused our attention on the use of the tris(methylamino)borane,  $B(NHCH_3)_3$ , first, since it is expected to produce the best ceramic yield within the series, depending on the low weight methylamino substituent used.<sup>13–15</sup>  $B(NHCH_3)_3$  underwent classic cyclization and polycondensation reactions in an argon atmosphere to yield the corresponding poly [*B*-(alkylamino)borazine] **1**, which displayed borazine rings linked through  $-N(CH_3)-$  bridges (scheme 1).



**Scheme 1**

Polymer **1** showed good processing properties in the molten state, as illustrated by the preparation of several meters of polymeric fibers. The fibers were obtained at a spinning temperature ( $T_{\text{spinning}}$ ) of 150°C using a piston-driven lab-scale spinning apparatus associated with a windup spool as a stretching tool. This equipment was set up in a nitrogen-filled glove box. The polymer-to-ceramic conversion was performed using a two-step process: the first step occurred in flowing ammonia up to 650°C to substitute the alkylamino groups by amino groups via transamination reactions (see scheme 2). This reduces carbon contaminants. The second step occurred in flowing nitrogen up to 1800°C to yield a well-crystallized material. The consequence of this thermochemical treatment was that most of the fibers split during annealing. Only a thin BN skin remained to generate BN microtubes with, in some cases, retention of the initial circular form (Fig. 1). This behavior is related to the effect of the ammonia atmosphere that is applied during the initial conversion steps according to the TGA results. It was demonstrated that the thermal decomposition is accompanied by a weight loss greater than the theoretical value and involves the elimination of boron species.

Polymer **1** is decomposed by reaction with ammonia, yielding methylamine and the intermediate *N*-trimethyl-*B*-tri(amino)borazine **2**, which was partially sublimed, resulting in a major loss of fiber integrity (scheme 2).

The tubular forms obtained after thermal treatment strongly suggest a different behavior between the core of the green fibers and their surface. Therefore, it is reasonable to propose that the sublimation of **2** is limited at low temperature, allowing the surface of the green fibers to undergo polymerization to give a solid skin on a cross-linked polymer. Although the preparation of BN microtubules can be interesting for some applications, these studies showed that tris(monoalkylamino)boranes

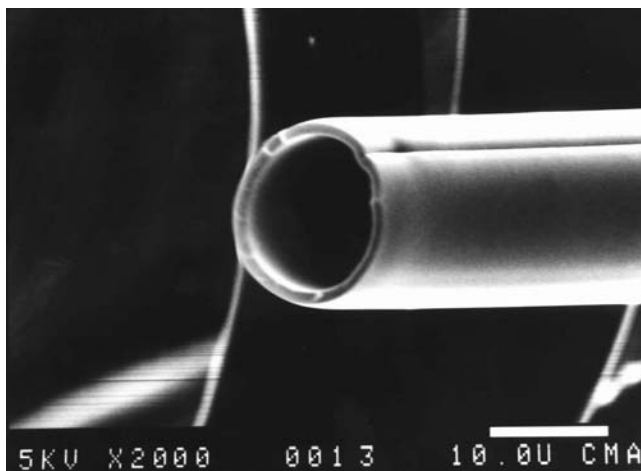


**Figure 1** D. Cornu et al., *J. Mater. Chem.* 2002, 12, 228. Reproduced by permission of the Royal Society of Chemistry.

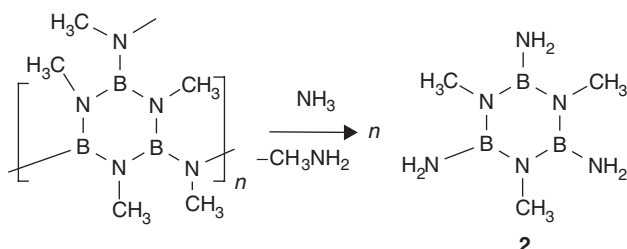


**Figure 2**

of the type  $B(NHR)_3$  ( $R = \text{Me}, \text{Pr}^i$ ) are not appropriate molecular precursors to BN fibers. Thus, an alternative route was sought.

### B. tris(*B*-Alkylamino)borazine–Derived Poly[*B*-(alkylamino)borazines]

In our research,<sup>16,17,18,19</sup> we first prepared a series of tris(*B*-alkylamino)borazines that possess different pendent groups. This allowed us to investigate the effect of the nature of the *B*-(alkylamino) substituents on both the viscoelastic behavior of the thermal properties and, therefore, the melt spinnability of the resulting poly[*B*-(alkylamino)-borazines] polymers.

Tris(*B*-Alkylamino)borazines of the type 2,4,6-[( $\text{CH}_3$ )<sub>2</sub>N]<sub>3</sub>B<sub>3</sub>N<sub>3</sub>H<sub>3</sub> (**3**), 2,4-[( $\text{CH}_3$ )<sub>2</sub>N]<sub>2</sub>-6-[ $\text{CH}_3\text{HN}$ ]B<sub>3</sub>N<sub>3</sub>H<sub>3</sub> (**4**), 2-[( $\text{CH}_3$ )<sub>2</sub>N]-4,6-[ $\text{CH}_3\text{HN}$ ]<sub>2</sub>B<sub>3</sub>N<sub>3</sub>H<sub>3</sub> (**5**), and 2,4,6-[ $\text{CH}_3\text{HN}$ ]<sub>3</sub>B<sub>3</sub>N<sub>3</sub>H<sub>3</sub> (**6**) are schematically represented in Figure 2. The thermolysis process was carried out at 200°C under argon at latm. pressure. Tris(*B*-Alkylamino)borazines **3**, **4**, **5**, and **6** underwent polycondensation reactions leading

to four different poly[*B*-(alkylamino)borazines] **7**, **8**, **9**, and **10**, respectively. The mechanisms that occur during thermolysis of tris(*B*-alkylamino)borazines are closely related to the nature of the pendent groups. As an illustration, polymer **7** derived from **3** displays only direct B—N linkages between borazine rings in agreement with the evolution of dimethylamine [(CH<sub>3</sub>)<sub>2</sub>NH] (scheme 3).<sup>16</sup> The molecular weight (*M<sub>w</sub>*) of the poly[*B*-(alkylamino)borazine] **7** is ~900, indicating that **3** is on average a hexamer. Its glass-transition temperature is 45°C.

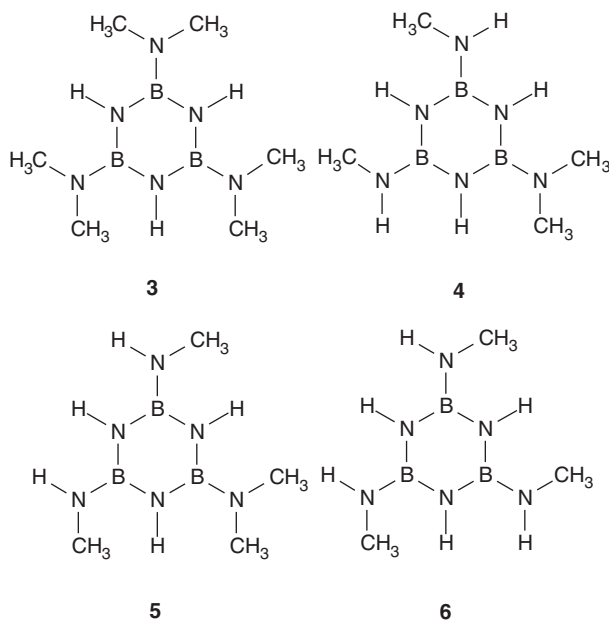
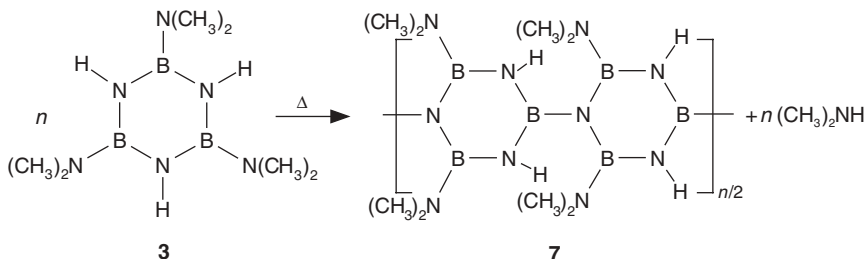


Figure 2



Scheme 3

The structure of polymers **8** to **10** contains the same two repeating units in different proportions. During thermolysis of **4** and **5** to polymers **8** and **9**, respectively,

both methylamine ( $\text{CH}_3\text{NH}_2$ ) and dimethylamine  $[(\text{CH}_3)_2\text{NH}]$  were released with two main polycondensation repeating structures being formed (Fig. 3). These structures involve the formation of  $-\text{N}(\text{CH}_3)-$  bridges [Fig. 3(a)], and direct B—N linkages between borazine rings [Fig. 3(b)].

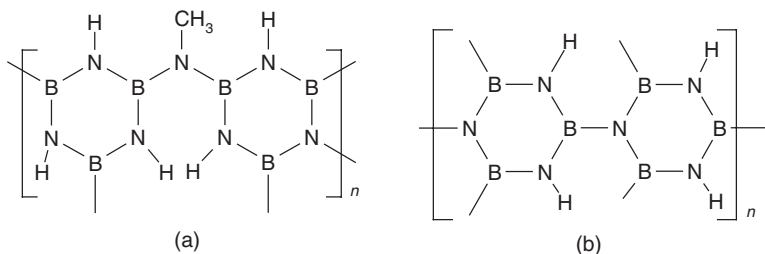


Figure 3

During the thermolysis of **5** to **9**, traces of ammonia were also detected during the last stages of the polymerization, typically above  $170^\circ\text{C}$ . This feature may be explained by the ring-opening pathway described by Toeniskoetter et al.<sup>20</sup> and clarified by Paciorek et al.<sup>21</sup> However, this mechanism has not been confirmed experimentally (see Chapter 5).

Finally, the thermolysis of **6** to **10** is characterized by the evolution of methylamine and ammonia, the former being the predominant gaseous product. The resulting polymer **10** displays a high proportion of  $-\text{N}(\text{CH}_3)-$  bridges [structure (a), Fig. 3] between the rings.<sup>22,23</sup>

The gas chromatography/mass spectroscopy (GC/MS) results indicated that the amount of  $(\text{CH}_3)_2\text{NH}$  evolved during thermolysis of **3–5**, increases with an increase in the number of  $-\text{N}(\text{CH}_3)_2$  substituents bonded to the monomer unit. This feature is related to the formation of direct intercyclic B—N linkages in the corresponding polymer, which increases going from polymer **9** to **7**. In contrast, the presence of  $-\text{NHCH}_3$  substituents on the borazine causes the formation of  $-\text{N}(\text{CH}_3)-$  bridges between the rings to be favored. This was supported by  $^{13}\text{C}$  nuclear magnetic resonance (NMR) spectra of polymers **8** and **9**, which displayed two major resonances near  $\delta = 27.7$  ppm and  $\delta = 37$  ppm. These signals correspond to carbon atoms of mono- and dimethylamino groups, respectively. Moreover, one weak signal at  $\delta = 31.0$  ppm was assigned to the carbon of the  $-\text{N}(\text{CH}_3)-$  bridging groups. Thus, the proportion of  $-\text{N}(\text{CH}_3)-$  bridges in the poly[B-(alkylamino)borazines] increases in the following order,  $7 < 8 < 9 < 10$ , to the detriment of direct intercyclic B—N bonds. The oligomeric nature of **8**, **9**, and **10** was confirmed by size exclusion chromatograms (SEC), which gave  $M_w$  values of  $\sim 500$ ,  $\sim 900$ , and  $\sim 1000$ , respectively, consistent with values of glass-transition temperatures, which increase from  $48^\circ\text{C}$  (**8**) to  $90^\circ\text{C}$  (**10**). The thermolysis conditions for all polymers were identical (Table 1).<sup>16,17,23,24</sup>

**Table 1** Glass-Transition Temperatures and Ceramic Yields Measured for Poly[*B*-(alkylamino)borazines] **10**, **9**, **8**, and **7**

	<b>10</b>	<b>9</b>	<b>8</b>	<b>7</b>
$T_g$ (°C)	90	65	48	45
Ceramic yield (%) <sup>(a)</sup>	57.7	52.4	51.3	— <sup>(b)</sup>

<sup>(a)</sup> Measured under ammonia from 25 to 1000°C.

<sup>(b)</sup> Yield not measured.

$T_g$  decreases from **10** to **7**, commensurate with the decrease of thermal reactivity of the tris(*B*-alkylamino)borazines going from **6** to **3**. As an illustration, **10** displays the highest degree of branching, which induces a low freedom of motion owing to the rigidity of the borazine rings. This leads to relatively high  $T_g$  values. In contrast, although **7** is composed of direct B—N linkages between borazine rings that increase the rigidity of the molecular network,<sup>22,23</sup> this polymer displays a low  $T_g$  that is attributed to the poor thermal reactivity of N(CH<sub>3</sub>)<sub>2</sub> in its precursor **3**.

Poly[*B*-(alkylamino)borazines] **7–10** exhibited suitable viscoelastic and thermal stabilities to be extruded in the molten state through the monohole spinneret of a lab-scale melt-spinning apparatus. Thus, an extruded filament (diameter, 200 μm) was drawn with a windup unit, that is, a graphite spool. This provided green fibers with a wide range of diameters ( $16 \leq \phi \leq 50$  μm; Table 2), depending on polymer architecture.

**Table 2** Spinning Parameters Observed for Polymers **10**, **9**, **8**, and **7**

	<b>10</b>	<b>9</b>	<b>8</b>	<b>7</b>
$T_g$ (°C)	90	65	48	45
$T_{\text{spinning}}$ (°C)	185	165	120	150–195
Green-fiber diameter (μm)	16	20	25	50
Drawdown ratio $\tau$	12.5	10	8	4

The stretchability of fibers derived from poly[*B*-(alkylamino)borazines] is estimated through the drawdown ratio  $\tau$  (emerging fiber diameter/stretched fiber diameter). The value of  $\tau$  significantly varied from **7** to **10**; the higher drawdown ratio, the better the polymer melt-spinnability. As an example, polymers **9** and **10** were easily extruded in the molten state and the emerging molten polymeric fiber could be continuously drawn several kilometers into a fine flexible, uniform fiber that was free of defects. Polymer **8** also displayed excellent extrusion properties in the molten state at a lower spinning temperature (consistent with the lower  $T_g$ ). Due to a high rigidity of the emerging fiber, however, the stretchability was less (lower drawdown ratio), and the green fiber diameter increased. Although polymer **7** exhibited adequate extrusion behavior over a wide range of temperatures (150–195°C), the emerging fiber displayed a poor stretchability owing to the polymer's poor flexibility.

Differences in the melt-extrusion of the poly[*B*-(alkylamino)borazines] and stretching of the resulting green fibers could be related to polymer architecture. In particular, both tris(*B*-alkylamino)borazine monomers **5** and **6** displayed the appropriate proportion of *B*-substituted  $\text{—N(H)CH}_3$  groups for developing  $\text{—N(CH}_3\text{)—}$  bridged bonds in the resulting poly[*B*-(alkylamino)borazines] **9** and **10**. These bridged bonds would have a favorable effect on both the chain mobility and the stretchability of the related green fiber. Such bridging units permit conformational rearrangements of the polymer backbone and greater freedom in the molecular motion. In contrast, borazine units branched by direct B—N bonds are less flexible. This naturally stiffens the polymer network and restricts molecular motion. Therefore, fiber stretchability decreases with decreasing proportions of  $\text{—N(CH}_3\text{)—}$  bridged bonds in the polymers going from **10** to **7** and with decreasing proportion of B-bonded-N(H)CH<sub>3</sub> substituents in the starting monomer precursor going from **6** to **3**.

Curing and pyrolysis of the fibers in flowing ammonia (25°C–1000°C) and then in nitrogen (1000°C–1800°C) produced BN fibers with a ceramic yield that depended on the nature of pendent substituents linked to the polymer (see Table 1). Ceramic yields obtained after heat treatment to 1000°C decreased from **10** to **7** in line with an increase of the B-substituted  $\text{—N(CH}_3\text{)}_2$  groups and concomitant with a major evolution of gaseous dimethylamine during the conversion. During the entire pyrolytic process, the green fibers are maintained around the spool to prevent crimping due to thermal shrinkage. Shrinkage is caused by polymer weight loss and an increase in the fiber density. As a consequence, the fiber diameter is considerably reduced after pyrolysis to 1800°C. However, fibers derived from **7** were not pyrolyzed under the mechanical tension imposed by the spool because of filament breakage during annealing. This polymer-to-ceramic conversion was monitored by GC/MS coupled with thermogravimetric analysis (TGA), Fourier-transform infrared (FTIR), X-ray diffraction (XRD), transition electron microscopy (TEM), and scanning electron microscopy (SEM) techniques. Mechanical tests were also performed. Four steps (cross-link curing, mineralization, ceramization, and crystallization) are generally identified as major processes during the pyrolysis procedure.<sup>22,24,25</sup>

After the pyrolysis process, BN fibers obtained from the four poly[*B*-(alkylamino)borazines], **7** (Fig. 4a) to **10** (Fig. 4d), showed some differences in microtexture. Excluding **7**-derived fibers, which underwent pyrolysis in the absence of mechanical tension (in a general way), a coarse-grained microtexture gradually appeared that becomes more pronounced going from the fibers derived from **10** (Fig. 4d) to **9** (Fig. 4c) to **8** (Fig. 4b). This means that the crystallinity of the BN fibers increases as the proportion of direct B—N ring-to-ring bonds increases in the starting polymer. XRD experiments strongly support this finding. The initiation of crystallization occurring at higher temperature for **10** (1500°C<sup>22,24–26</sup>) was shifted to lower temperature going to **9** and then to **8** (1350°C). Changes were also seen in the mechanical properties measured at room temperature. The first observations showed a decrease in the mechanical properties (tensile strength  $\sigma$ ) proceeding from **10**- to **7**-derived BN fibers in accordance with an increase in the fiber diameter (Table 3). BN fibers derived from **7** were too stiff and brittle to carry out mechanical tests. These changes are a direct result of a decrease from **10** to **7** in the melt-spinnability of the corresponding

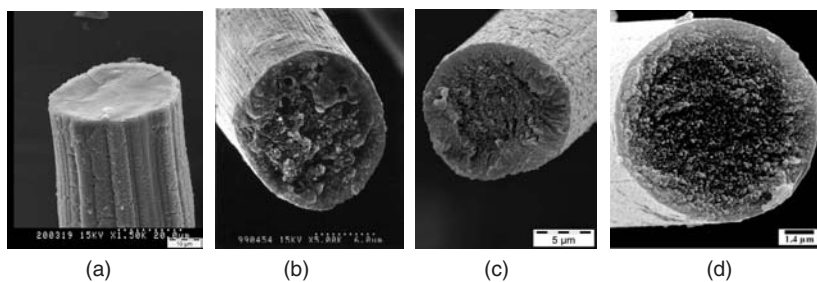


Figure 4

**Table 3** Mechanical Properties of the BN Fibers Prepared from Different Polymers

	Diameter ( $\mu\text{m}$ )	Young's Modulus $E$ (GPa)	Tensile Strength $\sigma$ (GPa)
<b>10</b> - Derived fibers	8	360	1.6
<b>9</b> - Derived fibers	11	315	1.4
<b>8</b> - Derived fibers	15	105	0.5
<b>7</b> - Derived fibers	40	— <sup>(a)</sup>	— <sup>(a)</sup>

<sup>(a)</sup> Quantity not measured.

polymer. As a consequence, **9** and **10** were excellent candidates for both melt-spinning and thermally induced processes and for the preparation of BN fibers with excellent mechanical properties. Finally, it can be postulated that variations in the quality of the mechanical properties and structural organization of the finished fibers are the result of the polymer's molecular characteristics, that is, type of linkage between the borazine rings and the thermal and rheological phenomena encountered that occur during the spinning process, that is, melt spinnability.

### C. Polymeric Precursors Derived from tris(Borylamino)borazines

This new class of boron- and nitrogen-containing polymers exhibits increased rings spacings, that is, multiatom bridges between the borazine rings. These polymers have been investigated since they are expected to exhibit improved processing properties compared to classic poly[*B*-(methylamino)borazines].

#### i. Two-Step Polycondensation (Thermal Route)

We have reported that the reaction of 2,4,6-tri(chloro)borazine  $\text{Cl}_3\text{B}_3\text{N}_3\text{H}_3$  with three equivalents of tris(isopropylamino)borane  $\text{B}(\text{NHPr}^i)_3$  led to the formation of 2,4,6-tri[bis(isopropylamino)boryl(isopropyl)amino]borazine **11** [Fig. 5(a)] in quantitative yield.<sup>26,27</sup> The subsequent polycondensation carried out in vacuo up to 150°C, led to the formation of the polymer **12** containing  $\text{B}_3\text{N}_3$  rings linked either through direct B—N interring bonds (minor pathway) or three-atoms —N—B—N— bridges

(major pathways) [Fig. 5(b)].<sup>28</sup> Polymer **12** was a slightly brown viscous oil at 150°C, which became a slightly brown glass after cooling. The polycondensation was stopped arbitrarily after 9 hours of heating in order to develop a tractable compound for fiber formation. Differential Scanning Calorimetry (DSC) and TGA experiments showed that this polymer exhibits a glass-transition temperature of 60°C and a ceramic yield of 31%, in accordance with the results obtained previously at 150°C over a shorter heating period.<sup>26,27</sup> The degree of polycondensation is calculated as the mole ratio of the evolved  $B(NHPr^i)_3$  to the starting monomer **11**; a degree of polycondensation of 1.4 was estimated.

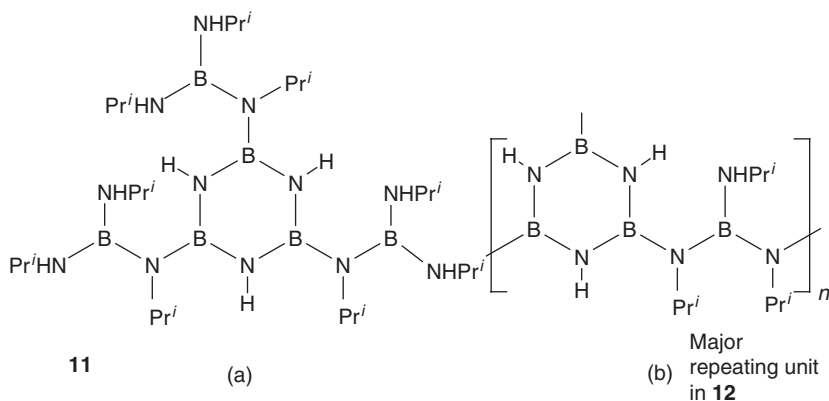
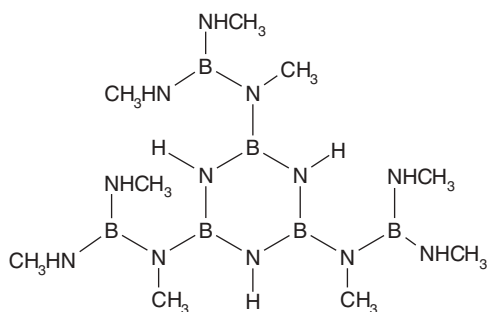


Figure 5

With the aim of increasing the ceramic yield, we have investigated the influence of the nature of the alkyl groups on both the processability of polymer and properties of the fibers. A similar reaction was therefore explored using the tris(methylamino)borane,  $B(NHCH_3)_3$ . Using a 3:1 equivalent of  $B(NHCH_3)_3$  to 1-2,4,6-trichloroborazine generated a viscous oil containing residual toluene, as evidenced by the  $^1H$  NMR spectrum.<sup>28</sup>

The  $^{11}B$  NMR spectrum of the product showed two broad signals at 27.7 ppm and 24.7 ppm, which are attributed to boron atoms of the borazine ring and the boryl substituents, respectively. These results are consistent with the formation of the *B*-tri[bis(methylamino)boryl(methyl)amino]borazine **13** as the main product (Fig. 6). No free  $B(NHCH_3)_3$  was detected.

The  $^1H$  NMR spectrum of the crude product was consistent with the formation of compound **13**. However, the ratio of the intensity of the signals corresponding to the boryl substituents to the borazine ring did not fit the calculated value for a pure compound. The lower intensity of the signals corresponding to the methylamino groups and the splitting of these signals supports the presence of small amounts of **13**-derived oligomers in the crude product. Even if the formation of direct interring bonds was also considered as a minor pathway (consistent with the results obtained



13

Figure 6

during the polycondensation of **11**), the ratio  $\text{NHCH}_3$  groups per  $\text{—N(CH}_3\text{)—}$  groups is consistent with the predominant formation of three-atom bridges between the  $\text{B}_3\text{N}_3$  rings in the oligomer derived from **13** (Fig. 7). Therefore, the direct synthesis of a pure oligomer-free **13** by a process similar to that used for **11** seems impossible. This is most likely due to the lower steric effect of the methylamino groups.

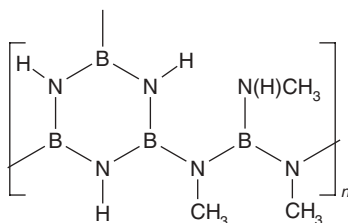


Figure 7

The polycondensation of **13** is conducted in vacuo using a process similar to that used for the polycondensation of **11**. After heating to  $150^\circ\text{C}$ , the product becomes solid and the mechanical stirring is stopped to yield polymer **14**. This product is a colorless waxy solid at  $150^\circ\text{C}$ , which becomes a white powder after cooling to  $T_{\text{room}}$ . DSC and TGA give a  $T_g = 55^\circ\text{C}$  and a ceramic yield of 47% (at  $1000^\circ\text{C}$ ). By presuming that trace amounts of oligomers are mixed with **13** in the starting material, the degree of polycondensation is calculated to be 1.5 based on the formula just given. It is interesting to note the similarities in  $T_g$  and degree of polycondensation for **12** (i.e., 1.4 and  $60^\circ\text{C}$ , respectively) and **14** (1.5 and  $55^\circ\text{C}$ ). The ceramic yield obtained at  $1000^\circ\text{C}$  is naturally higher for **14** than **12** owing to the nature of the pendent alkyl groups (methyl vs. isopropyl).

Using the melt-spinning equipment previously mentioned, **12** and **14** were both extruded on a piston-driven lab-scale spinning apparatus setup in a nitrogen-filled glove box. Green fibers could be obtained from **12** and **14** by melt-extrusion through a  $200\text{-}\mu\text{m}$ -diameter spinneret at  $151^\circ\text{C}$  and  $138^\circ\text{C}$ , respectively.<sup>29,30</sup> Their diameters were reduced by stretching the emerging molten filament using the windup spool.

The polymer-to-ceramic conversion was performed in flowing ammonia to 1000°C (heating rate 25°C/h), then in flowing nitrogen to 1800°C (heating rate 100°C/h).<sup>29,30</sup> Some of the properties of the final BN fibers are summarized in Table 4.

**Table 4** Main Characteristics of the Fibers Obtained from Polymers **12** and **14**

Samples	12-Derived Fibers	14-Derived Fibers
Green-fiber diameter ( $\mu\text{m}$ )	29.3	~40.0
BN-fiber diameter ( $\mu\text{m}$ )	8.4	23.6
$\sigma$ (GPa)	0.90	0.17
$E$ (GPa)	140	30
$\varepsilon$ (%)	0.62	0.54

The melt spinning of the polymer **12** allowed us to obtain endless green fibers whose diameters could be easily reduced by winding on a spool in a stable process. This clearly demonstrated the good processability of this polymer. In contrast, it was not possible to draw an endless green fiber from polymer **14**. Pure extrusion of such a polymer was barely achieved. As the filament emerged, swelling occurred. There was even a tendency for the emerging filament to fold back on itself rather than fall with gravity, which led to unstable spinning. The filaments obtained from **14** therefore exhibited larger and heterogeneous diameters (see Table 4).

As mentioned previously, the meltability of preceramic polymers derived from borylborazine precursors seems to be closely dependent on the nature of the pendant alkyl groups. When  $\text{B}(\text{NHPr}^i)_3$  is used, the polycondensation reaction has to be performed for a longer period to obtain the expected degree of polycondensation due to the steric bulk of such groups, which restricts the condensation's progress. The product, however, appears to be a more homogeneous polymer with enhanced processing properties. Using  $\text{B}(\text{NHCH}_3)_3$  significantly increases the polycondensation reaction rate, which results in a higher cross-linked network with reduced processability.

The measured tensile strength,  $\sigma$ , of fibers derived from **14** is low relative to their large diameter (Table 4). SEM images of these fibers (Fig. 8) showed the presence of fluting (left) on the surface along the fiber axis. A cross section (right) of the fiber exhibited a highly grainy homogeneous texture with numerous cavities.

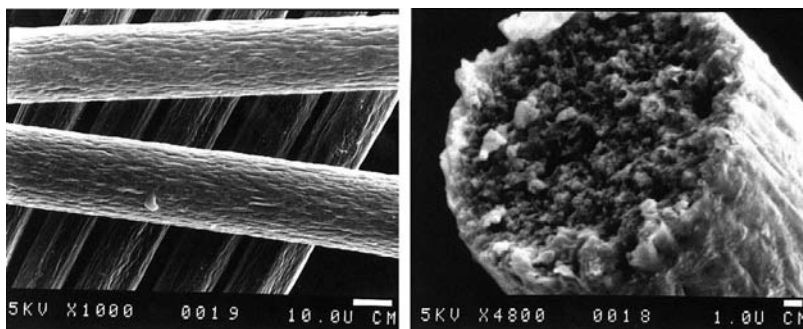


**Figure 8**

SEM images of fibers derived from **12** (Fig. 9) also indicated the presence of fluting on the surface along the fiber axis. However, the surface was smoother than that of fibers obtained from **14**. Also, the SEM images of the section showed fewer cavities.

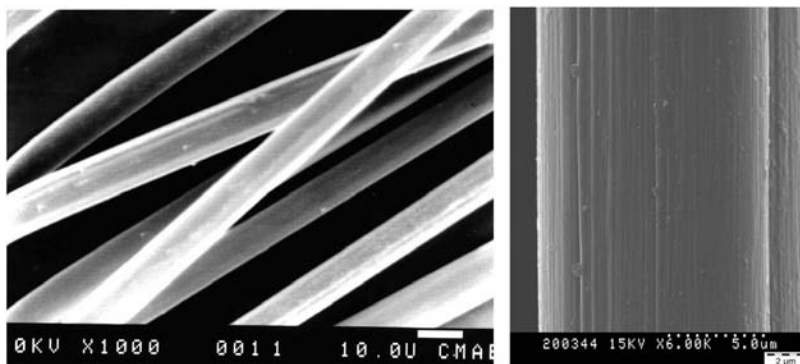
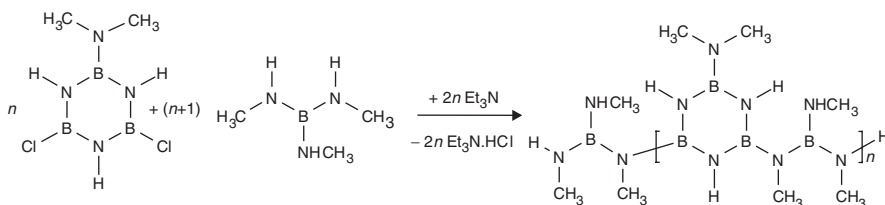


Figure 9

These results are closely related to the mechanical properties of the **12**-derived fibers, which are notably better. As an illustration, the tensile strength reached 0.90 GPa. These values are promising considering that these results have been obtained from a polymer whose characteristics (degree of polycondensation, glass-transition temperature) have been set arbitrarily. Thus, we can expect to increase these values significantly by optimizing the polymer properties. Such results show that obtaining both melt spinnability (polymer **12**) and suitable ceramic yield (polymer **14**) in a single polymer is an ambitious aim.

### ii. One-Step Polycondensation

As mentioned previously, the main drawbacks of the thermal route to polyborylborazine are (1) the presence of both direct intercyclic bonds and three-atom bridges between the rings, and (2) a difficulty in controlling the polycondensation rate. One solution we investigated to address these drawbacks is a route based on the room temperature reaction of *B*-chloroborazine with trialkylaminoborane.<sup>31,32</sup> We used 2-methylamino-4,6-dichloroborazine instead of 2,4,6-trichloroborazine to prepare a “two-point” polymer (scheme 4), which is theoretically less cross-linked.



Scheme 4

An excess of tertiary amine (e.g.,  $\text{Et}_3\text{N}$ ) was added to the reaction medium to trap evolving hydrogen chloride. The dimethylamino group bonded to the  $\text{B}_3\text{N}_3$  ring is poorly reactive and is therefore retained during the room-temperature reaction. Moreover, the dimethylamino function can be considered as a latent cross-linking agent since it can react at high temperature with ammonia. This affords reticulation, that is, shape-keeping after the melt-processing step. After reaction, the polyborylborazine, which remained soluble during the whole process, is easily obtained after filtration and solvent removal.

The main advantage of this technique is that the polyborylborazine displays only three-atom bridges,  $\text{—N—B—N—}$ , between the rings. As an illustration, a polyborylborazine has been prepared from  $[(\text{CH}_3)_2\text{N}]\text{Cl}_2\text{B}_3\text{N}_3\text{H}_3$  and  $\text{B}(\text{NHCH}_3)_3$  in a 1:1 molar ratio in the presence of triethylamine (scheme 4). Polymer characterization clearly supports the proposed structure. For instance, Figure 10 is a typical

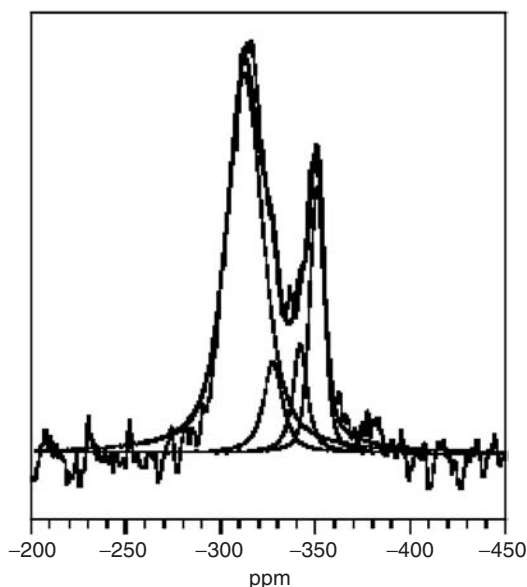
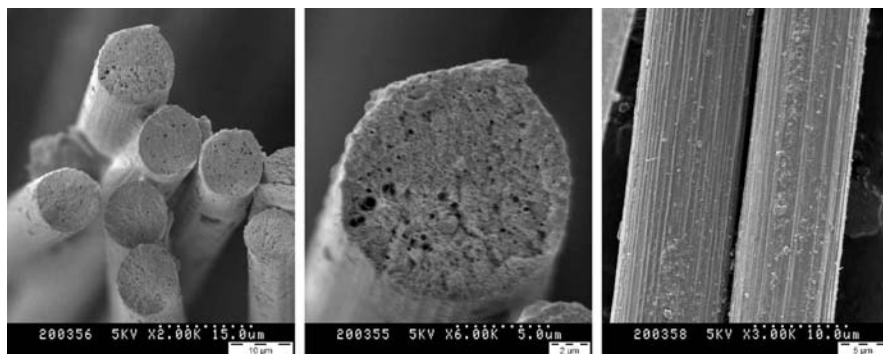


Figure 10

$^{15}\text{N}$  CPMAS solid-state NMR spectrum of the product showing four peaks after curve fitting.<sup>28</sup> These signals can be attributed to the four types of nitrogen environments found within the polymer: the chemical shift assignments are  $\text{BN}(\text{H})\text{CH}_3$ ,  $\text{BN}(\text{CH}_3)_2$ ,  $\text{B}_2\text{NCH}_3$ , and  $\text{B}_2\text{NH}$  from low to high field. As expected, this polymer is suitable for a spinning process, and continuous green fibers can be melt-spun.<sup>31,32</sup> Figure 11 shows the SEM images of the 10- $\mu\text{m}$ -diameter BN fibers obtained after a convenient thermal and chemical treatment to 1800°C. These fibers are striated lengthwise without surface defects. The circular cross section is retained, but numerous randomly distributed flakes appear. The presence of these defects can be related to the removal of the carbon species and the volatilization of low molecular-weight species



**Figure 11** B. Toury et al., *J. Mater. Chem.* 2004, 14, 2609. Reproduced by permission of the Royal Society of Chemistry and Reprinted from *J. Europ. Ceram. Soc.*, 25, B. Toury et al., Complete characterisation of BN fibres obtained from a new polyboryborazine, 137. Copyright Owner, Copyright (2007), with permission from Elsevier.

upon heating. Despite these defects, the BN fibers show promising mechanical properties, with a tensile strength slightly above 1.0 GPa and an average Young's modulus value of 200 GPa.

### III. OUTLOOK

The preparation of boron nitride fibers is the first step in producing composite materials intended for high-temperature specific applications. BN/BN composites composed of high-performance BN fibers derived from poly[*B*-(alkylamino)borazines] and BN matrices derived from borazine-based polymers with high ceramic yields are potential candidates for improving upon the performance provided by carbon/carbon composites in corrosive environments. An alternative approach is to prepare BN coatings on carbon fibers, which could improve the thermal stability of the latter in oxidizing environments. Then these BN-coated fibers could be incorporated into BN matrices. In this case, the polymer-derived BN coating might also play the role of an interphase and disturb or preclude the propagation of cracks along the fiber axis.

The most exciting challenge is probably the preparation of BN nanostructures, including nanofibers and nanotubules, using the template-assisted PDCs route. Such an approach could allow us to control the morphology and size of the nanostructured BN materials to be incorporated into the BN matrix. This should significantly enhance the mechanical performance of the resulting composites compared to composites reinforced by BN microfibers.

### IV. SUMMARY

Advanced technology in the areas of electronics, optoelectronics, optics, transport, aeronautics, and aerospace requires the synthesis of new materials displaying a

wide variety of functional or structural properties. This challenge can be tackled via the chemistry of molecular and polymeric precursors. This chapter has demonstrated that the pyrolysis of preceramic polymers allows the fabrication of ceramic fibers in a way unknown from traditional methods. Several borazine-based polymeric precursors of boron nitride have been described and compared in terms of their ability to lead to BN fibers. This chapter showed that meltable and spinnable poly[*B*-(alkylamino)borazines] can be prepared using the functionalization of boron atoms of borazinic derivatives. In our opinion, the borylborazine route, which allowed us to prepare linear polymers with —N—B—N— flexible bridges provided by the utilization of a “two-point” polymerization, is an excellent example of what the chemical mastery of the precursors can provide. In addition, the ceramic yield of a precursor, which is classically considered as a key point in materials science, must be counterbalanced with a chemical structure when the shaping of the ceramic must be controlled. It is clear that considerable effort still needs to be focused on the development and tailoring of molecular and polymeric precursors of BN fibers that display the mechanical properties required for integration into composite materials as reinforcing agents.

## V. REFERENCES

1. R. T. Paine, C. K. Narula, *Chem. Rev.*, **90**, 73 (1990).
2. R. Haubner, M. Wilhelm, R. Weissenbacher, B. Lux, in *High Performance Non-oxide Ceramics II, Structure and Bonding*, Vol. 102, M. Jansen, ed., p. 1, Springer-Verlag, Berlin Heidelberg, 2002.
3. J. Huang, Y. T. Zhu, *Defects Diffus. Forum*, **186**, 1 (2000).
4. P. G. Chantrell, E. P. Popper, in *Inorganic Polymers and Ceramics, Special Ceramics-4*, E. P. Popper, ed., p. 87, Academic Press, New York, 1964.
5. K. J. Wynne, R. W. Rice, *Ann. Rev. Mater. Sci.*, **14**, 297 (1984).
6. M. Peuckert, T. Vaahs, M. Brück, *Adv. Mater.*, **2**, 98 (1990).
7. J. Bill, F. Aldinger, *Adv. Mater.*, **7**, 775 (1995).
8. D. Segal, *J. Mater. Chem.*, **7**, 1297 (1997).
9. P. Greil, *Adv. Eng. Mater.*, **2**, 339 (2000).
10. L. Tanigushi, K. Harada, T. Maeda, *Chem. Abstr.*, **85**, 96582v (1976).
11. Y. Kimura, Y. Kubo, N. Hayashi, *Comput. Sci. Technol.*, **51**, 173 (1994).
12. T. Wideman, E. E. Remsen, E. Cortez, V. L. Chlanda, L. G. Sneddon, *Chem. Mater.*, **10**, 412 (1998).
13. B. Bonnetot, B. Frange, F. Guilhon, H. Mongeot, *Main Group Met. Chem.*, **17**, 583 (1994).
14. B. Bonnetot, F. Guilhon, J.-C. Viala, H. Mongeot, *Chem. Mater.*, **7**, 299 (1995); C. Doche, F. Guilhon, B. Bonnetot, H. Mongeot, J. Bouix, *J. Mater. Sci. Lett.*, **14**, 847 (1995).
15. D. Cornu, P. Miele, R. Faure, B. Bonnetot, H. Mongeot, J. Bouix, *J. Mater. Chem.*, **9**, 757 (1999).
16. B. Toury, P. Miele, D. Cornu, H. Vincent, J. Bouix, *Adv. Funct. Mater.*, **12**, 228 (2002).
17. B. Toury, S. Bernard, D. Cornu, J.-M. Létoffé, P. Miele, *J. Mater. Chem.*, **13**, 274 (2003).
18. P. Miele, B. Toury, S. Bernard, D. Cornu, J. Bouix, *Ceram. Trans.*, **135**, 153 (2002).
19. P. Miele, B. Toury, F. Chassagneux, R. Fulchiron, *J. Eur. Ceram. Soc.*, **25**, 157 (2005).
20. R. H. Toeniskoetter, F. R. Hall, *Inorg. Chem.*, **2**, 29 (1963).
21. K. J. L. Paciorek, D. H. Harris, R. H. Kratzer, *J. Polym. Sci.*, **24**, 173 (1986).

22. S. Duperrier, C. Gervais, S. Bernard, D. Cornu, F. Babonneau, P. Miele, *J. Mater. Chem.* **30**, 3126 (2006).
23. S. Duperrier, C. Gervais, S. Bernard, D. Cornu, F. Babonneau, C. Balan, P. Miele, *Macromolecules*, **40**(4), 1018 (2007).
24. S. Bernard, K. Fiaty, D. Cornu, P. Miele, P. Laurent, *J. Phys. Chem. B*, **110**, 9048 (2006).
25. S. Bernard, D. Cornu, P. Miele, H. Vincent, J. Bouix, *J. Organomet. Chem.*, **357**, 91 (2002).
26. D. Cornu, P. Miele, B. Bonnetot, P. Guenot, H. Mongeot, J. Bouix, *Main Group Met. Chem.*, **21**, 301(1998).
27. H. Mongeot, F. Guilhon, P. Miele, D. Cornu, B. Bonnetot, *J. Solid State Chem.*, **133**, 164 (1997).
28. B. Toury, C. Gervais, P. Dibandgo, D. Cornu, P. Miele, F. Babonneau, *Appl. Organomet. Chem.*, **18**, 227 (2004).
29. P. Miele, B. Toury, D. Cornu, S. Bernard, *J. Organomet. Chem.*, **690**, 2809 (2005).
30. D. Cornu, P. Miele, B. Toury, B. Bonnetot, H. Mongeot, J. Bouix, *J. Mater. Chem.*, **9**, 2605 (1999).
31. B. Toury, P. Miele, *J. Mater. Chem.*, **14**, 2609 (2004).
32. B. Toury, D. Cornu, F. Chassagneux, P. Miele, *J. Eur. Ceram. Soc.*, **25**, 137 (2005).

---

## CHAPTER 4

# Organoboron Polymers

**Yuuya Nagata and Yoshiki Chujo**

*Department of Polymer Chemistry, Graduate School of Engineering,  
Kyoto University, Katsura Nishikyo-ku, Kyoto 615-8510, Japan*

### CONTENTS

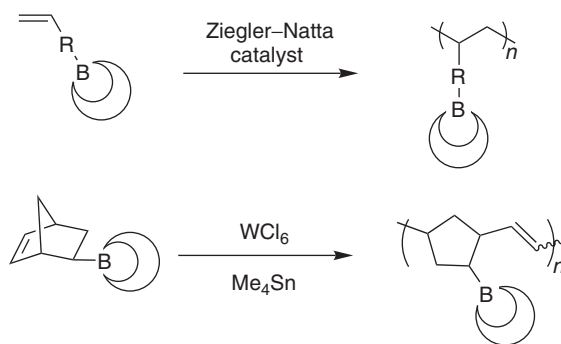
I. INTRODUCTION	122
II. HYDROBORATION POLYMERIZATION	123
A. Hydroboration Polymerization of Diene Monomers	123
B. Reactions of Organoboron Polymers Prepared by Hydroboration Polymerization	124
C. Hydroboration Polymerization of Diyne Monomers	129
D. Conjugated Organoboron Polymers	130
E. Poly(cyclodiborazane)s Prepared by Hydroboration Polymerization of Dicyano Monomers	132
F. Conjugated Poly(cyclodiborazane)s	134
G. Organoboron Polymers as an Anion Sensor	137
III. OTHER BORATION POLYMERIZATIONS	138
A. Haloboration Polymerization	138
B. Phenylboration Polymerization	139
C. Alkoxyboration Polymerization	140
IV. ORGANOMETALLIC ROUTES	141
A. Grignard and Organolithium Reagents	141

*Macromolecules Containing Metal and Metal-Like Elements,  
Volume 8: Boron-Containing Polymers*, edited by Alaa S. Abd-El-Aziz,  
Charles E. Carraher Jr., Charles U. Pittman Jr., and Martel Zeldin.  
Copyright © 2007 John Wiley & Sons, Inc.

B. Poly(cyclodiborazane)s via Cross-Coupling Reactions	142
C. Poly(pyrazabole)s via Cross-Coupling Reactions	143
V. SUMMARY	145
VI. REFERENCES	145

## I. INTRODUCTION

Since the discovery of the hydroboration reaction by H. C. Brown et al.,<sup>1</sup> organoboron compounds have been used as useful intermediates for a variety of functional groups. Polymeric organoboron compounds are therefore expected to act as a new class of reactive polymers. However, until recently the study of introducing boron atoms into polymers has been limited because of the instability of boron compounds toward air and moisture. A few stable polymers did appear. For example, T. C. Chung et al. reported the preparation of side-chain-type organoboron polymers by way of Ziegler–Natta polymerization<sup>2</sup> or ring-opening metathesis polymerization (ROMP)<sup>3,4</sup> of boron-containing monomers (scheme 1).



Scheme 1

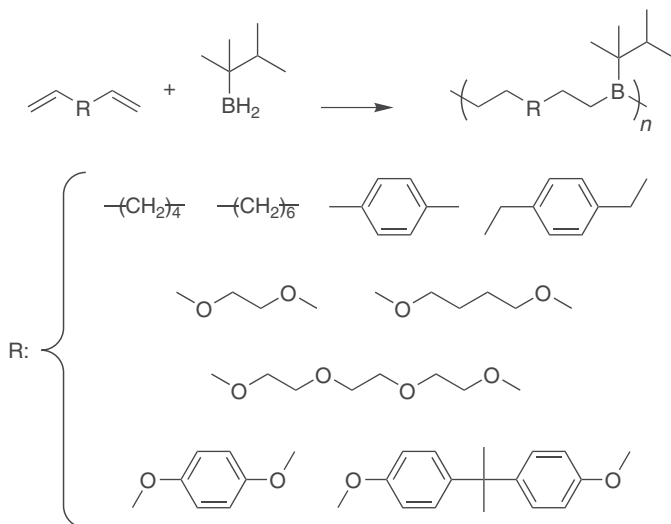
On the other hand, the synthesis of main-chain-type organoboron polymers have been studied in our group. A wide variety of organoboron polymers has been prepared and their properties revealed. The first class of main-chain-type organoboron polymers was synthesized by hydroboration polymerization between various diene monomers and hexylborane, which behaves as a Lewis acidic polymer. Therefore, organoboron polymers are regarded as reactive polymers that can be converted to versatile functionalized polymers. Second, conjugated organoboron polymers have been developed. These polymers exhibited various interesting properties due to the high electron affinity of boron, strong fluorescence emission, nonlinear optical properties, and n-type electronic conductivity. Because of their unique properties, these

polymers are regarded as novel optical and electronic materials. The preparation of these organoboron polymers and their properties are surveyed in this chapter.

## II. HYDROBORATION POLYMERIZATION

### A. Hydroboration Polymerization of Diene Monomers

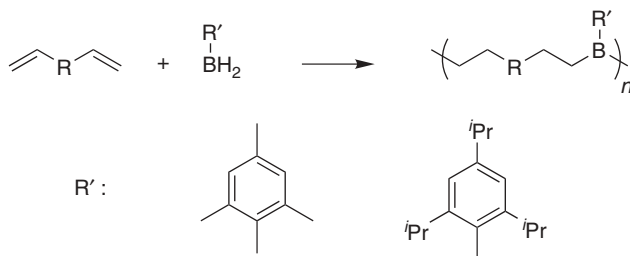
The synthesis of main-chain-type organoboron polymers has been achieved in our group by utilizing hydroboration polymerization. The polyaddition between diene and thexylborane gave the corresponding poly(alkylborane)s quantitatively (scheme 2). For instance, the reaction of thexylborane with 1,7-octadiene was carried out in tetrahydrofuran at 0°C under nitrogen atmosphere to produce an organoboron polymer. The molecular weight of the polymer obtained increased as the feed ratio approached unity. The dienes 1,9-decadiene, *p*-divinylbenzene, *p*-diallylbenzene, bis(allyl ether) of ethylene glycol, 1,4-butanediol, triethylene glycol, hydroquinone, and bisphenol A were used in this hydroboration polymerization to give the corresponding organoboron polymers. The thermal and oxidative stabilities of the obtained polymers were also examined. These polymers were more stable toward air in comparison with conventional "trialkylboranes."<sup>5</sup>



Scheme 2

Hydroboration polymerization between diene monomers and 2,4,6-trimethylphenylborane (mesitylborane)<sup>6</sup> or 2,4,6-triisopropylphenylborane (tripylborane)<sup>7</sup> gave organoboron main-chain polymers (scheme 3). The polymerization was

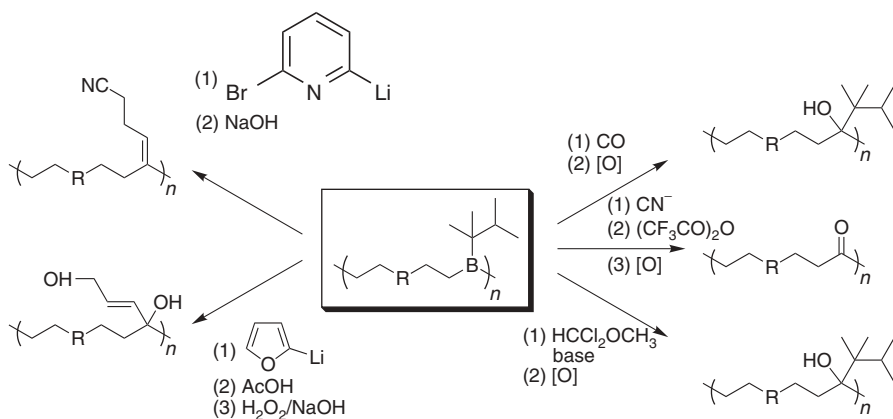
carried out by adding a diene monomer to a tetrahydrofuran (THF) solution of borane monomer at room temperature under nitrogen atmosphere. The polymers obtained were found to be more stable compared with the polymers prepared from hexylborane. This stability might be derived from the steric hindrance of bulkier substituent, which prevents the attack of oxygen on the boron atom.



Scheme 3

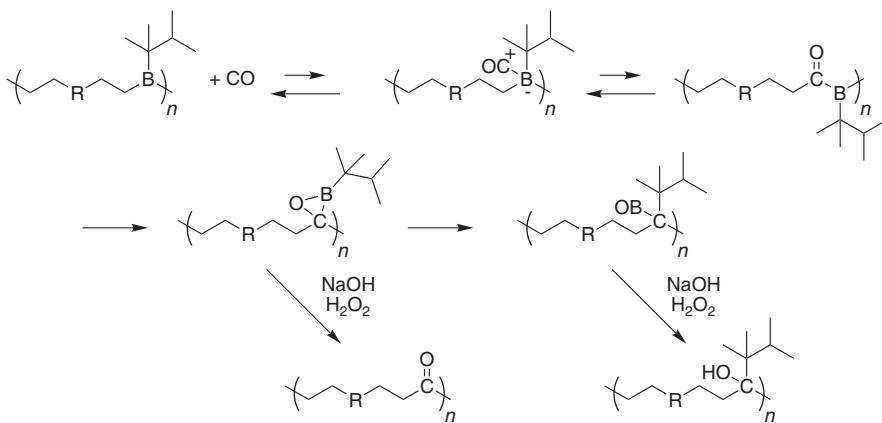
## B. Reactions of Organoboron Polymers Prepared by Hydroboration Polymerization

Generally, trialkylboranes are useful intermediates in the field of organic synthesis with versatile reactivity. The polymers prepared by polyaddition between diene monomers and hexylborane are polymer homologues of trialkylboranes, which can be converted to poly(alcohol)s, poly(ketone)s, and other polymers having some functional groups (scheme 4).<sup>8-12</sup>



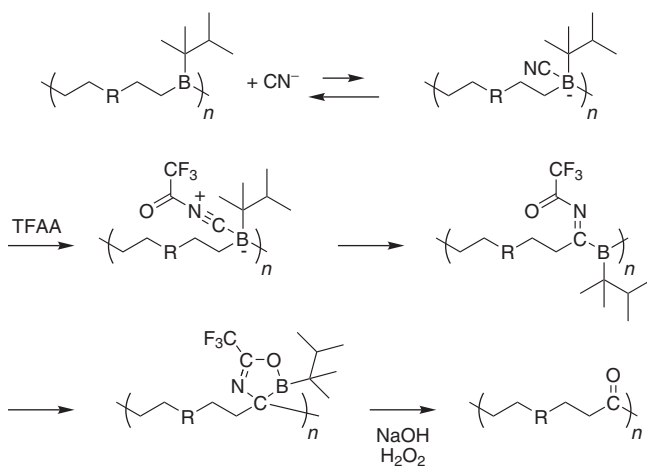
Scheme 4

The polymers prepared from hexylborane and diene monomers were reacted with carbon monoxide at 120°C, followed by treatment with NaOH and H<sub>2</sub>O<sub>2</sub> to produce a polyalcohol (scheme 5).<sup>13</sup> This conversion includes migration of the polymer chain and hexyl group from the boron atom to carbon, as shown in scheme 5. When this reaction was carried out under milder condition, poly(ketone) segments were included in the polymer backbone due to an incomplete migration of the hexyl group.



Scheme 5

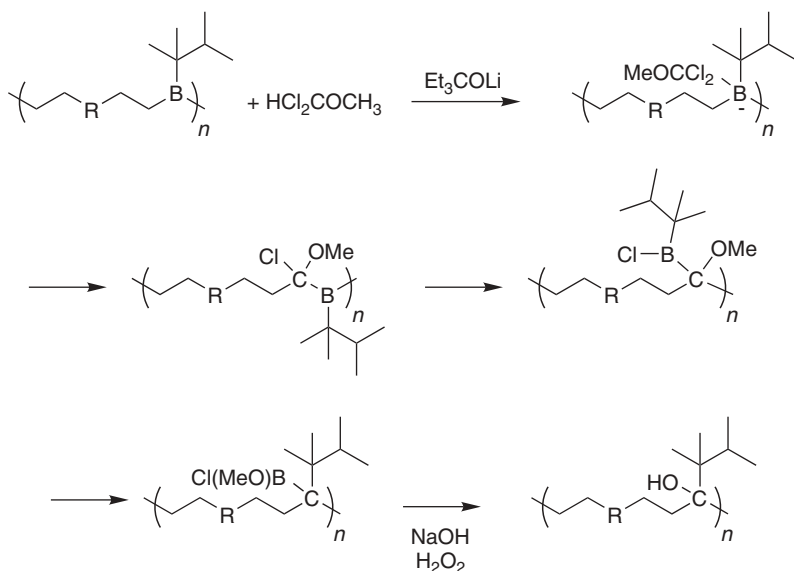
To synthesize the poly(ketone)s selectively, the reaction between the organoboron polymers and KCN was reported (scheme 6).<sup>8</sup> After oxidation of the reaction mixture, followed by coagulation, the desired poly(ketone)s were obtained. The yielded polymers



Scheme 6

were white, solid, and stable under air. This result indicates no carbon–boron bond remained in the product polymer backbone (scheme 6).

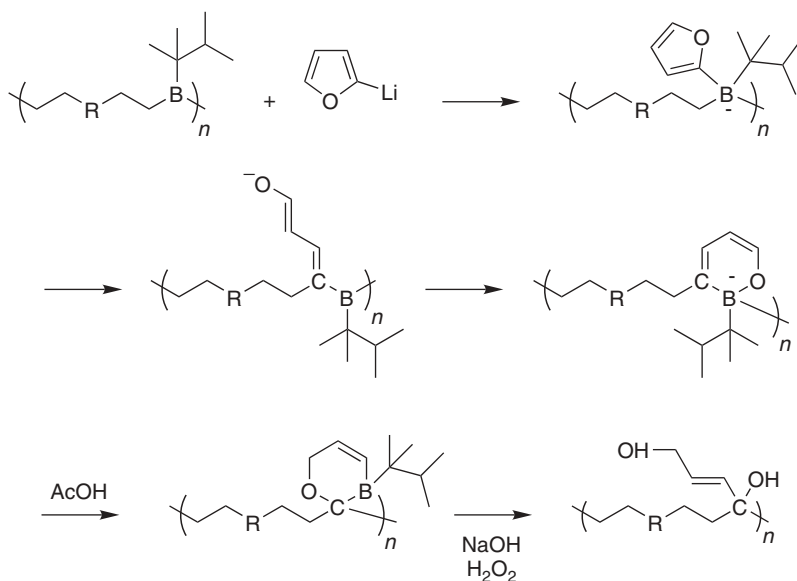
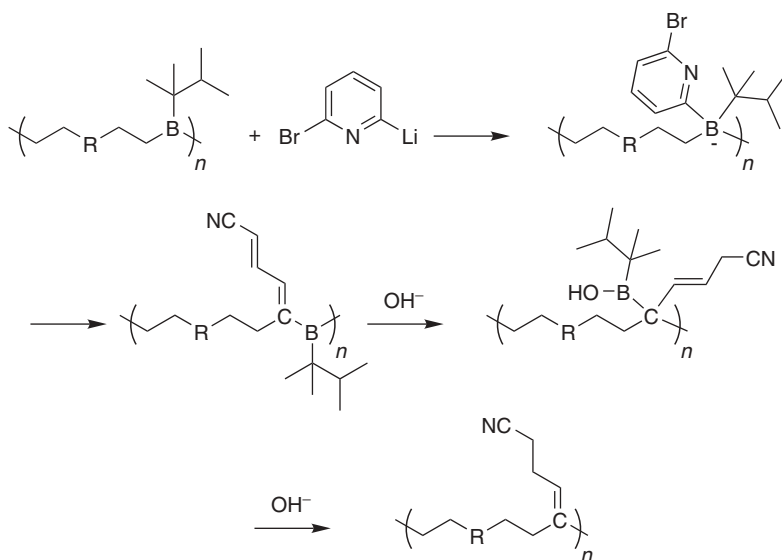
In another method for the preparation of poly(alcohol)s from organoboron polymers, dichloromethyl methyl ether (DCME) could be used (scheme 7).<sup>9</sup> Various organoboron polymers synthesized by hydroboration polymerization were reacted with DCME at 0°C in THF, followed by treatment with lithium triethylmethoxide. After oxidative treatment with NaOH and H<sub>2</sub>O<sub>2</sub>, the corresponding poly(alcohol)s were obtained. The structures of these resulting polymers were the same as those prepared by the reaction with carbon monoxide describe earlier. However, the reaction with carbon monoxide requires severe conditions (120°C, 30 kg/cm<sup>2</sup>). The reaction with DCME therefore provides a more convenient way for the conversion of organoboron polymers to poly(alcohol)s.



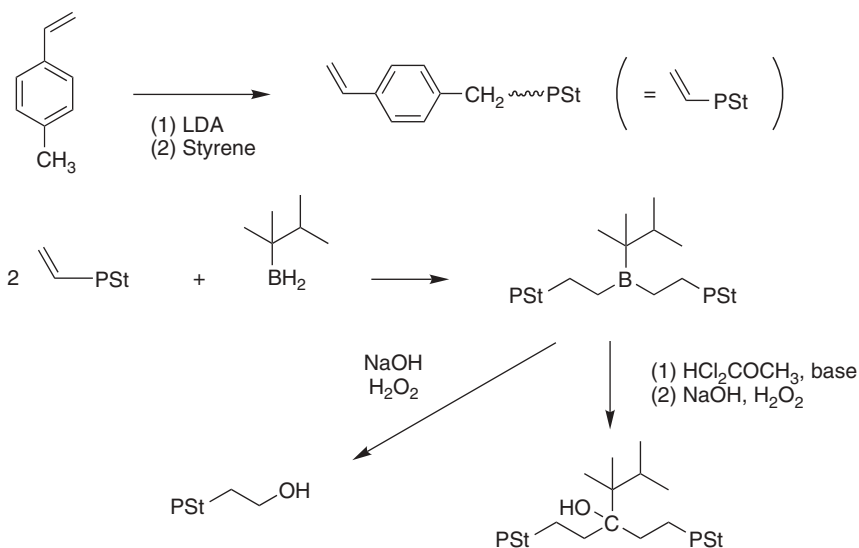
Scheme 7

The reactions of organoboron polymers via the ring opening of pyridine or furan moieties were also reported. As shown in scheme 8, the organoboron polymers were reacted with 2-bromo-6-lithiopyridine followed by treatment with NaOH to produce the cyano-group-containing polymers.<sup>10</sup> Conversely, the reaction of organoboron polymers with  $\alpha$ -furyllithium was followed by treatment with acetic acid and then with NaOH and H<sub>2</sub>O<sub>2</sub> to form a polymer having primary and tertiary alcohols (scheme 9).<sup>11</sup> These conversions include the migration of polymer chains on the boron atom and the ring-opening reactions of pyridine and furan, respectively.

Hydroboration reaction of the terminal double bond of polystyrene with thexylborane yielded a polymer bearing one organoboron unit at the center of the polymer

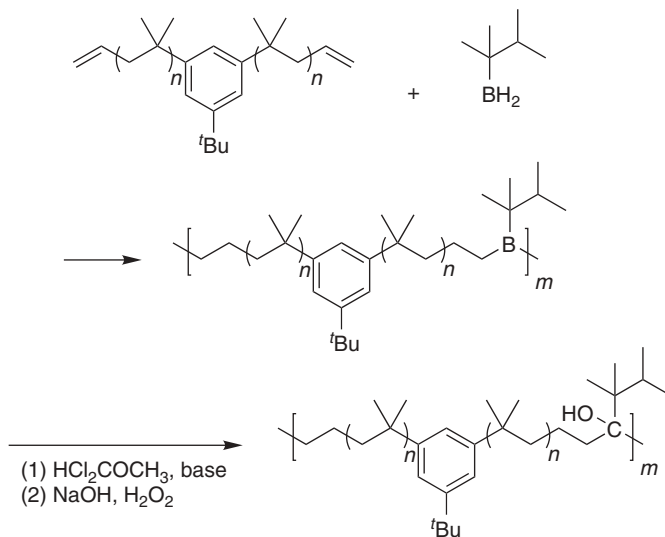


(scheme 10), whose molecular weight was found to be doubled in comparison with the starting polymer.<sup>14</sup> This polymer was subjected to the novel polymer reaction with  $\alpha,\alpha$ -dichloromethyl methyl ether, followed by the oxidative treatment. A polymer having one tertiary alcohol unit at the center in the main chain was produced without obvious decrease of the molecular weight.



Scheme 10

The preparation of a functional segmented block copolymer was also investigated (scheme 11).<sup>15</sup> First hydroboration polymerization of the oligomer using tetrabutylborane was carried out. Then the obtained organoboron polymer was subjected to a chain-transformation reaction (DCME rearrangement). DCME and lithium alkoxide of 3-ethyl-3-pentanol in hexane was added to a THF solution of the polymer at 0°C.

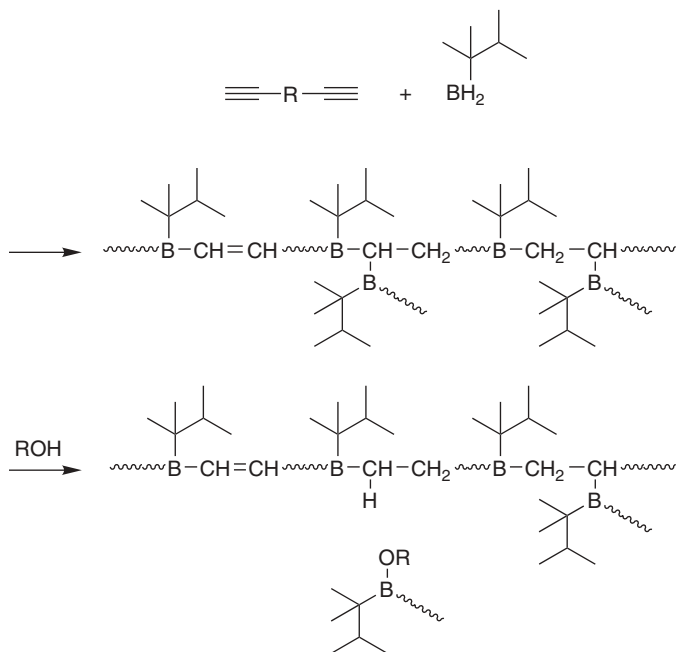


Scheme 11

The reaction mixture was stirred at room temperature for 24 hours, followed by oxidative treatment with  $\text{H}_2\text{O}_2/\text{NaOH}$  to give the corresponding segmented block poly(alcohol).

### C. Hydroboration Polymerization of Diyne Monomers

Synthesis of organoboron polymers by polyaddition between thexylborane and diynes are described here (scheme 12).<sup>13</sup> When a terminal diyne such as 1,7-octadiyne was used as a monomer, a moderate amount of cross-linking reaction occurred due to the further hydroboration of vinylborane units in the main chain of the polymer. Even when an organoboron polymer was prepared from a stoichiometric amount of thexylborane and 1,7-octadiyne, the obtained polymer showed in  $^1\text{H}$  nuclear magnetic resonance (NMR) only 60% of the vinyl protons expected on the basis of an assumption of linear structure. That is, the resulting polymer had a 20% branched structure. As a result of the cross-linking reaction, gelation was observed when an excess of thexylborane was used. The gel obtained with the excess of thexylborane, however, dissolved again upon treatment with methanol. This alcoholysis may cause the chain scission of polymers. Accordingly, an increase in the amount of this structure in the main chain resulted in the decrease in the molecular weight of the polymer after alcoholysis. Conversely when an internal diyne such as 3,9-dodecadiyne was used as a monomer, no gelation was observed even in the presence of excess

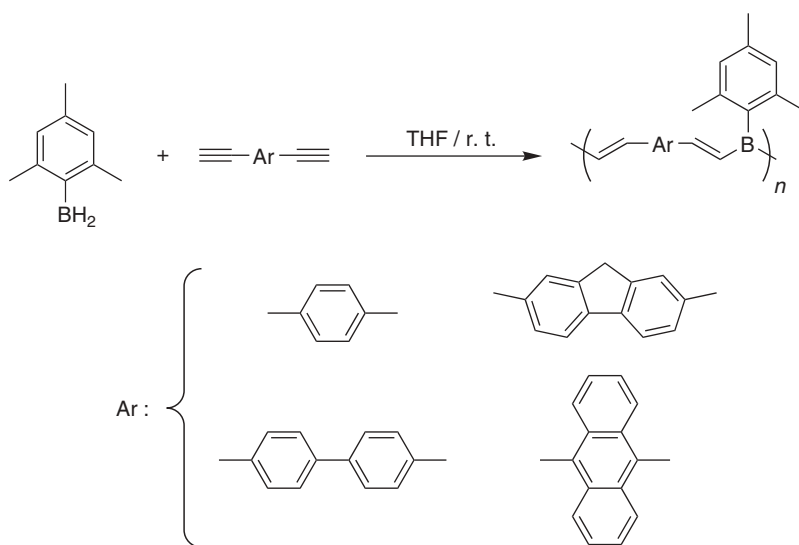


Scheme 12

thexylborane. There was little contribution of the branched structure detected by the spectroscopic analyses of the polymer prepared from an equimolar amount of thexylborane and 3,9-dodecadiyne.

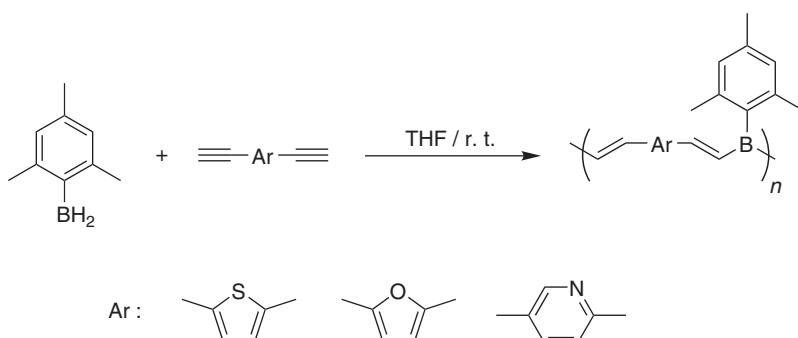
### D. Conjugated Organoboron Polymers

The conjugative interaction between the vinyl group and the boron atom has been investigated by using the spectral properties of low molecular-weight vinylborane derivatives.<sup>16–18</sup> Early studies found that the <sup>11</sup>B NMR and ultraviolet (UV) absorption maxima were in accordance with the calculated results from Hückel molecular orbital (MO) theory, which suggested considerable conjugative overlap of the  $\pi$ -orbitals of the vinyl groups with the p-orbital of the boron atom. Generally, aromatic organoboron compounds such as triphenylborane or trimesitylborane<sup>19,20</sup> are known as strong electron acceptors. Therefore, the polymeric homologues of these materials are expected to possess unique properties as novel n-type conjugated polymers. For example, these polymers include high electron affinity or extended  $\pi$ -conjugation length via the vacant p-orbital of the boron atom. The synthesis of a series of conjugated organoboron polymers was examined by hydroboration polymerization of aromatic diynes with mesitylborane, utilizing the highly regioselective nature of the hydroboration reaction of mesitylborane with the acetylene bond.<sup>21</sup> Various aromatic diynes were used in this hydroboration polymerization with mesitylborane, as shown in scheme 13. The polymers obtained were highly fluorescent. In every case, when a dilute chloroform solution was excited at 350 nm at room temperature, an intense emission was observed in a visible blue region.



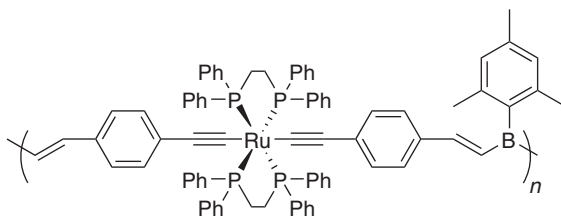
Scheme 13

The hydroboration polymerization of heteroaromatic diynes (2,5-diethynylthiophene, 2,5-diethynylfuran, and 2,5-diethynylpyridine) with mesitylborane was examined to give the corresponding donor–acceptor conjugated polymers (scheme 14).<sup>22</sup> Generally, incorporation of a donor–acceptor pair into a conjugated system is an interesting subject.<sup>23–28</sup> Narrow band gaps or improved third-order nonlinear-optical properties can be achieved, due to the charge-transferred structure in their backbone. The polymers are highly luminescent with especially large Stokes shifts for the heteroaromatic polymers containing pyridine and thiophene units in the backbone. Intriguingly, a white emission was observed for the polymer derived from diethynylpyridine.



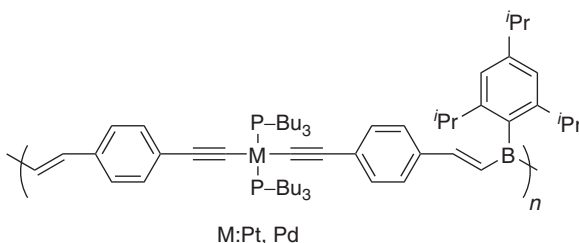
Scheme 14

A facilitated  $d\pi-p\pi^*$  transition was observed in a boron–ruthenium conjugated system prepared by hydroboration polymerization between mesitylborane and a ruthenium–phosphine tetrayne complex to give the polymer shown in scheme 15.<sup>29</sup> The UV–visible (vis) absorption spectrum of the polymer showed two absorption maxima at 359 and 514 nm, possibly due to  $\pi-\pi^*$  and  $d\pi-p\pi^*$  transitions in the main chain, respectively. The former indicates extended  $\pi$ -conjugation length through the boron atom. The latter is unusually bathochromically shifted by 141 nm in comparison with that of ruthenium monomer. It is hard to explain this phenomenon only in terms of the extension of  $\pi$ -conjugation. The high electron affinity of the organoboron unit and the push-pull effect between the electron-rich ruthenium complex and the electron-deficient organoboron unit might be responsible for this red shift.



Scheme 15

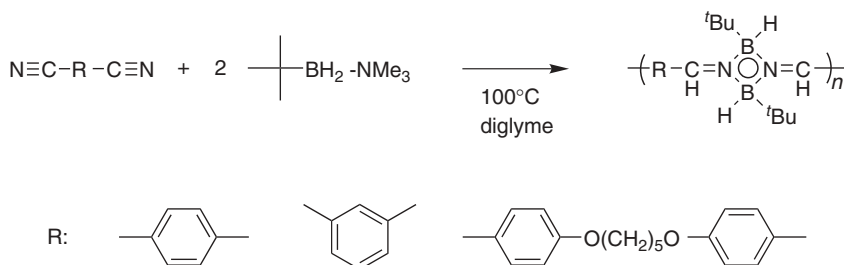
$\pi$ -Conjugated boron polymers containing platinum or palladium atom in the main chain were also prepared by hydroboration polymerization between tetrayne/metal complex monomers and triptylborane (scheme 16).<sup>30</sup> From gel permeation chromatographic analysis [THF, polystyrene (PSt) standards], the number-average molecular weights of the polymers obtained were found to be 9000. The polymers were soluble in common organic solvents such as THF, chloroform, and benzene. The absorption peaks due to  $\pi$ - $\pi^*$  transition were observed around 390 nm in the UV-vis spectra of these polymers. The fluorescence emission spectra exhibited intense peaks at 490 nm in chloroform.



Scheme 16

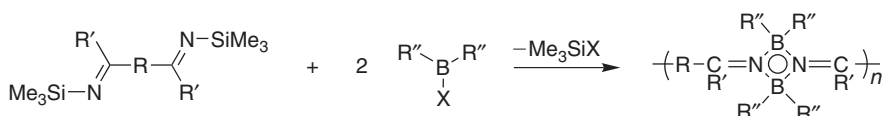
### E. Poly(cyclodiborazane)s Prepared by Hydroboration Polymerization of Dicyano Monomers

Poly(cyclodiborazane)s were synthesized by hydroboration polymerization or allylboration of dicyano compounds. Dimerization of iminoborane formed by monohydration of cyano groups leads to the formation of cyclodiborazane structures having four-membered boron nitrogen rings. For instance, hydroboration polymerization of aromatic dicyano compounds with the *tert*-butylborane-trimethylamine complex gave soluble boron containing polymers having cyclodiborazane backbones in good yields (scheme 17).<sup>31</sup> It required relatively drastic reaction temperature (100°C) to remove trimethylamine ligand moderating reactivity of borane monomers.



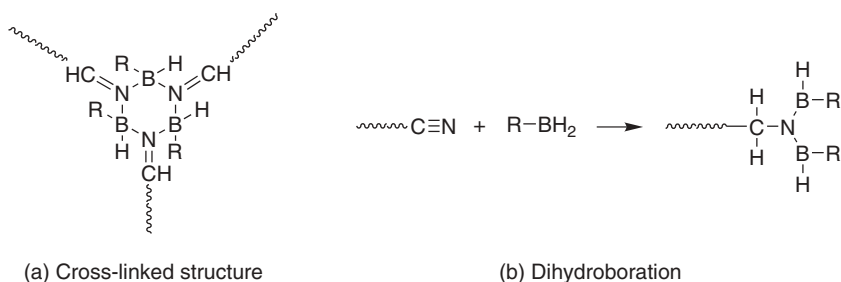
Scheme 17

As an alternative method, poly(cyclodiborazane)s were prepared by the reaction of bis(silylimine)s with chlorodialkylboranes or with methyl dialkylborinates (scheme 18).<sup>32</sup> This reaction proceeds via the condensation between *N*-silylimine and boron halide, eliminating trimethylsilyl halide followed by dimerization. However, the isolated polymer became insoluble after several hours of exposure under air, which resulted from the cross-linking reactions of unreacted trimethylsilyl groups to form trimerized hydrobenzamide derivatives.



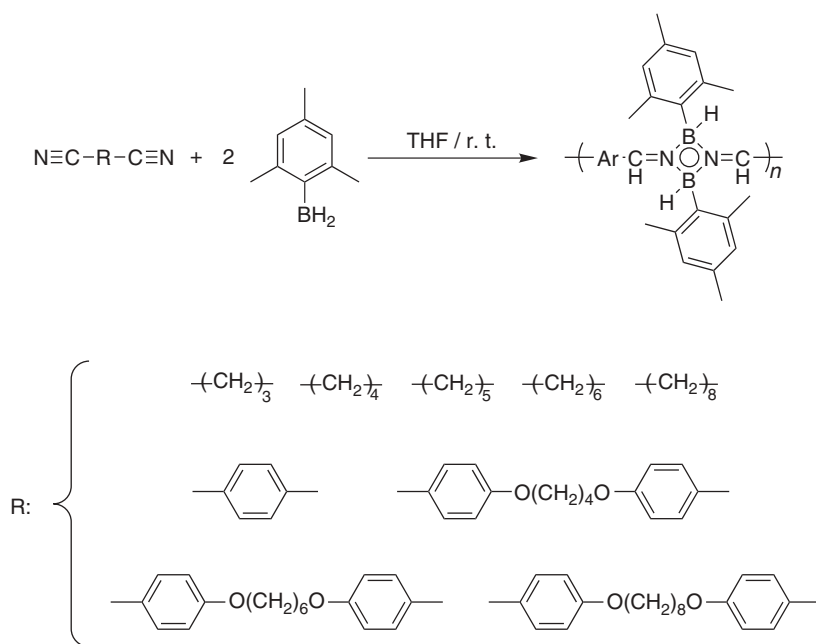
Scheme 18

Generally, during hydroboration polymerization of dicyano compounds, the formation of the borazine structures that have a six-membered boron–nitrogen ring (scheme 19a) and dihydroborated end groups (scheme 19b) as a structural defect is unavoidable. The borazine cross-linked structures often cause the gelation, and dehydroboration causes a decrease in molecular weight.



Scheme 19

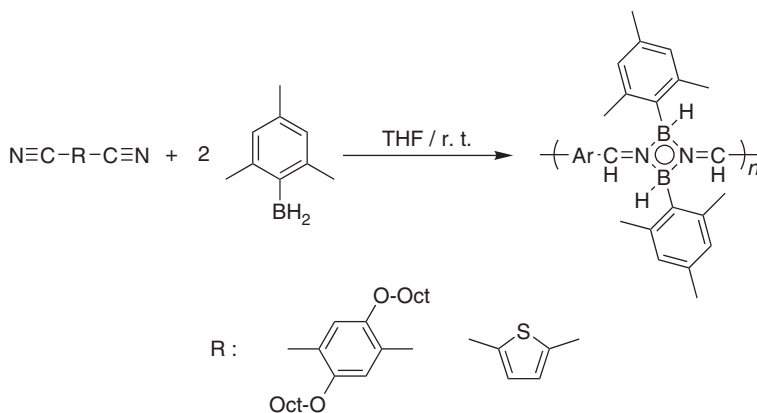
To obtain higher molecular weight and soluble polymers with a more regulated structure, the hydroboration polymerization was examined with sterically hindered borane monomers (scheme 20).<sup>33</sup> Hydroboration polymerization between mesitylborane and adiponitrile gave relatively high molecular-weight polymers when the reaction was carried out at 0°C to room temperature. Due to the bulky mesityl groups, further hydroboration reactions and the formation of borazine structures were almost negligible.



Scheme 20

## F. Conjugated Poly(cyclodiborazane)s

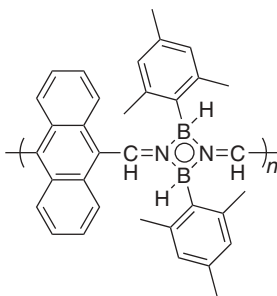
Fully aromatic poly(cyclodiborazane)s should be regarded as  $\pi$ -conjugated organoboron polymers via the vacant p-orbital of the boron atom. However, no significant extension of  $\pi$ -conjugation length was observed when 1,4-dicyanobenzene was employed as a dicyano monomer.<sup>33</sup> Recently, it was found that the incorporation of the electron donating structure in the poly(cyclodiborazane)s backbone (scheme 21)



Scheme 21

led to dramatically bathochromic-shifted absorption edges compared with their model compounds.<sup>34</sup> This indicates the existence of some intramolecular charge-transfer (ICT) interaction due to the electron-accepting cyclodiborazane moieties or interunit conjugation along the main chain of the polymer. This also suggests that the electronic state of poly(cyclodiborazane) is very sensitive toward the electronic environment around the cyclodiborazane unit. Accordingly, poly(cyclodiborazane)s bearing ICT structures are interesting and promising as optical and electronic materials. Therefore, we examined hydroboration polymerization with a wide range of dicyano compounds.

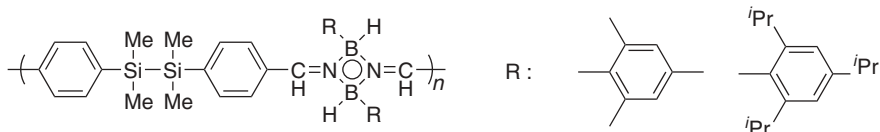
Hydroboration polymerization between mesitylborane and 1,9-dicyanoanthracene (DCA) gave the corresponding poly(cyclodiborazane) having anthracene as the repeating unit (scheme 22).<sup>35</sup> Polymerization was carried out under nitrogen by adding a THF solution of mesitylborane to a suspension of DCA in THF at room temperature. After the reaction mixture was stirred for 12 hours, an insoluble precipitate was filtered. The soluble part was purified by reprecipitation into MeOH to give a yellow powder. Gel permeation chromatography (chloroform, PSt) analysis showed that the number-average molecular weight of the polymer was 4400 (yield 91%). The polymer obtained was highly soluble in common organic solvents such as THF, chloroform, and benzene, despite the presence of an anthracene ring repeat unit. An intense green fluorescence emission spectrum was observed at 494 nm. The relatively high stability of the polymer was shown by its resistance to reaction with air or water and from thermogravimetric analysis behavior. The polymer is expected to be a novel type of electron-transporting material or polymer catalyst in photochemistry.



Scheme 22

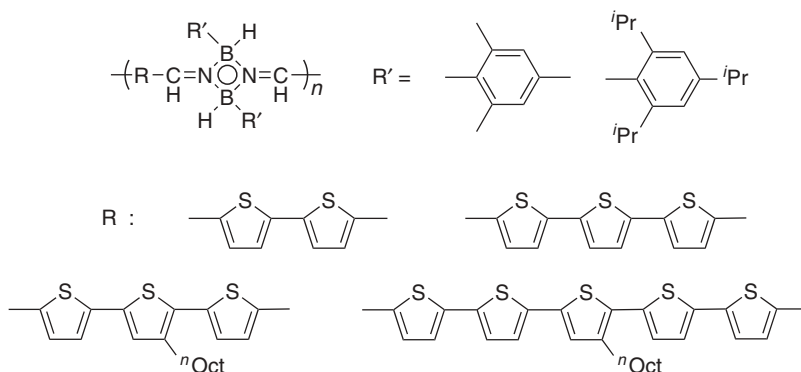
The presence of  $\sigma$ - $\pi$  conjugation utilizing the disilanylene structure also would be interesting. We synthesized poly(cyclodiborazane)s from 1,2-bis(*p*-cyanophenyl)-1,1,2,2-tetramethyldisilane and mesitylborane or tripylborane (scheme 23). The polymers obtained exhibited novel optical behavior for  $\sigma$ - $\pi$  conjugated polymers. The fluorescence emission spectra of the polymers showed an intense emission peak at 430 nm, due to their intramolecular charge-transfer structure. The potential of the peak (+0.87 V) obtained from cyclic voltammetric measurement was relatively smaller than those reported for  $\sigma$ - $\pi$  conjugated organosilicon copolymers prepared by Fang

and co-workers,<sup>36</sup> indicating the existence of enhanced  $\sigma$ - $\sigma$  interaction between the disilanylene unit and the adjacent cyclodiborazane unit.



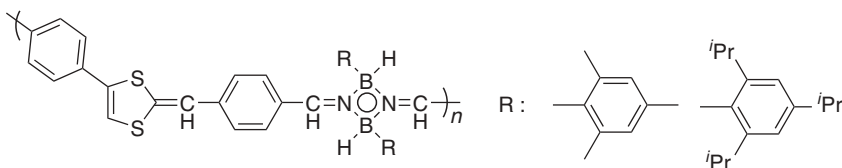
Scheme 23

The poly(cyclodiborazane)s containing oligothiophene units were also synthesized (scheme 24).<sup>37</sup> The longer the oligothiophene units of the polymers were, the more bathochromic-shifted their absorption maxima became. In other words, as the number of thiophene repeating units increases,  $\pi$ -conjugation length extends effectively and a red shift of absorption maxima in UV-vis absorption spectra was observed. The fluorescence emission maxima of the poly(cyclodiborazane)s were successfully controlled in this way (450–530 nm).



Scheme 24

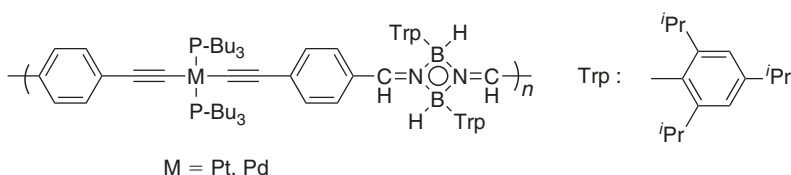
The poly(cyclodiborazane)s containing a dithiafulvene unit in the backbone were also reported (scheme 25).<sup>38</sup> This polymer showed an efficient extension of conjugation between the consecutive repeat units due to the strong electron donating property of the dithiafulvene unit. Before doping, this polymer exhibited an electrical



Scheme 25

conductivity of  $2 \times 10^{-5} \text{ S cm}^{-1}$  as measured on a cast film by the conventional two-probe technique. This relatively high conductivity is probably due to the donor-acceptor pair of the dithiafulvene and the cyclodiborazane units. Moreover, cast films of the charge-transfer complex between poly(cyclodiborazane) with 7,7,8,8-tetracyanoquinodimethane (TCNQ) had a conductivity of  $2 \times 10^{-4} \text{ S cm}^{-1}$ , one order of magnitude greater than that for the uncomplexed polymer.

The poly(cyclodiborazane)s containing the transition metals palladium and platinum in their backbone were prepared (scheme 26).<sup>39</sup> These polymers exhibited an extension of  $\pi$ -conjugation length via their transition metal and cyclodiborazane moieties.

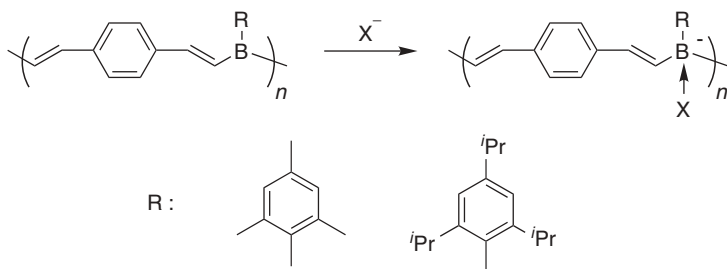


Scheme 26

## G. Organoboron Polymers as an Anion Sensor

Recently, chemosensors that convert molecular recognition into easily detected signals have been actively investigated. Especially, fluorescent chemosensors have attracted considerable interest because of their high sensitivity. Since the fluoride anion is highly significant to health and environmental issues, a large number of artificial chemosensors have been designed. Among them, the specific and strong Lewis acid-base interaction of a boron atom with fluoride ion were adopted as efficient approaches.<sup>40-51</sup>

$\pi$ -Conjugated organoboron polymers were also reported as a selective fluoride ion sensor.<sup>52</sup> A halide ion was added to a chloroform solution of  $\pi$ -conjugated organoboron polymer prepared from 1,4-diethynylbenzene and mesitylborane or triptylborane. After the addition of a fluoride ion, an absorption maximum was hypsochromic shifted and the intense blue emission was quenched (scheme 27).



Scheme 27

In conjugated organoboron polymers,  $\pi$ -conjugation length is extended via the vacant p-orbital of boron atom. If fluoride anion coordinates to the organoboron polymer, the hybridization of the boron atom should change from  $sp^2$  to  $sp^3$  and this change would interrupt the extension of  $\pi$ -conjugation and fluorescence emission.

### III. OTHER BORATION POLYMERIZATIONS

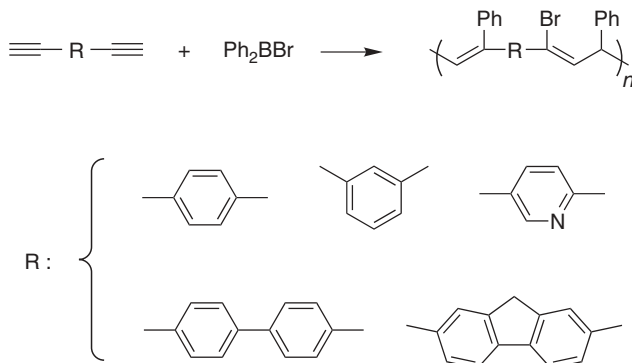
#### A. Haloboration Polymerization

Haloboration is known to provide key intermediates for the synthesis of substituted olefins. This reaction proceeds chemoselectively and stereoselectively under the appropriate reaction conditions. The reactivity of a boron-halide moiety toward haloboration is known to decrease with the decrease of its Lewis acidity in the following general order:  $BX_3 > RBX_2 > R_2BX$ . Dialkenylboron bromide, which may be produced by the haloboration of a diyne with B—Br, has a low Lewis acidity due to the two alkenyl groups on the boron atom. Thus, a large different reactivity between B—Br and dialkenylboron bromide makes possible the formation of a linear polymer without gelation by supplying two B—Br bonds from boron tribromide (scheme 28).<sup>53</sup>



Scheme 28

$\pi$ -Conjugated organoboron polymers were prepared by haloboration-phenylboration polymerization between diyne monomers and bromodiphenylborane (scheme 29).<sup>54</sup> The polymerization was carried out by adding a slight excess of bromodiphenylborane to a tetrachloroethane solution of diynes at room temperature

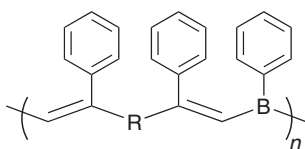


Scheme 29

under nitrogen and stirring the reaction mixture for 4 hours at 100°C. The obtained polymers were soluble in common organic solvents such as THF and chloroform. Their molecular weights were estimated to be several thousands by gel permeation chromatographic analysis. In UV–vis absorption spectra, bathochromic shifts of  $\lambda_{\max}$  and absorption edge in comparison with the corresponding monomers were observed. This indicates  $\pi$ -conjugation is occurring via vacant p-orbital of the boron atom.

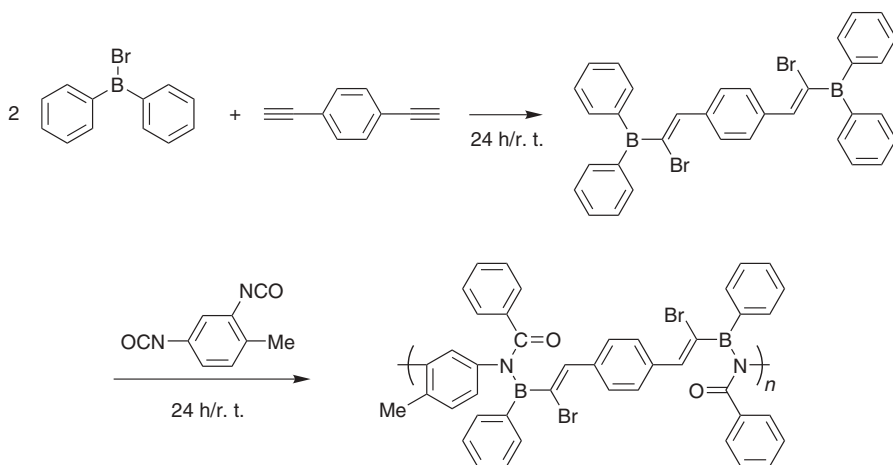
## B. Phenylboration Polymerization

The polymers prepared by phenylboration polymerization of diynes exhibit relatively high stability against air and thermal oxidation (scheme 30).<sup>55</sup>



Scheme 30

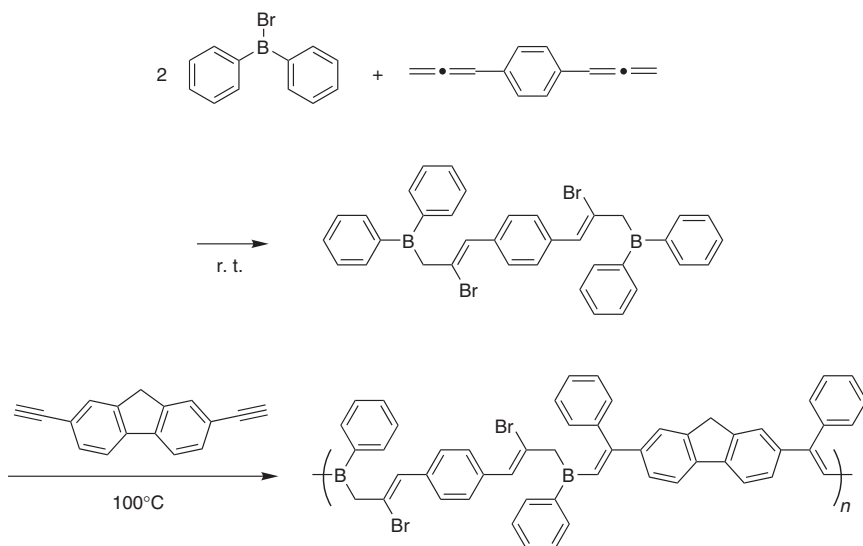
An alternating boration copolymerization methodology was explored by making use of different boration reactivities between diynes and diisocyanates (scheme 31).<sup>56</sup> To obtain the organoboron polymers bearing amidoalkenylborane units, a boration polymerization using the stepwise boration reaction should be required. Alternating boration copolymerization was achieved by utilizing the different boration reactivities between acetylene and isocyanate. Haloboration of aromatic acetylene bonds takes place under mild reaction conditions ( $\sim -78^\circ\text{C}$ ), while the phenylboration



Scheme 31

reaction requires more forcing reaction conditions ( $\sim 70^\circ\text{C}$ ). Conversely, both haloboration and phenylboration of isocyanates proceed smoothly at room temperature. Accordingly, the treatment of an aromatic diyne monomer with two molar equivalents of diphenylbromoborane (selective haloboration of the acetylene bond) and the subsequent reaction with an equimolar amount of diisocyanate would give a polymer having the alternating unit structure shown in scheme 31.

The alternating boration copolymerization between bisallene (1,4-allenylbenzene) and diyne (2,7-diethynylfluorene) was carried out to afford the corresponding alternating copolymer (scheme 32).<sup>57</sup> The alternating boration copolymerization would give the polymer having alkenylallylborane units, in which the B—C bond could be incorporated in the conjugation path. Since the B—C bond interacts conjugatively with the adjacent vinyl group similar to the behavior of a Si—Si bond,<sup>58</sup> the polymer produced in the present system is expected to be a polymeric precursor for a novel  $\sigma$ – $\pi$  conjugated polymers.

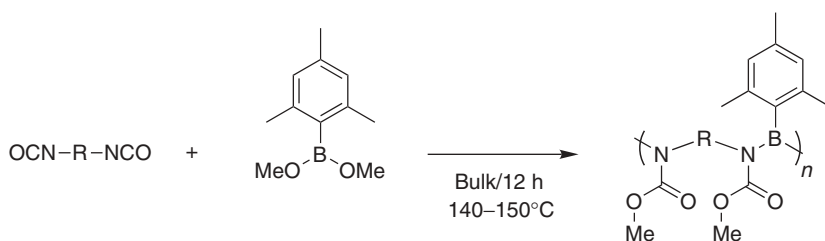


Scheme 32

### C. Alkoxyboration Polymerization

Poly(boronic carbamate)s were prepared by alkoxyboration polymerization of diisocyanates with mesityldimethoxyborane (scheme 33).<sup>59</sup> The polymers obtained have boronic carbamate functions in their repeating units and can be expected to be novel reactive polymers. First, alkoxyboration polymerization between mesityldimethoxyborane and 1,6-hexamethylene diisocyanate was examined, and the optimized reaction conditions were bulk reactions at  $140^\circ\text{C}$ . Both aliphatic and aromatic diisocyanates gave the corresponding polymers. When aromatic diisocyanates were employed, the

reactions required severe reaction conditions (150°C). The polymers prepared from aromatic diisocyanates have a high air stability.

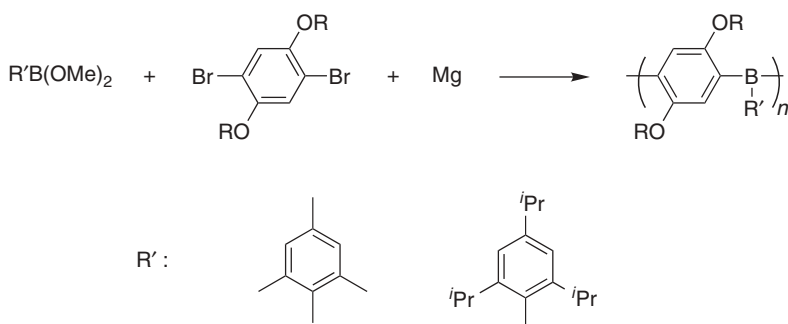


Scheme 33

## IV. ORGANOMETALLIC ROUTES

### A. Grignard and Organolithium Reagents

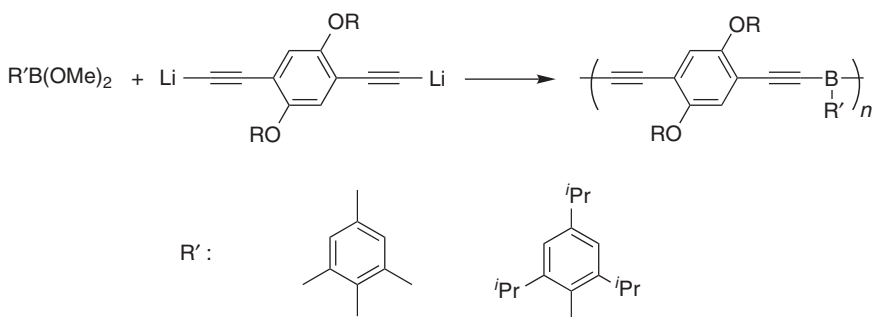
The organoboron polymers were prepared not only by hydroboration polymerization but also by organometallic approaches. Poly(*p*-phenylene-borane)s (PPBs) were prepared by polycondensation of aryldimethoxyboranes and bifunctional Grignard reagents (scheme 34).<sup>60</sup> This provides a novel methodology for the preparation of organoboron conjugated polymers, which is a useful alternative to hydroboration polymerization. The polymers obtained are expected to be novel n-type conjugated polymers with fairly high air and moisture stability. The higher thermal stability is also expected due to the absence of a retrohydroboration ( $\beta$ -elimination) process during their thermal degradation. The PPBs show absorption maxima in the range of 359–367 nm in chloroform solution and emit blue-green light upon excitation at 350 nm.



Scheme 34

Poly(ethynylene-*p*-phenylene-ethynylene-borane)s were also prepared by polycondensations of bifunctional lithium acetylides and aryldimethoxyborane, as shown in scheme 35.<sup>61</sup> The polymerization between dilithium 2,5-didodecyloxybenzene-1,4-diethynilide and triplydimethoxyborane gave the corresponding polymer in 67%

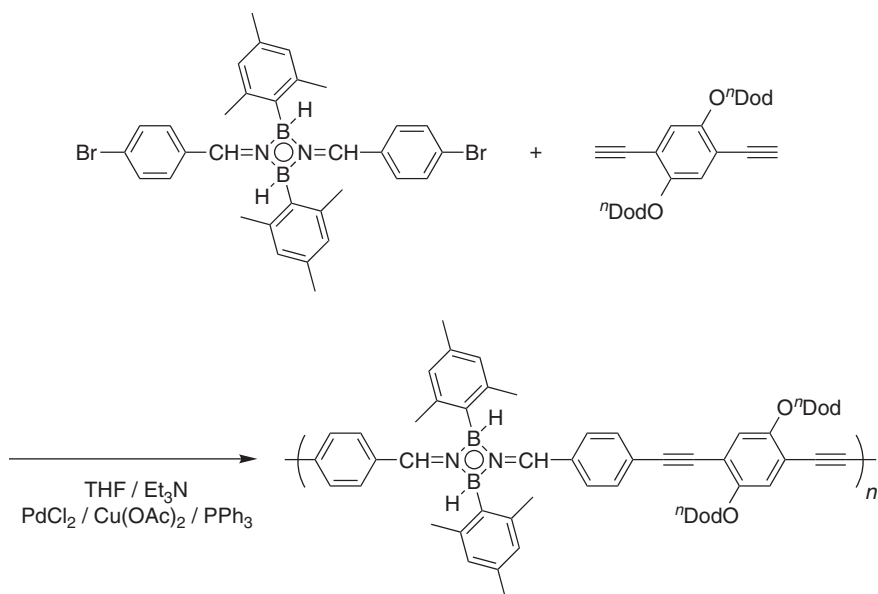
yield. From gel permeation chromatographic analysis (THF, PSt standards), the number-average molecular weight of the polymer was found to be 2700. In the UV–vis spectrum of the polymer (in chloroform at room temperature), an absorption maximum was observed at 397 nm. The fluorescence emission spectrum (in chloroform, room temperature, excitation wavelength at 400 nm) showed its emission wavelength maximum at 456 nm in the visible blue region.



Scheme 35

## B. Poly(cyclodiborazane)s via Cross-Coupling Reactions

Donor–acceptor type  $\pi$ -conjugated poly(cyclodiborazane)s were synthesized by organometallic polycondensation between cyclodiborazane-containing dibromides and diethynyl monomers utilizing Sonogashira–Hagihara coupling (scheme 36).<sup>62</sup>



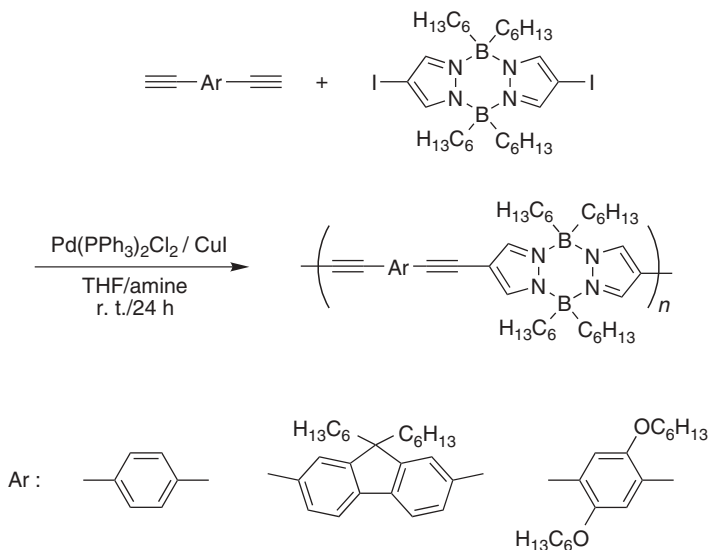
Scheme 36

The polymerization was carried out under a nitrogen atmosphere in THF/Et<sub>3</sub>N solution in the presence of a catalytic amount of copper acetate, palladium chloride, and triphenylphosphine at 80°C for 12 hours. After reprecipitation into MeOH, the resulting polymer was isolated as a brown powder in moderate yield. The polymer obtained was soluble in common organic solvents such as THF, chloroform. The number-average molecular weight of the polymer was 8500 from the gel permeation chromatographic analysis [gel permeation chromatography (GPC) THF, PSt standards]. The UV–vis absorption spectrum recorded in chloroform exhibited an absorption maximum at 414 nm, owing to extension of  $\pi$ -conjugation via the vacant p-orbital of the boron atom and intramolecular charge transfer. This polymer exhibited an intense blue-green light emission upon irradiation at 414 nm.

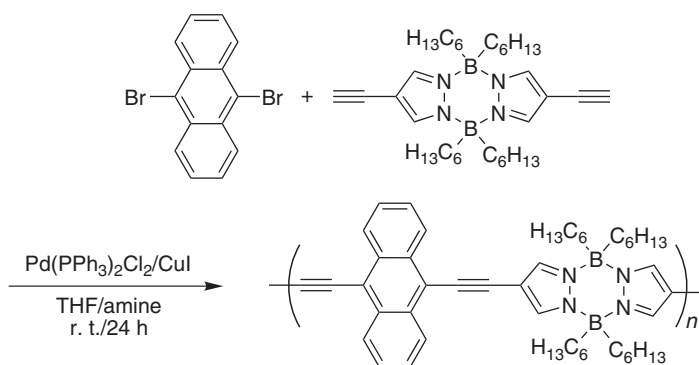
### C. Poly(pyrazabole)s via Cross-Coupling Reactions

Pyrazaboles are known as a novel class of boron heterocycles. Since its first synthesis<sup>63</sup> in 1967, a number of pyrazaboles have been prepared and characterized; however, their structures and properties are not fully understood. Pyrazaboles are highly stable, so that the derivatives containing various functional groups are easily prepared by the usual organic reaction. Several recent applications of pyrazaboles have been reported, including their use as possible building blocks for discotic liquid crystals<sup>64,65</sup> or good bridges for *ansa*-ferrocenes to form active container molecules for supramolecular applications.<sup>66,67</sup>

Organoboron polymers containing pyrazaboles in the main chain were prepared by Sonogashira–Hagihara coupling (schemes 37 and 38).<sup>68</sup> The coupling reaction between diyne monomers and pyrazabole derivatives gave the corresponding polymers



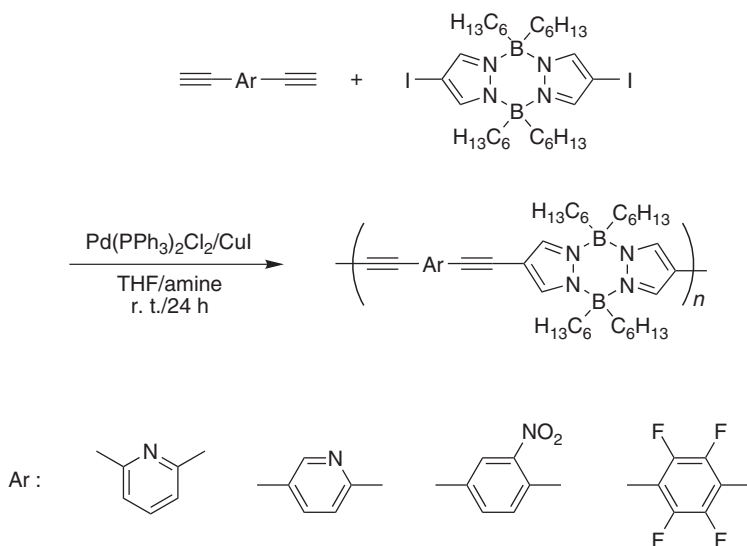
Scheme 37



Scheme 38

in good yields. Furthermore, these polymers were highly stable against air and moisture, and showed blue fluorescent emission (383–470 nm) with high quantum emission yields (0.43–0.67). As a result of UV–vis absorption measurements of the polymers and the model compounds, a slight extension of  $\pi$ -conjugation via the six-membered ring structure of boron and nitrogen was suggested in these polymers. Moreover, similar emission spectra were observed to be independent of the polymer structures. From these results, the pyrazole structures seemed to play a significant role in the emission properties.

Poly(pyrazole)s containing an electron withdrawing moiety in the main chain were prepared the same way (scheme 39).<sup>69</sup> The coupling reaction between



Scheme 39

various diyne monomers and the pyrazabole derivative gave the corresponding polymers in good yields. The polymers exhibited blue to near-UV emission. By incorporating the electron-withdrawing structure into the main chain, the electron density on the boron atom was reduced, and their emission wavelengths and fluorescence quantum yields were decreased accordingly. The emission spectra suggested a strong relation between the presence of pyrazabole and the polymer's emission properties. Furthermore, they were highly stable and exhibited good film formability.

Poly(pyrazabole)s were investigated as a neutron scintillator material.<sup>70</sup> Neutron scintillator materials require a high detection efficiency and a large  $n/\gamma$  ratio. For high detection efficiency and a large  $n/g$  ratio, the materials should contain light elements such as  $^3\text{He}$ ,  $^6\text{Li}$ , and  $^{10}\text{B}$ . The poly(pyrazabole)s consisting only of light elements such as C, N, B, and H, show luminescence by UV excitation with high efficiency. The luminescence of poly(pyrazabole) powder, poly(pyrazabole)/polystyrene, and poly(pyrazabole)/perylene/polymethylmethacrylate (PMMA) by UV-light, X-ray, and  $\alpha$ -ray excitation was observed in the blue-green region. The decay time of neutron excitation, the neutron detection efficiency, and the  $n/\gamma$  ratios are 3.7 ns,  $\sim 0.020$ ,  $\sim 1.0$  and 7.4 ns,  $\sim 0.013$ ,  $\sim 3.5$  for poly(pyrazabole)/polystyrene, and poly(pyrazabole)/perylene/PMMA, respectively.

## V. SUMMARY

In summary, a wide variety of main-chain-type organoboron polymers have been synthesized by hydroboration, haloboration, phenylboration, the organometallic route, and so on. These organoboron polymers exhibited interesting properties based on the high electron affinity of boron both as reactive polymers and optical/electronic materials. The organoboron material chemistry, based on mature organoboron chemistry, is in an early phase of development. In the future, novel organoboron polymer applications must be discovered through the design of polymer structures and the polymerization method.

## VI. REFERENCES

1. H. C. Brown, *Hydroboration*, W. A. Benjamin, New York, 1962.
2. T. C. Chung, *Macromolecules*, **21**, 865 (1989).
3. S. Ramakrishnan, T. C. Chung, *Macromolecules*, **22**, 3181 (1989).
4. S. Ramakrishnan, T. C. Chung, *Macromolecules*, **23**, 4519 (1990).
5. Y. Chujo, I. Tomita, Y. Hashiguchi, H. Tanigawa, E. Ihara, T. Saegusa, *Macromolecules*, **24**, 345 (1991).
6. Y. Chujo, Y. Sasaki, N. Kinomura, N. Matsumi, *Polymer*, **41**, 5047 (2000).
7. M. Miyata, F. Meyer, Y. Chujo, *Polym. Bull.*, **46**, 23 (2001).
8. Y. Chujo, I. Tomita, Y. Hashiguchi, T. Saegusa, *Polym. Bull.*, **25**, 1 (1991).

9. Y. Chujo, I. Tomita, Y. Hashiguchi, T. Saegusa, *Polym. Bull.*, **26**, 165 (1991).
10. Y. Chujo, M. Morimoto, I. Tomita, *Polym. J.*, **25**, 891 (1993).
11. Y. Chujo, M. Morimoto, I. Tomita, *Polym. Bull.*, **29**, 617 (1992).
12. Y. Chujo, *J. Macromol. Sci., Pure Appl. Chem.*, **A31**, 1647 (1994).
13. Y. Chujo, I. Tomita, Y. Hashiguchi, T. Saegusa, *Macromolecules*, **25**, 33 (1991).
14. Y. Chujo, I. Tomita, T. Asano, T. Saegusa, *Polym. Bull.*, **30**, 215 (1993).
15. M. Miyata, F. Meyer, Y. Chujo, *Polym. Bull.*, **52**, 25 (2004).
16. C. D. Good, D. M. Ritter, *J. Am. Chem. Soc.*, **84**, 1162 (1962).
17. C. D. Good, D. M. Ritter, *J. Phys. Chem. Ref. Data*, **1**, 416 (1962).
18. G. Zweifel, G. M. Clark, T. Leung, C. C. Whitney, *J. Organomet. Chem.*, **117**, 303 (1976).
19. H. C. Brown, V. H. J. Dodson, *J. Am. Chem. Soc.*, **79**, 2302 (1957).
20. B. G. Ramsey, L. M. J. Isabelle, *J. Org. Chem.*, **46**, 179 (1981).
21. N. Matsumi, K. Naka, Y. Chujo, *J. Am. Chem. Soc.*, **120**, 5112 (1998).
22. N. Matsumi, M. Miyata, Y. Chujo, *Macromolecules*, **32**, 4467 (1999).
23. E. E. Havinga, W. ten Hoeve, H. Wynberg, *Polym. Bull.*, **29**, 119 (1992).
24. J. P. Ferraris, A. Bravo, W. Kim, D. C. Hrnčir, *J. Chem. Soc., Chem. Commun.*, 991 (1994).
25. M. Karikomi, C. Kitamura, S. Tanaka, Y. Yamashita, *J. Am. Chem. Soc.*, **117**, 6791 (1995).
26. T. Kanbara, Y. Miyazaki, T. Yamamoto, *J. Polym. Sci., Part A: Polym. Chem.*, **33**, 999 (1995).
27. T. Yamamoto, Z. Zhou, T. Kanbara, M. Shimura, K. Kizu, T. Maruyama, Y. Nakamura, T. Fukuda, B. Lee, N. Ooba, S. Tomaru, T. Kurihara, T. Kaino, K. Kubota, S. Sasaki, *J. Am. Chem. Soc.*, **118**, 10389 (1996).
28. Q. T. Zhang, J. M. Tour, *J. Am. Chem. Soc.*, **119**, 5065 (1997).
29. N. Matsumi, Y. Chujo, O. Lavastre, P. H. Dixneuf, *Organometallics*, **20**, 2425 (2001).
30. F. Matsumoto, N. Matsumi, Y. Chujo, *Polym. Bull.*, **46**, 257 (2001).
31. Y. Chujo, I. Tomita, N. Murata, H. Mauermann, T. Saegusa, *Macromolecules*, **25**, 27 (1992).
32. Y. Chujo, I. Tomita, T. Asano, H. Mauermann, T. Saegusa, *Polym. J.*, **26**, 85 (1994).
33. N. Matsumi, K. Naka, Y. Chujo, *Polym. J.*, **30**, 833 (1998).
34. N. Matsumi, T. Umeyama, Y. Chujo, *Macromolecules*, **33**, 3956 (2000).
35. N. Matsumi, K. Naka, Y. Chujo, *Macromolecules*, **31**, 8047 (1998).
36. M. C. Fang, A. Watanabe, M. Matsuda, *Polymer*, **37**, 163 (1996).
37. M. Miyata, N. Matsumi, Y. Chujo, *Macromolecules*, **34**, 7331 (2001).
38. K. Naka, T. Umeyama, Y. Chujo, *Macromolecules*, **33**, 7467 (2000).
39. F. Matsumoto, N. Matsumi, Y. Chujo, *Polym. Bull.*, **48**, 119 (2002).
40. C. Dusemund, K. R. A. S. Sandanayake, S. Shinkai, *J. Chem. Soc., Chem. Commun.*, 333 (1995).
41. H. Yamamoto, A. Ori, K. Ueda, C. Dusemund, S. Shinkai, *Chem. Commun.*, 407 (1996).
42. C. R. Cooper, N. Spencer, T. D. James, *Chem. Commun.*, 1365 (1998).
43. M. Nicolas, B. Fabre, J. Simonet, *Chem. Commun.*, 1881 (1999).
44. S. Yamaguchi, S. Akiyama, K. Tamao, *J. Am. Chem. Soc.*, **122**, 6335 (2000).
45. S. Yamaguchi, S. Akiyama, K. Tamao, *J. Am. Chem. Soc.*, **123**, 11372 (2001).
46. S. Yamaguchi, T. Shirasaka, S. Akiyama, K. Tamao, *J. Am. Chem. Soc.*, **124**, 8816 (2002).
47. Y. Kubo, M. Yamamoto, M. Ikeda, M. Takeuchi, S. Shinkai, S. Yamaguchi, K. Tamao, *Angew. Chem., Int. Ed.*, **42**, 2036 (2003).
48. S. Solé, F. P. Gabbai, *Chem. Commun.*, 1284 (2004).
49. J. D. Hoefelmeyer, S. Solé, F. P. Gabbai, *Dalton. Trans.*, 1254 (2004).
50. S. Arimori, M. G. Davidson, T. M. Fyles, T. G. Hibbert, T. D. James, G. I. Kociok-Köhn, *Chem. Commun.*, 1640 (2004).

51. Y. Kubo, A. Kobayashi, T. Ishida, Y. Misawa, T. D. James, *Chem. Commun.*, 2846 (2005).
52. M. Miyata, Y. Chujo, *Polym. J.*, **34**, 967 (2002).
53. Y. Chujo, I. Tomita, T. Saegusa, *Macromolecules*, **23**, 687 (1990).
54. M. Miyata, N. Matsumi, Y. Chujo, *Polym. Bull.*, **42**, 505 (1999).
55. Y. Chujo, *ACS Symp. Ser.*, **572**, 398 (1994).
56. N. Matsumi, K. Kotera, Y. Chujo, *Macromolecules*, **33**, 2801 (2000).
57. N. Matsumi, Y. Chujo, *Polym. Bull.*, **43**, 117 (1999).
58. Y. Yamamoto, H. Yatagai, Y. Naruta, K. Maruyama, T. Okamoto, *Tetrahedron Lett.*, **21**, 3599 (1980).
59. N. Matsumi, Y. Chujo, *Macromolecules*, **31**, 3802 (1998).
60. N. Matsumi, K. Naka, Y. Chujo, *J. Am. Chem. Soc.*, **120**, 10776 (1998).
61. N. Matsumi, T. Umeyama, Y. Chujo, *Polym. Bull.*, **44**, 431 (2000).
62. N. Matsumi, Y. Chujo, *Macromolecules*, **33**, 8146 (2000).
63. S. Trofimenko, *J. Am. Chem. Soc.*, **89**, 3165 (1967).
64. J. Barberá, R. Giménez, J. L. Serrano, *Adv. Mater.*, **6**, 470 (1994).
65. J. Barberá, R. Giménez, J. L. Serrano, *Chem. Mater.*, **12**, 481 (2000).
66. F. Jäcle, T. Priermeier, M. Wagner, *Organometallics*, **15**, 3165 (1996).
67. E. Herdweek, F. Jäcle, G. Opromolla, M. Spigler, M. Waner, P. Zanello, *Organometallics*, **15**, 5524 (1996).
68. F. Matsumoto, Y. Chujo, *Macromolecules*, **36**, 5516 (2003).
69. F. Matsumoto, Y. Nagata, Y. Chujo, *Polym. Bull.*, **53**, 155 (2005).
70. E. Kamaya, F. Matsumoto, Y. Kondo, Y. Chujo, M. Katagiri, *Nucl. Instrum. Methods Phys. Res., A*, **529**, 329 (2004).



---

## CHAPTER 5

# Boron- and Nitrogen-Containing Polymers

**Philippe Miele, David Cornu, and Bérangère Toury**

*Laboratoire des Multimatériaux et Interfaces, Université Lyon 1, Villeurbanne, France*

### CONTENTS

I. INTRODUCTION	150
II. BACKGROUND	151
III. POLYMERS DERIVED FROM BORAZINE	151
IV. POLYMERS DERIVED FROM <i>B</i> -CHLOROBORAZINE	156
A. Poly( <i>B</i> -amino)borazines Prepared in a One-Step Process	156
B. Poly( <i>B</i> -borylamino)borazines Prepared in a One-Step Process	159
C. Poly( <i>B</i> -amino)borazines Prepared in a Two-Step Process	161
D. Poly( <i>B</i> -borylamino)borazines Prepared in a Two-Step Process	166
V. POLYMERS DERIVED FROM TRIS(ALKYLAMINO)BORANES	169
VI. SUMMARY	171
VII. REFERENCES	172

## I. INTRODUCTION

The main purpose of this chapter is to provide an overview of the chemistry of boron- and nitrogen-containing polymers. This topic was investigated before the 1960s in the same way that other inorganic polymers based on main-group elements and were reviewed in the past.<sup>1-3</sup> During this decade, Chantrell and Popper published in 1964 a seminal paper describing the possibility of converting inorganic polymers into ceramics with covalently bonded atoms.<sup>4</sup> However, it was only from the middle 1970s that a marked upsurge of interest concerning these systems was noticed after nonoxide SiC-based fibers prepared from preceramic polymers were produced.<sup>5</sup> The successful development of carbon fibers and components from organic polymers was based on the same concept.<sup>6</sup>

Generally, the precursor-to-ceramic route used is known as the polymer derived ceramics (PDCs) method. This technique has many advantages starting with the use of reagents, allowing the chemistry (purity, elemental composition, compositional homogeneity, and atomic architecture) of molecular precursors to be controlled and tailored. As for the versatile *p* element, a large number of possibilities in terms of chemical synthesis can be judiciously put to good use in order to provide preceramic polymers with desirable composition, structure, and thermal properties.<sup>7,8</sup> In addition, the main interest offered by these polymers lies in the fact that they can be shaped into unconventional forms before conversion into ceramic materials. Thus, this route has a conclusive advantage in many applications. Among the most obvious is the production of ceramic fibers, which cannot be fabricated from a powder source. Obviously, the reader should be aware that any monomer and any polymer cannot be considered as preceramic precursors; and, general characteristics have been proposed within this outlook.<sup>9</sup> The development of advanced materials requires the exploration of improved new molecular precursors simultaneously with the determination of the inorganic reactions taking place in the formation of the polymers from the monomers.

A number of studies have been devoted to boron's inorganic polymers. Also, most efforts have concentrated on polymeric B—N derivatives directed toward the production of boron nitride in different morphologies. These results were summarized in the 1990s within the context of ceramic materials science.<sup>10,11</sup> As might be imagined, when taking an interest to elaborate high-performances ceramic materials by the PDCs method, the design of molecular and polymeric precursors are crucially important. Particularly, the fabrication of BN fibers was very challenging since several constraints imposed by the process must be also taken into account at the precursor chemistry level. Among all these features, the ceramic yield of the precursors and the rheological properties of the polymers have guided most of our studies. However, these properties are not discussed in this chapter. In the following sections, we concentrate on the chemistry of the monomers and the derived polymers. These are presented according to the kind of polymeric species prepared and the polymerization mechanisms involved.

## II. BACKGROUND

For the most part, boron–nitrogen-containing polymers have the borazinic ring as the main building block. Since these rings may be linked by several ways in the inorganic backbone, it is difficult to classify polymers by their linking criterion. Instead, it seems relevant to use a classification based on the kind of monomer used and by taking into account the lack of a clear nomenclature of these polymers. This chapter is organized around three main parts corresponding to the three main classes of boron-containing preceramic polymers used for BN preparation: (1) polyborazylene and other polymers derived from borazine,  $\text{H}_3\text{B}_3\text{N}_3\text{H}_3$ ; (2) poly[*B*-aminoborazines] obtained from *B*-chloroborazines,  $(\text{Cl}_{3-x}\text{R}_x)\text{B}_3\text{N}_3\text{R}'_3$ ; and (3) poly[*B*-aminoborazines] prepared from tris(alkylamino)boranes,  $\text{B}(\text{NHR})_3$ . The potential of some preceramic polymers to generate nonoxide ceramics through the PDCs route are illustrated in Chapter 3. Finally, some future outlooks are explored, and, we will try to predict some further scientific challenges in the field.

## III. POLYMERS DERIVED FROM BORAZINE

The synthesis of borazine (Fig. 1) was first described in 1926 by Stock and Pohland.<sup>12</sup> More recently, Wideman and Sneddon reported interesting three one-step synthetic procedures using various starting compounds including 2,4,6-trichloroborazine, metal borohydrides, and ammonia-borane.<sup>13</sup> The B—N bond is isoelectronic with the C—C bond, which explains why borazine is often presented as the inorganic analog of benzene, that is, borazine has almost the same colligative properties as benzene.

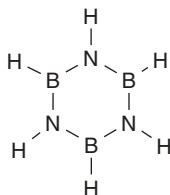
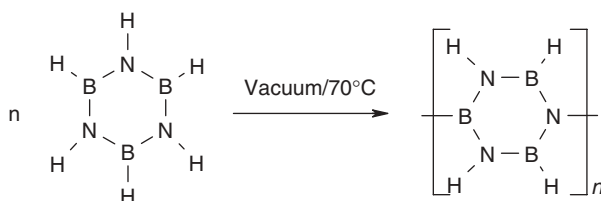


Figure 1

There is a great deal of potential interest in borazine as a precursor of boron nitride, since it offers the advantages of being a single source of boron and nitrogen with the correct B/N ratio and a high ceramic yield. In addition, borazine contains the elementary BN building block as its substituted derivatives. This is described later.

Borazine exhibits high reactivity and volatility at room temperature; however, there have been only a few attempts to prepare preceramic polymers from this compound. In the early 1990s, Sneddon et al. found that simply heating liquid borazine

*in vacuo* at a moderate temperature leads to a polyborazylene polymer analogous to organic polyphenylene (scheme 1).<sup>14-16</sup> The reaction involved dehydrocoupling of B—H and N—H moieties. This formed B—N linkages between the rings, thereby giving rather complex polymeric structures with linear, branched, cross-linked, and fused-rings portions, as supported by the empirical formula of the purified material, that is,  $B_{3.1}N_{3.0}H_{2.7}$ .



Scheme 1

From these data, it appears the polymer consists mainly of randomly arranged biphenyl-type and naphthalene-type dimeric units. These units appear to be related to the fragments found in polyphenylenes by taking into account that two oligomeric intermediates, 1,2'-diborazine ( $1,2'-[B_3N_3H_5]_2$ ) (Fig. 2a), and borazanaphthalene, ( $B_5N_5H_8$ ) (Fig. 2b), formed during the polymerization. The compounds have been isolated and characterized.

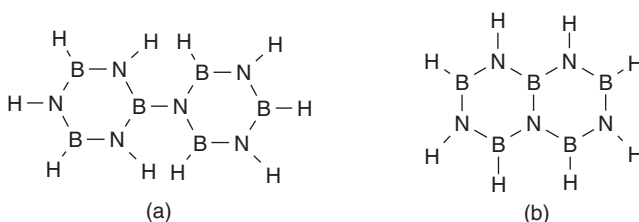


Figure 2

The formation of borazanaphthalene (Fig. 2b) implies that another mechanism occurs beside dehydropolymerization. This suggests that a ring-opening occurred, followed by formation of the bicyclic structure, as is detailed in the following.<sup>17,18</sup> Babonneau et al. have reexamined the structure of polyborazylene by  $^{11}B$  and  $^{15}N$  solid-state nuclear magnetic resonance (NMR) studies in the light of *ab initio* calculations.<sup>19</sup> They have determined that the polymer contains only two kinds of B sites ( $BHN_2$  and  $BN_3$ ) and two types of N sites ( $NHB_2$  and  $NB_3$ ) sites. This is consistent with the proposed fragments depicted in Figure 2(a) and 2(b). They also suggested that eight-membered ring structures (Fig. 3) coexist with the six-membered

borazine rings, although the exact structure of the polymer has not been established. However, the polymer is soluble in polar solvents such as glyme and tetrahydrofuran (THF), and can be purified as a powder by precipitation from pentane. An effort was made to determine the molecular weights and typical values are in the ranges 500–900 and 3000–8000 ( $M_n$  and  $M_w$ ).

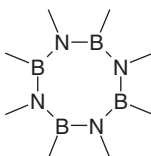


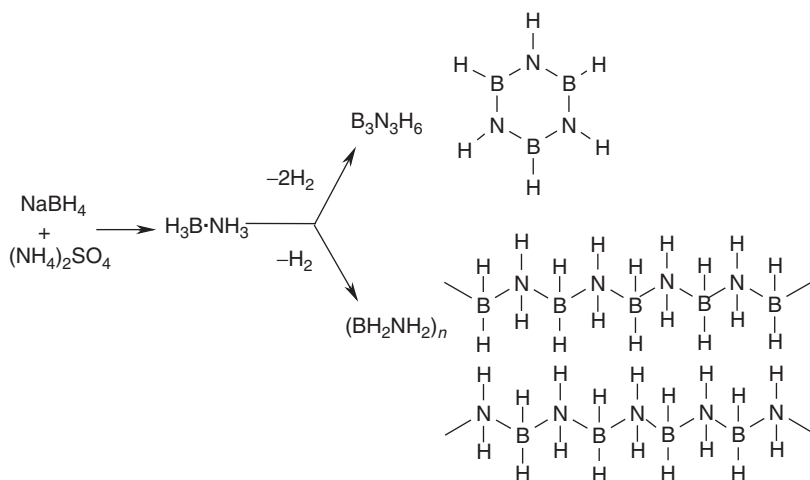
Figure 3

Polyborazylenes can be applied as coatings from solutions because of their solubility. In contrast, the latent reactivity of B—H and N—H fragments at relatively low temperatures results in cross-linking reactions prior to melting, which increases high polymer-chain entanglement and limits access to complex boron nitride structures through melt processing.

Following the general synthesis procedure reported by Sneddon et al.<sup>14–16</sup> (scheme 1), Economy and Kim<sup>20</sup> have proposed an alternative synthesis route to prepare more tractable polyborazylenes. Their objective was to develop a polymer with low viscosity that allows the preparation of BN matrices by an impregnation technique for carbon fiber–reinforced composite materials. In contrast to the synthetic procedure reported by Sneddon et al.,<sup>14–16</sup> they have performed the thermolysis of the borazine in a nitrogen atmosphere to 70°C for 40 hours. The as-obtained viscous polymer displayed a different chemical composition ( $B_{3.0}N_{3.6}H_{3.7}$ ), and could readily wet carbon fibers. In another paper,<sup>21</sup> these authors prepared the first inorganic mesophase, starting from borazine. First, they prepared a borazine-based polymer using the same thermolysis conditions. They showed consistently that the major components of this polymer are biphenyl-like and naphthalene-like. Then they applied a low-temperature treatment between 0 and 5°C, and obtained optically anisotropic mesophases similar to those derived from carbon pitch. In this process, the second low-temperature treatment is probably insufficient to produce polymerization; however, it did yield oligomers that maintained a certain mobility, thereby allowing molecular reorganization.

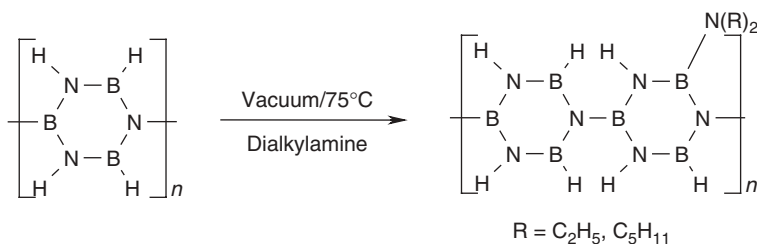
Conversely, Kim's group together with Babonneau's group<sup>22</sup> reinvestigated the products obtained from the reaction of  $NaBH_4/(NH_4)_2SO_4$  in tetraglyme, which was already known to form borazine.<sup>13</sup> They isolated poly(aminoborane)  $(NH_2BH_2)_x$  in a 5% yield during this reaction in addition to borazine  $H_3B_3N_3H_3$  (scheme 2). Dehydrogenation reactions between the chains subsequently gave fused-ring structures at higher temperatures than boron nitride.

Since the initial cross-linking reactions do not permit applications requiring a thermoplastic polymer, further studies have been devoted to the control of the dehydrocoupling reaction, in particular between the already established chains. For this purpose, Sneddon et al. demonstrated that the preparation of dialkylamine-modified



Scheme 2

polyborazylenes was an interesting strategy.<sup>23,24</sup> This novel method consisted of reducing the number of reactive B—H and/or N—H sites by grafting suitable substituents on the ring, since polyborazylene had been shown to react readily with dialkylamines. Under typical reaction conditions, both reagents were dissolved in glyme and heated at  $75^\circ\text{C}$  under vacuum (scheme 3). The resulting amine-modified polyborazylene exhibited interring B—N bonds with pendent amines. These bonds are formed by dehydrocoupling reactions of the amine N—H units and borazine B—H units, leading to the polyborazylene without destroying the borazine rings. The processability of the resulting modified polyborazylene was clearly demonstrated.

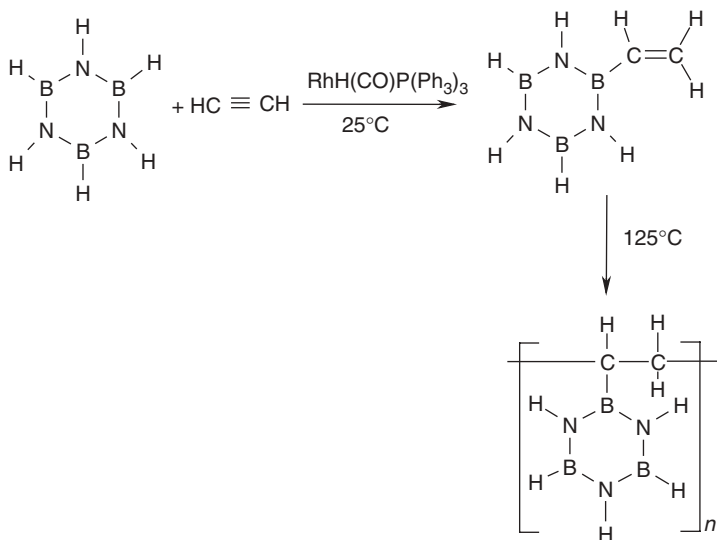


Scheme 3

The best results were obtained with dipentylamine-modified polyborazylenes. The dipentylamino substituents limit the extent of cross-linking during thermolysis. As a consequence, dipentylamine-modified polyborazylene was soluble in hydrocarbons

and, interestingly, melted above 75°C without evolution. Consistently, thermal analysis (differential scanning calorimetry) of a typically prepared polymer showed that the glass-transition temperature ( $T_g$ ) was below the cross-linking temperature, in contrast to what was observed with polyborazylene. It was concluded that the dipentylamino groups act as plasticizers, thereby lowering the glass-transition temperature of polyborazylene and rendering the polymer more tractable when heated at a sufficient temperature.

In a different approach, the same group drew inspiration from the widespread utilization of  $\text{RhH}(\text{CO})(\text{PPh}_3)_3$  as catalyst for reactions involving olefins. Numerous reactions of borazine with several olefins leading to mono-, di-, and tri-*B*-alkylborazines have been reported.<sup>25,26</sup> Among them, the formation of *B*-vinylborazine, 2-( $\text{CH}_2=\text{CH}$ )- $\text{B}_3\text{N}_3\text{H}_5$ , is of particular interest, since it can be polymerized at 125°C to yield a poly-*B*-vinylborazine homopolymer analogous to polystyrene (scheme 4).<sup>27</sup> However, this polymer is insoluble, and only the addition of excess borazine during the reaction at 125°C produced soluble polymers.



Scheme 4

The same authors proposed an alternative methods for obtaining soluble poly(*B*-vinylborazine) homopolymers and poly(styrene-*co*-*B*-vinylborazine) copolymers.<sup>28</sup> In fact, gentle polymerization conditions in solution at 80°C using Azobisisobutyronitrile (AIBN) (1.6 mol%) as an initiator provided soluble homopolymers. The polymer displays typical  $M_w$  and  $M_n$  values of ~18,000 and 11,000, respectively, whereas an increase in the AIBN concentration results in a decrease in the molecular weight, contrary to what is usually observed in free-radical polymerization.

This feature can be explained by intermolecular chain transfer, giving branched macromolecules with high molecular weight or by the occurrence of dehydrocoupling cross-linking reactions, such as described previously for polyborazylene (scheme 1).

The copolymers were obtained following this method by exploiting the similarity of *B*-vinylborazine and styrene. Several poly(styrene-*co*-*B*-vinylborazine) copolymers soluble in ethers were formed in solution at 80°C using AIBN.<sup>28</sup>

#### IV. POLYMERS DERIVED FROM *B*-CHLOROBORAZINE

A second variety of BN preceramic polymer, for example, poly[*B*-aminoborazine] prepared from borazine was studied and described previously. The resulting polymers are composed of  $B_3N_3$  rings linked mainly through nitrogen-bonded groups, for example, —NR— or —NH—. Such polymers can be synthesized starting either from aminoborane or *B*-chloroborazine. The use of aminoborane is described in the following section. An outline of typical methods, which involve the use of *B*-chloroborazines as a source of poly(*B*-alkylaminoborazines), is given here. Within this context, most researchers interested in materials chemistry focus their attention on the use of 2,4,6-trichloroborazine (Fig. 4).

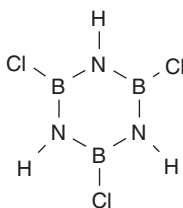


Figure 4

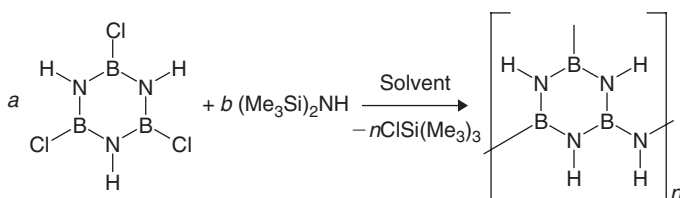
Two chemical approaches that involve nucleophilic substitution of the chlorine atoms attached to boron with linking reagents are reported in the literature. In both methods, the driving force is the formation of a stable by-product or one that can easily be stabilized. These substances contain chlorine. They can be distinguished by the number of steps, either one or two, required for preparing the polymer, starting from *B*-chloroborazine.

##### A. Poly(*B*-amino)borazines Prepared in a One-Step Process

These one-step reactions display the following characteristics: (1) the nitrogen-containing linking reagent is reactive at a relatively low temperature, (2) the reagents should be mixed carefully with the *B*-chloroborazine in such a way as to prevent the

statistical substitution of all the chlorine atoms of the *B*-chloroborazine in a monomeric molecule, and (3) the condensation coproduct should be stable. Furthermore, the chemical process should be mild since the linking species is very reactive and, a priori, well suited for the preparation of a low cross-linked polymer.

Paciorek et al. have investigated the direct formation of a polymer from the reaction of 2,4,6-trichloroborazine and hexamethyldisilazane.<sup>29,30</sup> This one-step synthetic procedure also has been studied by Paine et al.<sup>31</sup> The reaction in principle is depicted in scheme 5, and its main interest is that the driving force is the formation of stable and volatile  $\text{Me}_3\text{SiCl}$ .



Scheme 5

The earliest successful efforts to prepare poly[*B*-aminoborazine] according to this procedure are those made by Paine et al.<sup>31</sup> In that work, 2,4,6-trichloroborazine is cooled at  $-78^\circ\text{C}$ . Then hexamethyldisilazane is added. The mixture is allowed to warm slowly to  $25^\circ\text{C}$ . The stoichiometry of the reactions is  $a = (n + 2)$  and  $b = (3n + 4)/2$ , which corresponds to a lack of hexamethyldisilazane compared to the number of equivalents of chlorine atoms (scheme 5). Thus, polymerization is favored to the detriment of the formation of individualized completely substituted molecules. On the basis of model reactions of  $(\text{Me}_3\text{Si})_2\text{NH}$  with B— and N—, partly substituted borazines with unreactive groups yield a highly three-dimensional (3D) cross-linked polymer gel. The formula of this polymeric gel is  $\text{BN}_{1.49}\text{Cl}_{0.06}\text{Si}_{0.09}$ , which is consistent with the presence of  $-\text{HNSiMe}_3$  and Cl end groups. Paciorek et al. have also used the same general procedure under modified conditions.<sup>29,30</sup> In the latter case, 2,4,6-trichloroborazine was added to a hexamethyldisilazane solution at  $-35^\circ\text{C}$ . The stoichiometry of this reaction is  $a = 5$  and  $b = 11$ ; for example, compared to chlorine a slight excess of silazane is used. This leads to a trimethylsilylamino-substituted oligomer comprising five monomeric units ( $n = 5$ ; scheme 5). These authors postulated that the reaction conditions and the order of addition of the reagents control the nature of the polymer formed. The proposed structure is supported by the  $^1\text{H}$  NMR spectra and elemental analysis data, the latter confirming the absence of residual chlorine. This polymer is soluble in pentane, hexane, and benzene even though it is infusible. This suggests that the structure is, in fact, cross-linked.

In order to increase the organic solvent solubility of the polymers formed by reaction of 2,4,6-trichloroborazine with a disilazane, Paine et al. proposed the selective use of alkyl-substituted *B*-chloroborazines as monomers.<sup>32</sup> These polymers are intended for materials applications, where the methyl substituent is used to ensure

high potential ceramic yield. The reaction of 1,2,3,5-tetramethyl-4,6-dichloroborazine and heptamethyldisilazane led to a polymer, that is represented in Figure 5a.<sup>32</sup> This polymer, called a “two-point polymer,” is based on the number of reactive sites and is soluble in organic solvents. It resembles polymers described by Meller et al.<sup>33</sup> that were obtained from 1,2,3,5-tetramethyl-4,6-dichloroborazine and hexamethyldisilazane. A similar reaction involving 1,3,5-trimethyl-2,4,6-trichloroborazine and hexamethyldisilazane led to a gel insoluble in organic solvents (Fig. 5b).<sup>32</sup> Based on this information, it appears that the cross-linking of the polymers is the prevailing parameter to control in order to prepare a soluble material.

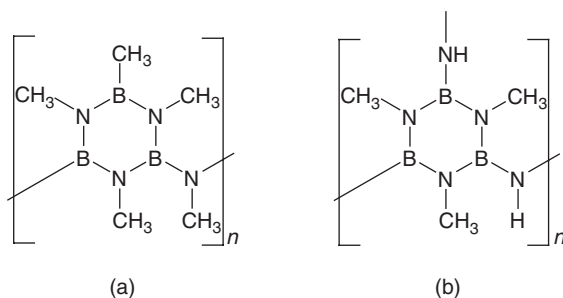
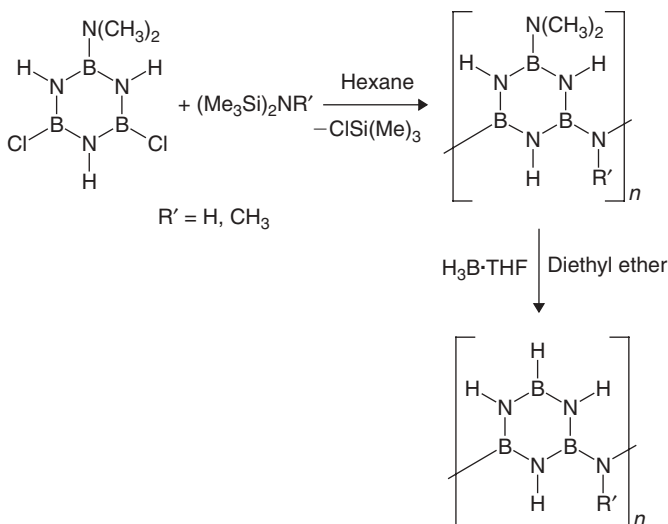


**Figure 5**

Following these studies, the same authors have reported that the combination of 6-dimethylamino-2,4-dichloroborazine and a disilazane yields “two-points polymers” (scheme 6).<sup>34</sup> Depending on the solvent used and the reaction conditions, the as-prepared polymer is recovered as a gel or as a solid with a low solubility. Subsequently, it is possible to remove the dimethylamino protecting group by the action



**Scheme 6**

of  $\text{H}_3\text{B} \cdot \text{THF}$ . The reaction performed on the gel in chlorobenzene at room temperature leads to a polymer containing a small quantity of carbon (<4%).

### B. Poly(*B*-borylamino)borazines Prepared in a One-Step Process

These studies were stimulated to search for an ideal polymeric precursor for the elaboration of BN fibers based on the conceptual relationship between graphite and hexagonal boron nitride described by Wynne and Rice.<sup>7</sup> In this 1984 paper, the authors summarized structures that should be the best polymers for this application. Indeed, they suggested that six-membered rings were needed to avoid the reverse reaction. Such rings are already the basal units of the polymers presented in this chapter. They are linked through 2 to 5 atom-bridges (to decrease rigidity) and represent the best compromise between ceramic yield and viscoelastic properties optimized for melt-shaping and melt-spinning operations (Fig. 6).

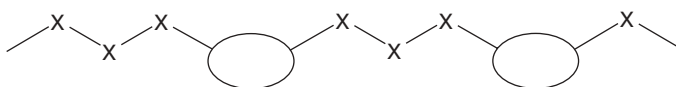
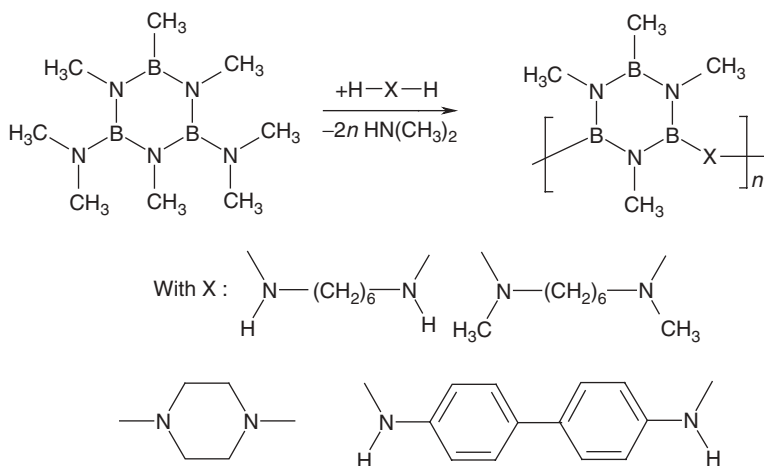


Figure 6

Even though the rheology of inorganic polymers is extremely complex, Wynne and Rice posed a worthy scientific challenge: How does one increase the length of the bridge (i.e., spacer) between the borazine rings in BN polymeric precursors? The first answer was given 37 years ago by Clement and Proux.<sup>35</sup> These authors demonstrated transamination reactions that permit conversion of *B*-tri(dimethyl)-*N*-trimethylborazine to various polymers exhibiting larger ring spacings compared to polyborazines derived from *B*-trialkylaminoborane or *B*-(trialkylamino)borazine (scheme 7). To our knowledge,



Scheme 7

these derivatives represent the first examples of borazine-derived polymers with several atoms bridges between the rings. The main drawback is that these species incorporate carbon atoms into the backbone, which drastically reduces their interest as BN precursors.

With this in mind, we have proposed an improvement on the Wynne and Rice<sup>7</sup> model, with the objective of designing an ideal polymeric precursor for melt drawing of BN fibers. The polymeric architecture that we were attempting to build, namely, poly(borylamino borazine), is depicted on Figure 7. According to the aforementioned assumptions, this structure can be considered ideal, since its “flexible” boron and nitrogen “spacers” correspond to the sequence found in hexagonal boron nitride ceramics.

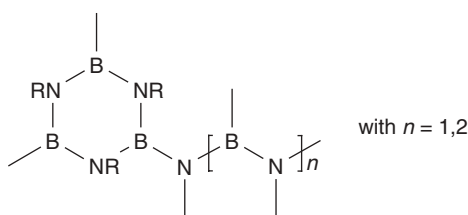
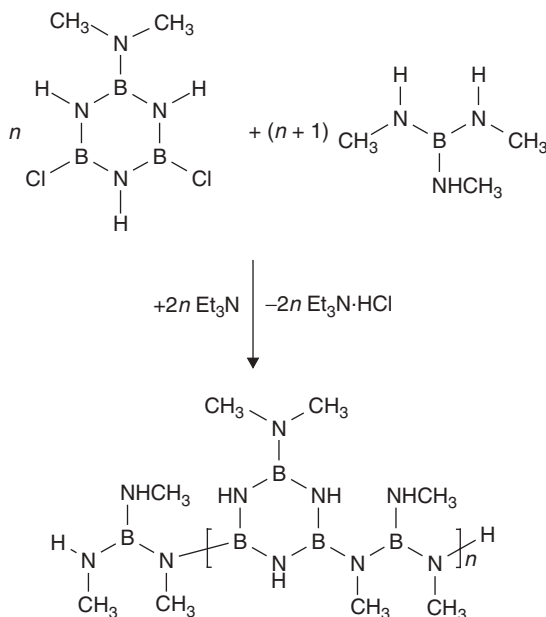


**Figure 7**

We chose the room temperature exchange reaction between chlorine and an aminoboryl group of *B*-chloroborazine with tris(alkylamino)borane. The synthesis is briefly described in the next section.<sup>36,37</sup> In order to reduce cross-linking in the resulting polymer structure and, therefore, potentially increase its melt-shaping ability, we started with 2-dimethylamino-4,6-dichloroborazine instead of 2,4,6-trichloroborazine. This is similar to the reactions forming polyborazines mentioned earlier. Conversely, tris(alkylamino)borane should have sufficient reactivity to perform condensation under mild conditions without competitive attack at sites other than B—Cl. In this respect, tris(methylamino)borane, B(NHCH<sub>3</sub>)<sub>3</sub>, is satisfactory and has the advantage of having the best ceramic yield in this family. Moreover, since no volatile leaving group is desired in this reaction, a tertiary amine (e.g., Et<sub>3</sub>N) must be added to precipitate the corresponding hydrochloride (e.g., Et<sub>3</sub>N·HCl). Although it is weakly bonded to the B<sub>3</sub>N<sub>3</sub> ring boron atom, the dimethylamino substituent cannot be replaced by B(NHR)<sub>2</sub>; therefore, it is retained during the reaction under mild conditions. In contrast, this dimethylamino group can be removed from boron ring atoms during the process following the monomer polymerization. After mixing 6-dimethylamino-2,4-dichloroborazine and tris(methylamino)borane, both in toluene solutions, the mixture is stirred at -10°C for 1 hour and at room temperature for 24 hours (scheme 8). When the reaction is complete, the poly(borylamino borazine), which remains soluble during the entire process, is easily isolated by filtration and solvent removal.

The proposed structure for the polymer is well supported by liquid state <sup>1</sup>H, <sup>13</sup>C, and <sup>11</sup>B NMR data and elemental analysis. The formula, BN<sub>1.6</sub>C<sub>1.5</sub>H<sub>3.5</sub>, is consistent with the theoretical N/B ratio of 1.7. Since no chlorine is detected in the product, the terminating groups are mainly borylamino, —N(CH<sub>3</sub>)B(NHCH<sub>3</sub>)<sub>2</sub>, groups.

Clearly, branching chains containing other borazine units on the free aminoboryl site cannot be excluded, even though such chains are difficult to obtain because of steric hindrance. Nevertheless, a structure that is consistent with the characterization data is proposed in scheme 8.



Scheme 8

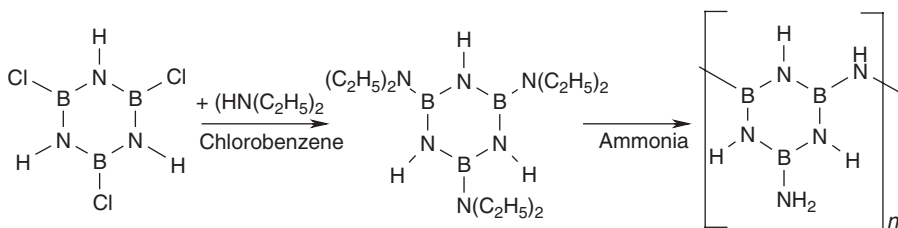
Thus, the main advantage of this one-step technique is that a judicious choice of chemicals and reaction conditions allows the formation of a poly(borylamino)borazine that displays only three-atom bridges, that is,  $-\text{N}-\text{B}-\text{N}-$ , between the rings. This polymer fulfills the Wynne and Rice criteria<sup>7</sup> about the nature of the backbone and the length of the bridge between the rings. Furthermore, the material has an extremely low glass-transition temperature,  $T_g = 20^\circ\text{C}$ , compared to values generally reported for polyborazines ( $\sim 30^\circ\text{C}$  higher), which strongly supports a low degree of cross-linking relative to the two-point polymer structure.

### C. Poly(*B*-amino)borazines Prepared in a Two-Step Process

Two-step synthetic routes to poly(*B*-aminoborazines) from *B*-chloroborazines involve initial nucleophilic reaction of the *B*-chloroborazine with appropriate linking reagents followed by a deamination reaction of the as-obtained *B*-aminoborazine. The *B*-trichloroborazine undergoes nucleophilic attack by ammonia or amine derivatives on the boron atom linked to chlorine atoms. For the same reasons previously quoted, a tertiary amine (e.g.,  $\text{Et}_3\text{N}$ ) must be added to precipitate the corresponding hydrochloride.

The *B*-aminoborazines that are formed display amino groups as linking agents and can be subsequently polymerized by deamination at moderate temperatures to generate poly[*B*-aminoborazine] with borazinic rings connected through the nitrogen-bonded H ( $-\text{NH}$ ) or the organic group ( $-\text{NR}$ ). Pioneering work in this area was the two-step preparation of *B*-aminoborazine-type polymers, which was accomplished in the late 1950s by Lappert.<sup>38</sup> However, this work did not consider precursors to BN materials in the same way as other early studies.<sup>39,40</sup> Moreover, several polyborazines were developed following the same approach during the 1960s. However, these polymers probably never found practical outlets, because they were not correctly characterized due to a lack of solubility.

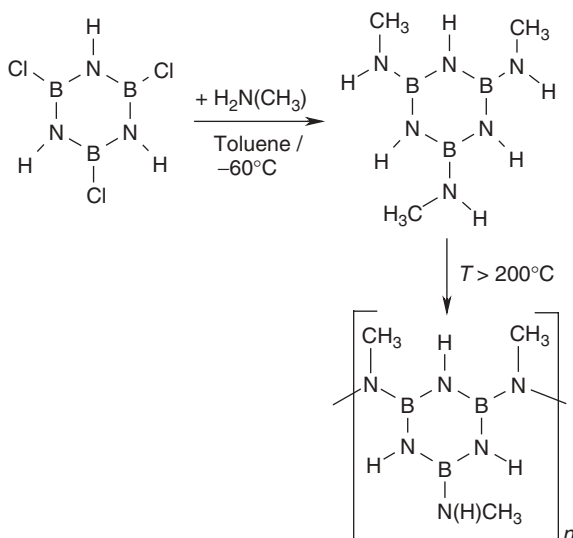
As early as the 1970s, research aimed at the fabrication of boron nitride fibers from polymeric precursors stimulated an increasing number of studies devoted to poly[*B*-amino]borazines. The first report<sup>41</sup> concerned the exchange of 2,4,6-trichloroborazine chlorine atoms by a dialkylamino group,  $-\text{NR}_2$ . Since the tri(dialkylamino)borazines that were prepared did not undergo deamination at modest temperatures, a further treatment with excess ammonia was needed to assure polymerization. Actually, this ammonolysis process involved the exchange of  $-\text{NR}_2$  groups with  $-\text{NH}_2$  groups and a nearly simultaneous polycondensation of the resulting triaminoborazine owing to its extremely high reactivity. Thus, Tanigushi et al. have used this technique to prepare the first boron nitride fibers from a melt-spinnable poly[*B*-aminoborazine] (scheme 9).<sup>41</sup>



Scheme 9

Following a similar approach starting from *B*-trichloroborazine, Kimura et al.<sup>42</sup> as well as Paine et al.<sup>43</sup> have reported the ammonolysis of *B*-trialkylaminoborazine ( $\text{R} = \text{C}_2\text{H}_5$ ,<sup>42</sup>  $\text{CH}_3$ <sup>43</sup>) followed by thermolysis to obtain untractable polymers composed of bridged units ( $-\text{N}(\text{H})-$ ) and fused rings (naphthalene-type units). The former segments are formed by a condensation reaction, while the latter are presumably formed by borazine ring-opening pathways, such as that shown in scheme 9.

To limit the number of steps, Kimura et al. used methylamine as a linking reagent.<sup>44</sup> Actually, the reaction of methylamine  $\text{CH}_3\text{NH}_2$  with 2,4,6-trichloroborazine followed by self-condensation of the resulting 2,4,6-(trimethylamino)borazine, leads relatively easily to the poly[*B*-(trimethylamino)borazine] above  $200^\circ\text{C}$  in a nitrogen atmosphere (scheme 10). Infusible polymers are produced by an important chain entanglement through  $-\text{N}(\text{CH}_3)-$  bridges.

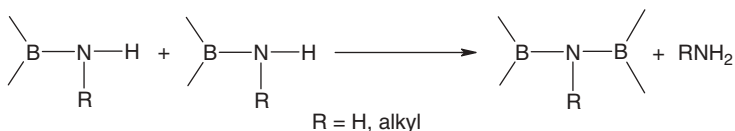


Scheme 10

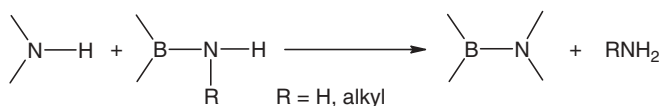
Kimura et al. also proposed a solution to lower cross-linking during thermolysis by making a cocondensate of 2,4,6-trimethylaminoborazine and laurylamine ( $\text{C}_{12}\text{H}_{25}\text{NH}_2$ ).<sup>45</sup> Since the reactivity of an alkylamino group attached to the borazinic boron atom decreases when its steric bulkiness increases, the large laurylamino substituent is less reactive toward thermal condensation. It also serves as a plasticizer through the long alkyl chain. The polymeric structure proposed in this chapter is in accordance with the  $^1\text{H}$  NMR data. The polyborazine that is obtained melts at  $200^\circ\text{C}$  and has a molecular weights  $M_n$  in the 400–800 range. This material can be melt spun at  $160\text{--}170^\circ\text{C}$  using an extruder.

Extending these studies, we have reexamined the synthesis of poly(*B*-trimethylaminoborazines) obtained by thermolysis of the 2,4,6-trimethylaminoborazine without the addition of other compounds.<sup>46</sup> A series of melt-spinnable poly [*B*-trimethylaminoborazines] have been synthesized by self-condensation of 2,4,6-trimethylaminoborazine at different thermolysis temperatures in an argon atmosphere. The main objective of this study was to determine correlations between the polymer structure and the polymers' melt-spinning ability. First, we demonstrated that self-condensation of 2,4,6-trimethylaminoborazine does not take place in an unequivocal fashion by formation of the well-known  $\text{---N}(\text{CH}_3)\text{---}$  bridges. By examining the  $^{11}\text{B}$ ,  $^{13}\text{C}$ , and  $^{15}\text{N}$  solid-state NMR spectra, the presence of direct interring  $\text{B---N}$  bonds was revealed. These interring bonds were present in very low quantities compared to a majority of  $\text{---N}(\text{CH}_3)\text{---}$  bridges between the rings. Obviously, terminal  $\text{---N}(\text{H})\text{CH}_3$  groups were also observed.<sup>47</sup> Bridging units were initially suggested by Lappert<sup>38</sup> in the preparation of polymers in which borazinic rings were linked by amino groups ( $\text{---N}(\text{R})\text{---}$ ) (scheme 11), whereas  $\text{NB}_3\text{---}$  containing motifs, for example, extraring

B—N bonds, were initially proposed by Gerrard et al.<sup>48</sup> and have been demonstrated by Paciorek et al.(scheme 12).<sup>18</sup>



Scheme 11



Scheme 12

Using gas chromatography/mass spectrometry (GC/MS) data allowed us to propose a structure of a typical melt-spinnable poly[*B*-trimethylaminoborazine] ( $[\text{BN}_{1.5}\text{C}_{0.67}\text{H}_{3.17}]$ ,  $T_{\text{synthesis}} = 180^\circ\text{C}$ ) (Fig. 8). It has been shown that —N(CH<sub>3</sub>)— bridges provide flexibility, while the —N(H)CH<sub>3</sub> end groups act as a plasticizer to provide a tractable polymer upon heating at a moderate temperature. The proportion of bridging units and methylamino end groups decreases upon heating above 195°C. This decreases interring B—N bonds, and melt spinnability is reduced.<sup>47</sup> Surprisingly, bridging —N(H)— units and/or —NH<sub>2</sub> end units are present in a low proportion in such systems. Therefore, the only likely pathway to explain this occurrence is a ring-opening rearrangement during thermolysis and the self-condensation of *B*-(trianilino)borazine. This was suggested by Toeniskoetter and Hall<sup>17</sup> and confirmed by Paciorek et al.<sup>18</sup> These authors have also described a series of concurrent

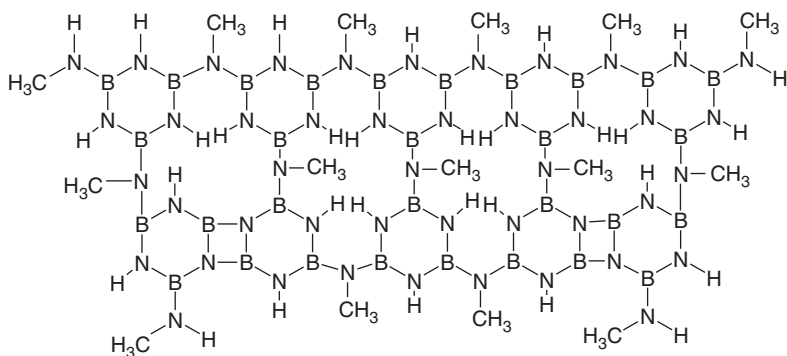
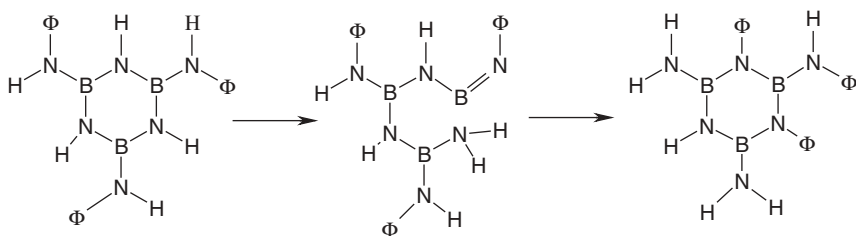


Figure 8

thermolysis mechanisms yielding a poly [*B*-(trianilino)borazine], in which ring-opening pathways (scheme 13) proceed according to this mechanism.



Scheme 13

The possibility of controlling the structure through thermal condensation of *B*-triaminoborazines is of crucial importance in designing and developing polymeric precursors for advanced ceramics. Therefore, we have studied the thermal polycondensation of a series of *B*-trialkylaminoborazines using various alkylamino linking reagents.<sup>49</sup> Interestingly, a detailed picture of both the thermolysis mechanism and the role of bonds that compose poly(*B*-alkylaminoborazines) on the degree of cross-linking, and processability can be provided by synthesizing model asymmetric *B*-alkylaminoborazines. Inspired by the early work of Beachley in the 1970s,<sup>50</sup> we have developed a two-step nucleophilic reaction route using 2,4,6-trichloroborazine with different mono- and diamino derivatives that yield compounds 1–3.<sup>51</sup> Comparison was made with the symmetric *B*-trimethylaminoborazine 4, which provided melt-spinnable polymers as previously described (Fig. 9).

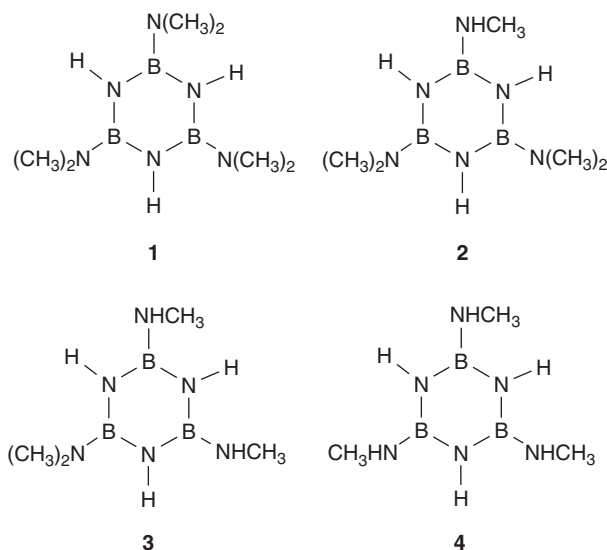
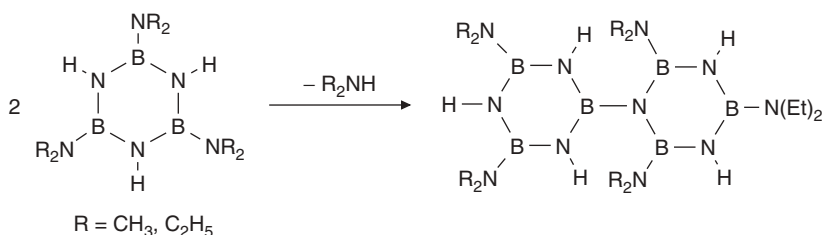


Figure 9

In accordance with Gerrard's observations,<sup>48</sup> when dialkylamino groups ( $R = \text{CH}_3, \text{C}_2\text{H}_5$ ) are attached to the boron atoms in 2,4,6-tri(dialkylamino)borazines only the corresponding dialkylamines,  $(\text{HN}(\text{CH}_3)_2)$  and  $(\text{HN}(\text{C}_2\text{H}_5)_2)$ , are evolved during self-condensation under argon, as evidenced by GC/MS. This is consistent with a mechanism where direct interring B—N bonds are formed exclusively (scheme 14).<sup>51</sup> Compared to the condensation of monoalkylamino analogs, this reaction is more difficult to achieve. This agrees with previous work.<sup>49</sup>



Scheme 14

During the thermal self-condensation of *B*-alkylaminoborazines **2** and **3** in an argon atmosphere, both  $\text{CH}_3\text{NH}_2$  and  $(\text{CH}_3)_2\text{NH}$  were evolved with the establishment of  $-\text{N}(\text{CH}_3)-$  bridge units as well as direct B—N bonds in the related polymer. This indicates a competition between the different reaction mechanisms (schemes 11 and 13). In both cases, the elimination of  $(\text{CH}_3)_2\text{NH}$  increases as the proportion of  $-\text{N}(\text{CH}_3)_2$  substituents on the monomer. A higher portion of bridging units decreases elimination of  $(\text{CH}_3)_2\text{NH}$  in agreement with the fact that a secondary amine is displaced more easily than a primary amine. This is observed going from polymers derived from **4** to **1**. These polymers are characterized by glass-transition temperatures in the range 45–60°C. Consistently, their molecular weights  $M_w$  are in the 500 to 900 range, which corresponds to oligomeric chains of 4 to 6 borazine rings.

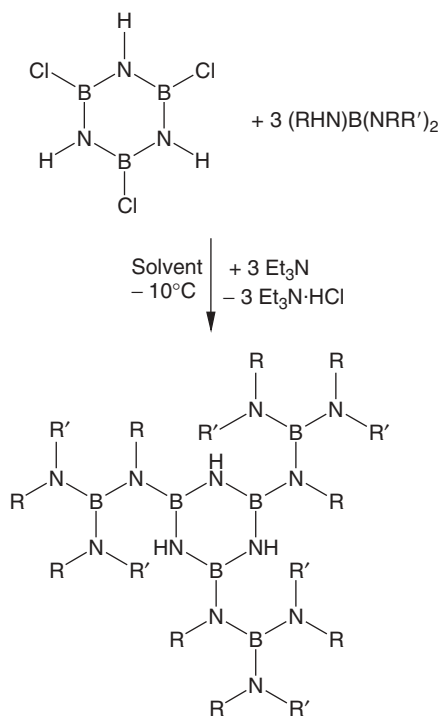
Conversely, we have also confirmed that the presence of bridge-type bonds in poly(*B*-alkylaminoborazines) confer flexibility and improve processability, thus leading to the conclusion that melt spinnability increases going from polymers derived from **1** to polymers derived from **4**.

#### D. Poly(*B*-borylamino)borazines Prepared in a Two-Step Process

By analogy with *B*-trialkylaminoborazine and polyborazine derived therefrom, the first route envisioned to poly(borylamino)borazine was the thermal condensation of molecular precursors under a convenient atmosphere. As detailed earlier the innovative idea behind this procedure is to tailor the polymeric precursor structure by increasing the distance between the two borazinic rings. For that purpose, we explored

the chemistry of a new class of 2,4,6-trialkylaminoborazines in which the alkylamino,  $-\text{N}(\text{H})\text{R}$ , groups born by the boron atoms of the  $\text{B}_3\text{N}_3$  rings incorporate boron atoms. As mentioned previously, 2,4,6-trialkylaminoborazines,  $(\text{NHR})\text{B}_3\text{N}_3\text{H}_3$ , can be easily prepared from the reaction of 2,4,6-trichloroborazine,  $\text{Cl}_3\text{B}_3\text{N}_3\text{H}_3$ , with a molar excess of the corresponding alkylamine,  $\text{RNH}_2$ . Both trisalkylaminoborane,  $\text{B}(\text{NHR})_3$ , and dialkylaminoborylamine,  $[(\text{RHN})_2\text{B}]\text{NH}$ , can play the role of the amine in the reaction pathway to generate the structure depicted in Figure 6. The chemistry and synthetic accessibility of *B*-trialkylaminoboranes are much easier than that of diborylamine derivatives. Therefore, we exclusively focused our attention on tris(alkylamino)boranes.

As a starting point, we examined the chemistry of borylborazine derivatives consisting of a  $\text{B}_3\text{N}_3$  core surrounded by three aminoboryl groups. As expected, this compound can be easily obtained from the reaction of  $\text{Cl}_3\text{B}_3\text{N}_3\text{H}_3$  with symmetric or asymmetric trialkylaminoboranes,  $(\text{R}(\text{H})\text{N})\text{B}(\text{NRR}')_2$  (with  $\text{R} = \text{alkyl}$ ,  $\text{R}' = \text{H}$  or alkyl) in a 1:3 molar ratio. A tertiary amine (e.g.,  $\text{Et}_3\text{N}$ ) was also present to precipitate the corresponding amine hydrochloride.<sup>51</sup> The general scheme to synthesize borylaminoborazines is depicted in scheme 15. It is important to note that this reaction must be run at a low temperature ( $-10^\circ\text{C}$ ) to avoid self-condensation of the aminoborane.<sup>52</sup>

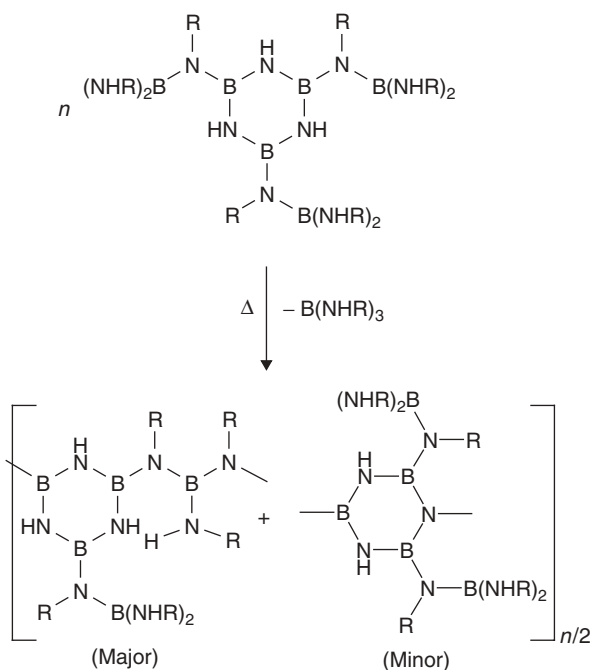


Scheme 15

The borylborazine is collected as a viscous liquid or a solid depending on the nature of the alkyl group. It can be prepared in quantitative yield due to the high reactivity of the B—Cl groups toward primary and secondary amines.

The second step is the thermal conversion of borylaminoborazine into poly(borylaminoborazine). Continuous elimination of parent alkylamine is the main by-product during the thermal polycondensation of 2,4,6-trialkylaminoborazine (see earlier). We expected the continuous elimination of the starting *B*-alkylaminoborane during the thermal polycondensation of borylborazine. However, the alkylaminoborane is a liquid, which requires that the thermal polycondensation must be performed *in vacuo* to continuously remove the evolving B(NHR)<sub>3</sub> from the reaction mixture. This procedure also precludes any competing polycondensation reaction from B(NHR)<sub>3</sub>.

As expected, borylaminoborazines behave like 2,4,6-trialkylaminoborazines. Two competitive mechanisms occurred during the thermal condensation *in vacuo*: the formation of direct B—N bonds between two borazinic rings and the formation of three-atom bridges of the —N—B—N— type between two rings (scheme 16).<sup>53</sup> Similar to the case of 2,4,6-trialkylaminoborazines, the latter linkage mechanism predominates according to liquid and solid-state NMR investigations.<sup>54</sup>



**Scheme 16**

Various molecular borylaminoborazinic derivatives of this type can be prepared by the synthetic pathway depicted earlier. Their polycondensation was realized and

the resulting polymers were characterized by multinuclei NMR analysis in particular.<sup>55</sup> From these data we propose an ideal polymeric structure for poly(borylamino-borazines) that are prepared by thermolysis of either symmetric methylated or isopropylated tri(borylamino)borazines (i.e.,  $[(\text{NHCH}_3)_2\text{B}(\text{NCH}_3)]_3\text{B}_3\text{N}_3\text{H}_3$  or  $[(\text{NHPr}^i)_2\text{B}(\text{NPr}^i)]_3\text{B}_3\text{N}_3\text{H}_3$ ; Fig. 10). The duration of the thermal polycondensation at 150°C was 1.5 hours for the former compound and 9 hours for the latter compound. This is consistent with their different reactivities. These polymers displayed interesting processability for fabrication of BN fibers, coatings, or matrices. In addition, we were able to determine the molecular structure of  $[(\text{NPr}^i)_2\text{B}(\text{NCH}_3)]_3\text{B}_3\text{N}_3\text{H}_3$  obtained from  $\text{Cl}_3\text{B}_3\text{N}_3\text{H}_3$  and the asymmetric alkylaminoborane,  $(\text{Pr}^i(\text{H})\text{N})\text{B}(\text{NPr}^i)_2$ , by single-crystal X-ray diffraction.<sup>56</sup>

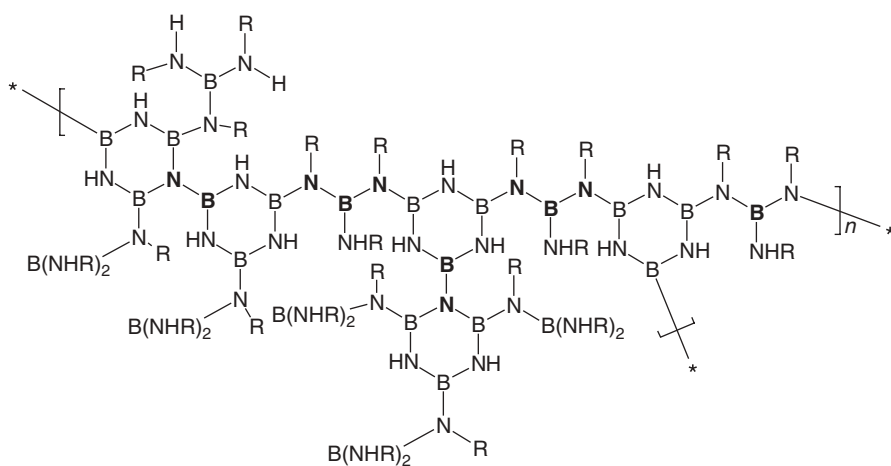
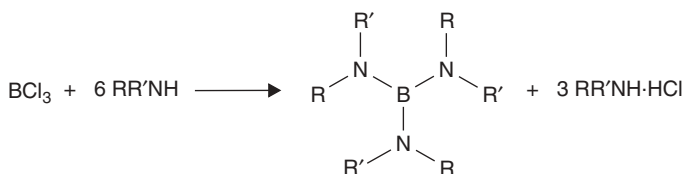


Figure 10

## V. POLYMERS DERIVED FROM TRIS(ALKYLAMINO)BORANES

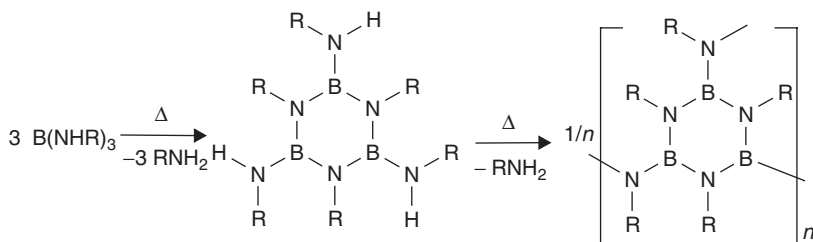
Tris(alkylamino)boranes,  $\text{B}(\text{NHR})_3$ , can be synthesized through a simple reaction involving boron trichloride and an excess of the corresponding primary alkylamine (scheme 17).<sup>57,58</sup> This reaction may also lead to alkylaminoborazines of



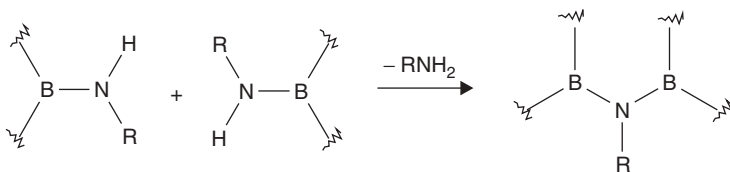
Scheme 17

formula  $(\text{RNBHR})_3$  as a side product. The amount of side products can be lowered by using both excess alkylamine and low-temperature reaction conditions. Thus, trisalkylaminoboranes can be obtained in high yield (60–70%) based on boron trichloride, which is the most expensive reagent.

Polymers can be prepared via a multistep thermal process. Heating tris(monoalkylamino)boranes,  $\text{B}(\text{NHR})_3$ , under reduced pressure or in an inert atmosphere, results in conversion to the corresponding *B*-(alkylamino)-*N*-(alkyl)borazine,  $[\text{R}(\text{H})\text{N}]_3\text{B}_3\text{N}_3\text{R}_3$ . The corresponding poly(alkylaminoborazine) is formed later (scheme 18). When the amine is bulky, the aminoborazine yield is low. The alkylamino— $\text{N}(\text{R})$ —bridges, which connect two neighboring boron atoms whether in rings or in tris(alkylamino)boryl fragments, are formed by elimination of alkylamine (scheme 19; similar to schemes 11 and 12). The main feature of alkylaminoborazines and poly(alkylaminoborazines) derived from tris(monoalkylamino)boranes is the fact that the borazine ring nitrogen atoms are bonded to alkyl groups.



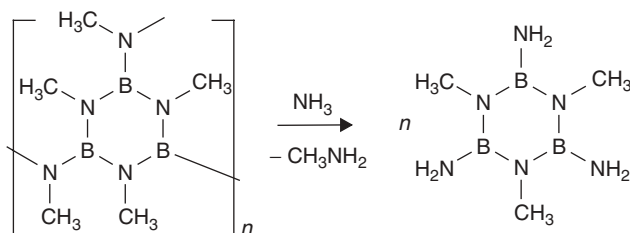
Scheme 18



Scheme 19

In order to evaluate the influence of the alkyl substituent's steric bulk on the polymerization, attention was focused on two derivatives: tris(methylamino)borane,  $\text{B}(\text{NHCH}_3)_3$ , and tris(isopropylamino)borane,  $\text{B}(\text{NHPr}^i)_3$ . Direct heating of  $\text{B}(\text{NHCH}_3)_3$  to  $180^\circ\text{C}$  under an argon flow leads to the formation of a thermoplastic polyborazine in a two-step process: 1,3,5-trimethyl-2,4,6-tri(methylamino)borazine is formed through deamination reactions, and it is subsequently converted to the polymer with borazine rings connected by  $-\text{N}(\text{CH}_3)-$  bridges (scheme 18;  $\text{R} = \text{CH}_3$ ).<sup>59</sup> Size exclusion chromatography gave an  $M_w$  value of  $\sim 900$  and differential scanning calorimetry (DSC) gave a glass-transition temperature of  $73^\circ\text{C}$ . Subsequent heating

at 80°C under ammonia provoked the partial decomposition of the poly(aminoborazine) to volatile 1,3,5-trimethyl-2,4,6-tri(amino)borazine and methylamine via a transamination reaction (scheme 20). By comparison,  $B(NHPr^i)_3$  exhibits very high thermal stability, which can be attributed to the steric bulk of the isopropylamino group. A small amount of thermal polymerization of this derivative occurs under an inert atmosphere up to 180°C, whereas most of the aminoborane is stripped off.<sup>60</sup>



Scheme 20

To achieve the goal of preparing pure boron nitride materials, polymerizations under an ammonia flow have been studied to displace the carbon-containing moieties from the polymers. An exchange of the  $-N(H)R$  group of  $B(NHR)_3$  for  $-NH_2$  of ammonia takes place, resulting in an unstable aminoborane  $B(NH_2)_3$ , which subsequently polymerizes. During the first step, a  $NH_2$  B-substituted borazine ( $HNBNH_2$ )<sub>3</sub> is obtained, which polycondenses very rapidly into a polymer based on borazine rings linked through  $-N(H)-$  bridges.<sup>61</sup> Obviously, the aminoborane reactivity toward ammonia depends on the nature of the amino group. The more bulky the amino group becomes, the more the exchange reaction is favored. For example, the exchange of the isopropylamino group occurred at room temperature in a 50% yield, whereas a temperature of at least 50°C is needed to initiate the methylamino group exchange in  $B(NHCH_3)_3$ .

## VI. SUMMARY

Owing to its unique set of properties, advanced boron nitride materials have a bright future. However, the design of new precursors should be developed by linking novel substituents to the borazinic monomers in order to introduce new kinds of linkages in the derived polymers. Developing novel bonding, with different stabilities and reactivities is crucial in synthesizing linear polymers with a controlled architecture.

Conversely, since a great many routes for precursor design are now known, improvements in the control of polymerization reactions will be essential. Studies should be directed to the accurate measurement of the molecular weights,  $M_n$  and  $M_w$ , of the inorganic polymers by using size-exclusion chromatography techniques.

This is not trivial because of the air and moisture sensitivity of these boron-based polymers. It will be necessary to mobilize people from different scientific communities to overcome this impediment. Methods must be developed to determine the rheological parameters of polymers during melt processing to generate complex shapes or fibers. Viscosity as a function of processing temperature and time should be investigated. In this specific area, advances will also come from complementary advances in materials science, rheology, and modeling.

## VII. REFERENCES

1. H. Steinberg, R. J. Brotherton, *Organoboron Chemistry*, Vol. 2, Wiley, New York, 1966.
2. W. Maringgele, *The Chemistry of Inorganic Homo- and Heterocycles*, Vol. 1, I. Haiduc, Ed., Academic Press, London, 1987.
3. M. F. Lappert, *Developments in Inorganic Polymer Chemistry*, M. F. Lappert, G. J. Leigh, Eds., p. 20, Elsevier, Amsterdam, 1962.
4. P. G. Chantrell, E. P. Popper, *Inorganic Polymers and Ceramics, Special Ceramics-4*, E. P. Popper, Ed., P. 87, Academic Press, New York, 1964.
5. S. Yajima, J. Hayashi, M. Omori, K. Okamura, *Nature*, **261**, 683 (1976).
6. Driggs, R. J. Shufford, R. W. Lewis, in *Handbook of Composites*, G. Lubin, Ed., Van Nostrand Reinhold, New York, 1982.
7. K. J. Wynne, R. W. Rice, *Annu. Rev. Mater. Sci.*, **14**, 297 (1984).
8. Y. D. Blum, K. B. Schwartz, R. M. Laine, *J. Mater. Sci.*, **24**, 1707 (1989).
9. D. Seyferth, *Transformation of Organometallics into Common and Exotic Materials: Design and Activation*, R. M. Laine, Ed., M. Nijhoff Publishers, P. 133, Dordrecht, The Netherlands, 1988.
10. R. T. Paine, C. K. Narula, *Chem. Rev.*, **90**, 73 (1990).
11. R. T. Paine, L. G. Sneddon, *Chemtech.*, **24**, 29 (1994).
12. A. Stock, E. Pohland, *Chem. Ber.*, **59B**, 2215 (1926).
13. T. Wideman, L. G. Sneddon, *Inorg. Chem.*, **34**, 1002 (1995).
14. P. J. Fazen, J. S. Beck, A. T. Lynch, E. E. Remsen, L. G. Sneddon, *Chem. Mater.*, **2**, 96 (1990).
15. P. J. Fazen, E. E. Remsen, L. G. Sneddon, *Polym. Preprints*, **32**, 544 (1991).
16. P. J. Fazen, E. E. Remsen, P. J. Carroll, J. S. Beck, L. G. Sneddon, *Chem. Mater.*, **7**, 1942 (1995).
17. R. H. Toeniskoetter, F. R. Hall, *Inorg. Chem.*, **2**, 29 (1963).
18. K. J. L. Paciorek, D. H. Harris, R. H. Kratzer, *J. Polym. Sci.*, **24**, 173 (1986).
19. C. Gervais, J. Maquet, F. Babonneau, C. Duriez, E. Framery, M. Vaultier, P. Florian, D. Massiot, *Chem. Mater.*, **13**, 1700 (2001); C. Gervais, E. Framery, C. Duriez, J. Maquet, M. Vaultier, F. Babonneau, *J. Eur. Ceram. Soc.*, **25**, 129 (2005).
20. D.-P. Kim, J. Economy, *Chem. Mater.*, **5**, 1216 (1993).
21. D.-P. Kim, J. Economy, *Chem. Mater.*, **6**, 395 (1994).
22. D.-P. Kim, K.-T. Moon, J.-G. Kho, J. Economy, Gervais, F. Babonneau, *Polym. Adv. Technol.*, **10**, 702 (1999).
23. T. Wideman, L. G. Sneddon, *Chem. Mater.*, **8**, 3 (1996).
24. T. Wideman, E. E. Remsen, E. Cortez, V. L. Chlanda, L. G. Sneddon, *Chem. Mater.*, **10**, 412 (1998).
25. A. T. Lynch, L. G. Sneddon, *J. Am. Chem. Soc.*, **109**, 5867 (1987).
26. P. J. Fazen, L. G. Sneddon, *Organometallics*, **13**, 2867 (1994).

27. A. T. Lynch, L. G. Sneddon, *J. Am. Chem. Soc.*, **111**, 6201 (1989).
28. K. Su, E. E. Remsen, H. M. Thompson, L. G. Sneddon, *Macromolecules*, **24**, 3760 (1991).
29. K. J. L. Paciorek, S. R. Masuda, R. H. Kratzer, *Chem. Mater.*, **3**, 88 (1991).
30. K. J. L. Paciorek, R. H. Kratzer, *Eur. J. Solid State Inorg. Chem.*, **29**, 101 (1992).
31. C. K. Narula, R. Schaeffer, R. T. Paine, *J. Am. Chem. Soc.*, **109**, 5556 (1987).
32. C. K. Narula, D. A. Lindquist, M.-M. Fan, T. T. Borek, Z. N. Duesler, A. K. Datye, R. Schaeffer, R. T. Paine, *Chem. Mater.*, **2**, 377 (1990).
33. A. Meller, H. J. Z. Füllgrabe, *Naturforsch. B*, **33B**, 156 (1978).
34. C. K. Narula, R. Schaeffer, A. K. Datye, T. T. Borek, B. M. Rapko, R. T. Paine, *Chem. Mater.*, **2**, 384 (1990).
35. R. Clement, Y. Proux, *Bull. Soc. Chim. Fr.*, **2**, 558 (1969).
36. B. Toury, P. Miele, *J. Mater. Chem.*, **14**, 2609 (2004).
37. B. Toury, D. Cornu, F. Chassagneux, P. Miele, *J. Eur. Ceram. Soc.*, **25**, 137 (2005).
38. M. F. Lappert, *Proc. Chem. Soc.*, 59 (1959).
39. W. Gerrard, H. R. Hudson, E. F. Mooney, *J. Chem. Soc.*, 113 (1962).
40. R. H. Toeniskoetter, F. R. Hall, *Inorg. Chem.*, **2**, 29 (1963).
41. L. Tanigushi, K. Harada, T. Maeda, *Chem. Abstr.*, **85**, 96582v (1976).
42. Y. Kimura, Y. Kubo, N. Hayashi, *J. Inorg. Organomet. Polym.*, **2**, 231 (1992).
43. C. K. Narula, R. Schaeffer, A. Datye, R. T. Paine, *Inorg. Chem.*, **28**, 4053 (1989).
44. Y. Kimura, Y. Kubo, N. Hayashi, *Comput. Sci. Technol.*, **51**, 173 (1994).
45. Y. Kimura, Y. Kubo, N. Hayashi, *Compost. Sci. Technol.*, **51**, 173 (1994). Y. Kimura, Y. Kubo, *Inorg. Organomet. Polym. II: Adv. Mater. Intermed.*, ACS Symp. Ser. 572, 375 (1993).
46. P. Miele, B. Toury, S. Bernard, D. Cornu, K. Ayadi, L. Rousseau, G. Beauhaire, U.S. Patent 200 4044 162 (2004).
47. S. Duperrier, A. Calin, S. Bernard, C. Balan, P. Miele, *Polym. Eng. Sci.*, in press (2006).
48. W. Gerrard, H. R. Hudson, E. F. Mooney, *J. Chem. Soc.*, 113 (1962).
49. B. Toury, P. Miele, D. Cornu, B. Bonnetot, H. Mongeot, *Main Group Met. Chem.*, **22**, 231 (1999).
50. O. T. Beachley, *J. Am. Chem. Soc.*, **94**, 4223 (1972); O. T. Beachley, T. R. Durkin, *Inorg. Chem.*, **13**, 1768 (1974).
51. B. Toury, P. Miele, D. Cornu, H. Vincent, J. Bouix, *Adv. Funct. Mater.*, **12**, 228 (2002).
52. D. Cornu, P. Miele, B. Bonnetot, P. Guenot, H. Mongeot, J. Bouix, *Main Group Met. Chem.*, **21**, 301 (1998).
53. B. Toury, B. Bonnetot, H. Mongeot, J. Bouix, *J. Mater. Chem.*, **9**, 2605 (1999).
54. B. Toury, C. Gervais, P. Dibandgo, D. Cornu, P. Miele, F. Babonneau, *Appl. Organomet. Chem.*, **18**, 227 (2004).
55. P. Miele, B. Toury, D. Cornu, S. Bernard, *J. Organomet. Chem.*, **690**, 2809 (2005).
56. B. Toury, D. Cornu, S. Lecocq, P. Miele, *Appl. Organomet. Chem.*, **17**, 58 (2003).
57. D. W. Aubrey, M. F. Lappert, *J. Chem. Soc.*, 2927 (1959); D. W. Aubrey, M. F. Lappert, M. K. Majumbar, *J. Chem. Soc.*, 4088 (1962); B. Bonnetot, B. Frange, F. Guilhon, H. Mongeot, *Main Group Met. Chem.*, **17**, 583 (1994).
58. D. Cornu, *Ph.D. Thesis*, University Lyon 1, France (1998).
59. D. Cornu, P. Miele, R. Faure, B. Bonnetot, H. Mongeot, J. Bouix, *J. Mater. Chem.*, **9**, 757 (1999).
60. F. Guilhon, B. Bonnetot, D. Cornu, H. Mongeot, *Polyhedron*, **15**, 851 (1996).
61. F. Thévenot, C. Doche, H. Mongeot, F. Guilhon, P. Miele, B. Bonnetot, *J. Eur. Ceram. Soc.*, **17**, 1911 (1997); F. Thévenot, C. Doche, H. Mongeot, F. Guilhon, P. Miele, D. Cornu, B. Bonnetot, *J. Solid State Chem.*, **133**, 164 (1997), and refs. therein.



# Organoboron Polymer Electrolytes for Selective Lithium Cation Transport

**Noriyoshi Matsumi and Hiroyuki Ohno**

*Department of Biotechnology, Tokyo University of Agriculture and  
Technology, Koganei, Tokyo 184-8588, Japan*

## CONTENTS

I. INTRODUCTION	176
II. ANION-TRAPPING-TYPE ORGANOBORON POLYMER ELECTROLYTES VIA HYDROBORANE MONOMER	177
III. COMBLIKE ORGANOBORON POLYMER ELECTROLYTES	180
IV. FACILE PREPARATION OF ORGANOBORON POLYMER ELECTROLYTES VIA DEHYDROCOUPLING REACTION OF 9-BORABICYCLO[3.3.1]NONANE AND POLY(PROPYLENE OXIDE)	182
V. POLY(ORGANOBORON HALIDE)-IMIDAZOLE COMPLEXES	183
VI. LITHIUM BORATE-TYPE POLYMERS VIA POLYMER REACTIONS	186
VII. DIRECT SYNTHESIS OF POLY(LITHIUM ORGANOBORATE)S	188

VIII. POLYMER/SALT HYBRID INCLUDING BORON-STABILIZED IMIDOANION	190
IX. SUMMARY	193
X. REFERENCES	194

## I. INTRODUCTION

Recent development in mobile electronic devices, such as the Note PC, the cellular phone, personal digital assistants (PDA), music players and so forth, has been sustained by a remarkable advance of energy storage devices. The lithium secondary battery is one of the most common devices that has relatively high energy density and a long life. These days, the lithium secondary battery is also thought to be a promising candidate for auxiliary power in the hybrid car. In such devices, polymer electrolytes have played a key role as ion conductive media and an electrode separator. Most typically, poly(ethylene oxide) (PEO) derivatives<sup>1-3</sup> have been widely employed for a long time. However, because of crystalline properties, PEO derivatives generally do not show very high ionic conductivity. Among the solid polymer electrolytes reported so far, some inorganic polymer electrolytes such as polyether grafted polyphosphazene<sup>4,5</sup> and double-comb-type polysiloxanes<sup>6,7</sup> show high conductivity, demonstrating that the molecular design of polymer electrolytes utilizing inorganic elements is quite a valuable approach.

However, a problem still remains to be solved. In most polymer electrolytes, both anions and cations are mobile under a potential gradient. In such bi-ionic systems, a potential gradient is generated within the electrolyte so that the inner device voltage is offset. This retards the high-energy density and reliable performance of battery systems. Moreover, efficient cationic transport is also prevented by the binding of lithium cations by polar ether oxygens (Fig. 1). Generally, the lithium transference number of polyether-type electrolytes is no more than 0.1~0.2 at ambient temperature due to this ion-dipole interaction.

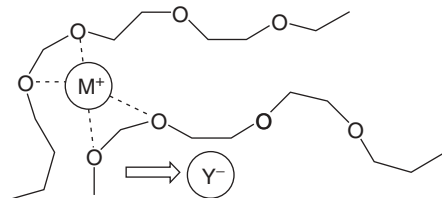


**Figure 1** A schematic illustration of ether oxygens binding to lithium ions.

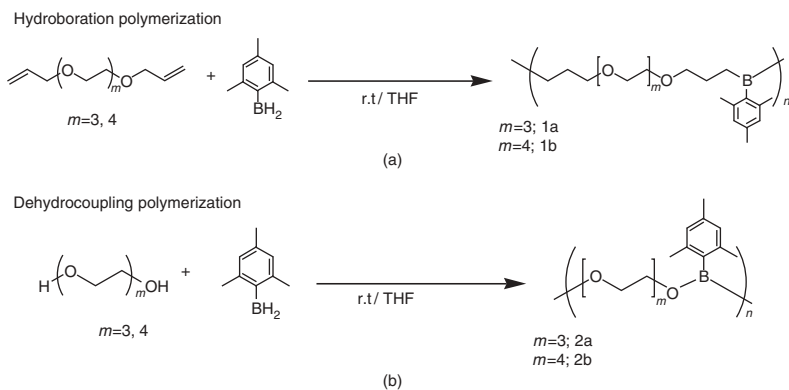
To improve the lithium transference number, a typical approach has been the preparation of a polymer/salt hybrid,<sup>8-17</sup> in which an ionic group is immobilized in

the polymer chain. However, most of these polymer/salt hybrids show limited ionic conductivity, because small numbers of carrier ions are present.

As an alternative approach, the addition of Lewis acidic organoboron compounds<sup>18–25</sup> into electrolytes has been studied by several groups. Conversely, we have examined the syntheses of defined organoboron polymer electrolytes by hydroboration polymerization<sup>26–29</sup> or dehydrocoupling polymerization.<sup>30</sup> Chujo et al. have published many papers on boration polymerization, in which they depict a synthetic approach for organoboron main-chain polymers. Hydroboration polymerization is a simple and reliable method for obtaining well-defined organoboron main-chain polymers effectively. Hydroboration polymerization of various bifunctional monomers proceeds under mild reaction conditions without being accompanied by disproportionation of the main chain or generation of any by-product. We have extended these methods for the preparation of various organoboron polymer electrolytes,<sup>31–39</sup> which are capable of transporting lithium cations selectively. In this chapter, synthesis and the ion-conductive characteristics of anion-trapping-type organoboron polymer electrolytes, organoboron polymer/salt hybrids, and nonpolyether-type organoboron polymer electrolytes are described in detail.

## II. ANION-TRAPPING-TYPE ORGANOBORON POLYMER ELECTROLYTES VIA HYDROBORANE MONOMER

First of all, synthesis of organoboron polymer electrolytes<sup>31,32</sup> was examined by hydroboration polymerization between mesitylborane<sup>40</sup> and triethyleneglycol diallylether (scheme 1). The polymerization was carried out by adding drop by drop a slight excess amount of mesitylborane to a tetrahydrofuran (THF) solution of oligo(ethylene oxide) diallyl ether. After stirring the solution for 6 hours, the solvent was removed, after which the crude polymer was purified by reprecipitation into *n*-hexane or washing with diethylether. The polymer obtained was a white powder or



Scheme 1

colorless gum (25–27% yield). Dehydrocoupling polymerization between mesitylborane and oligo(ethylene oxide) was also examined to give the corresponding boric-ester-type polymers in an 80–81% yield. In both polymerization systems, polymerization using oligo(ethylene oxide) monomer with longer ethylene oxide (EO) chains was not successful, probably because of stronger interactions between the EO chain and the boron atom.

The polymer structures obtained were supported by  $^1\text{H}$ - and  $^{11}\text{B}$ -nuclear magnetic resonance (NMR) spectra (Fig. 2). In the  $^1\text{H}$ -NMR spectra, peaks owing to the mesityl group was observed.  $^{11}\text{B}$ -NMR spectra exhibited only one main peak around 30 ppm. It should be noted that alkylborane polymers also show their main peak around 30 ppm. This is probably due to coordination of ether oxygen to the boron atom. From the  $^1\text{H}$ -NMR spectra, the number-average molecular weight of these polymers was estimated to be 1000~2900, after reacting the terminal hydroborane group with an excess amount of *tert*-butylphenol.

Ion-conductive properties of anion-trapping-type organoboron polymer electrolytes was evaluated after adding lithium salts (Fig. 3). In these systems, ionic conductivity of  $3.05 \times 10^{-5} \sim 5.22 \times 10^{-6} \text{ Scm}^{-1}$  was observed at  $50^\circ\text{C}$ . This indicates

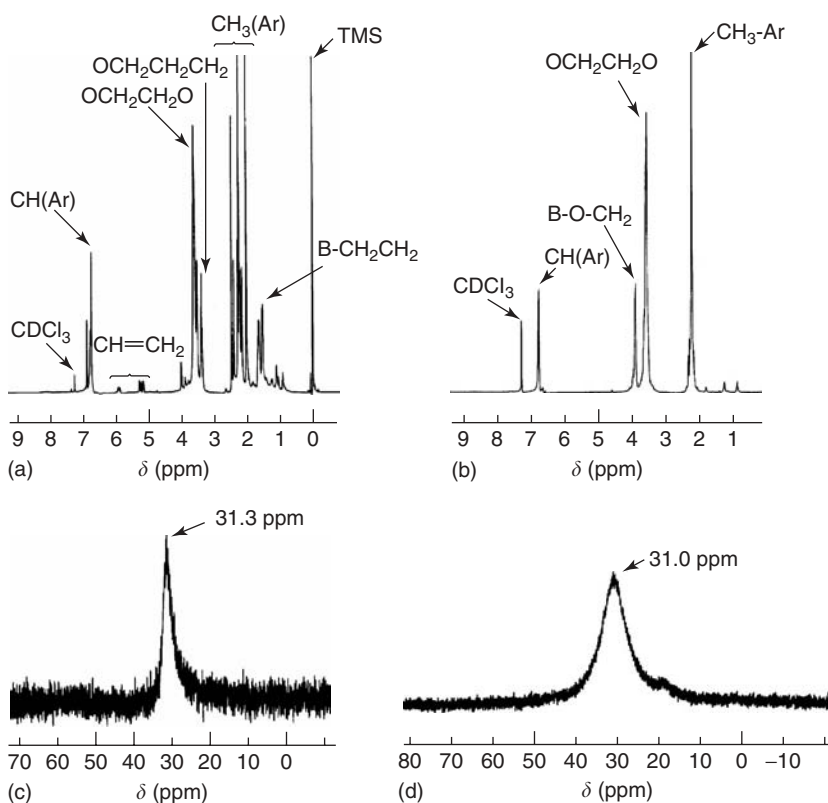


**Figure 2**  $^1\text{H}$ - and  $^{11}\text{B}$ -NMR spectra for polymer 1a and 2a. (a)  $^1\text{H}$ -NMR for 1a; (b)  $^1\text{H}$ -NMR for 2a; (c)  $^{11}\text{B}$ -NMR for 1a; (d)  $^{11}\text{B}$ -NMR for 2a.

that ionic conductivity of these polymers was not interrupted by bulky substituents on the boron atom. The highest ionic conductivity was observed when highly dissociable LiTFSI was added to boric-ester-type polymer. The ionic conductivity of alkylborane-type polymer was one order of magnitude lower than that of boric-ester-type polymers. Alkylborane-type polymers showed a larger temperature dependence of ionic conductivity in comparison with boric-ester-type polymers. This is due to lower alkylborane polymer segmental mobility, as implied from their higher glass-transition temperature.

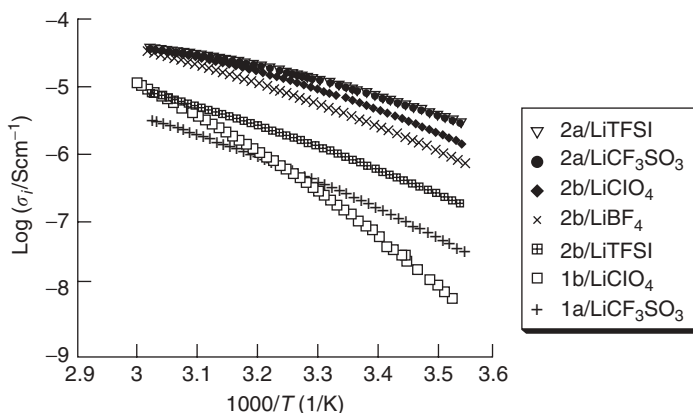


**Figure 3** Temperature dependence of ionic conductivity for polymers 1 and 2 in the presence of various lithium salts.

To obtain further information on ion conductive behavior, a Vogel–Fulcher–Tamman (VFT) plot<sup>41–43</sup> was fitted to give a linear line. This indicates that ions were transported by the segmental motion of the polymer main chain, similar to typical polymer electrolytes such as PEO derivatives. Interestingly, the difference between  $T_g$  and the optimized ideal  $T_0$  was relatively small in these systems, which implies a relatively small polymer–salt interaction. This might be due to a decrease of electron density on the oxygen atom adjacent to the boron atom via  $\pi$ - $\pi$  O–B back bonding.

The lithium transference number ( $t_+$ ) of these organoboron polymer electrolytes was evaluated by combination of dc polarization and ac impedance methods, as reported by Evans et al.<sup>44</sup> (Table 1). The observed  $t_+$  at 30°C was 0.50–0.35, indicating that anions were significantly trapped in these systems. Owing to the stronger Lewis acidity of the alkylborane unit, alkylborane-type polymers showed relatively higher  $t_+$ .

**Table 1** Lithium Transference Number  $t_+$  for Organoboron Polymer Electrolytes

Polymer/Salt or Lithium Reagent	$t_+$ <sup>a</sup>	Conductivity (Scm <sup>-1</sup> ) <sup>b</sup>
1a/LiCF <sub>3</sub> SO <sub>3</sub>	0.50	$2.11 \times 10^{-6}$
2b/LiClO <sub>4</sub>	0.35	$2.79 \times 10^{-5}$
2b/LiCF <sub>3</sub> SO <sub>3</sub>	0.39	$3.39 \times 10^{-5}$

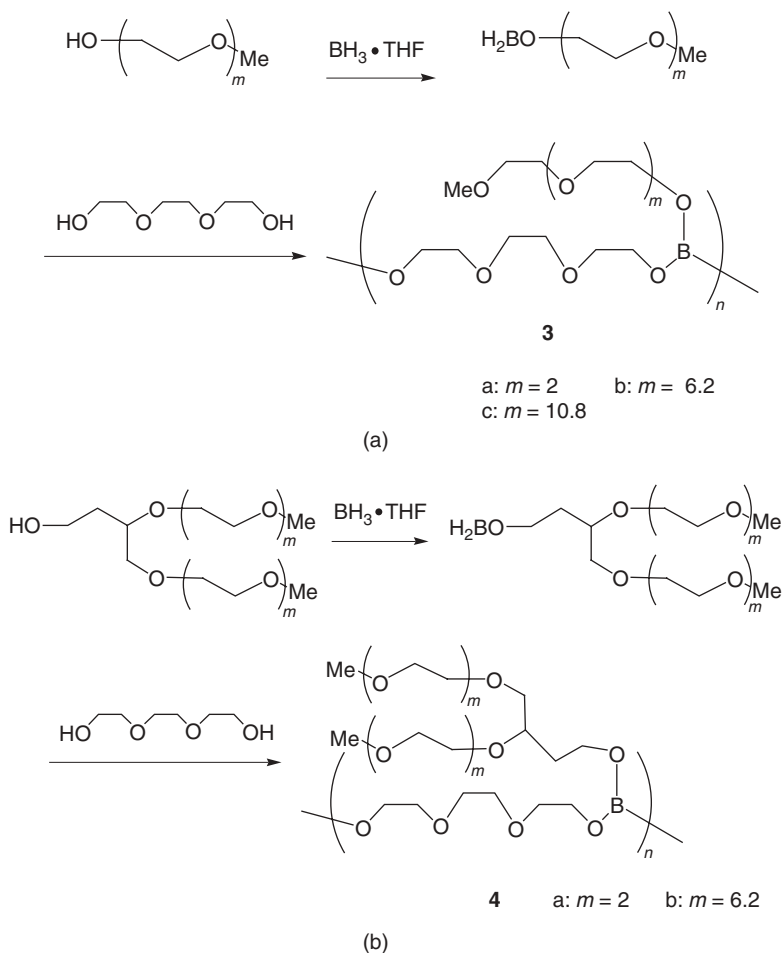
<sup>a</sup> Determined by combination of ac impedance/dc polarization methods, at 30°C.

<sup>b</sup> Determined by ac impedance method, at 50°C.

### III. COMBLIKE ORGANOBORON POLYMER ELECTROLYTES

As a major approach to prepare highly conductive polymer electrolytes, design of comblike polymer electrolytes has been widely examined. Both oligo(ethylene oxide) grafted polyphosphazene<sup>4,5</sup> reported by Allcock et al. and double comblike polysiloxane<sup>6,7</sup> developed by West et al. are successful examples. We have undertaken the preparation of comblike organoboron polymer electrolytes<sup>33</sup> to extend this strategy toward single-ion conductive polymers.

The synthesis of comblike organoboron polymer was examined (see scheme 2) by dehydrocoupling polymerization of hydroborane monomers bearing an



Scheme 2

oligo(ethylene oxide) tail. Similarly, comblike organoboron polymers bearing branched PEO side chains were also designed.

First, oligo(ethylene oxide) monomethylether was treated with excess  $\text{BH}_3\text{-THF}$  complex in THF. After solvent and borane-THF were removed under reduced pressure, the resulting hydroborane with an oligo(ethylene oxide) tail was polymerized with triethyleneglycol in THF at room temperature (r.t.). The polymers obtained were purified by reprecipitation into *n*-hexane or by washing with diethylether to give colorless or translucent gums in 61~76% yield.

In the presence of various lithium salts, the temperature dependence of ionic conductivity for comblike organoboron polymers was investigated (Fig. 4). When LiTFSI was employed, the maximum ionic conductivity was observed. The polymer bearing the longer EO chain exhibited higher ionic conductivity. For instance, an ionic conductivity of  $8.48 \times 10^{-5} \text{ Scm}^{-1}$  was observed for a polymer bearing PEO550 as the side chain (**3c**). Such behavior is different from other comblike polymer electrolytes where higher ionic conductivity was observed when a short PEO side chain was employed. This should be due to a much lower side-chain density of comblike organoboron polymers compared with PEO grafted polysiloxanes and polyphosphazenes.

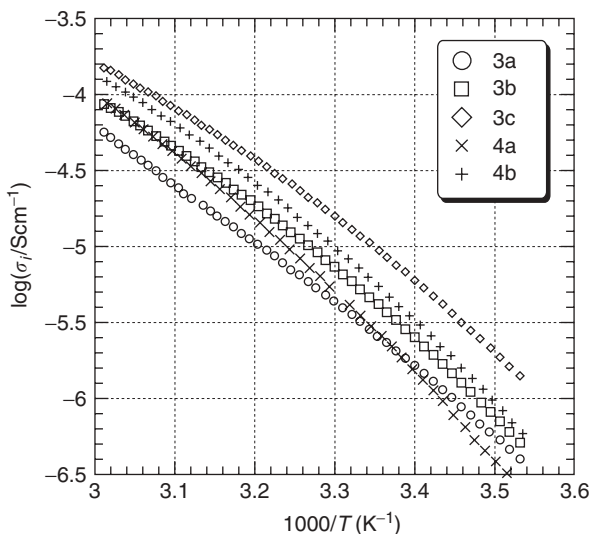


**Figure 4** Temperature dependence of ionic conductivity for comblike polymers 3 and 4 in the presence of LiTFSI.

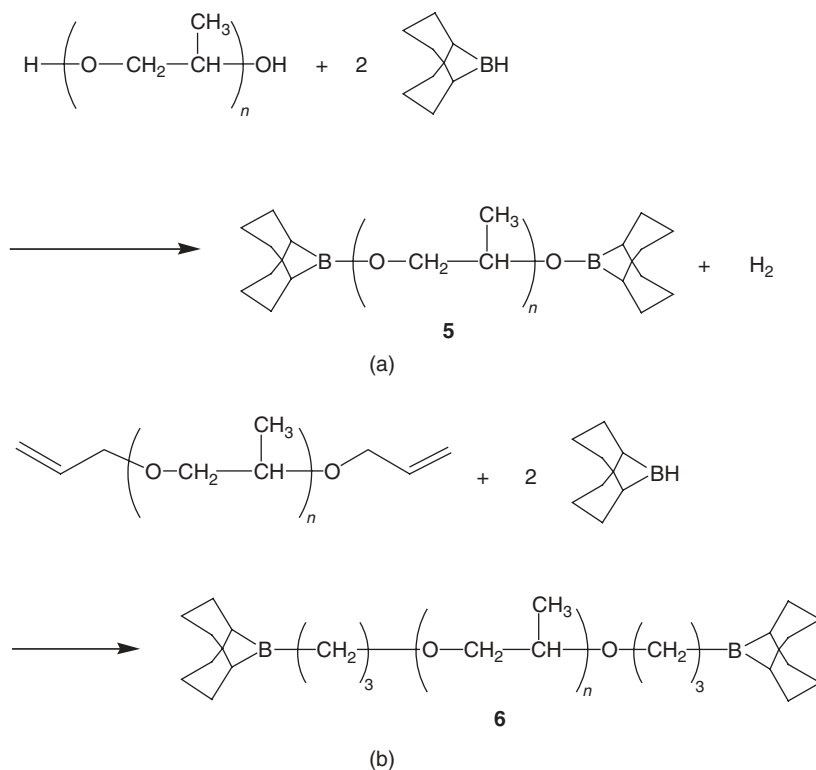
The lithium transference number ( $t_+$ ) of a polymer bearing PEO550 side chain/ $\text{LiCF}_3\text{SO}_3$  was found to be 0.38 at 30°C. This value implies that anions were effectively trapped by organoboron units, similar to linear organoboron polymer electrolytes.

#### IV. FACILE PREPARATION OF ORGANOBORON POLYMER ELECTROLYTES VIA DEHYDROCOUPLING REACTION OF 9-BORABICYCLO[3.3.1]NONANE AND POLY(PROPYLENE OXIDE)

A 9-borabicyclo[3.1.1]nonane (9-BBN)<sup>45</sup> is one of the most well-known hydroborane reagents. Because of the commercial availability of 9-BBN, facile preparation of organoboron polymer electrolytes using this reagent should be an industrially beneficial approach.<sup>34,36</sup>

The reaction was carried out by adding a THF solution of 9-BBN [equimolar to the poly(propylene oxide) (PPO) chain ends] drop by drop to PPO or PPO diallylether and stirring the resulting mixture for 5–7 hours (scheme 3). The structure of polymers obtained was confirmed by <sup>1</sup>H- and <sup>11</sup>B-NMR spectra. From the differential scanning calorimetric (DSC) measurement, no peak due to the melting point was observed to show that the polymer was fully amorphous.

In the presence of lithium salts, the temperature dependence of ionic conductivity for the polymer electrolytes obtained was evaluated. In the presence of LiCF<sub>3</sub>SO<sub>3</sub>,



Scheme 3

the polymers **5** and **6** ( $n = 7$ ) showed ionic conductivities of  $4.57 \times 10^{-6} \text{ Scm}^{-1}$  and  $2.83 \times 10^{-6} \text{ Scm}^{-1}$  at  $50^\circ\text{C}$ , respectively. The observed ionic conductivity was lower than that of a mixture of PPO and  $\text{LiCF}_3\text{SO}_3$ . This can be understood by considering the smaller number of carrier ions due to efficient anion trapping.

The lithium transference numbers calculated for **5**/ $\text{LiCF}_3\text{SO}_3$  and **6**/ $\text{LiCF}_3\text{SO}_3$  were 0.67 and 0.57 at  $30^\circ\text{C}$ . The high  $t_+$  value, comparable to PPO/salt hybrids bearing highly dissociable sulfonamide structures, indicates that anions were effectively trapped by the terminal organoboron unit. Even though the ionic conductivity of **5**/ $\text{LiTFSI}$  was higher ( $2.15 \times 10^{-5} \text{ Scm}^{-1}$ ; at  $50^\circ\text{C}$ ) than the  $\text{LiCF}_3\text{SO}_3$  systems,  $t_+$  was 0.28 at  $30^\circ\text{C}$ , indicating much less efficient anion trapping.

## V. POLY(ORGANOBORON HALIDE)-IMIDAZOLE COMPLEXES

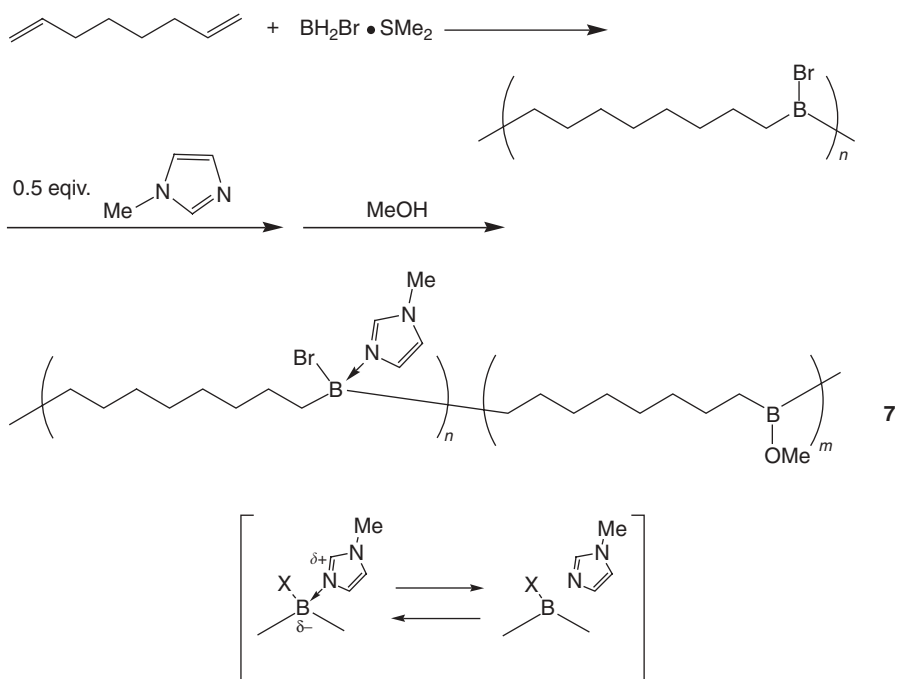
In recent years, as an alternative to polyether derivatives, ionic liquids (ILs)<sup>46,47</sup> have been intensely studied because of their high ionic conductivity and good electrochemical stability. However, selective cation transport is not easily achieved in IL-based systems either, because component ions of ILs are also prone to migrate under the potential gradient. To improve the selectivity for target cation transport, several approaches have been examined so far. Zwitterionic molten salts,<sup>48–50</sup> in which both anion and cation are covalently tethered, were found to exhibit relatively high lithium transference numbers. Molten salts bearing an organoboron anion receptor<sup>51</sup> were also prepared via hydroboration of 1-allylimidazolium bromide and a subsequent ion exchange reaction, to show a maximum  $t_+$  of 0.71.

As a further approach for novel electrolytes appropriate for selective cation transport, we have prepared poly(organoboron halide)-imidazole complexes.<sup>35</sup> Even though boron-amine complexes are widely known materials reported by the early works of H. C. Brown et al.,<sup>52–54</sup> they had not been investigated as solvents or electrolytes to the best of our knowledge.

The organoboron polymer complex was prepared as follows. First, poly(organoboron halide)<sup>55</sup> was prepared according to the reported method, by hydroboration polymerization between 1,7-octadiene and the monobromoborane dimethylsulfide complex. The polymer obtained was then reacted with half an equivalent of methanol and 1-methylimidazole to give the corresponding copolymer efficiently (scheme 4). The structure of the polymer was characterized by  $^1\text{H}$ - and  $^{11}\text{B}$ -NMR spectra.

It is known that organoboron halide–imidazole complexes dissociate during equilibrium;<sup>56</sup> however, charges disappear upon dissociation. In such a matrix, mobile ions should not originate from the matrix. Therefore, the polymer electrolytes composed of boron halide–imidazole complexes were considered to be appropriate for selective ion transport.

After adding lithium salts, ionic conductivity was measured by the ac impedance method (Fig. 5). Lithium salt concentration was first optimized by measurements



**Scheme 4** Fratiello et al., *Inorg. Chem.*, 7(8), 1581 (1968).

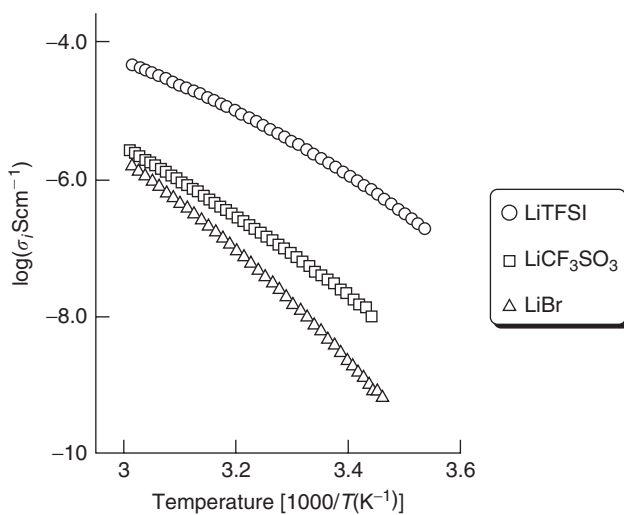


**Figure 5** Temperature dependence of ionic conductivity for poly(organoboron halide)-imidazole complexes in the presence of various lithium salts.

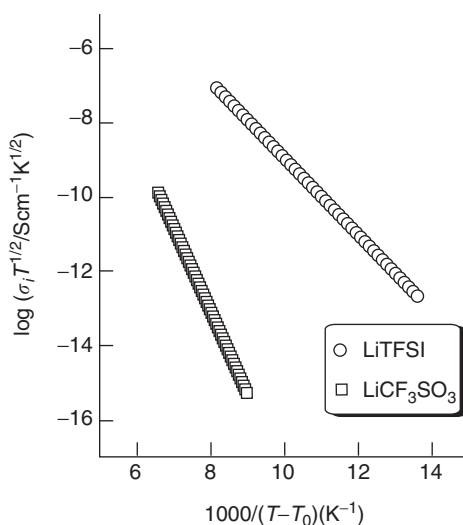


**Figure 6** VFT plots for poly(organoboron halide)-imidazole complexes.

with varying concentrations of LiTFSI. The ionic conductivity reached maximum when 0.5 equivalent of LiTFSI per organoboron unit was added ( $2.59 \times 10^{-5} \text{ Scm}^{-1}$ ; at  $50^\circ\text{C}$ ). In the presence of LiBr or  $\text{LiCF}_3\text{SO}_3$ , instead of LiTFSI, ionic conductivity was much lower than in the LiTFSI system. This should be due to much higher activation energies in these matrixes, as indicated from VFT plots (Fig. 6) and VFT parameters (Table 2).

**Table 2** VFT Parameters for Poly(organoboron halide)-imidazole Complexes

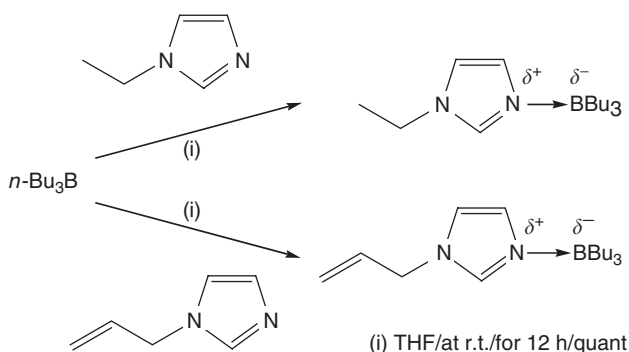
Salt	$T_g$ (K)	$T_0$ (K)	A (S/cm)	B (K)	$E_a$ (eV) <sup>a</sup>	rms <sup>b</sup>
$\text{LiCF}_3\text{SO}_3$	214	180	138.5	2263	18,490	0.9999
LiTFSI	209	209	4.011	1041	8504	0.9999

<sup>a</sup>  $E_a = B \times 8.1674 (10^{-5} \text{ eV})$ .

<sup>b</sup> Root mean square.

The lithium transference number calculated for 7/LiTFSI was 0.47 at  $30^\circ\text{C}$ , showing that anions were effectively trapped by methoxyboron unit.

Very recently, we reported liquid imidazole–borane complexes (scheme 5)<sup>57</sup> that are air stable. Judging from their polarity and viscosity (Table 3), they are expected to be a new class of solvent or electrolyte. Preparation of polymer homologues of imidazole–alkylborane complexes will also be reported elsewhere in the near future.



Scheme 5

**Table 3** Physical Properties of Imidazole–Borane Complexes

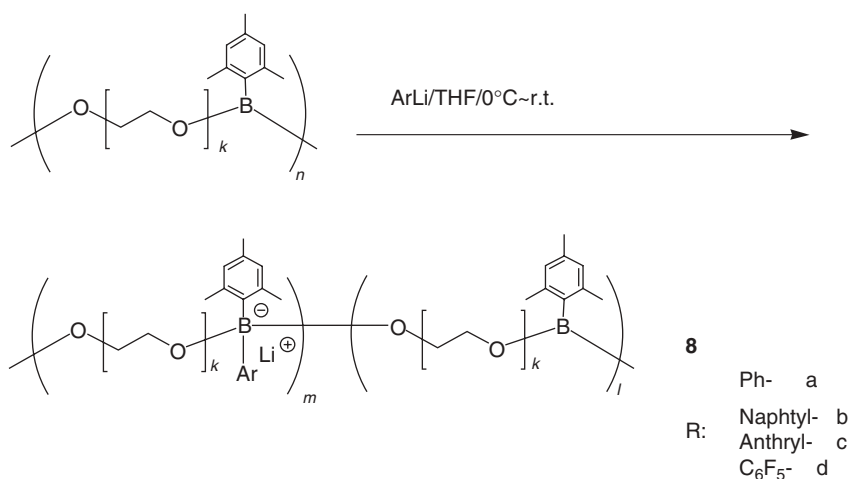
Complex	$T_g(^{\circ}\text{C})^a$	$T_m(^{\circ}\text{C})^a$	Viscosity $\eta(\text{cP}; \text{at } 25^{\circ}\text{C})$	Polarity Et(30)	Ionic Conductivity ( $\text{Scm}^{-1}$ ) <sup>b</sup>
	-78	9.1	36	43.6	$2.22 \times 10^{-4}$
	-81	-3.5	28	42.8	$2.07 \times 10^{-4}$

<sup>a</sup> At the heating rate of 10°C/min.<sup>b</sup> In the presence of 0.25 M LiTFSI.

## VI. LITHIUM BORATE-TYPE POLYMERS VIA POLYMER REACTIONS

To immobilize such anions as borate, organoboron polymers were reacted with aryllithium reagents.<sup>31,32</sup> The reaction of alkylborane polymers with *n*-BuLi was examined first; however, the ionic conductivity of the resulting material was very low. Moreover, complicated peaks were observed in the <sup>1</sup>H-NMR spectrum. Conversely, selective lithium borate formation was observed in the <sup>11</sup>B-NMR spectrum when PhLi was employed (scheme 6). An ionic conductivity of  $9.45 \times 10^{-7} \text{ Scm}^{-1}$  was observed at 50°C. The observed ionic conductivity was relatively low because of the decreased number of carrier ions compared with dissolved salt systems. However, the lithium transference number of this polymer was markedly high (0.82; at 30°C).

The reactions of organoboron polymer electrolytes were examined using various organolithium reagents (Fig. 7 and Table 4). When pentafluorophenyllithium was used, ionic conductivity increased by one order of magnitude compared with the use of phenyllithium. This occurs because of the greater degree of dissociation of lithium borate in the presence of electron withdrawing C<sub>6</sub>F<sub>5</sub>- groups. A similar enhancement of ionic conductivity was also observed when 2-naphthyllithium or 9-anthryllithium was employed.



Scheme 6

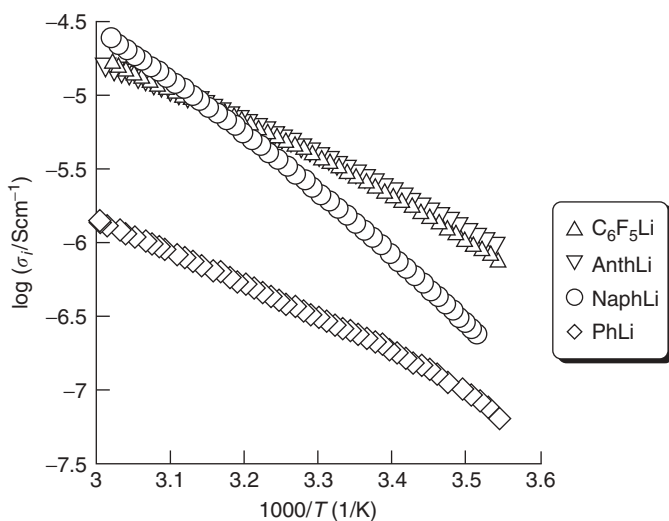


**Figure 7** Temperature dependence of ionic conductivity for lithium borate polymer electrolytes prepared via polymer reactions.

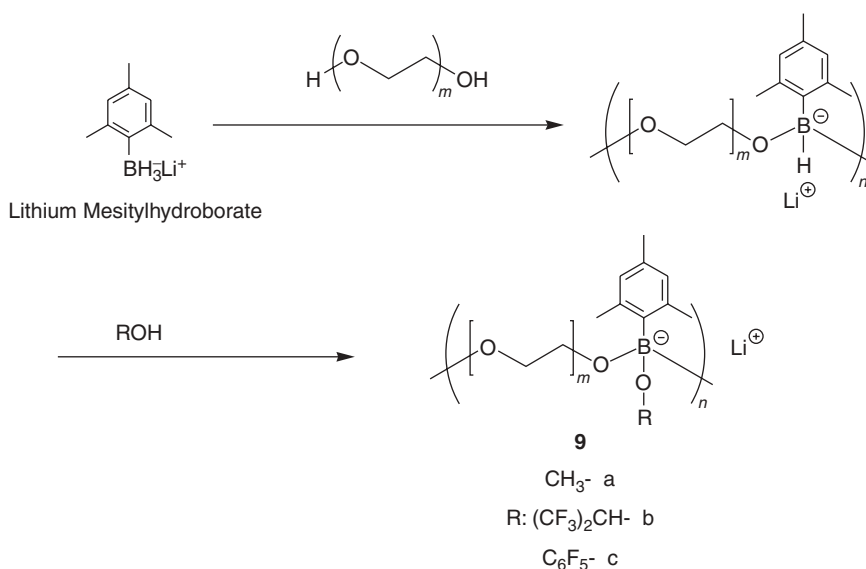
**Table 4** Ionic Conductivity of Lithium Borate Polymers Prepared via Polymer Reactions

ArLi	Phenyllithium	2-Naphthyllithium	9-Anthryllithium	Pentafluoro-phenyllithium
Conductivity (Scm <sup>-1</sup> )	$9.45 \times 10^{-7}$	$1.30 \times 10^{-5}$	$1.11 \times 10^{-5}$	$1.13 \times 10^{-5}$

## VII. DIRECT SYNTHESIS OF POLY(LITHIUM ORGANOBORATE)S

Reactions of organoboron polymer electrolytes with aryllithium reagents suffered low conversion due to relatively low reactivity of the mesitylborane unit. Moreover, incorporation of aryl substituent in side chains resulted in higher glass-polymer electrolyte-transition temperatures.

To avoid problems associated with these polymer reactions, the direct synthesis of lithium borate polymer electrolytes<sup>37</sup> was undertaken by dehydrocoupling polymerization using lithium mesitylhydroborate<sup>40</sup> (scheme 7).



**Scheme 7**

Lithium mesitylhydroborate was prepared by reaction of mesitylmagnesium bromide with trimethoxyborane and subsequent reduction with LiAlH<sub>4</sub>. The polymerization was performed by adding a THF solution containing a slight excess of lithium mesitylhydroborate to oligo(ethylene oxide) in THF. After treatment with alcohol, the lithium borate polymers were obtained as transparent soft solids soluble in methanol, THF, and chloroform.

Before treatment with alcohol, the ionic conductivity of lithium borate polymers was  $6.23 \times 10^{-5}$  to  $2.07 \times 10^{-7} \text{ Scm}^{-1}$  at 50°C. The maximum ionic conductivity was observed for the polymer with a PEO<sub>400</sub> spacer unit. After the polymer reaction with alcohols, glass-transition temperatures of these polymers were found to be -52 to 39°C, which was higher than that of poly(lithium mesitylhydroborate) (-69°C).

The ionic conductivity of this lithium borate polymer bearing the methoxyborate unit (**9a**) was  $8.77 \times 10^{-6} \text{ Scm}^{-1}$  at 50°C (Fig. 8). This value was lower than that observed before the polymer reacted with methanol. However, it was still greater

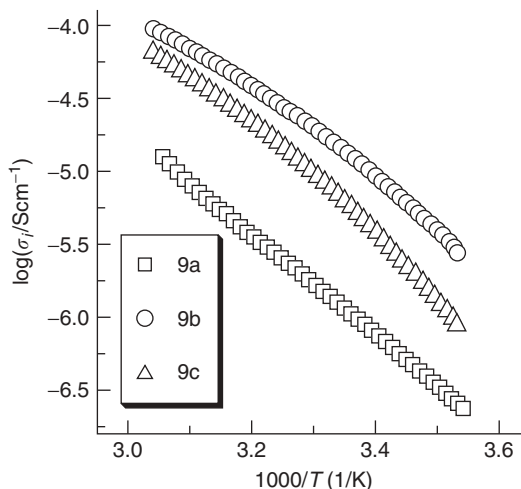


**Figure 8** Temperature dependence of ionic conductivity for lithium borate polymers 9.

than that for lithium borate polymers prepared by reacting the polymers with phenyllithium (**8a**). When poly(lithium mesitylhydroborate) was reacted with fluorinated alcohols such as hexafluoro-2-propanol and pentafluorophenol instead of methanol, the resulting lithium borate polymers exhibited further improved ionic conductivity. This occurs because of the higher degree of dissociation for the lithium borate unit in the presence of electron withdrawing groups. The maximum ionic conductivity of  $7.44 \times 10^{-5} \text{ Scm}^{-1}$  was observed at  $50^\circ\text{C}$  for lithium borate polymer with hexafluoropropoxy side groups (**9b**).

When the VFT equation was applied, every system gave a linear fit (Fig. 9). This implies that ion transport was assisted by segmental motion of polymer chains in a

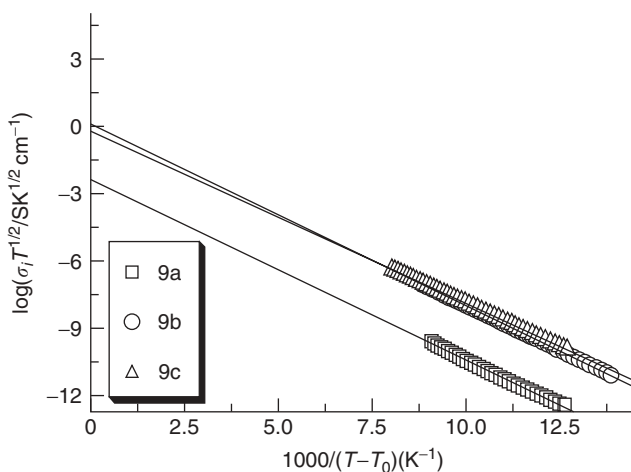


**Figure 9** VFT Plots for lithium borate polymers 9.

manner similar to ordinary PEO derivatives. From the VFT parameters (Table 5) corresponding to activation energy and carrier-ion number, a greater number of carrier ions for polymers with fluorinated groups (**9b** and **9c**) were indicated. This causes the observed higher ionic conductivity of these polymers compared with that bearing methoxyborate unit.

**Table 5** VFT Parameters for Lithium Borate Polymers 9

Polymer	$\sigma_i$ (Scm <sup>-1</sup> ) at 323 K	A (Scm <sup>-1</sup> K <sup>1/2</sup> )	B (K)	$T_g$ (K)	$T_0$ (K)
9a	$8.77 \times 10^{-6}$	0.31	731	221	203
9b	$7.44 \times 10^{-5}$	0.83	751	226	204
9c	$4.52 \times 10^{-5}$	1.13	818	234	211

## VIII. POLYMER/SALT HYBRID INCLUDING BORON-STABILIZED IMIDOANION

As described in previous sections (Sections VI and VII), macromolecular design of polymer/salt hybrids with a highly dissociable lithium borate unit proved to be a valuable approach for single-ion conductive polymers. To further improve the degree of lithium salt dissociation, we have designed a polymer/salt hybrid bearing the boron-stabilized imidoanion (BSI)<sup>38</sup> (Fig. 10).

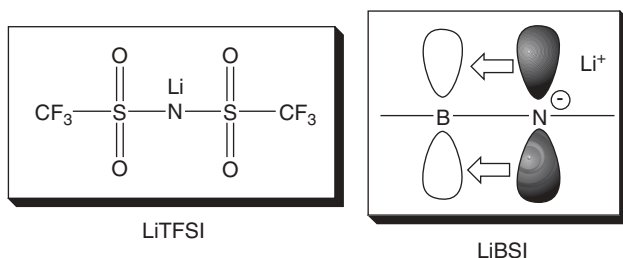


**Figure 10** Stabilized imidoanions.

The boron atom is capable of stabilizing adjacent anions. Boron-stabilized carbanions<sup>58</sup> have been utilized as valuable nucleophilic reagents in the field of organic synthesis. Recently, we have investigated the bulk ionic conductivity of boron-stabilized carbanions.<sup>59</sup> Since it is commonly known that a lone pair electron of the nitrogen atom efficiently flows into the vacant p orbital of the adjacent boron atom ( $p\pi$ - $p\pi$  interaction),<sup>60</sup> use of imidoanions stabilized by a boron atom should be a promising approach to prepare nonhalogenated salts showing high degrees of dissociation.

A synthesis of comblike organoboron polymer/boron stabilized imidoanion hybrids was examined via reactions of poly(organoboron halides) with 1-hexylamine and oligo(ethylene oxide) monomethyl ether and subsequent neutralization with lithium hydride (scheme 8). The obtained polymers (**10**) were amorphous soft solids soluble in common organic solvents such as methanol, THF, and chloroform. In the <sup>11</sup>B-NMR spectra (Fig. 11), neutralization of the iminoborane unit with lithium hydride



resulted in an up-field shift of the peak due to the iminoborane unit. The peak belonging to the boric ester unit remained unchanged, indicating that neutralization proceeded quite selectively. Generally, an alkylamine does not undergo neutralization with lithium hydride. The observed reactivity of the iminoborane unit is explained by strong  $p\pi-p\pi$  interaction in the iminoborane unit.

The ionic conductivity of these polymer/salt hybrids was evaluated after the polymers were thoroughly dried under vacuum (Fig. 12a). These polymers showed

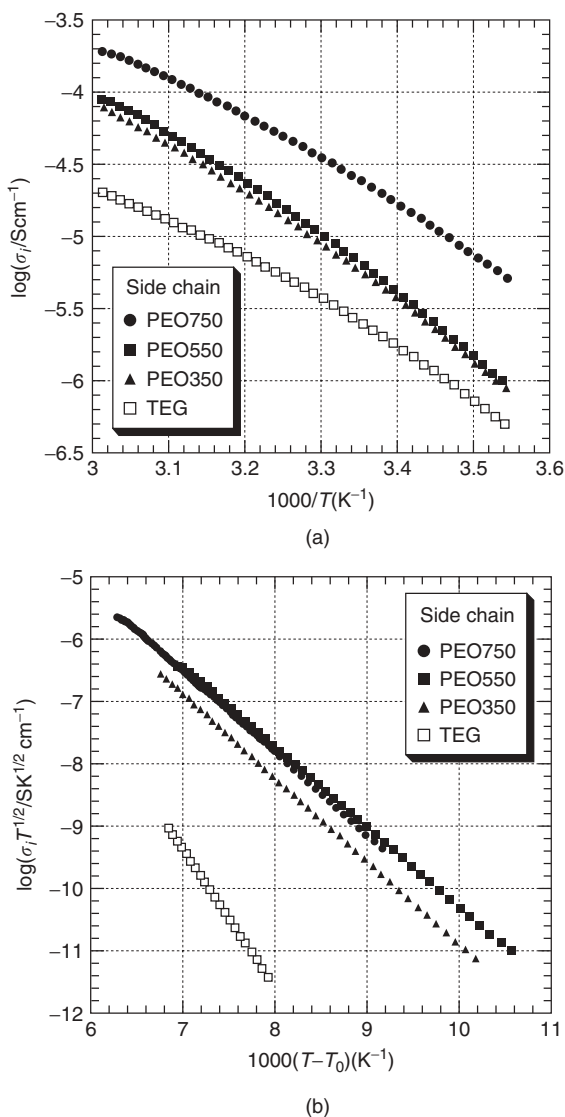


**Figure 12** (a) Temperature dependence of ionic conductivity. (b) VFT plots for polymer/salt hybrids 10.

ionic conductivities of  $1.31 \times 10^{-4}$  to  $1.32 \times 10^{-5} \text{ Scm}^{-1}$  at  $50^\circ\text{C}$ , which are very high values for single-ion conductive polymers. The highest ionic conductivity was observed when the side chain was PEO<sub>750</sub>. Conversely, the polymer bearing a triethylene glycol (TEG) side chain showed one order of magnitude lower ionic conductivity, possibly due to the restricted segmental motion of the polymer, as indicated from higher  $T_g$ .

VFT plots were fit for obtained polymer/salt hybrids (Fig. 12b). Except for the polymer having TEG side chains, linear fitting was possible. In the higher temperature region, linear VFT fitting was also obtained for the polymer with a TEG side chain. From the VFT parameters (Table 6) corresponding to carrier-ion number and activation energy, the carrier-ion number was lower when the PEO chain length was longer. However, the activation energy of the matrix was also lower for these systems, which led to improved ionic conductivity, as observed in ac impedance measurements.

**Table 6** Glass Transition Temperature, Ionic Conductivity and VFT Parameters For Polymer/Salt Hybrids 10

Side Chain	$[\text{Li}^+]/[\text{EO}]$	$T_g$ (K)	$T_0$ (K)	$\sigma_i$ at 323 K ( $\text{Scm}^{-1}$ )	A ( $\text{Scm}^{-1}$ )	B (K)
TEG ( $k = 3.0$ )	0.333	239	186	$1.32 \times 10^{-5}$	1,201,000	2207
PEO350 ( $k = 8.0$ )	0.125	232	184	$4.49 \times 10^{-5}$	332.9	1342
PEO550 ( $k = 13$ )	0.077	227	188	$5.40 \times 10^{-5}$	351.3	1284
PEO750 ( $k = 18$ )	0.056	223	173	$1.31 \times 10^{-4}$	430.4	1306

## IX. SUMMARY

A variety of organoboron polymer electrolytes were successfully prepared by hydroboration polymerization or dehydrocoupling polymerization. Investigations of the ion conductive properties of these polymers are summarized in Table 7. From this systematic study using defined organoboron polymers, it was clearly demonstrated that incorporation of organoboron anion receptors or lithium borate structures are fruitful approaches to improve the lithium transference number of an ion conductive matrix.

Among anion trapping-type electrolytes, alkylborane polymer electrolytes (run 1) were found to show relatively high lithium transference numbers owing to stronger Lewis acidity of the alkylborane unit. Although most polymer electrolytes exhibited maximum ionic conductivity in the presence of highly dissociable LiTFSI, the lithium transference number was not very high in these systems because of inefficient interaction between TFSI anion and organoboron units, possibly due to steric hindrance. When  $\text{LiCF}_3\text{SO}_3$  was employed as an additive, most systems showed significantly improved lithium transference numbers.

Interestingly, the nonpolyether-type polymer electrolyte 7 showed a relatively high lithium transference number of 0.47 in the presence of LiTFSI. This is possibly due to the absence of strong binding of ether oxygen to the lithium cation. Moreover, anion trapping of the boron atom is not retarded by coordination of oxygen to the

**Table 7** Ion-Conductive Properties of Organoboron Polymer Electrolytes

Run	Polymer	$T_g$ (°C)	Salt	Ionic	Lithium
				Conductivity	Transference Number
				$\sigma_i$ (Scm <sup>-1</sup> ) at 50°C	$t_+$ at 30°C
1	1a	-45	LiCF <sub>3</sub> SO <sub>3</sub>	$2.11 \times 10^{-6}$	0.50
2	2b	-	LiClO <sub>4</sub>	$2.79 \times 10^{-5}$	0.35
3	2b	-	LiCF <sub>3</sub> SO <sub>3</sub>	$3.39 \times 10^{-5}$	0.39
4	3c	-	LiTFSI	$8.48 \times 10^{-5}$	-
5	3c	-	LiCF <sub>3</sub> SO <sub>3</sub>	$2.01 \times 10^{-5}$	0.38
6	4b	-	LiTFSI	$6.63 \times 10^{-5}$	-
7	5	-44	LiTFSI	$2.15 \times 10^{-5}$	0.28
8	5	-22	LiCF <sub>3</sub> SO <sub>3</sub>	$4.57 \times 10^{-6}$	0.67
9	6	-32	LiCF <sub>3</sub> SO <sub>3</sub>	$2.83 \times 10^{-6}$	0.57
10	7	-64	LiTFSI	$2.59 \times 10^{-5}$	0.47
11	8a	-45	(PhBLi)	$9.45 \times 10^{-7}$	0.82
12	8c	-	(C <sub>6</sub> F <sub>5</sub> BLi)	$1.13 \times 10^{-5}$	-
13	9a	-52	(MeOBLi)	$8.77 \times 10^{-6}$	-
14	9b	-47	[(CF <sub>3</sub> ) <sub>2</sub> CHOBLi]	$7.44 \times 10^{-5}$	-
15	10	-50	(LiBSI)	$1.31 \times 10^{-4}$	-

boron atom in a nonpolyether-type system. Such efficient anion trapping was also observed in molten salts bearing organoboron anion receptors.

Generally, polymer/salt hybrids, in which salt is immobilized onto a polymer framework, do not exhibit very high ionic conductivity. However, incorporation of a fluorinated unit on lithium borate resulted in ionic conductivities as high as those for ordinary "salt in polymer" systems. A design of polymer/salt hybrids, including the highly dissociable LiBSI structure, also led to ionic conductivities as high as a single-ion conductive system.

Design of organoboron polymer electrolytes will continue to have a great deal of potential based on the ability to tailor boron atoms. This is an attractive approach for single ion conductive materials.

## X. REFERENCES

1. D. E. Fenton, J. M. Parker, P. V. Wright, *Polymer*, **14**, 589 (1973).
2. P. V. Wright, *Br. Polym. J.*, **7**, 319 (1975).
3. P. V. Wright, *J. Polym. Sci., Polym. Phys. Ed.*, **14**, 955 (1976).
4. P. M. Blonsky, D. F. Shriver, H. R. Allcock, P. E. Austin, *J. Am. Chem. Soc.*, **106**, 6854 (1984).
5. H. R. Allcock, S. J. M. O'Connor, D. L. Olmeijer, M. E. Napierala, C. G. Cameron, *Macromolecules*, **29**, 7544 (1996).
6. R. Hopper, L. J. Lyons, D. A. Moline, R. West, *Organometallics*, **18**, 3249 (1999).

7. R. Hopper, L. J. Lyons, M. K. Mapes, D. Schmacher, D. A. Moline, R. West, *Macromolecules*, **34**, 931 (2001).
8. L. C. Hardy, D. F. Shriver, *J. Am. Chem. Soc.*, **107**, 3823 (1985).
9. E. Tsuchida, H. Ohno, N. Kobayashi, H. Ishizaka, *Macromolecules*, **22**, 1771 (1989).
10. G. Zhou, I. M. Khan, J. Smid, *Macromolecules*, **26**, 2202 (1993).
11. W. Xu, K. S. Siow, Z. Gao, Y. Lee, *Chem. Mater.*, **10**, 1951 (1998).
12. K. E. Doan, M. A. Ratner, D. F. Shriver, *Chem. Mater.*, **3**, 418 (1991).
13. T. Fujinami, A. Tokimune, M. A. Metha, D. F. Shriver, G. C. Rawsky, *Chem. Mater.*, **9**, 2236 (1997).
14. T. Hamaide, C. L. Deore, *Polymer*, **34**, 1038 (1993).
15. K. Xu, C. A. Angell, *Electrochim. Acta*, **40**, 2401 (1995).
16. H. Ohno, K. Ito, *Polymer*, **36**, 891 (1995).
17. K. Ito, N. Nishina, H. Ohno, *J. Mater. Chem.*, **7**, 1357 (1997).
18. H. S. Lee, X. Q. Yang, C. L. Xiang, J. McBreen, *J. Electrochem. Soc.*, **145**, 2813 (1998).
19. J. McBreen, H. S. Lee, X. Q. Yang, X. Sun, *J. Power Sources*, **89**, 163 (2000).
20. M. A. Mehta, T. Fujinami, *Chem. Lett.*, 915 (1997).
21. M. A. Mehta, T. Fujinami, *Solid State Ionics*, **113–115**, 187 (1998).
22. M. A. Mehta, T. Fujinami, T. Inoue, *J. Power Sources*, **81–82**, 724 (1999).
23. M. A. Mehta, T. Fujinami, S. Inoue, K. Matsushita, T. Miwa, T. Inoue, *Electrochim. Acta*, **45**, 1175 (2000).
24. T. Hirakimoto, M. Nishiura, M. Watanabe, *Electrochim. Acta*, **46**, 1609 (2001).
25. X. Sun, C. A. Angell, *Electrochim. Acta*, **46**, 1467 (2001).
26. Y. Chujo, I. Tomita, Y. Hashiguchi, H. Tanigawa, E. Ihara, T. Saegusa, *Macromolecules*, **24**, 345 (1991).
27. Y. Chujo, I. Tomita, N. Murata, H. Mauermann, T. Saegusa, *Macromolecules*, **25**, 27 (1992).
28. N. Matsumi, K. Naka, Y. Chujo, *J. Am. Chem. Soc.*, **120**, 5112 (1998).
29. N. Matsumi, Y. Chujo, *Contemporary Boron Chemistry*; M. G. Davidson, A. K. Hughes, T. B. Marder, K. Wade, Eds., p. 51, Royal Society of Chemistry, London, 2000.
30. Y. Chujo, I. Tomita, T. Saegusa, *Polym. J.*, **23**, 743 (1991).
31. N. Matsumi, K. Sugai, H. Ohno, *Macromolecules*, **35**, 5731 (2002).
32. N. Matsumi, K. Sugai, H. Ohno, *Macromolecules*, **36**, 2321 (2003).
33. N. Matsumi, T. Mizumo, H. Ohno, *Chem. Lett.*, **33**, 372 (2004).
34. T. Mizumo, K. Sakamoto, N. Matsumi, *Chem. Lett.*, **33**, 369 (2004).
35. N. Matsumi, T. Mizumo, H. Ohno, *Polym. Bull.*, **51**, 389 (2004).
36. T. Mizumo, K. Sakamoto, N. Matsumi, H. Ohno, *Electrochim. Acta*, **50**, 3928 (2005).
37. N. Matsumi, K. Sugai, K. Sakamoto, T. Mizumo, H. Ohno, *Macromolecules*, **38**, 4951 (2005).
38. N. Matsumi, M. Nakashiba, T. Mizumo, H. Ohno, *Macromolecules*, **38**, 2040 (2005).
39. A. Narita, W. Shibayama, N. Matsumi, H. Ohno, *Polym. Bull.*, in press (2006).
40. K. Smith, A. Pelter, Z. Jin, *Angew. Chem. Int. Ed. Engl.*, **33**, 851 (1994).
41. H. Vogel, *Phys. Z.*, **22**, 645 (1921).
42. G. S. Fulcher, *J. Am. Ceram. Soc.*, **8**, 339 (1925).
43. G. Tamman, W. Z. Hesse, *Anorg. Allg. Chem.*, **156**, 245 (1926).
44. J. Evans, C. A. Vincent, P. G. Bruce, *Polymer*, **28**, 2325 (1987).
45. E. F. Knights, H. C. Brown, *J. Am. Chem. Soc.*, **90**, 5280 (1968).
46. T. Welton, *Chem. Rev.*, **99**, 2071 (1999).
47. H. Ohno, (ed.), *Electrochemical Aspects of Ionic Liquids*, Wiley-Interscience, New York, 2005.
48. M. Yoshizawa, M. Hirao, K. Ito-Akita, H. Ohno, *J. Mater. Chem.*, **11**, 1057 (2001).

49. M. Yoshizawa, H. Ohno, *Chem. Commun.*, 1828 (2004).
50. A. Narita, W. Shibayama, K. Sakamoto, T. Mizumo, N. Matsumi, H. Ohno, *Chem. Commun.*, 1926 (2006).
51. N. Matsumi, M. Miyake, H. Ohno, *Chem. Commun.*, 2852 (2004).
52. H. C. Brown, H. I. Sclesinger, S. Z. Cardon, *J. Am. Chem. Soc.*, **64**, 325 (1942).
53. H. C. Brown, *J. Am. Chem. Soc.*, **67**, 1452 (1945).
54. H. C. Brown, H. Pearsall, *J. Am. Chem. Soc.*, **67**, 1765 (1945).
55. Y. Chujo, N. Takizawa, T. Sakurai, *J. Chem. Soc., Chem. Commun.*, 227 (1994).
56. A. Fratiello, R. E. Schuster, *Inorg. Chem.*, **7**(8), 1581 (1968).
57. N. Matsumi, A. Mori, K. Sakamoto, H. Ohno, *Chem. Commun.*, 4489 (2005).
58. B. G. Ramsey, L. M. Isabelle, *J. Org. Chem.*, **46**, 179 (1981).
59. N. Matsumi, M. Nakashiba, H. Ohno, *Polym. Bull.*, **50**, 259 (2003).
60. K. Niedenzu, J. W. Dawson, *Boron-Nitrogen Compounds*, Springer-Verlag, New York (1965).

---

# Index

---

- Acidic polymers, use as cocatalysts, 27
- Acyclic diene metathesis (ADMET) polymerization, 28, 29
- Advanced ceramics, polymeric precursors for, 265
- Advanced materials, boron- and nitrogen-containing polymers for, 103–120
- AIBN (azobisisobutyronitrile), 155, 156
- Air-stable organoboron segmented block copolymers, 9
- Alcoholysis, 129
- Aldehyde reduction, 30
- Alkoxyboration polymerization, 140–141
- Alkylaluminumoxane (MAO) cocatalyst, 25, 27
- B*-Alkylaminoborazines, 166
- asymmetric, 165
- Alkylborane polymer electrolytes, 193
- Alkylborane-type polymers, 186
- ionic conductivity of, 179
- Alkyl-substituted *B*-chloroborazines, as monomers, 157–158
- Allylcarborane-containing polymers, 99
- $\alpha$ -olefin polymerization, supported catalysts for, 26
- Alternating boration copolymerization, 139
- Alternating poly(*m*-carborane-disiloxane-diacetylene)s, 43–45
- Amine-modified polyborazylene, 154
- B*-Aminoborazines, display of amino groups by, 162
- Aminosilane reaction, 6
- Ammonolysis process, 162
- Anion sensors, organoboron polymers as, 137–138
- Anion-trapping-type electrolytes, 193
- Anion-trapping-type organoboron polymer electrolytes
- ion-conductive properties of, 178–179
- via hydroborane monomer, 177–179
- Antimony pentachloride, 84
- Aromatic acetylene bonds, haloboration of, 139–140
- Aromatic ethers, condensation of, 97
- Aromatic organoboron compounds, 130
- Atomic emission spectroscopy (AES) studies, 90–91
- Atomic Weapons Establishment (AWE) studies, 84
- B*-alkylaminoborazines, 166
- asymmetric, 165
- B*-aminoborazines, display of amino groups by, 162
- 9-BBN dimer, 24. *See also* 9-Borabicyclo[3.3.1]nonane (9-BBN)
- 9-BBN-modified allylhydridopolycarbosilane polymers, 36
- B*-chloroborazine, polymers derived from, 156–169
- <sup>10</sup>B enriched compounds, 96
- Benzocyclobutadiene carborane analog, 40
- 5-Benzyl-2-phenyl-5-(4-vinylbenzyl)-[1,3,3]-dioxaborinane, 31, 32
- Bernard, Samuel, v, 103
- $\beta$ -elimination process (retrohydroboration), 141
- Bifunctional monomers, hydroboration polymerization of, 177
- Bi-ionic systems, 176
- 1,12-Bis-(4-chlorophenyl)-1,12-dicarbodecaborane, polycondensation of, 41
- Bis-adduct decaborane, 79
- 1,7-Bis-(di-methylmethoxysilyl)-*m*-carborane, 85
- 1,2-Bis(*N*-nitroso-acetylaminophenyl)-*o*-carborane (NAFC), 100
- Bisphenol-A resins, boron-containing, 31
- Bisureidosilane monomers, 6

- Bis(ureido)silanes, condensation reaction with *m*-carborane di-hydrocarbyl-disilanol, 86–87
- Blocky poly(*m*-carborane-disiloxane-diacetylene)s, 43–45
- <sup>11</sup>B MAS NMR spectra, 94. *See also* <sup>11</sup>B-NMR spectra; Boron; Nuclear magnetic resonance (NMR) spectroscopy
- BN/BN composites, 118. *See also* Boron nitride (BN)
- B—N bond, 151
- BN-coated fibers, 118
- BN fiber elaboration, polymeric precursor for, 159
- B(NHMe)<sub>3</sub> boranes, 105–106, 113, 115
- B—N linkages, 109, 152
- <sup>11</sup>B-NMR spectra, 190–191. *See also* <sup>11</sup>B MAS NMR spectra; Boron; Nuclear magnetic resonance (NMR) spectroscopy
- 9-Borabicyclo[3.3.1]nonane (9-BBN), 182. *See also* 9-BBN entries
- 9-Borabicyclo[3.3.1]nonane–poly(propylene oxide) dehydrocoupling reaction, 182–183
- Borandiyl-bridged poly(ferrocenylene)s, 20, 21
- Borane monomer tetrahydrofuran solution, adding a diene monomer to, 124
- Borane-terminated isotactic polypropylene (*I*-PP), preparing, 25
- Boration copolymerization, between bisallene and diyne, 140
- Boration reactivities, between diynes and diisocyanates, 139
- Borazanaphthalene, 152
- Borazine, 33–34
- polymers derived from, 151–156
  - as a precursor of boron nitride, 151
  - precursors, 36
  - reactions with olefins, 155
  - thermolysis of, 153
- Borazine-based polymers, 105
- Borazine-containing organoboron polymers, 34–37
- Borazine polymer systems, SiC-producing, 34–36
- Borazine structures, formation of, 133
- Borazinic ring, 151
- Boron. *See also* <sup>10</sup>B enriched compounds; <sup>11</sup>B MAS NMR spectra; <sup>11</sup>B-NMR spectra; Boron atoms
- characteristics of, 8
  - historical perspective on, xi, 2–8
  - in “inorganic benzene-like” ring systems, 3
  - inorganic polymers of, 150
  - sources of, 3
- Boronate-functionalized polymers, 28
- Boron atoms
- in polymer backbone or pendent groups, 8–33
  - synthesis of unsaturated polymers containing, 10
- Boron-bridged [1]ferrocenophanes, polymerization of, 19–20
- Boron chromophore-containing polyurethanes, 12
- Boron cluster compounds, 78
- for neutron capture applications, 96
- Boron clusters, in polymer backbone or pendent groups, 38–71
- Boron cluster systems, monomeric and polymeric organic analogs of, 38–42
- Boron-containing advanced ceramics, preparation of, 104
- Boron-containing polymers, xi
- advances in, 8–33
  - chemistry of, 8
  - preceramic, 104–105
- Boron-delivery agents, 55
- Boron hydrides, 3
- Boronic acid-containing polyanilines, 14
- Boronic acids, 33
- Boron isotopes, 54, 78
- Boron ligands/polymers, used in olefin polymerization reactions, 22–29
- Boron main-chain polymers, 9
- Boron neutron-capture therapy (BNCT), 54
- drug-delivery platforms for, 55–57
- Boron nitride (BN). *See also* BN entries
- preparation of, 118
  - properties of, 104
- Boron nitride fibers
- mechanical properties of, 112
  - microtexture differences in, 111–112
  - polymeric precursors of, 105
- Boron nitride materials, preparing pure, 171
- Boron nitride microtubes, 106
- Boron–nitrogen-containing polymers, 151
- Boron oxide/boron carbide crust, 94
- Boron polymers
- containing organometallic moieties, 17–22
  - containing P atoms, 15–17
  - formation of, 3
  - $\pi$ -conjugated, 21
  - silicon-containing, 17
- Boron-rich dodeca(carboranyl)-substituted closomers, 55–57
- Boron ring systems
- alternative, 38
  - planar structures of, 33
  - in polymer backbone or pendent groups, 33–38
- Boron–ruthenium conjugated system, 131
- Boron–silicon–diacetylene polymers, linear, 17
- Boron-stabilized carbanions, 190
- Boron-stabilized imidoanion (BSI), 190–193
- Boroxine, 33–34
- Boroxine ring systems, 37

- Borylaminoborazine, thermal conversion into poly(borylaminoborazine), 168
- Borylborazine derivatives, chemistry of, 167
- Borylborazine route, 119
- B*-trialkylaminoborazine, ammonolysis of, 162
- B*-tri[bis(methylamino)boryl(methyl)amino]borazine, 113
- B*-trichloroborazine
- nucleophilic attack on, 161
  - reaction with trialkylaminoborane, 116–117
- B*-tri(dimethyl)-*N*-trimethylborazine, conversion to polymers, 159–160
- B*-vinylborazine, 155
- Cancer therapy research, <sup>10</sup>B nucleus in, 54. *See also* Tumor treatment
- Carbanions, boron-stabilized, 199
- Carboracycles, examples of, 64
- Carboracycle systems, 63–64, 65
- m*-Carborane, 39, 40
- o*-Carborane, 39, 40
- enthalpy of formation of, 99
  - polymer-supported, 62
- p*-Carborane, 39, 40
- Carborane cages, 78, 91
- electron-deficient, 93
  - impact of heat and ionizing radiation on, 94–95
- Carborane clusters
- conducting polymers containing, 52–54
  - grafted onto organometallic dendrimers, 62
- Carborane cluster systems, 39
- Carborane-containing grid-shaped polymers, molecular-size construction kit for, 66–67
- Carborane-containing polymers, other than polysiloxanes, 97–98
- Carborane polyhedra, 78
- Carborane polymers, 5
- in catalytic reactions, 61–63
  - in high-performance fiber production, 57–60
  - in medicine, 54–57
  - of polyetherketones, 60–61
- Carborane polymer systems, energetic, 99–100
- Carboranes, characteristics of, 39–40. *See also* *o*-Carborane
- Carborane-siloxane polymers, 93
- Carborane supramolecular chemistry, 63–71
- Carborane units, bearing energetic groups, 99–100
- p*-Carborane units, 5
- Carboranophanes, synthesis of, 41
- Carboranosiloxane rubbers, 4
- Carboranylenesiloxane polymers, 5–6
- incorporation of smaller carboranes in, 7
- Carboranyl polymer systems, elastomeric behavior in, 82
- Carboranyl units, polyphosphazene incorporating, 98
- Carbosilane dendrimers, 17, 18
- Catalytic reactions, carborane polymers in, 61–63
- Ceramic fibers, 105
- production of, 150
- Ceramic yield, 114
- increasing, 113
- Chain scission, 129
- Chain-transfer strategy, 25
- Chemosensors, 137
- B*-Chloroborazine, polymers derived from, 156–169
- Chujo, Yoshiki, v, 121
- closo*-dicarboranes, 39, 78
- Cobaltabisdicarbollide {Cs[Co(C<sub>2</sub>B<sub>9</sub>H<sub>11</sub>)<sub>2</sub>]<sup>-</sup>}, 52
- Cocatalysts, industrial, 27
- Combllike organoboron polymer/boron stabilized imidoanion hybrids, synthesis of, 190–193
- Combllike organoboron polymer electrolytes, 180–181
- Combllike organoboron polymers, temperature dependence of ionic conductivity for, 181
- Condensation polymerization, 86–87
- Conducting polymers, containing carborane clusters, 52–54
- Conjugated organoboron polymers, 122–123, 130–132
- Conjugated poly(cyclodiborazane)s, 134–137
- Coordination-driven carborane-containing self-assembled polymers, 67–69
- Coordination polymers, xiv
- construction of, 67–68, 70
- Cornu, David, v, 149
- Corriu/Douglas polymers, 10
- Covalently attached carborane-containing polypyrrole, 53–54
- Covalently carborane-bound polymer, 52–53
- Cross-coupling reactions
- poly(cyclodiborazane)s via, 142–143
  - poly(pyrazabole)s via, 143–145
- Cross-linking, 84, 85, 86
- Cyclodiborazane structures, 132
- Cyclooctaphane, 41–42
- Cyclopentadienylmolybdenum tricarbonyl dimer, 45
- Cyclophane, carboranophane analogs of, 41
- Decaborane-based polymeric material, 57–58
- Decaborane-based polymer systems, 79–80
- Decaborane carboranes, properties of, 82
- Decaborane complexes, 79–80
- Decaborane polymer, 4
- Dehydrocoupling polymerization, 177, 178

- Dehydrocoupling reactions, 16–17  
control of, 153  
organoboron polymer electrolyte preparation via, 182–183
- 1,2-Dehydro-*o*-carborane, 40
- Density Functional Theory (DFT), 39
- DEXSIL 200, 5
- DEXSIL 201, 5
- DEXSIL polymers, 4, 82
- Diacetylene-carboranylenesiloxane block polymers, synthesis of, 45
- Diacetylene-diluted alternating poly(*m*-carborane-disiloxane-diacetylene)s, 43–45
- Diacetylene group, in poly(carboranylenesiloxanes), 42, 43
- Diacetylene-silarylene block polymers, synthesis of, 45
- Dialkenylboron bromide, 138
- Dialkylamine-modified polyborazylenes, 153–154
- Dialkylaminoborylamine, 167
- Dialkylamino groups, attached to boron atoms, 166
- Diborane adducts, 3
- 1,2'-Diborazine, 152
- Diborylated ferrocene polymers, 18–19
- Dibromoborylated PS (PS-BBr), 27. *See also* Polystyrene (PS)
- Di-chlorobenzyl peroxide, 86
- Dichloromethyl methyl ether (DCME), in poly(alcohol) preparation, 126
- 1,9-Dicyanoanthracene (DCA), hydroboration polymerization with mesitylborane, 135
- Dicyano monomers, hydroboration polymerization of, 132–134
- Diethylborazine, 35
- Dilithiocarborane, salt elimination reaction with dichlorosiloxane, 88
- 6-Dimethylamino-2,4-dichloroborazine, reaction with disilazane, 158–159
- Dioxobenzene dianion, 39
- Dioxoborane tetraanion, 39
- Dipentylamine-modified polyborazylenes, 154–155
- Direct synthesis, of poly(lithium organoborate)s, 188–190
- Diyne monomers, hydroboration polymerization of, 129–130
- Diyne, phenylboration polymerization of, 139–140
- Donor-acceptor conjugated polymers, 131
- Donor-acceptor type  $\pi$ -conjugated poly(cyclodiborazane)s, 142–143
- Elastomeric materials, producing, 43–45
- Elastomeric networked polymers, 48–49
- Elastomers, glass-transition temperature of, 90
- Electrophilic substitution, 40
- Ene reaction, 40
- Energetic carborane polymer systems, 99–100
- Enthalpy of combustion, 99
- Enthalpy of formation, 99
- Ethylenediamine-borane reagent, polymer-bound, 30
- Ethynyl monomer, 48
- Exopolyhedral B—O bond lengths, 39
- FeCl<sub>3</sub>-catalyzed condensation reaction strategy, 46–47. *See also* Ferric chloride-catalyzed bulk condensation copolymerization
- <sup>57</sup>Fe Mössbauer studies, 91, 92
- Ferric chloride-catalyzed bulk condensation copolymerization, 82. *See also* FeCl<sub>3</sub>-catalyzed condensation reaction strategy
- Ferrocene-bridged tris(1-pyrazolylborate) oligomeric systems, 20, 37
- Ferrocene [33-bipy]<sub>n</sub> polymer, 18–19
- Ferrocene compound chemistry, 18
- [1]Ferrocenophanes, ring-opening reactions of, 19–20
- Ferrocenyl-carboranylenesiloxyl-diacetylene polymers, 43
- Fire-resistant carborane-containing polyetherketones, 60
- Flame-retardant materials, organoboron polymers as, 31–33
- Fluorescent chemosensors, 137
- Fluorescent organoboron polymers, 37, 38
- Foamed polysiloxanes, 92  
synthesis of, 91
- Gas chromatography/mass spectroscopy(GC/MS), during thermolysis, 109
- Gel-permeation chromatography (GPC), 89
- Glass-transition temperature, 89–90
- Glyme, 153
- Green fibers, 114–115
- Grignard chemistry, 11
- Grignard reagents, 141
- Haloboration, 10
- Haloboration-phenylboration polymerization, 138–139
- Haloboration polymerization, 138–139
- Heteroaromatic diynes, hydroboration polymerization of, 131
- 6-Hexynyl-decaborane, 58
- High molecular-weight polyphosphinoborane polymer, 16–17
- High-performance fiber production, carborane polymers in, 57–60

- High-performance fibers, borazine-containing organoboron polymers in, 34–37
- High-temperature polymers, 5
- $^1\text{H}$ -NMR spectra, 178. *See also* Nuclear magnetic resonance (NMR) spectroscopy
- Homogeneous fluorescein-labeled *nido*-carboranyl oligomeric phosphate diesters (*nido*-OPDs), 54–55
- $^1\text{H}$  spin-echo decay measurements, 95
- $^1\text{H}$  spin-echo NMR relaxation techniques, 88–89. *See also* Nuclear magnetic resonance (NMR) spectroscopy
- $^1\text{H}$  spin-echo relaxation profile, 95–96
- Hückel molecular orbital (MO) theory, 130
- Hybrid Density Functional Theory (DFT), 39
- Hydroborane monomer, anion-trapping-type organoboron polymer electrolytes via, 177–179
- Hydroborane reagent, 182–183
- Hydroboration polymerization, 123–138, 177
- of dicyano monomers, 132–134
- of diyne monomers, 129–130
- between mesitylborane and triethyleneglycol diallylether, 177–178
- reactions of organoboron polymers prepared by, 124–129
- Hydroboration reaction, 8–11
- of polystyrene with hexylborane terminal double bond, 126–127
- Hydrogen. *See*  $^1\text{H}$  entries; Hydro- entries
- Hydrogen-bond interaction-driven coordination, 68–69
- Hydrosilated network polymers, 48
- Hydrosilation reactions, 47–48
- Icosahedral carborane cages, 96
- Icosahedral carboranes, 78
- properties of, 82
- thermal and radiation stability from, 93–97
- Icosahedral *closo*-dicarbaborane units, polymers incorporating, 77–102
- Imidazole–borane complexes, physical properties of, 186
- Imidoanion, boron-stabilized, 190–193
- Immunoconjugates, boron-rich, 54
- Industrial SiC fibers, 34
- Infusible polymers, 162
- Inorganic benzenes, 33
- Inorganic polymer electrolytes, 176
- Inorganic polymers, rheology of, 159
- Intramolecular charge-transfer (ICT) interaction, 135
- Ionic conductivity
- of lithium borate polymers, 188–189
- of polymer/salt hybrids, 192–193
- temperature dependence of, 181, 184, 187, 191–192
- Ionic liquids, 183
- Iron. *See* Fe entries; Ferric entries; Ferro-entries
- Isocyanates, 87
- haloboration and phenylboration of, 140
- Karstedt catalyst, 48, 49
- Kekule-like structures, 34
- Keller, Teddy M., v, 1
- Kolel-Veetil, Manoj K., v, 1
- Lewis acidic organoboron compounds, 177
- Lewis acids, polymeric, 28
- Linear boron–silicon–diacetylene polymers, 17
- Linear toluene swell, 90
- Liquid imidazole–borane complexes, 185
- LiTFSI, 179, 181, 185, 193
- Lithium borate polymers, ionic conductivity of, 187, 188–189
- Lithium borate-type polymers, via polymer reactions, 186–187
- Lithium ion conducting borosiloxane polymers, 17
- Lithium mesitylhydroborate, 188
- Lithium salt dissociation, 190
- Lithium secondary battery, 176
- Lithium transference numbers, 176–177, 179, 181, 183, 185, 193
- improving, 193
- Lowest unoccupied molecular orbital (LUMO), extending, 13
- Luminescent organoboron quinolate polymers, 13
- Lysine dendrimers, carborane-containing, 57
- Macromolecules, containing metal and metal-like elements, xiii–xiv
- Main-chain boronate polymers, 28
- Main-chain-type organoboron polymers, 122, 145
- Mass loss
- dimethylsiloxane groups and, 94
- of poly(ether-ketone-carbaborane), 98
- Matsumi, Noriyoshi, v, 175
- Medicine, carborane polymers in, 54–57
- Melting temperature, 89–90
- Melt-spinnable poly[*B*-aminoborazine], boron nitride fibers from, 162
- Melt-spinnable poly[*B*-trimethylaminoborazine]s, 163
- structure of, 164–165
- Melt spinning, 114–115
- Mercuracarborands, 66, 67
- Mesitylborane
- hydroboration polymerization with 1,9-dicyanoanthracene, 135

- Mesitylborane (*Continued*)  
  hydroboration polymerization with adiponitrile, 133  
  hydroboration reaction with acetylene bond, 130  
Metal-containing polymers, xiii  
Metal–halogen interchange reaction, 7  
Metallacarborane oligomers, 64, 66  
Metal-like elements, xiv  
Metallocene catalysts, polymer-supported, 26  
Methylvinylsiloxane, 87  
Miele, Philippe, v, 103, 149  
  + Mo<sub>2</sub>C superconducting nanoparticles, 45–46  
Mobile electronic devices, lithium secondary battery for, 176  
Molecular borylaminoborazinic derivatives, 168–169  
Molecular orbital (MO) theory, 130  
Molecular precursors, thermal condensation of, 166–167  
Molecular tools, carborane-containing, 68  
Molybdenum (Mo) metathesis catalyst, 28, 29. *See also* Cyclopentadienylmolybdenum tricarbonyl dimer; + Mo<sub>2</sub>C superconducting nanoparticles  
Monoanionic boron clusters, 53  
Monomeric organic analogs, of boron cluster systems, 38–42  
Mössbauer studies, 91, 92  
“Motorized nanocar” structure, 69, 71
- NaBH<sub>4</sub>/(NH<sub>4</sub>)<sub>2</sub>SO<sub>4</sub>, reaction in tetraglyme, 153  
Nagata, Yuuya, v, 121  
Nanostructured boron carbide materials, 57–58  
  —N—B—N— bridges, 117, 119  
  —N(CH<sub>3</sub>)— bridges, 109, 111  
  —N(CH<sub>3</sub>)— bridge units, 166  
Networked polymers, synthesis of, 47–48  
Neutron capture approach, 96  
Neutron scintillator materials, 145  
Neutron shields, 96  
New materials, synthesis of, 118–119  
*nido*-carboranyl oligomeric phosphate diesters (*nido*-OPDs), 54–55, 56  
*nido*-carboranylporphyrins, metal-free, 57  
9-BBN dimer, 24. *See also* 9-Borabicyclo[3.3.1]nonane (9-BBN)  
9-BBN-modified allylhydridopolycarbosilane polymers, 36  
NLO materials, from polyurethanes, 11–13  
  —NMe— bridges, 109  
NMR relaxation measurements, 95. *See also* Nuclear magnetic resonance (NMR) spectroscopy  
Nonoxide precursor route, 104  
Nonpolyether-type polymer electrolyte, 193–194  
Norbornene monomers, ring-opening metathesis polymerization of, 28–29  
Novolac resins, boron-containing, 31, 32  
n-type conjugated polymers, 130  
Nuclear magnetic resonance (NMR) spectroscopy, 88–89. *See also* <sup>11</sup>B MAS NMR spectra; <sup>11</sup>B-NMR spectra; <sup>1</sup>H-NMR spectra; <sup>1</sup>H spin-echo NMR relaxation techniques; NMR relaxation measurements  
Nucleophilic reaction route, two-step, 165
- Ohno, Hiroyuki, v, 175  
Olefinic monomers, functionalizing, 22  
Olefin polymerization reactions, boron ligands/polymer used in, 22–29  
Olefin protection strategy, 25  
Olefin reactions, 155  
Oligo(ethylene oxide) grafted polyphosphazene, 180  
Oligomeric boron-bridged (1-pyrazolyl)borate systems, 7–8  
Olin polymers, 4–5  
One-step poly(*B*-amino)borazine process, 156–159  
One-step poly(*B*-borylamino)borazine process, 159–161  
One-step polycondensation, 116–118  
Optical/sensing applications,  $\pi$ -conjugated organoboron polymers used in, 8–15  
Organic transformations, organoboron polymers used as catalysts in, 22–30  
Organoboron compounds, 122  
Organoboron main-chain polymers, 123–124  
Organoboron polymer electrolytes  
  comblike, 180–181  
  design of, 194  
  ion-conductive properties of, 194  
  lithium transference number of, 179  
  preparation via dehydrocoupling reaction, 182–183  
  reactions with organolithium reagents, 186  
  reaction with aryllithium reagents, 188  
  for selective lithium cation transport, 175–196  
Organoboron polymer reactions  
  prepared by hydroboration polymerization, 124–129  
  via ring opening of pyridine or furan moieties, 126  
Organoboron polymers, 121–147  
  as anion sensors, 137–138  
  conjugated, 130–132, 141  
  containing alternative boron ring systems, 38  
  containing borazine- or 9-BBN, 34–37  
  containing boroxine or triphosphatborin ring systems, 37  
  containing polypyrazolylborate or pyrazabole ring systems, 37–38

- containing pyrazoboles, 143  
as flame-retardant materials, 31–33  
formed by hydroboration route, 9–11  
formed by synthetic routes, 11–15  
reaction with aryllithium reagents, 186  
used as catalysts in organic transformations, 22–30  
used in organic transformations, 29–30
- Organoboron quinolate polymers, luminescent, 13
- Organolithium reagents, 141
- Organometallic dendrimers, 62–63
- Organometallic macromolecules, xiv
- Organometallic moieties, boron polymers containing, 17–22
- Organometallic routes, 141–145
- ortho*-carborane, preparation of, 79
- ortho*-oligomeric phosphate diesters (*ortho*-OPDs), 55, 56
- Overoxidation resistance limit (ORL), 53
- Palladium(0) catalysts, 30
- Patel, Mogon, v, 77
- Pendant carborane groups, polymers with, 80–81
- Phenylboration, 10  
polymerization via, 139–140
- Phenyl-modified poly(*m*-carborane-siloxane), 90
- Phosphine-borane adduct studies, 16–17
- Phosphorus-containing boron polymers, 15–17
- $\pi$ -conjugated boron polymers, 131–132. *See also*  
 $\pi$ -conjugated organoboron polymers
- $\pi$ -conjugated dendritic polymers, 12
- $\pi$ -conjugated organoboron polymers, 21, 22, 134.  
*See also*  $\pi$ -conjugated boron polymers  
in optical and sensing applications, 8–15  
as selective fluoride ion sensors, 137
- $\pi$ -conjugated poly(*p*-phenylene-boranes), 11
- $\pi$ -conjugation length, 138
- $\pi$ -extended conducting polymeric system, 13
- Pinacolborane-modified PVS polymers, 35
- Polar solvents, 153
- Poly(1-pyrazolyl)borate synthesis, 7–8
- Poly(alcohol)s, preparation from organoboron polymers, 125–126
- Poly(aniline boronic acid)-based conductimetric sensor, 14
- Poly(aryletherketone-carborane)s, synthesis of, 97
- Poly(azophenylene-*o*-carborane), 100
- Poly[*B*-(alkylamino)borazine-derived fibers  
curing and pyrolysis of, 111  
stretchability of, 110
- Poly[*B*-(alkylamino)borazines], 156  
bridge-type bonds in, 166  
as fiber precursors, 105  
glass-transition temperatures and ceramic yields for, 110  
melt-extrusion of, 111  
tris(alkylamino)borane-derived, 105–107  
tris(*B*-alkylamino)borazine-derived, 107–112  
viscoelastic and thermal stabilities of, 110
- Poly[*B*-aminoborazines], 151, 156  
one-step process for, 156–159  
studies of, 162  
two-step process for, 161–166
- Poly(*B*-borylamino)borazines  
one-step process for, 159–161  
two-step process for, 166–169
- Polyborazine additive, 35
- Polyborazylene polymer, 152
- Polyborazylenes, 151  
alternative synthesis route for, 153  
structure of, 152
- Poly(boronic carbamate)s, 140
- Polyborylamino borazines, polymeric structure for, 169
- Polyborylborazine, thermal route to, 116
- Poly[*B*-(trianilino)borazine], 165
- Poly[*B*-(trimethylamino)borazine], 162
- Poly-*B*-vinylborazine homopolymer, 155
- Poly(carboranedimethylsiloxane) elastomer, 90
- Poly(carboranylensiloxanes), 42–52
- Polycarbosilane-based polymers, incorporation of decaborane into, 60
- Polycarbosilane polymers, modification with 9-borabicyclo[3.3.3]nonane, 36
- Polycarbosilanes (PCS), 34–35
- Polycondensation  
calculating the degree of, 113, 114  
one-step, 116–118  
two-step, 112–116
- Poly(cyclodiborazane)s  
charge-transfer complex with 7,7,8,8-tetra-cyanoquinodimethane, 137  
conjugated, 134–137  
containing a dithiafulvene unit, 136–137  
containing oligothiophene units, 136  
containing palladium and platinum, 137  
electronic state of, 135  
prepared by hydroboration polymerization of dicyano monomers, 132–134  
via cross-coupling reactions, 142–143
- Poly(cyclooctenyl-decaborane), 59
- Poly(dioxaboralane)s, 38
- Poly(ether-ketone-carborane), 97–98
- Polyetherketones, carborane polymers of, 60–61
- Polyethylene (PE), high molecular weight, 62
- Poly(ethylene oxide) (PEO) derivatives, 176

- Poly(ethynylene-phenylene-ethynylene-borane)s, 11
- Poly(ethynylene-*p*-phenylene-ethynylene-borane)s, 141–142
- Poly(ferrocenylphosphines), 20
- Polyhexenyldecaborane, 57–58, 59
- Poly(isobutylphosphinoborane)s, 15–16
- Poly(lithium mesitylhydroborate), reaction with fluorinated alcohols, 189
- Poly(lithium organoborate)s, direct synthesis of, 188–190
- Poly(*m*-carborane-siloxane) elastomers, characterization of, 88–92
- Poly(*m*-carborane-siloxane) rubbers, 46, 47, 81–82  
polymerization method for, 85–86  
synthesis of, 82–88
- Poly(*m*-carborane-siloxane)s, 82  
with carborane units, 93  
phenyl and vinyl modified versions of, 86
- Polymer backbone/pendent groups  
boron ring systems in, 33–38  
containing boron clusters, 38–71
- Polymer derived ceramics (PDCs) method/route, 104, 156
- Polymer electrolytes, 176
- Polymer fibers, properties of, 115
- Polymeric B–N derivatives, 150
- Polymeric organic analogs, of boron cluster systems, 38–42
- Polymeric precursors, derived from tris(borylamino)borazines, 112–118
- Polymeric sensing systems, 13
- Polymerization. *See also* Polymerization reactions; Polymers  
alkoxyboration, 140–141  
haloboration, 138–139  
hydroboration, 123–138  
phenylboration, 139–140
- Polymerization reactions, improvements in the control of, 171–172
- Polymer reactions, lithium borate-type polymers via, 186–187
- Polymers. *See also* Polymer reactions  
*B*-chloroborazine-derived, 156–169  
borazine-derived, 151–156  
boron- and nitrogen-containing, 149–172  
carborane-containing, 97–98  
incorporating icosahedral *closo*-dicarbaborane units, 77–102  
organic solvent solubility of, 157–158  
organoboron, 121–147  
with pendent carborane groups, 80–81  
prepared from thexylborane and diene monomers, 124–125  
spinning parameters for, 110  
thermal and chemical properties of, 89–92  
transition temperatures of, 90  
tris(alkylamino)borane-derived, 169–171
- Polymer/salt hybrids, 176–177, 190–193, 194  
ionic conductivity of, 192–193  
VFT parameters for, 193
- Polymer-supported organoboron catalysts, 29
- Polymer-to-ceramic conversion, 115  
monitoring of, 111  
steps in, 106
- Poly(methylmethacrylate) (PMMA), production from methylmethacrylate monomer, 24
- Poly(norbornenyl-decaborane), 59
- Poly(*o*-carboranyl-organo-siloxane)s, synthesis of, 80–81
- Polyolefin diblock copolymers, 25
- Poly(organoboron halide), 183
- Poly(organoboron halide)–imidazole complexes, 183–186  
VFT parameters for, 185
- Poly(oxydimethylsilanediy)l)s, 84
- Poly(phenyl-carboranyl-di-trifluoroethoxy-phosphazene), 81
- Poly(phenylphosphinoborane), syntheses of, 15
- Poly(*p*-phenylene-borane)s (PPBs), 141
- Poly(*p*-phenylene) carborane-based analog, 40–41
- Polyphosphazenes  
containing alkyl- or phenyl-carborane, 81  
incorporating carboranyl units, 98
- Polyphosphinoborane polymer, high molecular-weight, 16–17
- Polyphosphinoboranes, 4
- Polypropylene (PP), hydroboration strategy of chain end olefinic unsaturation in, 23. *See also* PP/maleic anhydride (MA) copolymers
- Polypropylene-*b*-polymethylmethacrylate (PP-*b*-PMMA), synthesis of, 22–23
- Poly(pyrazabole)/perylene/polymethylmethacrylate (PMMA), 145
- Poly(pyrazabole)s  
containing an electron withdrawing moiety, 144–145  
as a neutron scintillator material, 145  
via cross-coupling reactions, 143–145
- Polypyrazolylborate ring systems, 37–38
- Polypyrrole (PPy), boronate-functionalized, 10.  
*See also* (PPy)-Cs[Co(C<sub>2</sub>B<sub>9</sub>H<sub>11</sub>)<sub>2</sub>]<sup>−</sup> polymer
- Polypyrrole–Cs[Co(C<sub>2</sub>B<sub>9</sub>H<sub>11</sub>)<sub>2</sub>]<sup>−</sup> polymer, 52
- Polypyrrole materials, overoxidation resistance limit of, 53
- Polypyrrole precursor reaction scheme, 11
- Polypyrroles, development of, 29–30

- Polysiloxanes (silicones), xiii  
double comblike, 180
- Polystyrene (PS), organoboron polymers of, 28.  
*See also* Dibromoborylated PS (PS-BBr)
- Poly(styrene-*co*-*B*-vinylborazine), 155–156
- Polythiophenes,  $\pi$ -conjugated, 10
- Poly vinyl chloride (PVC), 62
- Polyvinylstyrene polymers, diethylborazine- and pinacolborane-modified, 35
- Porphyrins, carboranylated, 57
- Potential gradient, 176
- Potentiometric sensors, boronic acid-containing polyaniline-based, 15
- PP/maleic anhydride (MA) copolymers, synthesis of, 23. *See also* Polypropylene (PP)
- (PPy)-Cs[Co(C<sub>2</sub>B<sub>9</sub>H<sub>11</sub>)<sub>2</sub>]<sup>-</sup> polymer, 52. *See also* Polypyrrole (PPy)
- Preceramic polymer route, 105
- Preceramic polymers, 104  
meltability of, 115  
pyrolysis of, 119
- Precursors-to-ceramic route, 150
- Propellant binders, polymers and copolymers used as, 99
- Pyrazabole ligands, 37
- Pyrazabole polymers, 37
- Pyrazabole ring systems, 37–38
- Pyrazaboles, 143
- Radiation stability, from icosahedral carboranes, 93–97
- Residual catalyst content, 91
- Retrohydroboration ( $\beta$ -elimination) process, 141
- RhH(CO)(PPh<sub>3</sub>)<sub>3</sub> catalyst, 155
- Rhodium (Rh)-catalyzed dehydrocoupling procedure, 16
- “Rigid-rod”-type polymers, 81
- Ring-opening metathesis polymerization (ROMP), 28–29
- Ring-opening polymerization (ROP) strategy, 19
- (RNBHR)<sub>3</sub> alkylaminoborazines, 170
- Ruthenium (Ru) metathesis catalyst, 28, 29
- Salt elimination reaction, 88
- Segmented block poly(alcohol)s, preparation of, 128–129
- Selective lithium cation transport, organoboron polymer electrolytes for, 175–196
- Self-condensation, carboranedisilanol, 6
- Semi-metal-containing polymers, xiii
- Si/B/C/N-producing systems, 36–37. *See also* Silicon-containing boron polymers
- SiC-producing borazine polymer systems, 34–36
- SiC-producing resins, introducing boron into, 35
- Side-chain-type organoboron polymers, 122
- $\sigma$ - $\pi$  conjugation, using the disilanylene structure, 135–136
- Silicon-containing boron polymers, 17. *See also* Si/B/C/N-producing systems; SiC entries
- Silicones (polysiloxanes), xiii  
double comblike, 180
- Siloxane-carborane ratio, 82
- Siloxane content, glass transition as a function of, 83
- Siloxane units, incorporation of, 82
- Silyl-carborane hybrid diethynylbenzene-silylene polymer, 50–52
- Size exclusion chromatogram (SEC), 109
- Sodium. *See* NaBH<sub>4</sub>/(NH<sub>4</sub>)<sub>2</sub>SO<sub>4</sub>
- Sonogashira–Hagihara coupling, 142, 143
- Speier’s catalyst, 47
- Spinnable polymers, properties of, 105
- Spin–spin (transverse) relaxation time, 95
- Styrenic monomer, boron-containing, 31–33
- Superaromatic carboranes, 49
- Supported catalysts, 26
- Supramolecular architectures, 70
- Supramolecular chemistry, carborane, 63–71
- Supramolecular structure assembly, 54
- Swain, Anthony C., v, 77
- Symmetric oligomers, 64, 66
- Syndiotactic polystyrene (PS) polymers, 24
- 7,7,8,8-Tetracyanoquinodimethane (TCNQ), 137
- Tetraethylene glycol (TEG) side chain, 193
- Tetrahydrofuran (THF), 153
- Tetrahydrofuran soluble fraction, GPC on, 89
- 1,2,3,5-Tetramethyl-4,6-dichloroborazine, reaction with hexamethyldisilazane, 158
- Thermal degradation pathway, influence of steric congestion on, 98
- Thermal neutron attenuation properties, 96
- Thermal stability, from icosahedral carboranes, 93–97
- Thermal transition temperatures, 90
- Thermoplastic polyborazine, 170–171
- Thexylborane, 122, 126–127  
reaction with 1,7-octadiene, 123
- Three-dimensional (3D) X-ray microtomography, 92
- Toury, Bérange, v, 149
- Transamination reactions, 159–160
- Transamination reaction, 171
- Transition metal-catalyzed synthetic methodology, 16
- Transverse (spin–spin) relaxation time, 95
- B*-Trialkylaminoborazine, ammonolysis of, 162
- 2,4,6-Trialkylaminoborazines, 167

- Trialkylboranes, polymer homologues of, 124
- 2,4,6-Tri[bis(isopropylamino)boryl(isopropylamino)]borazine, 112–113
- B*-Tri[bis(methylamino)boryl (methylamino)]borazine, 113
- B*-Trichloroborazine
- nucleophilic attack on, 161
  - reaction with trialkylaminoborane, 116–117
- 2,4,6-Trichloroborazine chlorine atoms, exchange by a dialkylamino group, 162
- 2,4,6-Trichloroborazine–hexamethyldisilazane reaction, polymer formation from, 157
- B*-Tri(dimethyl)-*N*-trimethylborazine, conversion to polymers, 159–160
- Trifluoroborate-substituted polythiophene system, conjugated, 13
- Trifluoromethanesulfonic acid (TFSA)-promoted polycondensation reaction, 60–61
- 2,4,6-Trimethylaminoborazine, self-condensation of, 163
- 2,4,6-Trimethylaminoborazine–laurylamine condensate, 163
- N*-Trimethyl-*B*-tri(amino)borazine, 106
- Trimethylsilylamino-substituted oligomer, 157
- Triphosphatriborin, 33–34
- ring systems of, 37
- Tris(alkylamino)borane-derived poly[*B*-(alkylamino)borazines], 105–107
- Tris(alkylamino)boranes, 160, 167
- polymers derived from, 169–171
  - thermal process for, 170
- Tris(*B*-alkylamino)borazine-derived poly[*B*-(alkylamino)borazines], 107–112
- Tris(*B*-alkylamino)borazines, thermolysis of, 108–109
- Tris(borylamino)borazines, polymeric precursors derived from, 112–118
- Trisiloxy groups, 45
- Tris(isopropylamino)borane, 170
- Tris(methylamino)borane, 160, 170
- Tumor treatment, neutron capture approach in, 96.
- See also* Cancer therapy research
- 2 + 2 reaction, 40
- “Two-point polymers,” 158
- Two-step poly(*B*-amino)borazine process, 161–166
- Two-step poly(*B*-borylamino)borazine process, 166–169
- Two-step polycondensation, 112–116
- Ultra-high molecular weight carboranylenesiloxane polymers, 6
- Ureidosilane reaction, 6. *See also* Bisureidosilane entries
- Valence bond (VB) theory, 34
- VFT equation, 189. *See also* Vogel–Fulcher–Tamman (VFT) plot
- VFT parameters
- for lithium borate polymers, 190
  - for polymer/salt hybrids, 193
- Vinylborane units, hydroboration of, 129
- B*-Vinylborazine, 155
- Vinylcarborane-containing polymers, 99
- Vinylcarboranylenesiloxane, 48
- Vinyl group, conjugative interaction with boron atom, 139
- Vinyl-phenyl-modified polymer, boron content of, 91
- Vogel–Fulcher–Tamman (VFT) plot, 179. *See also* VFT entries
- Ziegler–Natta (Z-N) polymerization, 22
- Zwitterionic molten salts, 183